Estimating forest attributes using laser scanning data and dual-band, single-pass interferometric aperture radar to improve forest management

Alicia Peduzzi

Dissertation submitted to the faculty of the Virginia Polytechnic Institute and State University in partial fulfillment of the requirements for the degree of

Doctor of Philosophy
In
Forestry

Randolph H. Wynne, Chair
Thomas R. Fox
Valerie A. Thomas
Ross F. Nelson

September 08, 2011
Blacksburg, Virginia

Keywords: forest mensuration, remote sensing, leaf area index, stem density, height to live crown

Estimating forest attributes using laser scanning data and dual-band, single-pass interferometric aperture radar to improve forest management

Alicia Peduzzi

ABSTRACT

The overall objectives of this dissertation were to (1) determine whether leaf area index (LAI) (Chapter 2), as well as stem density and height to live crown (Chapter 3) can be estimated accurately in intensively managed pine plantations using small-footprint, multiple-return airborne laser scanner (lidar) data, and (2) ascertain whether leaf area index in temperate mixed forests is best estimated using multiple-return airborne laser scanning (lidar) data or dual-band, single-pass interferometric synthetic aperture radar data (from GeoSAR) alone or both in combination (Chapter 4). In situ measurements of LAI, mean height, height to live crown, and stem density were made on 109 (LAI) or 110 plots (all other variables) under a variety of stand conditions. Lidar distributional metrics were calculated for each plot as a whole as well as for crown density slices (newly introduced in this dissertation). These metrics were used as independent variables in best subsets regressions with LAI, number of trees, mean height to live crown, and mean height (measured in situ) as the dependent variables. The best resulting model for LAI in pine plantations had an R^2 of 0.83 and a cross-validation (CV) RMSE of 0.5. The CV-RMSE for estimating number of trees on all 110 plots was 11.8 with an R^2 of 0.92. Mean height to live crown was also well-predicted (R^2 = 0.96, CV-RMSE = 0.8 m) with a one-variable model. In situ measurements of temperate mixed forest LAI were made on 61 plots (21 hardwood, 36 pine, 4 mixed pine hardwood). GeoSAR metrics were calculated from the X-band backscatter coefficients (four looks) as well as both X- and P-band interferometric heights and magnitudes.

Both lidar and GeoSAR metrics were used as independent variables in best subsets regressions with LAI (measured in situ) as the dependent variable. Lidar metrics alone explained 69% of the variability in temperate mixed forest LAI, while GeoSAR metrics alone explained 52%. However, combining the LAI and GeoSAR metrics increased the R^2 to 0.77 with a CV-RMSE of 0.42. Analysis of data from active sensors shows strong potential for eventual operational estimation of biophysical parameters essential to silviculture.

Acknowledgements

I would like to thank my major professor Dr. Randolph H. Wynne for his unconditional support and encouragement throughout my PhD program. I am deeply grateful to him and committee member Dr. Valerie A. Thomas for their professional and personal support throughout. Also, I would like to thank Dr. Ross F. Nelson and Thomas R. Fox for their input and contribution to my research. I am grateful for the financial support provided by the Virginia Tech Department of Forest Resources and Environmental Conservation, the Forest Productivity Cooperative, and for the field collaboration provided by the personnel from the Virginia Department of Forestry and the Forest Service Appomattox-Buckingham office.

I want to extend special thanks to every person that helped me with the field data collection: Rupesh Shrestha, Jessica Walker, Jose Zerpa, Nilam Kayastha, Asim Banskota, Dan Evans, Omar Carrero, and Lee Allen, and to the people who timely provided data and support from several of my study sites: Christine Blinn, Colleen Carlson, Leandra Blevins, Tim Albaugh, Ruth Lanni, and Jose Alvarez. My words of gratitude go also to all the friends in Blacksburg, VA and Raleigh, NC for their moral support throughout these years, especially in the most difficult moments.

My deepest gratitude goes to my family for their love and support, especially to my parents, whose example gave me the strength and inspiration to pursue this degree, and to my husband, whose support was essential to complete this journey.

Table of Contents

List of Figures

List of Tables

1. INTRODUCTION

Forest management relies on information on forest conditions and the use of descriptors, such as tree height, tree diameter, number of trees per unit area, and amount of leaves, which are fundamental for estimations of forest growth, biomass, wood volume, and productivity. Ground-based forest inventories are traditionally used to collect most of these parameters. Although they are the most simple and direct way to acquire this information, they represent a high cost and time consuming activity that can be prone to errors.

The use of remote sensing technologies to monitor and therefore help to improve the management of forest resources at regional and global scales has exponentially increased over the last 30 years. Aerial photography has been and continues to be utilized primarily for sampling and forest type classification, while satellite data are used to describe, classify, and quantify vegetation by relating reflectance values to ground-based assessments (Huete et al. 1997; Jensen et al. 1997; Lefsky et al. 2002). However, some limitations of using optical imagery are that: (1) reflectance values can be affected by atmospheric characteristics and the background optical properties of the ground, (2) the vegetation indices developed from satellite imagery, used to quantify green vegetation, have shown saturation points at high leaf area index values (3 to 5), (3) it can be used to examine the variation of features on a horizontal distribution basis only, so cannot account for tree architecture, crown length or foliage clumping effects, and their dynamics (Fassnacht et al. 1994; le Maire et al. 2006; Zheng and Moskal 2009).

Newer remote sensing technologies such as laser (lidar, Light Detection and Ranging) and radar interferometry (InSAR) can overcome the problems identified from optical sensors. These technologies generate data related to ground object heights; both are physically oriented, and in the case of lidar the data are acquired as three-dimensional cloud of points, which can be used to evaluate vertical variation of forest attributes. The InSAR (Interferometric Synthetic Aperture Radar) system used in this study, GeoSAR (Geographic Synthetic Aperture Radar), acquires two bands of data at spatial resolutions of 3 m (X-band) and 5 m (P-band), representing a lower density 'cloud' of three dimensional points when compared to lidar data.

The development of models and indices from remotely sensed data to estimate height, stem density, or LAI offers not only a cost-effective and non-destructive estimation, but also an accurate way to retrieve information over the landscape at different spatial and temporal scales. The use of newer remote sensing technologies, such as LiDAR and GeoSAR, for the examination of forest ecophysiological parameters might still be in an early research phase, but its potential to aid forest resource assessments and management has rapidly evolved over the past ten years. These technological developments represent an opportunity to improve regional LAI models and estimation of tree heights derived from optical remote sensing data, where success in many cases has been limited and the estimates are often not precise enough to be widely used by forest managers.

However, developing good models from airborne remote sensing datasets requires considerable investment due to the high cost of acquiring data, their subsequent preprocessing and analysis, and validation on the ground. The relatively small number of industrial forest managers currently using lidar technology might be influenced by both the ratio of high cost to the limited number of products that are being generated (basically height, biomass and volume), and by the relative newness of the remote sensing tool; quoting Stanturf et al. (2003) … "We have seen that over the years some forest companies adopt new technologies at early stages, while others wait until the technology has been proven".... Fortunately, the previous traditional way of management where most of the forest industries or organizations tried to minimize wood production costs, is no longer valid; nowadays, forest organizations are managing their forestlands as assets, focusing on maximizing return on investment. Allocation of capital to the land creates the need to make efficient decisions, which inevitably generates the need for information (Smith et al. 2003). Adding the ability to estimate leaf area and stem density to the suite of the already validated forest applications of LiDAR and GeoSAR will likely increase forest managers use of these tools for monitoring purposes.

1.1 Objectives and general hypotheses

The primary goal of this study is to help improve forest management and silvicultural prescriptions by developing methods to accurately estimate key forest attributes in intensively managed pine plantations and temperate mixed forests using newer, active, remote sensing technologies. The general objectives are as follows:

- Determine whether leaf area index (LAI) can be accurately estimated in pine plantations under a large range of silvicultural regimes and management purposes using multiple-return small-footprint airborne laser scanner (lidar) data.
- Estimate the usefulness and performance of multiple-return small-footprint airborne lidar data to predict stem density, tree height, and mean crown height in pine plantations with different establishment densities and silvicultural management.
- Evaluate the effectiveness of estimating LAI in eastern U.S. mixed temperate forests using a set of metrics derived from two remote sensing technologies: light detection and ranging and interferometric synthetic aperture radar alone and combined.

For the leaf area index estimations, this research is approached on the basis that leaf biomass and crown development is related to site and climate conditions, the number of vegetation strata, the combination of plant species per forest type, the species tree crown architecture, the size and amount of leaves, and the tree responses to applied silvicultural management, among other factors. If the number, size, location of branches, and leaves vary among forest types and silviculture regimes, and there are well-defined understory, midstory, and canopy layers within the forest, then the density and heights of the data points from these remote sensing technologies should be able to describe such structural differences within the forest stands.

In pine plantations, the estimation of number of trees per unit area at mid-rotation or at the end of the rotation is an important parameter for forest management because, although initial stem density is known at the beginning of the rotation, as trees start growing and competing for resources, tree mortality, as well as planned thinning operations, incorporates changes in number of trees per unit area over time. It was hypothesized that lidar distributions and return ratios should be a function of canopy gaps, current number of canopy trees, and understory vegetation. For instance, groups of trees closely located should have more canopy returns and less ground returns (within those trees) than those more separated from each other (i.e., thinned).

2. ESTIMATING LEAF AREA INDEX IN INTENSIVELY MANAGED PINE PLANTATIONS USING AIRBORNE LASER SCANNER DATA

2.1 Abstract

The objective of this study was to determine whether leaf area index (LAI) can be accurately estimated in intensively managed pine plantations using multiple-return airborne laser scanner (lidar) data. In situ measurements of LAI were made using the LiCor LAI-2000 Plant Canopy Analyzer on 109 plots under a variety of stand conditions (i.e., stand age, nutritional regime, and stem density) in North Carolina and Virginia, USA in late summer, 2008. Distributional metrics were calculated for each plot using small footprint lidar data (average pulse density 5 pulses per square meter; up to four returns per pulse) acquired in the month preceding the field measurements. Distributional metrics were calculated for each plot as a whole as well as for ten one meter deep crown density slices (newly introduced in this study), five above and five below the mode of the vegetation returns for each plot. These metrics were used as independent variables in best subsets regressions with LAI (measured in situ) as the dependent variable. The best resulting models had an R^2 ranging from 0.61 (for a 2-variable model) to 0.83 (for a 6-variable model). The laser penetration index (LPI) was an important variable regardless of the number of variables used. Other important variables included the mean intensity value, the mean and 20th percentile of the vegetation returns, and various crown density slice metrics. These results indicate that LAI can be estimated accurately using lidar data in intensively managed pine plantations over a wide variety of stand conditions.

2.2 Introduction

Stemwood production is influenced by climate, nutrients, and water, but is also determined by the amount of light intercepted and the photosynthetic efficiency of canopies (Vose and Allen 1988). Canopy structure throughout the vertical and horizontal profiles can be described by biophysical forest parameters such as leaf area and tree height. Leaf area is a structural parameter of vegetation canopies that plays an important role in several key ecosystem processes by the exchange of energy and gases (e.g., CO_2 and water-vapor fluxes) between terrestrial ecosystems and the atmosphere. It is also central to describing rainfall interception. As a result, leaf area varies along with hydrological, biogeochemical, and biophysical processes, either due to natural stand development or forest management practices (e.g., thinning, fertilization, and vegetation control).

Leaf area index (LAI) is defined as the total one-sided area of leaf tissue per ground surface area (Watson 1947). Along with leaf biomass, leaf area has a strong relationship with productivity (Cannell 1989). In loblolly pine (*Pinus taeda* L.) for example, leaf biomass dynamics are dependent on phenology, climatic conditions, site factors and stand density, thus LAI represents a measure of site occupancy that integrates tree size, stand density and site resource supply (Vose and Allen 1988). Based on these relationships, forest managers have observed crown development and leaf production as responses to fertilization and thinning; such responses are consequently related to carbon accumulation and tree growth (Albaugh et al. 1998; Carlyle 1998; Martin and Jokela 2004). Traditional approaches to directly estimate leaf area index, such as using destructive sampling, although very accurate, are labor intensive, time consuming, and costly. The resulting paucity of samples limits their utility for forest management.

The use of remote sensing technologies to monitor, and therefore to improve the management of forest resources at regional and global scales has increased exponentially over the last 30 years (Lefsky et al. 2002b; Lu 2006; Lutz et al. 2008). Previous research has shown that satellite data can be used to estimate LAI accurately in areas where LAI has been empirically related to satellite-measured reflectance values (Curran et al. 1992; Flores et al. 2006; Gholz et al. 1997; Jensen and Binford 2004). Green vegetation amounts and leaf area index have been associated with spectral reflectance, and frequently with vegetation indices. Nonetheless, researchers have observed that optically-derived vegetation indices reach an asymptote or saturation point when LAI values are on the order of 3 to 5 (Anderson et al. 2004; Birky 2001; Spanner et al. 1990b; Turner et al. 1999).

The estimation of LAI using satellite data can be complicated by variation in atmospheric characteristics, the background optical properties (i.e., understory vegetation, senescent leaves, soil, bark and shadows) (Eriksson et al. 2006; Spanner et al. 1990a), and the challenge of accounting for tree architecture (Soudani et al. 2002). A drawback of optical imagery is that it is only appropriate for examining the variation of features on horizontally distributed basis. Newer remote sensing technologies such as lidar (light detection and ranging), which is physically oriented and generates data points in a three-dimensional cloud, can be suitable to evaluate variation in vertically distributed canopy features. Researchers have employed lidar to estimate forest biophysical parameters, especially in forest inventory applications, such as estimating stand height and volume (Næsset 1997a, b; Nilsson 1996; Popescu et al. 2002); forest biomass (Bortolot and Wynne 2005; Drake et al. 2003; Lefsky et al. 2002a; Nelson et al. 1997; van Aardt et al. 2006); canopy structure (Lovell et al. 2003; Nelson et al. 1984); tree crown diameter (Popescu et al. 2003); stem density (Maltamo et al. 2004; McCombs et al. 2003), species classification (Farid et al. 2006; Ørka et al. 2009) and leaf area index (Jensen et al. 2008; Morsdorf et al. 2006; Zhao and Popescu 2009). The studies in which lidar data were used to estimate LAI did not find a maximum LAI or saturation problems. However, none of the past studies have used multiple return lidar data, nor have they examined the accuracy of lidar-based LAI estimates in stands that have been fertilized at different rates and have different stem densities. The primary objective of this study was to predict LAI accurately across multiple sites of loblolly pine plantations and under a variety of intensive silviculture regimes using laser technology. Traditional approaches, used in previous published work, to extract information from lidar data were followed, as well as the calculation and evaluation of new metrics to better explain variation in LAI.

2.3 Methods

2.3.1 Study sites

Five study sites located in North Carolina and Virginia, USA were used for this research. All five sites were established and maintained in support of research studies investigating the role of intensive management in optimizing loblolly pine (*Pinus taeda* L.) production. These studies were established and/or maintained as a joint effort among the Forest Productivity Cooperative (FPC 2011), academic institutions, the USDA Forest Service, the Virginia Department of Forestry, and private industry.

The *Nutrient by Stand Density Study (NSD)* was installed in 1998 and is located in Buckingham County, Virginia (37°34'59" N, 78°26'49" W) (fig. 2.1), at 184 meters above sea level. The aim of the study was to investigate the effects of two tree planting spacings and fertilization on tree growth development. It has 3 different fertilization regimes: low, medium and high, (designed to achieve a site index (SI) at 25 years of 15, 21 and 24 meters, respectively), and 2 different stem densities (897 and 1794 trees per hectare). Fertilizer applications mainly contained nitrogen and phosphorus. Plot size is 676 m^2 (26 m x 26 m) with each block containing 6 plots, for a total of 18 plots. Refer to Carlson et al. (2009) for a more detailed explanation of the treatments.

The second study site was a recently established trial, *RW195501 (RW19),* which is part of a regionwide study examining the effects of fertilization and thinning in mid-rotation stands. This trial is located in the Piedmont of Virginia in Appomattox County at 37º26'32" N and 78º39'43" W (fig. 2.1). A total of 32 plots were installed in a 13 year old stand. The plots vary in size from approximately 400 m^2 to 1280 m^2. At the time of the lidar acquisition in summer 2008, only the plots had been established and no additional silvicultural technique had been applied besides the traditional forest operation practices used in the area.

The third study in Virginia, *RW180601* (*RW18*), is also part of a regionwide study designed with the objective of understanding optimal rates and frequencies of nutrient additions for rapid growth in young stands. The trial is located in a Piedmont site of Brunswick County at 36°40'51" N and 77°59'13" W (fig. 2.1). A total of 40 plots were installed in 1999 in a 6-yr-old planted stand. These plots had complete weed control and 5 nutrient treatments, as follows: 0, 67, 134, 201, and 269 kg/ha nitrogen (N) applied with phosphorus (0.1 x N), potassium (0.40 x N) and boron (0.005 x N). Nutrient application frequencies were at 1, 2, 4 and 6 year intervals. 30 plots were thinned in 2008. Plots vary in size from approximately 400 m^2 to 470 m^2.

One of the two sites located in North Carolina, is *The Southeast Tree Research and Education Site (SETRES),* geographically positioned in the sand hills at 34º54'17" N and 79º29' W (Scotland County) (fig. 2.1). This trial was established in 1992 in an 8-yr-old plantation. The aim of the study was to quantify the effects of nutrient and water availability on above and below ground productivity and growth efficiency in loblolly pine. Treatments consisted of nutrient additions (nitrogen, phosphorous, potassium, calcium and magnesium), and irrigation. See Albaugh et al. (1998) for complete site and treatment descriptions. Plot size is 900 m^2 (30 m x 30 m), 4 blocks and 4 plots per block, for a total of 16 plots.

The final site in North Carolina, and also the oldest stand measured, is the *Henderson Long Term Site Productivity Study (Henderson)* located at 36º26'52" N, 78º28'23" W (Vance County) (fig.2.1). It was established in 1982 with the objective of monitoring the effects of soil management practices on soil structure, organic matter and nutrient contents, and pine growth. Treatments consisted of two levels of biomass harvest, stem wood only or whole tree removals; two site preparation methods, chop and burn, or shear, pile and disk; and vegetation control for the first 5 years or no vegetation control. Plot measurement size is 450 m^2 (15 m x 30 m), and there are 3 blocks, with 8 plots per block, totaling 24 plots in the study. For a detailed description of the treatments and study see Vitousek and Matson (1985).

*2.3.2 **Field data collection and analysis***

2.3.2.1 Inventory data

All studies were measured during the 2008 dormant season. Total tree height (HT) and height to live crown (HLC) were assessed for every tree within the measurement plots using a Haglöf Vertex hypsometer.

2.3.2.2 *Leaf area measured with an optical sensor*

Leaf area index data were assessed using the LiCor LAI-2000 Plant Canopy Analyzer on each plot during late summer (September 7 to September 19, 2008) except for the RW19 trial, which was measured in January 2009. Above canopy readings were recorded remotely every 15 seconds by placing an instrument in an open field adjacent to the stand during the same date and time that measurements were taken inside the stand. The measurements inside the stand were made holding the instrument at a height of 1 m facing upwards. This same procedure was repeated in every single plot regardless of the presence of understory or mid-story vegetation, such as that found in some plots part of the Henderson study. Due to the instrument's design, measurements were taken under diffuse sky conditions to ensure that the sensor measured only indirect light. Thus, measurements were taken during the dawn and predusk periods, with the above and below instruments facing north, using a 90º view cap. Sampling points were distributed systematically in the plots along a transect perpendicular to the tree-rows. Two transects were used, one close to the plot edge and the other in the middle of the plot. Between fourteen and twenty five readings were recorded, based on the plot dimensions. The calculation of LAI was accomplished using the FV-2000 software which averaged all the readings per plot. The canopy model used to calculate LAI was Horizontal (Li-COR 2010); the ring number 5 was masked to reduce the error introduced by the stem and branches of pine trees; the option of skipping records with transmittance > 1 was used in order to avoid bad readings that can alter the mean values of LAI per plot. The above and below canopy records were matched by time (Welles and Norman 1991).

Since RW19 leaf area was measured in early winter (January 2009), a regression model was developed to generate an approximation of the summer 2008 LAI values. The model was based on Licor LAI ground measurements made in summer (August) 2005 and winter (February) 2006 from 17 plots (100 m x 100 m) established in 7 and 10-year old loblolly pine stands. See Peduzzi et al. (2010) for a description of the plots. The resulting equation was $LAI_{summer} = 1.2768(LAI_{winter})$ and had an R^2 of 0.8. Previous research has shown that loblolly pine LAI differences between summer and winter estimates, based on litterfall, are higher than the differences of seasonal LAI estimates using the Licor LAI-2000 (Dewey et al. 2006; Hebert and Jack 1998), this is probably due to Licor underestimations of LAI (Sampson and Allen 1995); hence, predicted LAI values from the developed equation were low compared to litter trap estimates (Dalla-Tea and Jokela 1991; Greshman 1982) but in agreement with Licor measurements (Sampson et al. 2003). In addition, an unrealistic estimated LAI value (0.12) collected in one of the heavily thinned plots of the RW18 study was deleted from the dataset.

2.3.2.3 Lidar data

Small footprint lidar data were acquired for all the study areas in late August 2008. The system was an Optech ATLM 3100 with an integrated Applanix DSS 4K x 4K DSS camera. The data have multiple returns with a sampling density of 5 pulses per square meter, with at least 4 returns per pulse. The scan angle was less than 15 degrees. Instrument vertical accuracy over bare ground is 15 cm, and horizontal accuracy is 0.5 m.

Ground returns were already extracted by the lidar provider, and the data were reviewed to determine whether the ground return classification had any flaws. Based on the size of the lidar dataset, these study sites represent a relatively small area, which is an advantage in terms of the computation time necessary to run interpolation models. Therefore, the kriging method was applied to the provided ground returns to generate a digital elevation model (DEM) for the area

(Popescu et al. 2002). Next, lidar data points per plot were separated in three classes: "ground returns" (hag = 0 m), "all returns" (hag > 0.2 m), and "vegetation returns" (hag > 1 m). Vegetation returns were classified using a 1 m threshold because the instrument used to estimate LAI in situ was held at approximately 1 m above the ground. The metrics derived from the ground returns class (Gr) were: frequency (count) of returns and frequency (count) of pulses (table 2.1). The metrics derived from the all returns class (All) were: frequency (count), mean height, standard deviation, coefficient of variation, minimum, maximum, percentiles (10, 20, 25, 40, 50, 75, and 90), and frequency (count) of pulses (Holmgren 2004; Magnussen and Boudewyn 1998; Popescu et al. 2002). The metrics derived from the vegetation returns class (Veg) were the same described for the all returns class with the addition of the mode. The distribution of intensity values (I) were described using the mean, minimum, maximum, standard deviation, and coefficient of variation. First, second, third and fourth returns were classified as such and divided by the total number of "vegetation returns" (R). The Laser Penetration Index (LPI) (Barilotti et al. 2005) was calculated per plot as the proportion of ground pulses to the total pulses (ground pulses + all pulses). Density metrics (d) were calculated following Naesset (2002), as the proportion of returns found on each of 10 sections equally divided within the range of heights of vegetation returns for each plot. Additionally, another set of metrics, crown density slices (Cd), was calculated using the mode value of vegetation returns. Ten 1-meter sections of vegetation returns (5 above and 5 below the mode value, based on the maximum value of crown length observed) were classified and proportion of returns to the total number of returns, mean, standard deviation, and coefficient of variation were calculated (fig. 2.2). Frequency of returns (count), calculated from each of the lidar data point classes, were used only to estimate other metrics, such as proportions of returns, but they were not used in the development of the models (table 2.1).

The height values obtained from the lidar data collected in RW18 were too high in one portion of the study area, with values several meters higher than the forest stand heights. A threshold, maximum return hag ≥ 1 m higher than field-measured tree height per plot was used to eliminate erroneous lidar measurements. After this threshold was applied only 19 plots remained in this study area.

2.3.2.4 Statistical analysis

A dataset of 109 plots was assembled with all lidar derived metrics and ground truth measurements. Results from the data diagnostic methods applied to the dataset showed normality between the Studentized residuals and the predicted values, and normal order statistics. There was no need to transform the dependent variable, and because the existing outliers were also influential points, they were not deleted from the dataset. Pearson correlation coefficients were used to evaluate relationships among lidar metrics, ground data, and LAI. Multiple regressions were used to fit the dataset. Best subset regression models were examined using the RSQUARE method for best subsets model identification (SAS 2010). This method generates a set of best models for each number of variables (1, 2, …, 6, etc.). The criterion to choose the models was a combination of several conditions as follows:

- High coefficient of determination (R^2) value.
- Low residual mean square (RMSE).

- Similarity between the adjusted coefficient of determination R^2_{adj}, and R^2 values. The R^2_{adj}, is a rescaling of R^2 by degrees of freedom, hence involves the ratio of mean squares instead of sum of squares.
- Mallows' C_p statistic values (Hocking, 1976). When the model is correct, the C_p is close to the number of variables in the model.
- Low values from two information criteria, the Akaike (1969) Information Criterion (AIC) and Schwarz (1978) Bayesian Criterion (SBC). The AIC is known for its tendency to select larger subset sizes than the true model; hence the SBC was used for comparison, since it penalizes models with larger number of explanatory variables more heavily than AIC.

The best models chosen per subset size (based on number of variables in the models) were evaluated for collinearity issues. Computational stability diagnostics were then used to check for near-linear dependencies between the explanatory variables. In order to make independent variables orthogonal to the intercept and therefore remove any collinearity that involves the intercept, independent variables were centered by subtracting their mean values (Belsley 1984; Marquart 1980). The variance Inflation Factor (VIF) quantifies how much the variance of an estimated regression coefficient is inflated, and a threshold of 10 is commonly used, which in the case of higher values, suggests weak ($10 < VIF < 30$) to high ($VIF > 30$) collinearity problems. However, since VIF neither detects multiple near-singularities nor identifies the source of singularities (Rawlings et al. 2001), condition index (CI) was evaluated for all variables within the models. This index is the square root of the ratio of the largest eigenvalue to the corresponding eigenvalue from the matrix. Similar to VIF, the CI indicates weak dependencies when $10 > CI > 30$ to high dependencies when $CI > 30$.

Additional data to test the models were not available, thus cross-validation analysis was performed using the predicted residual sum of the squares (PRESS) statistics (Allen 1971), which is the sum of squares of the difference between each observation and its prediction when that observation was not used in the prediction equation. The root mean square error from the cross validation analysis (CV-RMSE) was then calculated as the square root of the ratio between the PRESS statistic and the number of observations. The CV-RMSE is an indicator of the predictive power of the model, thus a small CV-RMSE is desirable. The significance level used for all the statistical tests was $\alpha = 0.05$ (p-value < 0.05). This p-value was used to evaluate if the variables included in the model were statistically significant as well. The squared semipartial correlation coefficients (SSCC) were calculated using partial sum of squares to determine the contribution from each variable to the models, while controlling the effects of other independent variables within the model. These coefficients represent the proportion of the variance from the dependent variable associated uniquely with the independent variable.

2.4 Results

*2.4.1 **Summary statistics from ground measurements and lidar metrics***

Stand age ranged from 11 to 26-yr-old. Forest canopy was closed in all plots, except for the plots in NSD that had the spacing twice as large as that traditionally used in forest operations, and the plots from RW18 that were thinned. Table 2.2 summarizes the average growth metrics of plots, within the study sites, as treatment and control, and in the case of NSD, these were distinguished by the number of trees per hectare. In RW19 all plots were classified as fertilized, since the stand had been under traditional forest management. Studies in which there were different levels of fertilization were classified together as fertilized, regardless of the rate and frequency of nutrient additions. In RW18, thinning was recently applied to some of the control and fertilized plots, thus the plots at this site were also classified by the number of trees per hectare. Individual tree height ranged from 4.8 m to 27.9 m and averaged 15.7 m among all the study areas, the highest standard deviation (> 2 m) from the mean of tree height was observed in the SETRES and Henderson studies. Crown length ranged between 0.8 m (a damaged tree) and 10.8 m, and averaged 6.9 m. Leaf area index measured on the ground ranged from 0.45 to 4.91. The lowest values of LAI were observed in the plots from the RW18 study, and they corresponded to the thinned plots which had an average of 16 trees distributed in a 400 – 470 m^2 plot area. Leaf area index assessment in these plots was expected to be low, not only due to the reduced number of trees, but also due to the difficulty of using an indirect method to measure it. The highest LAI values were observed in the control plots in Henderson. Regardless of the other treatments applied to these plots (harvesting and site preparation), the control plots had consistently higher LAI than the vegetation control plots. In most plots, the presence of competing vegetation (mostly hardwood trees) increased the LAI as much as twice the LAI value from the plots with vegetation control.

Lidar ground returns were lowest (131) at the control plots in Henderson (table 2.3). This set of plots can be compared to the vegetation control plots (297) from the same study and to the fertilized plots (223) from RW18, which had comparable tree densities. However, when the number of vegetation returns are taken into account, the proportion of ground pulses relative to the total number of pulses (LPI = 0.08) shows that the canopy in the control plots from Henderson generated more returns (1601) and hence did not penetrate to the ground as much as the other two set of plots. The opposite was observed in the thinned plots from RW18, which had the highest LPI (0.42 and 0.50), and the lowest number of trees per plot, ground penetration was high (461 and 427), and canopy interception low (478 and 670).

Heights of vegetation returns were consistently lower than the tree heights measured on the ground, except for a few returns that were a few centimeters higher than the maximum tree height of the plot. These minor anomalies could be attributable to measurement and estimation errors. Fertilized plots showed higher intensity mean values than control plots; however, as expected, Henderson control plots had higher intensity means than the treated plots, since classification of these plots is not based on nutrient additions but on competing vegetation control.

The vertical profiles (fig. 2.3) show graphically the range of heights for the vegetation returns according to their frequency. The mode for each of the sites is highlighted on the profiles; this metric had a Pearson correlation coefficient of 0.92 with the mean mid-crown height of the individual plots (n = 109). The frequency of returns at the Henderson site, and at the RW18 and RW19 sites (fig. 2.3) show that there are a number of returns that come from below the canopy, whereas SETRES and NSD frequencies are closer to zero. The latter two sites have been maintained with no understory vegetation. RW18 unthinned plots are also free of understory vegetation, but they represent only 4 of the 19 plots used from this study. The site that showed less frequency of returns was RW18 (fig. 2.3); this observation could be due to the fact that most of the 15 plots at this site had been intensively thinned (313 to 470 TPH) and they are also the smallest plots among all the study sites. SETRES and Henderson have a higher number of trees per hectare than RW19; however the frequency of returns in fig. 2.3 was higher in RW19 than in the other two sites. This result could be explained by the number and area of the plots: 32 plots

($400\ m^2$ to $1280\ m^2$) in RW19, compared to 24 plots ($450\ m^2$) in Henderson, and only 16 plots ($900\ m^2$) in SETRES.

2.4.2 ***Variable selection and modeling***

Among all the lidar metrics, LPI has the highest correlation with LAI (-0.757) (table 2.4). A graphic representation of the LAI and the LPI contrast is shown in fig. 2.4, where the high values of LAI are in concordance with the low values of LPI. The crown density slices (1 m section) were calculated with the objective of examining the relationship of the shape of the frequency profiles to LAI. The metrics that contributed to the best models were the proportion of returns at 1 m above the mode (Cd+1) and its standard deviation, the coefficient of variation at 4 m above the mode ($Cd{+}4_{cv}$), and the proportion of returns at 4 m below the mode (Cd-4). Correlations of these metrics are shown in table 2.4. Although the standard deviation at 1 m above the mode ($Cd{+}1_{stdv}$) was the only one to have a statistically significant correlation with LAI, the other three metrics (Cd+1, $Cd{+}4_{cv}$, and Cd-4) had a highly significant contribution to the LAI predictive models when used in combination with other variables. The other variables, which were significantly correlated with LAI included Veg_{stdv}, and I_{mean} (table 2.4). Also, variables such as the Veg-percentiles, crown density slices, and the rest of the densities, had significant correlations with LAI, but since their correlations were similar to the ones from the variables shown in table 2.4, and they were not part of the best models observed, their Pearson coefficients have not been reported. Variables derived from all returns > 0.2 m were also significantly correlated with LAI, but not as highly correlated as the variables derived from vegetation returns > 1 m. Due to collinearity problems among these metrics, only one set of variables was used at a time in the best subset analysis, and ultimately variables with higher correlations and models with better R^2 were chosen.

All variables from ground measurements showed significant correlations with LAI, that is mean tree height (0.270), mean crown length (-0.343), and number of trees (0.427). However, the best models generated from the best subsets analysis, did not have an increase in R^2 compared to the models using lidar metrics only. Therefore, these models were not reported.

Combinations of the metrics reported in table 2.4 for models including 2, 3, 4, 5 and 6 variables are summarized in table 2.5. R^2_{adj}, values ranged between 0.60 and 0.82 for 2 and 6 variable models respectively. Despite the collinearity issues that lidar derived metrics can produce in predictive models, all parameters had variance inflation factors (VIF) lower than 6. All variables had a CI lower than 5 (table 2.5). The increment in R^2 and R^2_{adj}, gained from adding a variable to the model is more noticeable where 2 to 3 and 3 to 4 variables were included. The root mean square error (CV-RMSE) and PRESS statistics (from the cross validation analysis) became lower as the number of variables included in the models increased. LPI, which was highly correlated with LAI, was found in all the models, as well as I_{mean} except for the 2-variable model; and as these two variables were added to the models, the Veg_{mean} and Veg_{20th} became common variables also. The variable contributions among the models, in descending order of importance, were LPI, Veg_{mean}, Veg_{20th}, and I_{mean}; except for the 6-variable model were I_{mean} had higher contribution than Veg_{20th}. Crown density metrics were the lesser contributors compared to the rest of the variables, nonetheless these were responsible for increasing the R^2 values from the models. Among all the models reported, the 4-variable model represents the best way to estimate LAI, in terms of maximizing R^2 while minimizing the number of variables. However, predicted LAI values using this model were plotted against the observed LAI from all the plots (fig. 2.5) and it was noticeable that one of the plots from RW18 control thinned stands with very low LAI (0.6) was predicted as no LAI (0) whatsoever. Therefore, for comparison purposes, LAI estimations using the 6-variable model were plotted versus the observed LAI values (fig. 2.6), in which the same plot was estimated with and LAI of 0.4. Although, the R^2 and R^2_{adj}, values are similar between these two models, the 6-variable model predicted low LAI values better (more realistically) than the 4-variable model. Data distribution within the graphs tended to cluster at the center, since this was the range of the observed LAI from most of the sampled plots.

In addition, a modified dataset was used to evaluate the influence that plot size had on the models. As described previously, the area of the plots differed from one site to another. For this modified dataset, all plots were buffered and reduced to the smallest area plots (between 400 and 450 m^2), and lidar metrics for this new set of plots were then calculated. Despite the expectation that the results using similar plot sizes could improve, the models derived using same plot size consistently showed lower R^2 values than those generated using different plot size. Nonetheless, the combination of variables within the models was very similar. This result was supported by the absence of correlation between LAI and plot area (r = -0.010).

2.5 Discussion

Good correlations of certain lidar metrics with LAI were expected. Laser penetration index is physically related to the level of canopy development; the closer and denser the vegetation, the less the laser pulses penetrate to reach the ground. This index has been used in previous research to predict LAI, and reported models were able to explain 80% or more of the variation of leaf area in natural forest ecosystems (Barilotti et al. 2005; Kwak et al. 2007).

Vegetation return percentiles, and canopy densities have also correlated well with other stand attributes, including tree height, diameter, and volume (Holmgren 2004; Magnussen and Boudewyn 1998; Naesset 2002; Popescu et al. 2002). Recurrent variables in the models, besides LPI, were:

1) The average intensity of the returns (I_{mean}), which as a measure of the return signal strength, depends, among other things, on the reflectance and reflectivity of the target. This metric is therefore closely related to the amount of vegetation (leaves and branches) when a forest is such target. Previous research has used metrics calculated from intensity values to estimate forest biomass (van Aardt et al. 2006); however, since the intensity values from lidar sensors are frequently not calibrated, researchers have advised to using them with caution (Bater et al. 2011). Fortunately, the dataset used in this research encompasses large variability in many aspects. Lidar data acquisition dates were not the same for most sites, the terrain relief ranged from flat to hilly, and the forest stands varied in age, stem density and fertilization rates. Therefore, the intensity metrics used for developing the models inherently possessed a large amount of variation.
2) The average height from the vegetation returns (hag > 1 m) and the Veg_{20th} percentile. These two metrics are lidar return height values, hence they are descriptors of the canopy density and height of the forest stands. The mean values from the lidar returns are related to the distribution of return heights across the stand vertical profiles, and such heights will therefore relate to the target heights (on the ground). The more targets (i.e. branches, leaves, etc.) the laser would encounter within a range of heights, the more returns will be obtained from that section of the stand. Thus, the mean value from all the vegetation returns will be influenced by the heights from where most of the returns were acquired.

Similarly, the percentile values, in this case the 20^{th}, meaning that 80% of the return heights are above that height; can refer to the density of such targets on the ground.

3) The standard deviation of the returns found between 1 and 2 meters above the mode of the height values of vegetation returns ($Cd+1_{stdv}$). This variable had a negative correlation with LAI, meaning that the higher the LAI, the less the dispersion observed from the mean of the height values. This section is located above the mode, within the top part of the tree crowns, which in closed canopy stands such as these is likely to be where most of the foliage would be located.

Despite the fact that ground-based variables (number of trees, mean tree height, and crown length) showed significant correlations with LAI, these were not strong enough to increase the performance of lidar metrics when added to the models.

Previously developed leaf area predictive models (that used discrete lidar data, first and last returns) were reported to explain between 40% and 89% of the variance. Interestingly enough, the tendency observed is that relationships (between LAI and lidar metrics) favor the sampling of mixed species forests more than pure coniferous stands. For example, Riaño et al. (2004) measured forests in Spain and reported $R^2 > 0.8$ for deciduous species and $R^2 < 0.4$ for pines. Other researchers modeling pure pine stands reported an R^2 of 0.69 in Sweden (Morsdorf et al. 2006), and an R^2 of 0.70 in the U.S. (Jensen et al. 2008); but the results from mixed species stands have R^2 values of 0.89 (Barilotti et al. 2005), 0.80 (adjusted R^2) (Sasaki et al. 2008), and 0.84 (Zhao and Popescu 2009). Using loblolly pine plantations only, Roberts et al. (2005) developed a model that explained 69% of the variation.

Based on these previous results, and considering that the stands sampled in the current study were not only pure coniferous stands, but also of uniform age within each site, and growing under intensive management (with different fertilization rates, little or no understory vegetation, and different tree spacing), the models obtained performed close to the best models reported in the literature, since they explained up to 83% of the variation. The use of multiple return data might have made the characterization of such variation across the study sites feasible, since many of the variables included in the model were based on the number of returns, instead of using the number of pulses.

A group of models explaining between 61% and 83% of the LAI variation was reported. The reason for this range is the number of variables in each model. Although the most parsimonious model is generally considered best, this applies to cases when the stability of the model can be compromised or when the estimation of an additional variable impact on the research or operation costs, which is usually the case in biological sciences (Rawlings, 2001). Adding a lidar metric to the model will not increase the cost in a significant matter, since the highest cost is the acquisition of the lidar data itself. It will only add computational time, therefore a 6-variable model (with stable regression estimates) for predicting LAI can only increase the accuracy of the predictions. The decision of which model should be used will depend on a forest manager's needs. If a good approximation of the estimates and relative variation of LAI values is sufficient, the 2-variable model will be appropriate, but if higher accuracy is wanted, a 6-variable model will be the best choice.

LAI is a useful index for intensive plantation management because it provides an estimate of the amount of light captured by the stand and is thus a proxy variable that defines the stand's current growing conditions. For instance, LAI allows foresters to identify stands that are in need of fertilization (e.g., when LAI is low) or thinning (e.g., when LAI is high), in order to improve tree growth and maximize returns. The 6-variable model, with an RMSE for prediction

(CV-RMSE) of 0.46, provides a precise tool for this type of management, in which decisions are usually made based on LAI thresholds. In this case, an error of this magnitude in estimating LAI for forest management purposes is not as important as the consistency of the estimated values across stands under different conditions (the ability to use the same model across different stand ages, fertilization regimes, vegetation controls, etc.). For forest managers, the advantage of having a model that estimates LAI using remotely sensed data resides in the accuracy and robustness of such models. Although satellite-derived LAI estimates rely on models with R^2 values similar to those of the lidar model developed in this research (Flores et al. 2006), such estimates have not been consistent, mainly due to issues associated with sensor saturation, atmospheric conditions, and the inability to account for the vertical structure of the stand (Peduzzi et al. 2010). Lidar data are not without acquisition issues; in the past, there have been concerns about the consistency of metrics derived from lidar returns given variations in lidar sensor configurations, flight characteristics, atmospheric conditions, topography, and target objects (Bater et al. 2011). In view of creating a robust model, this research has taken into account much of the variation associated with these issues. For all sites, the sensor configuration was similar; however, the acquisition date and time did not coincide for most of them, topography differed, and, given the different stand ages, stem densities and fertilization regimes included in the dataset, target objects also varied.

Laser technology has been successfully used in the past to estimate forest height, volume and biomass to the stand and plot levels. Lately, attempts to estimate leaf area index have broadened the potential of this tool. The results from this research complement these efforts. A robust model with a unique set of variables was developed that explained 83% of the variation of LAI in loblolly pine plantations. The model was constructed from and tested through cross validation on multiple research studies across a wide range of site conditions and silvicultural regimes, giving foresters managing for different purposes (i.e. sawtimber, pulp, etc.) the opportunity to use it as a robust application in decision making.

2.6 Literature cited

Akaike, H. 1969. Fitting autoregressive models for prediction. Ann. Inst. Stat. Math. 21:243-247.

Albaugh, T.J., H.L. Allen, P.M. Dougherty, L.W. Kress, and J.S. King. 1998. Leaf area and above- and belowground growth responses of loblolly pine to nutrient and water additions. For. Sci. 44(2):317-328.

Allen, D. 1971. The prediction sum of squares as a criterion for selection of predictor variables. Univ. of Ky. Dept. of Statistics, Tech. Report 23.

Anderson, M.C., C.M.U. Neale, F. Li, J.M. Norman, W.P. Kustas, H. Jayanthi, and J. Chavez. 2004. Upscaling ground observations of vegetation water content, canopy height, and leaf area index during SMEX02 using aircraft and Landsat imagery. Remote Sens. Environ. 92:447-464.

Barilotti, A., S. Turco, R. Napolitano, and E. Bressan. 2005. La tecnologia LiDAR per lo studio della biomassa negli ecosistemi forestali. in 15th Meeting of the Italian Society of Ecology, Torino, Italy.

Bater, C.W., M.A. Wulder, N.C. Coops, R.F. Nelson, T. Hilker, and E. Naesset. 2011. Stability of sample-based scanning-LiDAR-derived vegetation metrics for forest monitoring. IEEE Trans. Geosci. Remote Sens. 49(6):2385-2392.

Belsley, D.A. 1984. Demeaning conditioning diagnostics through centering (with discussion). Amer. Statistician 38:73-77.

Birky, A.K. 2001. NDVI and a simple model of deciduous forest seasonal dynamics. Ecol. Model. 143:43-58.

Bortolot, Z.J., and R.H. Wynne. 2005. Estimating forest biomass using small footprint LiDAR data: an individual tree-based approach that incorporates training data. ISPRS-J. Photogramm. Remote Sens. 59(6):342-360.

Cannell, M.G.R. 1989. Physiological basis of wood production: a review. Scand. J. Forest Res. 4:459-475.

Carlson, C.A., T.R. Fox, J. Creighton, P.M. Dougherty, and J.R. Johnson. 2009. Nine-year growth responses to planting density manipulation and repeated early fertilization in a loblolly pine stand in the Virginia Piedmont. South. J. Appl. For. 33(3):109-114.

Carlyle, J.C. 1998. Relationships between nitrogen uptake, leaf area, water status and growth in an 11-year-old *Pinus radiata* plantation in response to thinning, thinning residue, and nitrogen fertiliser. Forest Ecol. Manag. 108(1-2):41-55.

Curran, P.J., J.L. Dungan, and H.L. Gholz. 1992. Seasonal LAI in slash pine estimated with Landsat TM. Remote Sens. Environ. 39:3-13.

Dalla-Tea, F., and E.J. Jokela. 1991. Needlefall, canopy light interception, and productivity of young intensively managed slash and loblolly pine stands. For Sci 37(5):1298-1313.

Dewey, J.C., S.D. Roberts, and I. Hartley. 2006. A comparison of tools for remotely estimating leaf area index in loblolly pine plantations. P. 71-75 *in* Proceedings of the 13th biennial southern silvicultural research conference. U.S. Department of Agriculture, Forest Service, Southern Research Station, Asheville, NC.

Drake, J.B., R.G. Knox, R.O. Dubayah, D.B. Clark, R. Condit, B.J. Blair, and M.A. Hofton. 2003. Above-ground biomass estimation in closed canopy neotropical forests using lidar remote sensing: factors affecting the generality of relationships. Global Ecol. Biogeogr. 12:147-159.

Eriksson, H.M., L. Eklundh, A. Kuusk, and T. Nilson. 2006. Impact of understory vegetation on forest canopy reflectance and remotely sensed LAI estimates. Remote Sens. Environ. 103:408-418.

Farid, A., D. Rautenkranz, D.C. Goodrich, S.E. Marsh, and S. Sorooshian. 2006. Riparian vegetation classification from airborne laser scanning data with an emphasis on cottonwood trees. Can. J. Rem. Sens. 32(1):15-18.

Flores, F.J., H.L. Allen, H.M. Cheshire, J.G. Davis, M. Fuentes, and D.L. Kelting. 2006. Using multispectral satellite imagery to estimate leaf area and response to silvicultural treatments in loblolly pine stands. Can. J. For. Res. 36:1587-1596.

FPC. 2011. Forest Productivity Cooperative. Shaping the future of plantation forestry (http://www.forestnutrition.org/, August 2009). Raleigh, NC.

Gholz, H.L., P.J. Curran, J.A. Kupiec, and G.M. Smith. 1997. Assessing leaf area and canopy biochemistry of Florida pine plantations using remote sensing. in The Use of Remote Sensing in the Modeling of Forest Productivity., Gholz, H.L., K. Nakane, and H. Shimoda (eds.). Kluwer Academic Publishers, Dordrecht, The Netherlands.

Gresham, C.A. 1982. Litterfall patterns in mature loblolly and longleaf pine stands in coastal South Carolina. For. Sci. 28(2):223-231.

Hebert, M.T., and S.B. Jack. 1998. Leaf area index and site water balance of loblolly pine (Pinus taeda L.) across a precipitation gradient in east Texas. Forest Ecology and Management 105(1-3):273-282.

Hocking, R. 1976. The analysis and selection of variables in linear regression. Biometrics. 32:1-49.

Holmgren, J. 2004. Prediction of tree height, basal area and stem volume in forest stands using airborne laser scanning. Scand. J. Forest Res 19(6):543-553.

Jensen, J.L.R., K.S. Humes, L.A. Vierling, and A.T. Hudak. 2008. Discrete return lidar-based prediction of leaf area index in two conifer forests. Remote Sens. Environ. 112(10):3947-3957.

Jensen, R.R., and M.W. Binford. 2004. Measurement and comparison of leaf area index estimators derived from satellite remote sensing techniques. Internat. J. Rem. Sens. 25(20):4251-4265.

Kwak, D.-A., W.-K. Lee, and H.-K. Cho. 2007. Estimation of LAI using lidar remote sensing in forest. P. 248-252 in ISPRS Workshop on Laser Scanning and SilviLaser, Espoo, Finland.

Lefsky, M.A., W.B. Cohen, D.J. Harding, G.C. Parker, S.A. Acker, and S.T. Gower. 2002a. Lidar remote sensing of above-ground biomass in three biomes. Global Ecol. Biogeogr. 11:393-399.

Lefsky, M.A., W.B. Cohen, G.G. Parker, and D.J. Harding. 2002b. Lidar remote sensing for ecosystem studies. BioScience 52(1):19-30.

LI-COR. 2010. FV2000 the LAI-2000 data file viewer. P. 73. LI-COR Biosciences, Lincoln, NE USA.

Lovell, J.L., D.L.B. Jupp, D.S. Culvenor, and N.C. Coops. 2003. Using airborne and ground-based ranging lidar to measure canopy structure in Australian forests. P. 607-622 *in* Workshop on 3-D Analysis of Forest Structure and Terrain Using LiDAR Technology. Canadian Aeronautics Space Inst, Victoria, Canada.

Lu, D. 2006. The potential and challenge of remote sensing-based biomass estimation. Internat. J. Rem. Sens. 27(7):1297-1328.

Lutz, D.A., R.A. Washington-Allen, and H.H. Shugart. 2008. Remote sensing of boreal forest biophysical and inventory parameters: a review. Can. J. Forest Res. 34(2):S286-S313.

Magnussen, S., and P. Boudewyn. 1998. Derivations of stand heights from airborne laser scanner data with canopy-based quantile estimators. Can. J. Forest Res. 28(7):1016-1031.

Maltamo, M., K. Eerikäinen, J. Pitkänen, J. Hyyppä, and M. Vehmas. 2004. Estimation of timber volume and stem density based on scanning laser altimetry and expected tree size distribution functions. Remote Sens. Environ. 90(3):319-330.

Marquart, D.W. 1980. Comment: you should standarize the predictor variables in your regression models. J. Amer. Stat. Assoc. 75:87-91.

Martin, T.A., and E.J. Jokela. 2004. Developmental patterns and nutrition impact radiation use efficiency components in southern pine stands. Ecol. Appl. 14(6):1839-1854.

McCombs, J.W., S.D. Roberts, and D.L. Evans. 2003. Influence of fusing lidar and multispectral imagery on remotely sensed estimates of stand density and mean tree height in a managed loblolly pine plantation. For. Sci. 49(3):457-466.

Morsdorf, F., B. Kötz, E. Meier, K.I. Itten, and B. Allgöwer. 2006. Estimation of LAI and fractional cover from small footprint airborne laser scanning data based on gap fraction. Remote Sens. Environ. 104(1):50-61.

Næsset, E. 1997a. Determination of mean tree height of forest stands using airborne laser scanner data. ISPRS-J. Photogramm. Remote Sens. 52(2):49-56.

Næsset, E. 1997b. Estimating timber volume of forest stands using airborne laser scanner data. Remote Sens. Environ. 61(2):246-253.

Naesset, E. 2002. Predicting forest stand characteristics with airborne scanning laser using a practical two-stage procedure and field data. Remote Sens. Environ. 80:88-99.

Nelson, R., W. Krabill, and G. MacLean. 1984. Determining forest canopy characteristics using airborne laser data. Remote Sens. Environ. 15(3):201-212.

Nelson, R., R. Oderwald, and T.G. Gregoire. 1997. Separating the ground and airborne laser sampling phases to estimate tropical forest basal area, volume, and biomass. Remote Sens. Environ. 60(3):311-326.

Nilsson, M. 1996. Estimation of tree heights and stand volume using an airborne lidar system. Remote Sens. Environ. 56(1):1-7.

Ørka, H.O., E. Næsset, and O.M. Bollandsås. 2009. Classifying species of individual trees by intensity and structure features derived from airborne laser scanner data. Remote Sens. Environ. 113(6):1163-1174.

Peduzzi, A., H.L. Allen, and R.H. Wynne. 2010. Leaf area of overstory and understory in pine plantations in the flatwoods. South. J. Appl. For. 34(4):154-160.

Popescu, S.C., R.H. Wynne, and R. Nelson. 2002. Estimating plot-level tree heights with lidar: local filtering with a canopy-height based variable window size. Comput. Electron. Agr. 37:71-95.

Popescu, S.C., R.H. Wynne, and R.F. Nelson. 2003. Measuring individual tree crown diameter with lidar and assessing its influence on estimating forest volume and biomass. Can. J. Rem. Sens. 29(5):564-577.

Rawlings, J.O., S.G. Pantula, and D.A. Dickey. 2001. Applied Regression Analysis: A Research Tool. Springer.

Riaño, D., F. Valladares, S. Condes, and E. Chuvieco. 2004. Estimation of leaf area index and covered ground from airborne laser scanner (lidar) in two contrasting forests. Agr. Forest Meteorol. 124(3-4):269-275.

Roberts, S.D., T.J. Dean, D.L. Evans, J.W. McCombs, R.L. Harrington, and P.A. Glass. 2005. Estimating individual tree leaf area in loblolly pine plantations using LiDAR-derived measurements of height and crown dimensions. Forest Ecol. Manag. 213(1-3):54-70.

Schwarz, G. 1978. Estimating the dimension of a model. Annals of Statistics. 6:461-464.

Sampson, D.A., T.J. Albaugh, K.H. Johnsen, H.L. Allen, and S.J. Zarnoch. 2003. Monthly leaf area index estimates from point-in-time measurements and needle phenology for Pinus taeda. Can. J. For. Res. 33(12):2477-2490.

Sampson, D.A., and H.L. Allen. 1995. Direct and indirect estimates of leaf-area index (lai) for lodgepole and loblolly-pine stands. Trees-Struct. Funct. 9(3):119-122.

SAS. 2010. The SAS System for Windows Release 9.1.3. SAS Institute Inc., Cary, NC USA.

Sasaki, T., J. Imanishi, K. Ioki, Y. Morimoto, and K. Kitada. 2008. Estimation of leaf area index and canopy openness in broad leaved forest using an airborne laser scanner in comparison with high-reslution near-infrared digital photography. Landscape Ecol. Eng. 4:47-55.

Soudani, K., J. Trautmann, and J.M.N. Walter. 2002. Leaf area index and canopy stratification in scots pine (*Pinus sylvestris* L.) stands. Internat. J. Rem. Sens. 23:3605-3618.

Spanner, M.A., L.L. Pierce, D.L. Peterson, and S.W. Running. 1990a. Remote-sensing of temperate coniferous forest leaf-area index - the influence of canopy closure, understory vegetation and background reflectance. Internat. J. Rem. Sens. 11(1):95-111.

Spanner, M.A., L.L. Pierce, S.W. Running, and D.L. Peterson. 1990b. The seasonality of AVHRR data of temperate coniferous forests: relationship with leaf area index. Remote Sens. Environ. 33(2):97-112.

Turner, D.P., W.B. Cohen, R.E. Kennedy, K.S. Fassnacht, and J.M. Briggs. 1999. Relationships between leaf area index and Landsat TM spectral vegetation indices across three temperate zone sites. Remote Sens. Environ. 70(1):52-68.

van Aardt, J., R.H. Wynne, and R.G. Oderwald. 2006. Forest volume and biomass estimation using small-footprint lidar-distributional parameters on a per-segment basis. For. Sci. 52(6):636-649.

Vitousek, P.M., and P.A. Matson. 1985. Disturbance, nitrogen availability, and nitrogen losses in an intensively managed loblolly-pine plantation. Ecology 66(4):1360-1376.

Vose, J.M., and H.L. Allen. 1988. Leaf area, stemwood growth, and nutrition relationships in loblolly pine. For. Sci. 34(3):547-563.

Watson, D.J. 1947. Comparative physiological studies in the growth of field crops. I. Variation in net assimilation rate and leaf area between species and varieties, and within and between years. Ann. Bot-London(11):41-76.

Welles, J.M., and J.M. Norman. 1991. Instrument for indirect measurement of canopy architecture. Agron. J. 83(5):818-825.

Zhao, K., and S. Popescu. 2009. Lidar-based mapping of leaf area index and its use for validating GLOBCARBON satellite LAI product in a temperate forest of the southern USA. Remote Sens. Environ. 113(8):1628-1645.

Figure 2.1 Geographic representation of the study sites in North Carolina and Virginia, USA.

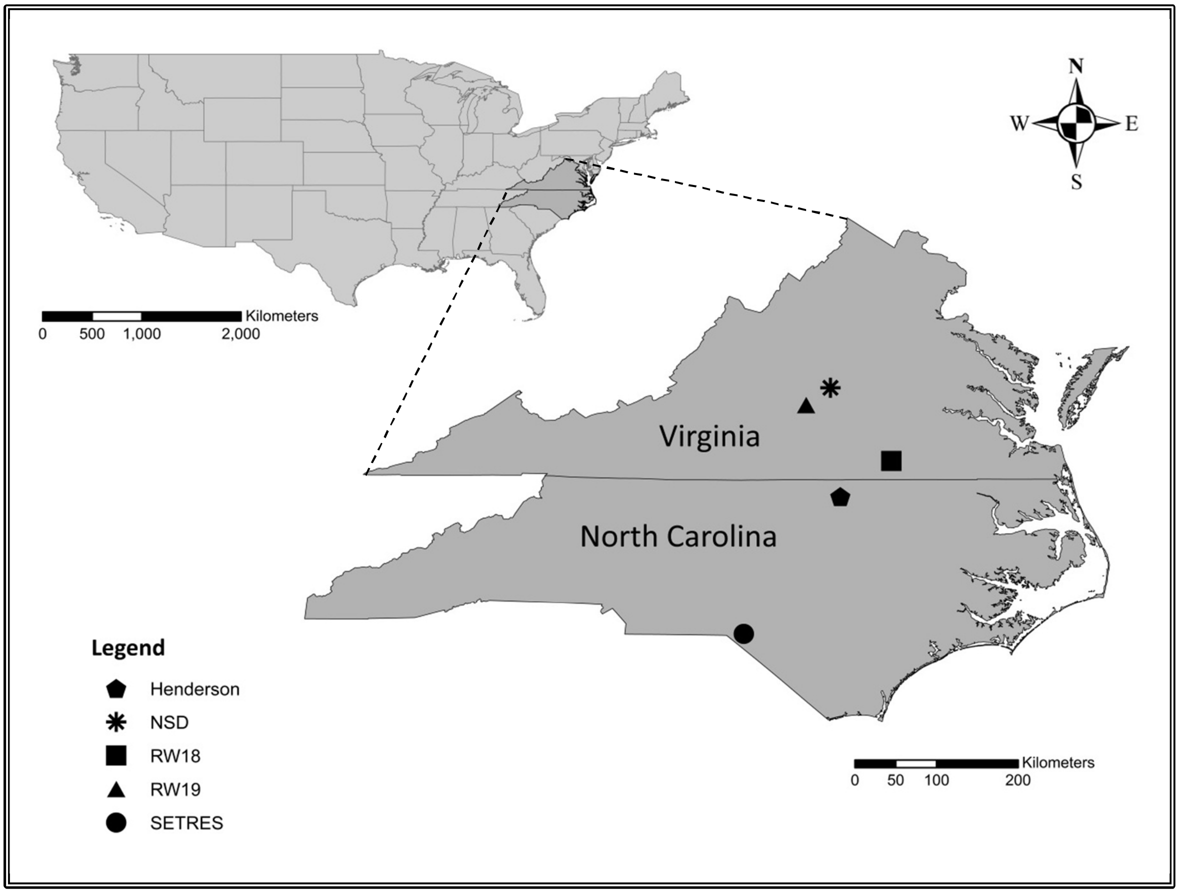

Figure 2.2 Graphic description of crown density slices derived from lidar Veg_{mode} value. Mode value per plot was significantly correlated (0.92) with mid-crown height, which was calculated as follows: Tree total height – (crown length/2). Five 1 m sections above and below the mode were defined, and the descriptive statistics (i.e., frequency, mean, standard deviation, and coefficient of variation) from the returns within each section were obtained. See table 2.1 for variable names and how they were calculated. (a) Crown density values for a vegetation control plot from the Henderson site.

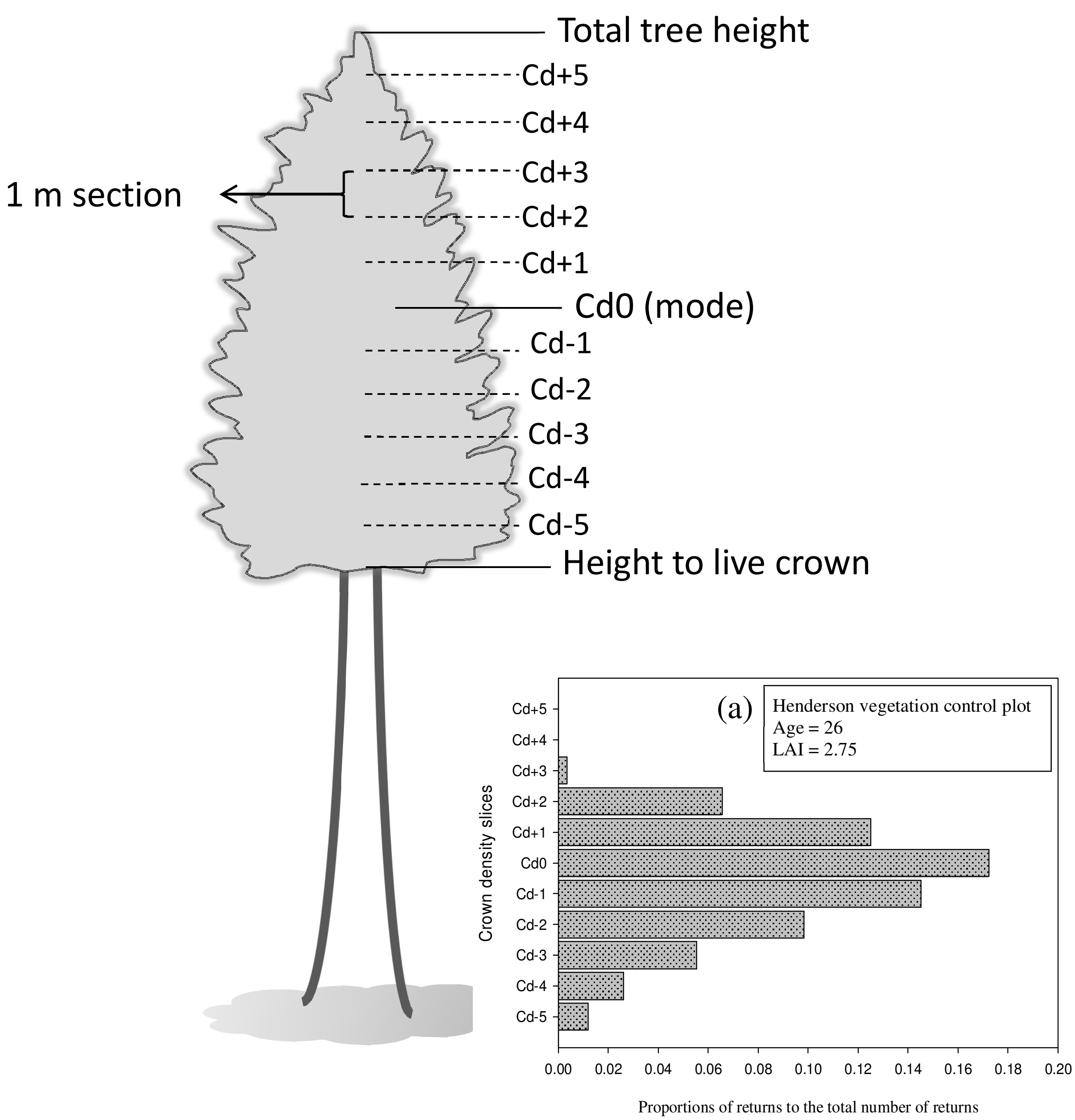

Figure 2.3 Vertical profiles for lidar vegetation returns (hag > 1 m) in each study site. The mode for the vegetation returns is circled on the *y* axis. Study sites are: (a) NSD, (b) RW19, (c) RW18, (d) SETRES, and (e) Henderson.

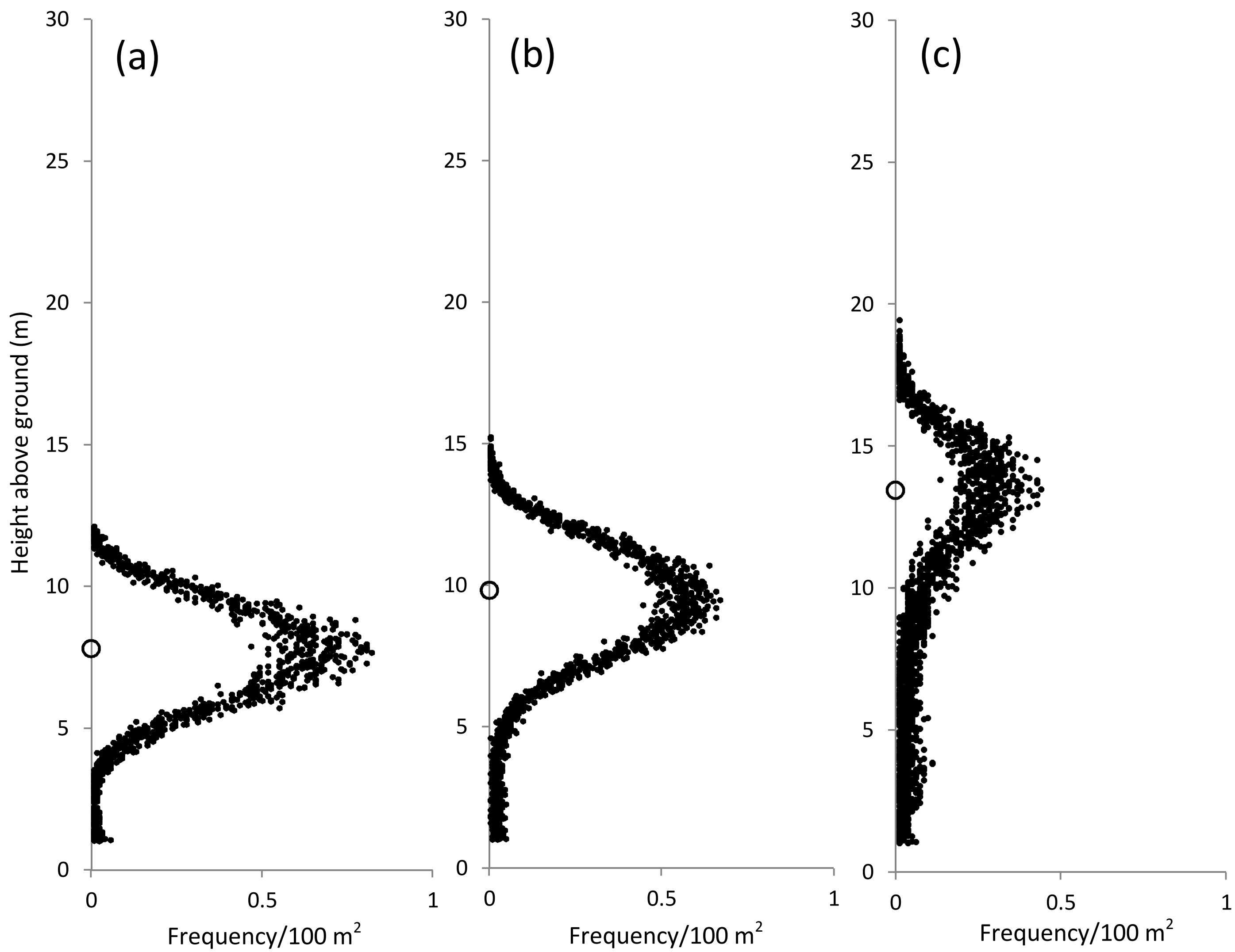

Figure 2.3. Continued.

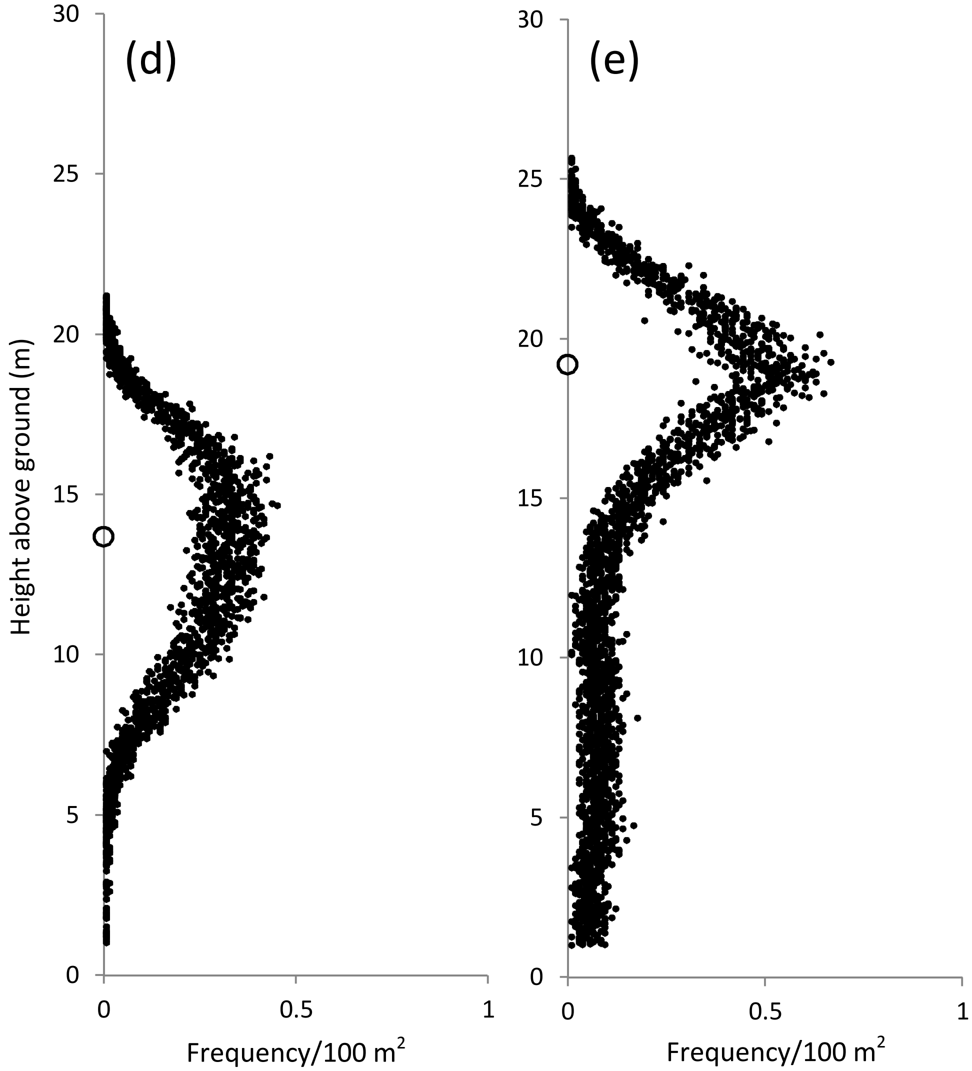

Figure 2.4 Graphic representation of LAI and LPI mean values for a subset of plots at the SETRES study site. LAI and LPI have a negative correlation (-0.76), hence when LAI is high (dark) the LPI should be low (light). Aerial photography was taken at the same time that lidar data were acquired (Summer 2008).

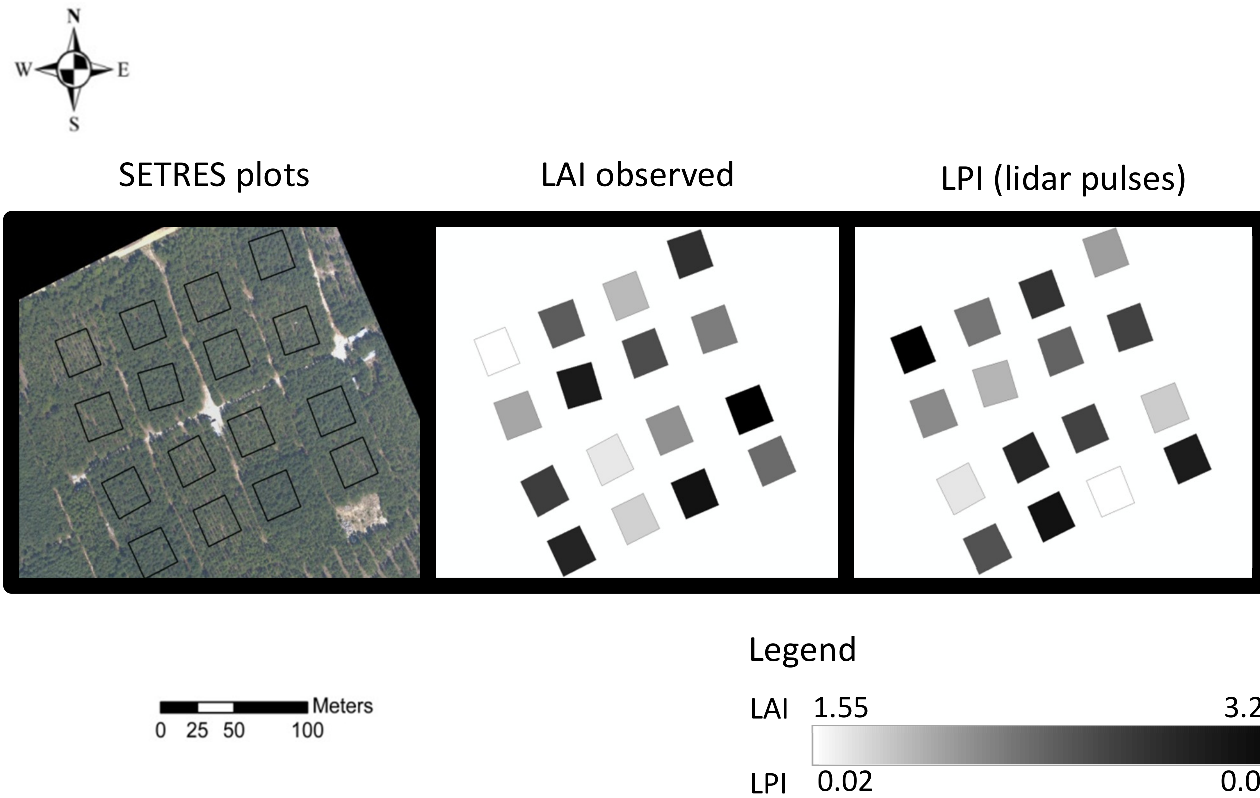

Figure 2.5 Relationship between estimated LAI and measured LAI using the 4-variable model with lidar metrics only (n = 109). Plots were classified first by stem density, and then by control and treatment.

Model (refer to table 2.1 for variable names):

$$LAI = 2.767 + 0.330\,(Veg_{mean}) - 0.268\,(Veg_{20th}) - 5.522\,(LPI) + 0.106\,(I_{mean})$$

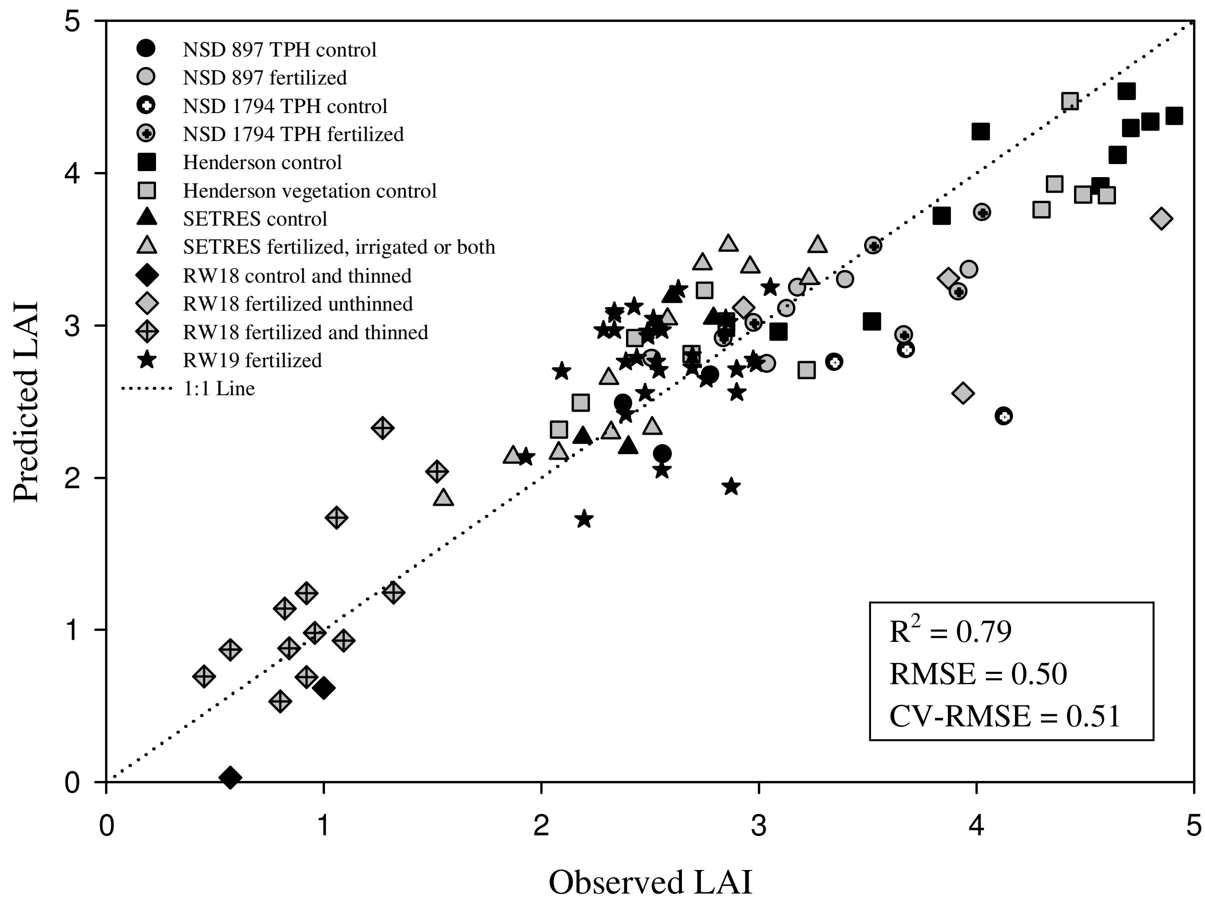

Figure 2.6 Relationship between estimated LAI and measured LAI using the 6-variable model with lidar metrics only (n = 109). Plots were first separated by stem density, and then by control and treatment.

Model (refer to table 2.1 for variable names):

$$LAI = 2.767 + 0.345\ (Veg_{mean}) - 0.236\ (Veg_{20th}) - 6.475\ (LPI) + 0.113\ (I_{mean}) - 10.772\ (Cd+1) - 18.581\ (Cd\text{-}4)$$

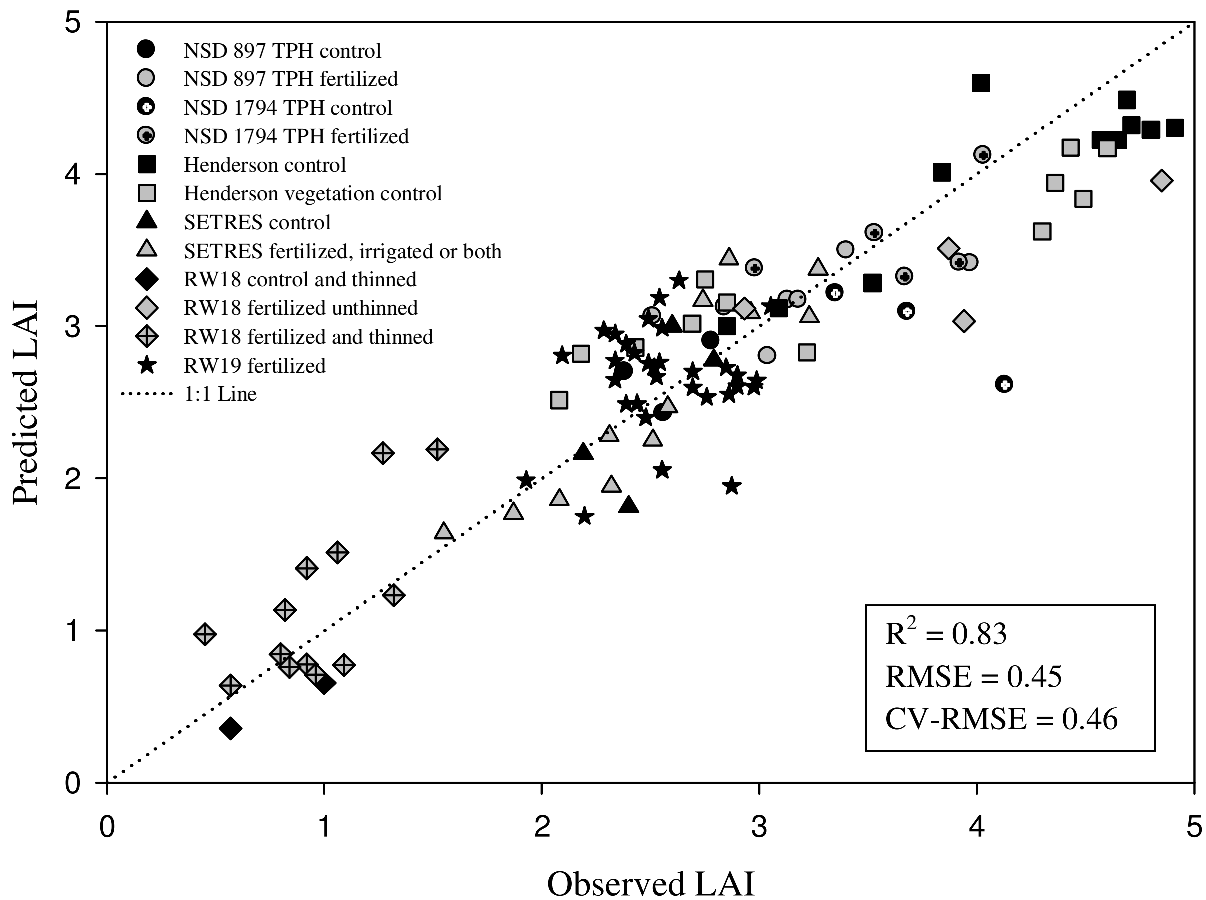

Table 2.1 Explanatory variables derived from lidar. Return hag refers to the return height above the ground. Statistics in subscripts were as follows: frequency (total), mean, mode, standard deviation (stdv), coefficient of variation (cv), minimum (min), maximum (max), and height percentiles (10^{th}, 20^{th}, …, 90^{th}). The metrics Gr_{total}, All_{total}, Veg_{total}, Gr_{pulses}, All_{pulses}, and Veg_{pulses} were determined for calculation of other metrics (i.e. proportions of returns), but were not used for model development.

Lidar metrics	**Symbol**
Total number of ground returns	Gr_{total}
All returns (return hag > 0.2 m) *Units are meters for all metrics except for* All_{total} *and* All_{cv}.	All_{total}, All_{mean}, All_{stdv}, All_{cv}, All_{min}, All_{max}, All_{10th},…, All_{90th}
Vegetation returns (return hag > 1 m) *Units are meters for all metrics except for* Veg_{total} *and* Veg_{cv}.	Veg_{total}, Veg_{mean}, Veg_{mode}, Veg_{stdv}, Veg_{cv}, Veg_{min}, Veg_{max}, Veg_{10th},...,Veg_{90th}
Pulses (number of lidar pulses per return class)	Gr_{pulses}, All_{pulses}, Veg_{pulses}
Laser penetration index (LPI)	$LPI = Gr_{pulses}/(Gr_{pulses} + All_{pulses})$
Intensity values (returns hag > 1 m) *Units are watts for all metrics except for* I_{cv}.	I_{mean}, I_{min}, I_{max}, I_{stdv}, I_{cv}
Proportion of 1^{st}, 2^{nd}, 3^{rd} and 4^{th} returns R*i is a proportion of returns*	R_i = total number of i returns/ Veg_{total} $i = 1^{st}$, 2^{nd}, 3^{rd}, and 4^{th}
Density d*i is a proportion of returns*	$d_i = [x + (Veg_{max} - Veg_{min})/10]/Veg_{total}$ $x = Veg_{min}$,1,..,10 i= 1, 2, …,10
Crown density slices around Veg_{mode} See fig. 2.2 for a graphic representation of slices. *Units are meters for* Cdi_{mean}, Cdi_{stdv}, *and* Cdi_{cv}. Cd*i is a proportion of returns*	Cdi, Cdi_{mean}, Cdi_{stdv}, Cdi_{cv} Cd_i = [number of returns in i / ($All_{total} + Gr_{total}$)] (i=+1,+ 2,+3,+4,+5, 0, -1, -2, -3, -4, and -5) i=+1,…,+ 5 at i meters above Veg_{mode} i = 0 at Veg_{mode} i = -1,…,-5 at i meters below Veg_{mode}

Table 2.2 Descriptive statistics for tree height, crown length and leaf area index (LAI) at control and treatment plots per study site. Statistics for total were calculated based on plot means. Column annotation: *n* (number of observations or plots), TPH (trees per hectare), N_{trees} (number of trees per plot), and Stdv (standard deviation).

Study	Stand age	Treatment	*n*	TPH	N_{trees}	Height (m)				Crown length (m)				LAI			
					(mean)	Mean	Stdv	Range		Mean	Stdv	Range		Mean	Stdv	Range	
NSD	11	Control	3	897	61	11.0	0.9	7.1	12.9	7.2	1.0	6.5	7.6	2.57	0.20	2.38	2.78
			3	1794	125	11.1	0.9	6.5	13.2	5.8	0.9	5.6	6.1	3.72	0.39	3.35	4.13
		Fertilized	6	897	61	11.1	1.0	5.7	13.3	7.3	1.1	6.7	7.9	3.21	0.48	2.51	3.97
			6	1794	123	11.2	0.9	6.7	14.6	5.9	1.0	5.7	6.2	3.50	0.49	2.84	4.03
RW19	13	Fertilized	32	1176	94	13.1	1.3	5.0	18.8	7.3	1.2	6.5	8.0	2.56	0.27	1.93	3.05
RW18	16	Control and thinned	2	(346 - 395)	16	16.7	0.7	15.5	18.0	7.7	1.0	5.7	10.8	0.79	0.30	0.57	1.00
		Fertilized unthinned	4	1678	60	16.9	1.8	10.5	20.6	6.3	1.6	0.8	10.7	3.90	0.78	2.93	4.85
		Fertilized and thinned	13	(313 - 470)	16	17.0	0.8	13.8	19.4	7.6	1.0	4.9	10.7	0.96	0.30	0.45	1.52
SETRES	24	Control	4	1665	100	12.9	2.1	4.8	17.8	6.2	1.6	5.7	6.6	2.09	0.38	1.55	2.40
		Fertilized, irrigated or both	12	1665	95	16.6	2.5	6.0	22.1	6.9	1.7	6.1	7.9	2.66	0.41	1.87	3.27
Henderson	26	Control	12	1665	51	21.1	2.4	13.4	27.9	6.3	1.8	5.6	8.2	4.47	0.31	3.84	4.91
		Vegetation control	12	1665	63	21.9	2.2	14.0	26.9	6.2	1.7	5.0	7.1	3.07	0.83	2.08	4.69
Total			109	____	73	15.7	3.7	4.8	27.9	6.9	0.8	0.8	10.8	2.77	1.06	0.45	4.91

Table 2.3 Means of lidar returns per plot at each study site. Minimum values for vegetation returns heights above ground were set at 1 m. Intensity minimum value was 1 for all plots (n = 109). Column annotation: n (number of observations or plots), Gr_{total} (total number of ground returns), Veg_{total} (total number of all returns), Stdv (standard deviation), Max (maximum value), and LPI (Laser Penetration Index).

Study	**Treatment**	***n***	**N_{trees} (mean)**	**Gr_{total} (mean)**	**Veg_{total} (mean)**	**Veg return heights (m)**			**Intensity (watts)**			**LPI**
						Mean	**Stdv**	**Max**	**Mean**	**Stdv**	**Max**	
NSD	Control	3	61	592	1286	6.9	1.7	11.5	33.5	14.1	93	0.32
		3	125	719	1965	7.8	1.5	12.1	36.7	13.9	75	0.28
	Fertilized	6	61	589	1912	7.3	1.7	12.1	38.9	14.9	91	0.24
		6	123	660	2218	8.0	1.5	12.1	40.8	14.7	80	0.23
RW19	Fertilized	32	94	1042	2201	9.2	2.1	15.2	36.8	16.0	115	0.30
RW18	Control and thinned	2	16	461	478	12.6	1.9	16.7	28.9	14.5	66	0.50
	Fertilized unthinned	4	60	223	1031	12.5	3.7	18.6	34.5	13.2	71	0.18
	Fertilized and thinned	13	16	427	670	11.9	3.5	19.4	31.4	15.2	87	0.42
SETRES	Control	4	100	814	2806	10.4	2.2	18.1	28.9	13.3	69	0.23
	Fertilized, irrigated or both	12	95	757	2456	14.0	2.7	21.2	34.1	14.6	80	0.24
Henderson	Control	12	63	131	1601	15.2	5.0	24.7	32.0	19.4	103	0.08
	Vegetation control	12	51	297	1395	17.1	5.6	25.7	30.4	15.8	105	0.18

Table 2.4 Pearson correlation coefficients for the independent variables used to predict leaf area index (LAI) (n = 109). For a description of the variable names refer to table 2.1. LAI was measured on the ground. Bold values were significant at $\alpha = 0.05$.

	LAI	**LPI**	**Veg_{mean}**	**Veg_{stdv}**	**Veg_{20th}**	**I_{mean}**	**Cd+1**	**$Cd+1_{stdv}$**	**$Cd+4_{cv}$**	**Cd-4**
LAI	1	**-0.757**	0.187	**0.397**	-0.046	**0.271**	0.086	**-0.328**	-0.029	0.101
LPI		1	-0.045	**-0.271**	0.060	**-0.183**	**-0.254**	**0.239**	**-0.213**	-0.185
Veg_{mean}			1	**0.693**	**0.873**	**-0.436**	0.153	-0.004	**-0.453**	**0.391**
Veg_{stdv}				1	**0.366**	**-0.491**	0.024	0.016	**-0.249**	**0.227**
Veg_{20th}					1	**-0.271**	**0.250**	0.045	**-0.450**	**0.298**
I_{mean}						1	0.172	-0.075	0.086	-0.179
Cd+1							1	0.002	**0.304**	**-0.326**
$Cd+1_{stdv}$								1	0.135	0.125
$Cd+4_{cv}$									1	-0.093
Cd-4										1

Table 2.5 Best predictive models of LAI using lidar metrics only, n = 109. The statistics R^2_{adj}', CV-RMSE, SSCC, VIF, and CI are the adjusted coefficient of determination, the RMSE from the cross validation analysis, the squared semipartial correlation coefficient from partial sum of squares, the variance inflation factor and the condition index, respectively. Since all the explanatory variables were centered, the intercept parameter for all models is 2.767. All variables in the models were highly significant at a p-value < 0.0001, except for $Cd+1_{stdv}$ with a p-value < 0.01 (in the 5-variable model), and $Cd+4_{cv}$ with a p-value < 0.005 (in the 2-variable model). For a description of the variable names refer to table 2.1.

# var.	R^2	R^2_{adj}'	RMSE	CV-RMSE	Variable	Coefficient	SSCC	VIF	CI
2	0.61	0.60	0.67	0.67	LPI	-7.518	0.61	1.05	1.10
					$Cd+4_{cv}$	-0.237	0.04	1.05	1.24
3	0.71	0.70	0.58	0.59	Veg_{stdv}	0.318	0.11	1.60	1.14
					LPI	-5.393	0.26	1.26	1.23
					I_{mean}	0.099	0.09	1.54	2.07
4	0.79	0.779	0.50	0.51	Veg_{mean}	0.330	0.19	5.68	1.40
					Veg_{20th}	-0.268	0.14	4.86	1.45
					LPI	-5.522	0.30	1.14	1.72
					I_{mean}	0.106	0.11	1.44	4.67
5	0.80	0.791	0.48	0.50	Veg_{mean}	0.324	0.19	5.70	1.29
					Veg_{20th}	-0.262	0.13	4.89	1.45
					LPI	-5.275	0.26	1.19	1.60
					I_{mean}	0.104	0.11	1.45	1.75
					$Cd+1_{stdv}$	-13.046	0.01	1.07	4.68
6	0.83	0.82	0.45	0.46	Veg_{mean}	0.345	0.20	5.93	1.27
					Veg_{20th}	-0.236	0.10	5.26	1.42
					LPI	-6.475	0.34	1.38	1.52
					I_{mean}	0.113	0.12	1.47	1.84
					Cd+1	-10.772	0.03	1.64	2.68
					Cd-4	-18.581	0.04	1.64	4.98

3. ESTIMATING STEM DENSITY AND HEIGHT TO LIVE CROWN IN INTENSIVELY MANAGED PINE PLANTATIONS USING AIRBORNE LASER SCANNING DATA

3.1 Abstract

The objective of this study was to determine whether stem density and mean height to live crown can be estimated accurately in intensively managed pine plantations using metrics derived from multiple-return airborne laser scanning (lidar) data with and without knowledge of establishment density. Field measurements of mean height, height to live crown, and stem density were measured on 110 plots under a variety of stand conditions (i.e., nutritional regimes, stand ages, and stem densities) in North Carolina and Virginia, USA. Lidar distributional metrics were calculated for all returns as well as for ten one meter deep crown density slices (newly introduced in this study), five above and five below the mode of the vegetation returns for each plot. These metrics, along with establishment density, were used as independent variables in best subsets regressions with stem density, mean height to live crown, and mean height (all measured in situ) as the dependent variables. The cross-validation (CV) RMSE for estimating number of trees on all 110 plots was 11.8 with an R^2 of 0.92. Mid-rotation age stands alone (70 plots) had a CV-RMSE of 8.7 and an R^2 of 0.97, and end-of-rotation stands (40 plots) had a CV-RMSE of 5.5% and an R^2 of 0.96. Initial establishment density, the laser penetration index, and the ratio of the returns in a given crown density slice to the total number of returns per plot were all important variables when estimating stem density. Mean height to live crown was also well-predicted (R^2 = 0.96, CV-RMSE = 0.8 m) with a model containing only one independent variable, the 90th percentile of the heights of all returns more than 0.2 m above ground. These

results indicate that if initial planting density is known, stem density can be estimated accurately using lidar data in intensively managed pine plantations over a wide variety of stand conditions. Mean height to live crown, in contrast, requires only lidar data for accurate estimation on these sites.

3.2 Introduction

Forest volume, forest biomass, and site quality are some of the parameters used to quantify forest growth and productivity. The values and units of measurements vary depending on what they describe, but they always rely on primary forest biophysical parameters, such as tree diameter, tree height, height to live crown, and stem density. These parameters, especially tree height and stem density are critical elements of forest inventories; and they are used extensively by forest managers to define silviculture prescriptions in plantations throughout a rotation, and, more importantly at the end of the rotation, when standing timber volume estimations are necessary. However, field-based estimations or measurements of these variables by traditional cruising inventories can require large amounts of time and expense; since inventories are conducted periodically, such investments tend to multiply. There is a general interest in the development and application of new, non-field-based techniques that can more easily and inexpensively quantify forest metrics. Remotely sensed data has been attractive for collecting forestry attributes given their rapid acquisition and synoptic views; aerial photography has been and continues to be utilized primarily for the estimation of number of trees and tree crown diameters, while satellite imagery, as a substitute to aerial photos, has primarily contributed information on quantifying and classifying vegetation and, most recently, aerial-based laser technology have emerged as a valuable source of three-dimensional data.

Lidar sensors measure the time between the emission and reception of laser pulses, which multiplied by the constant speed of light results in the distance (round trip) between the sensor and a target feature. This information is used to obtain accurate surface representations (i.e., elevation, slope and aspect) for topographic applications (Anderson et al. 2006; Xiaoye Liu 2008). Furthermore, the vertical distribution of the lidar returns provides the ability to estimate important forest parameters, such as canopy heights (Goodwin et al. 2006).

Previous work has reported strong correlations between lidar-based and field-based mean tree heights (Bortolot and Wynne 2005; Harding et al. 2001; Jupp et al. 2005; Lefsky et al. 2002). There have also been attempts to estimate stem density using lidar datasets through a variety of different methods, such as segmentation techniques (Holmgren and Persson 2004; Persson et al. 2002); tree crown (outlines) extractions (Lee and Lucas 2007); canopy height models (Dalponte et al. 2009; Popescu et al. 2002); and clustering (Morsdorf et al. 2004). Other procedures have incorporated the use of high spatial resolution images (i.e., aerial photography and multispectral satellite imagery) with lidar, consequently increasing forest inventory costs. However, the majority of these studies were based in natural or unmanaged forest environments. Little work has been done in intensively managed loblolly pine plantations. One of the few studies that estimated stand density in a 15-year-old loblolly pine spacing trial with high and low initial density plots (1736 and 1111 trees ha^{-1}, 32 plots of 149 m^2 per stem density) reported accuracies in the range of 65% to 87% using lidar data only, and 84% to 95% using fused lidar and multispectral imagery data (McCombs et al. 2003), but results from datasets constrained by age and management regime are difficult to extrapolate to other situations.

The accuracy and precision of inventory estimations in pine plantations is very important; an error in estimated height and number of trees at mid-rotation would have an effect on forest management decisions, while an error towards the end of the rotation would lead to inaccurate estimates of wood standing volumes.

In the past, predictive models developed using remotely sensed data, although accurate, have been developed based on uniform stand conditions or low variation. Therefore, a reliable, accurate, and comprehensive way to estimate stand biometric attributes in pine plantations is needed. The general goal of this work was to generate methods that can accurately estimate key forest attributes in intensively managed plantations using small-footprint lidar data, regardless of the silvicultural history of the planted stands. The specific goals were to (1) evaluate the relationships between lidar-derived variables and ground-based stand biophysical parameters under a range of forest management regimes and stem densities, and (2) investigate differences in the stem density predicted accuracies for mid-rotation and end-of-rotation stand ages.

3.3 Methods

3.3.1 Study sites

In order to cover a wide range of sites (Sandhills to Piedmont), silvicultural regimes (low to high fertilization intensities), stand ages (11 to 26 years), and densities (313 to 1794 trees per hectare, TPH), five loblolly pine (*Pinus taeda* L.) plantation silviculture research trials were used as study sites representing a total of 110 plots and 8056 trees. Three of these sites are located in Virginia: The *Nutrient by Stand Density Study (NSD)* trial is located in Buckingham County at 37° 34' 59" N and 78° 26' 49" W (fig. 3.1). It was initiated in 1998 as a randomized complete block design with a 3x2 factorial: 3 different fertilization regimes of low, medium and high (site index (SI) at 25 years of 15, 21 and 24 m, respectively), and 2 different stem densities (897 and 1794 trees per hectare). Each plot size is 676 m^2 (26 m x 26 m) and each block has 6 plots, for a total of 18 plots. Refer to Carlson et al. (2009) for a more detailed explanation about the treatments.

The Forest Productivity Cooperative (FPC) *RW195501 (RW19)* trial established in 2009, in a 13-year-old stand as part of a mid-rotation thinning and fertilization region-wide study. This trial is located in the Piedmont area in Appomattox County (37º26’32” N, 78º39’43” W) (fig. 3.1). There are 32 plots varying in size from approximately 400 m^2 to 1280 m^2. At the time of lidar acquisition in the summer of 2008, only the plots had been established; no additional silviculture treatments had been applied other than the traditional forest operation practices used in the area.

The FPC *RW180601* (*RW18*) is located in Virginia (Brunswick County) at 36°40’51” N and 77°59’13” W (fig. 3.1). It was established in 1999 on a 6-year-old planted stand as part of a region-wide study with the objective of understanding optimal rates and frequencies of nutrient additions for rapid growth in young stands. A total of 40 plots of various sizes ranging from 400 m^2 to 470 m^2 had complete weed control and nutrient additions (nitrogen, phosphorus, potassium, and boron) at different frequencies (1, 2, 4 and 6 year intervals). 30 plots were thinned in 2008.

The *Southeast Tree Research and Education Site (SETRES)* site is located in the sand hills of Scotland County, North Carolina (34º54’17” N and 79º29’0” W) (fig. 3.1). This trial, established in 1992 in an 8-year-old plantation, was designed as randomized complete block design (4 blocks and 4 plots per block) with treatments of nutrient additions (nitrogen, phosphorous, potassium, calcium and magnesium), irrigation, and both. See Albaugh et al. (1998) for complete site and treatment descriptions. There are 16 plots of 900 m^2 (30 m x 30 m) size.

The *Henderson Long Term Site Productivity Study (Henderson)* is located in Vance County, North Carolina (36º 26’52” N, 78º28’23” W) (fig.3.1). Established in 1982, this 2x2x2 factorial split plot design consisted of two levels of harvest (stem wood only or whole tree removals) , two site preparation methods (chop and burn or shear, pile and disk), and vegetation control (during the first 5 years) or not. There are 3 blocks and 8 plots per block (24 plots total), with a plot size of 450 m^2 (15 m x 30 m). For a detailed description of treatments and study see Vitousek and Matson (1985).

These studies were established and/or maintained as a joint effort among the Forest Productivity Cooperative (FPC 2011), academic institutions, the USDA Forest Service, the Virginia Department of Forestry, and private industry.

3.3.2 ***Field data collection and analysis***

3.3.2.1 Inventory data

The studies were measured during the 2008 dormant season (December 2008 – February 2009). Every tree, within the measurement plots, was measured using a diameter tape and a Haglöf Vertex hypsometer to obtain diameter at breast height (dbh), total tree height (ht), and height to live crown (htlc). Initial number of trees ($Tree_0$) was defined as the number of trees that fit within each plot area based on planting tree spacing; this information was known from the time of plot establishment for 4 of the study sites (NSD, RW18, Henderson, and SETRES). For RW19, the initial number of trees was estimated by using the tree planting spacing and the area of the plots. The tree spacing in this study was not always uniform since the stand was planted manually, so an average of several random measures between trees was used. In addition, number of trees (N_{trees}) was defined as the current number of trees in each plot; this information was obtained from the tree growth measurements, since all trees within the plots are measured every year for research purposes.

3.3.2.2 Lidar data

Small footprint lidar data were acquired for all study areas in late August 2008. Using an Optech ATLM 3100 system with an integrated Applanix DSS 4K x 4K DSS camera. The data had multiple returns with a sampling density of 5 pulses per square meter, with at least 4 returns per pulse. The scan angle was < 15 degrees. The vertical accuracy over bare ground was 15 cm, and the horizontal accuracy was 0.5 m.

Although ground returns had been extracted by the lidar data provider, an initial examination of the data was first made to determine if the ground/vegetation classification was true to the terrain reality. Since the size of the study sites was relatively small, so was the lidar dataset; this allowed the application of the kriging interpolation method to generate a DEM (Popescu et al. 2002) from the provided ground returns without compromising computational time. The rest of the non-ground returns were classified as "all returns" using a threshold of 0.2 m of height from the ground and as "vegetation returns" for heights greater than 1 m. The metrics derived from the ground returns class (Gr) were: frequency (count) of returns and frequency (count) of pulses (table 3.1). The metrics derived from the all returns class (All) were: frequency (count), mean height, standard deviation, coefficient of variation, minimum, maximum, percentiles (10, 20, 25, 40, 50, 75, and 90), and frequency (count) of pulses (Holmgren 2004; Magnussen and Boudewyn 1998; Popescu et al. 2002). The metrics derived from the vegetation returns class (Veg) were the same described for the all returns class with the addition of the mode. The distribution of intensity values (I) were described using the mean, minimum, maximum, standard deviation, and coefficient of variation. First, second, third and fourth returns were classified as such and divided by the total number of "vegetation returns" (R). The Laser Penetration Index (LPI) (Barilotti et al. 2005) was calculated per plot as the proportion of ground pulses to the total pulses (ground pulses + all pulses). Density metrics (d) were calculated following Naesset (2002), as the proportion of returns found on each of 10 sections equally divided within the range of heights of vegetation returns for each plot. Additionally, another set of metrics, crown density slices (Cd), was calculated using the mode value of vegetation returns. Ten 1-meter sections of vegetation returns (5 above and 5 below the mode value, based on the maximum value of crown length observed) were classified and proportion of returns to the total number of returns, mean, standard deviation, and coefficient of variation were calculated (fig. 3.2). Frequency of returns (count), calculated from each of the lidar data point classes, were used only to estimate other metrics, such as proportions of returns, but they were not used in the development of the models (table 3.1).

The height values obtained from the lidar data collected in RW18 were too high in one portion of the study area, with values several meters higher than the forest stand heights. A threshold, maximum return hag ≥ 1 m higher than field-measured tree height per plot, was used to eliminate erroneous lidar measurements. After this threshold was applied only 20 plots remained in this study area.

3.3.2.3 Statistical analysis

Data diagnostic methods were applied to the dataset of 110 plots (8056 trees) lidar derived metrics, and ground truth measurements, to evaluate each for normality, necessary transformations, outliers, influential points, and correlations among all variables. Multiple regressions were used to fit the dataset. Best subset regression models were examined using the RSQUARE method for best subsets model identification (SAS 2010). This method generates a set of best models for each number of variables (1, 2,…, 6, etc.). The criterion to select the best models was based on several conditions: (a) high coefficient of determination (R^2) value, (b) low residual mean square (RMSE), (c) similarity between the adjusted coefficient of determination R^2_{adj} and R^2 values. The R^2_{adj} is a rescaling of R^2 by degrees of freedom; hence it involves the ratio of mean squares instead of sum of squares, (d) Mallows' C_p statistic values (Hocking 1976). When the model is correct, the C_p is close to the number of variables in the model, and (e) low values from two information criteria, the Akaike (1969) Information Criterion (AIC) and Schwarz (1978) Bayesian Criterion (SBC). The AIC is known for its tendency to select larger subset sizes than the true model; hence the SBC was used for comparison, since it penalizes models with larger number of explanatory variables heavier than AIC.

The best models chosen per each subset size (based on number of variables in the models) were evaluated for collinearity issues. Computational stability diagnostics were then used to check for near-linear dependencies between the explanatory variables. In order to make independent variables orthogonal to the intercept and therefore remove any collinearity that involves the intercept, independent variables were centered by subtracting their mean values (Belsley 1984; Marquart 1980). The variance inflation factor (VIF) was used to quantify the variance inflation of estimated regression coefficients; a threshold of 10 was used, as it is common in most statistical analyses. High VIF values (10 < VIF < 30) suggest weak to severe (VIF > 30) collinearity problems. Since VIF neither detects multiple near-singularities nor identifies the source of singularities (Rawlings et al. 2001), the condition index (CI) was also evaluated for all variables within the models. This index is the square root of the ratio of the largest eigenvalue to the corresponding eigenvalue from a data matrix. Similar to VIF, the CI indicates weak dependencies when $10 < CI < 30$ and severe dependencies when $CI > 30$.

Additional data to test the models were not available, thus cross-validation analysis was performed using PRESS statistics (Allen 1971), which is the sum of squares of the difference between each observation and its prediction when that observation was not used in the prediction equation. The root mean square error from the cross validation analysis (CV-RMSE) was then calculated as the square root of the ratio between the PRESS statistic and the number of observations. The CV-RMSE is an indicator of the predictive power of the model, thus a small PRESS statistics is desirable. The significance level used for all the statistical tests was $\alpha = 0.05$. This p-value was used to evaluate if the variables included in the model were statistical significant as well. The squared semipartial correlation coefficients (SSCC) were calculated using partial sum of squares to determine the contribution from each variable to the models, while controlling the effects of other independent variables within the model. These coefficients represent the proportion of the variance from the dependent variable associated uniquely with the independent variable.

The previously described procedures were also used to evaluate models for subsets at different n values: $n = 78$, when excluding RW19 plots; $n = 70$ for mid-rotation age plots; and $n = 40$ for end-of-rotation age plots.

3.4 Results

3.4.1 Summary statistics from ground measurements and lidar metrics

The plantation age for all the study sites was between 11 to 26 years-old. Trees per hectare ranged from 313 to 1794, and plot sizes were between 400 m^2 to 1280 m^2. Given the tree planting spacing, and the fact that some plots had been thinned, the number of trees per plot ranged from 12 to 184. Tree mortality, which was based on the initial number of trees (when planted), ranged from 0 to 82%; 0% mortality was observed in some plots at the NSD and RW19 studies, and 82% mortality was observed at the RW18 plots that had been thinned, thus it is an artificial mortality. Plots were classified as control and fertilized. Summary statistics were calculated, mean dbh ranged from 15.2 to 21.8 cm (table 3.2), mean height was highest (21.9 m) in the plots at the Henderson study, as was the mean height to live crown. However, the differences between control plots and vegetation control plots were very small due to the previous application of other treatments to these plots (i.e. harvest type and soil preparation). The lowest ht (10.9 m) and hlc (3.8 m) values were observed at NSD, the youngest study site (table 3.3).

Lidar returns per group of plots are summarized in table 3.4. The number of ground returns was very high in RW19 plots, SETRES and NSD, while at Henderson and RW18 unthinned plots it was low. The difference between these two groups of plots is the level of canopy closure; the more vegetation found at the canopy level, the less the laser penetrated to reach the ground. Mean return height values for the lidar returns were always several meters lower than the mean tree heights measured from the ground; nevertheless, the maximum heights of the lidar returns were closer to the maximum tree heights observed on the ground (shown in table 3.3). Mean intensity values ranged from 28.9 in SETRES to 40.8 in NSD, but the range of intensities within each plot was large; this is noticeable in the standard deviations of the group of plots, which varied from 13.2 and 19.4. Maximum intensities ranged from 66 to 115.

3.4.2 *Variable selection and modeling*

Several lidar metrics showed highly significant correlations with number of trees (N_{trees}), but only the variables that appeared in the models are reported in table 3.5. Variables such as I_{cv} (-0.441), d_9 (-0.432), LPI (-0.384), d_7 (0.359), Cd-1 (0.348), Cd-5 (-0.297), and All_{90th} (-0.338) were not only significant when using the entire dataset (n = 110) but also for the subsets of plots. Other variables (All_{10th}, I_{stdv}, d_5, d_6, Cd-2, and Cd+4_{stdv}) had significant correlations whether for the entire dataset or for some of the subsets. Although there are other variables in table 3.5 that showed no significant correlation with N_{trees}, once they were combined with other variables in the models their contributions became statistically significant. This was the case with Cd+2 and Cd-4 for the 110 plots; however in the model with the same number of plots Cd-4 was correlated with All_{10th} and also with Cd+2. Also, I_{cv} had significant correlations with LPI, All_{10th}, All_{90th}, I_{stdv}, d_6, d_9 and Cd-1 at any of the subsets of plots evaluated. Among the ground based variables, initial number of trees ($tree_0$) had highly significant correlations with N_{trees} when using any of the datasets. This was the only ground variable that consistently appeared in the best models.

Best models (for n = 110) using lidar metrics explained between 51%, using five variables in the model (table 3.6). Once the number of variables in the model was higher than 5, the adjusted R^2 remained approximately the same; thus, this was as much variation in number of trees that could be explained by lidar-metrics-only models while using this particular dataset. The variable with the largest contribution in the model was d_9 (0.23), followed by LPI (0.09), d_5 (0.08), Cd-5 (0.06) and Cd-1 (0.02). Near dependencies were evaluated by the variance inflation factor (VIF) and condition index (CI), which were both < 5 for all the parameters in the models. The RMSE from the cross-validation analysis (CV-RMSE) was high (29.3), as expected with a low R^2 of 0.51.

After evaluating lidar metrics alone, ground based data were added to the best subset analyses. The top best models were reported in table 3.7, which was a 2-variable model using initial number of trees ($Tree_0$) and LPI that explained 83% of the variation (CV-RMSE = 16.9), and a 5-variable model with an R^2 of 0.92. The R^2 from the 5-variable lidar-ground model was twice as much as the R^2 from the 5-variable lidar only model. The statistics for the 5-variable lidar-ground model were also reduced, having an RMSE of 11.8 compared to 29.3 from the lidar-only model. The biggest contribution in these two models was from the $Tree_0$ ground variable (0.68 in the 2-variable model and 0.75 in the 5-variable model), followed by LPI (0.09 and 0.13, in the 2 and 5-variable models respectively), Cd-4 (0.05), Cd+2 (0.02) and All_{10th} (0.01). No near dependencies among the variables were flagged by VIF or CI (< 5). Although the squared semi-partial correlation coefficient values of some variables were very low, those variables were highly significant at $p < 0.0001$.

After comparing the relationships between predicted and observed values from the models using the entire dataset (*n* = 110), the addition of $Tree_0$ to the models showed a more accurate estimation with a CV-RMSE of 17 and 12, compared to 29.2 from the lidar-only model. This accuracy can be observed graphically in figure 3.3, as the points distribute close and along the 1:1 line in the 5-variable model.

Among all the study sites evaluated, the estimation of initial number of trees for RW19 was based on the average tree spacing. As this site was manually planted, the range in tree spacing was larger than the spacing at the rest of the study sites, which could have contributed to a larger error when calculating the initial number of trees. An aerial view of the studies shows the difference in the straightness of plantation rows between RW19 and the rest of the sites (fig. 3.4). Based on this discrepancy, the best subsets were evaluated using the other 4 sites only (*n* =

78). Best models using lidar metrics and ground data, showed a plateau in the adjusted R^2 values when more than 5 variables were included in the model. Therefore a 5-variable model was reported (table 3.7), which explains 95% of variation in number of trees. $Tree_0$ contributed the most (0.30), and the variables LPI (0.26), Cd-4 (0.08), and Cd+2 (0.05) were included in this model and were common with the model fitted using 110 plots. Another contributor was d_6 (0.01). Despite the exclusion of RW19, the R^2 and $R^2_{adj'}$ values increased but not largely compared to those from the model with all plots, and the CV-RMSE was reduced from 12 to 9 (fig. 3.5). Similarly, study sites were later grouped by stand age; a mid-rotation age group including NSD, RW18 and RW19, and an end-of-rotation age group composed by SETRES and Henderson. Aside from stand age, the differences between these two groups were that the majority of the plots in SETRES and Henderson were closed canopy stands compared to the many open canopy stands in the other group of sites, and that the trees per hectare was similar within the end-of-rotation age group, while in the mid-rotation age group TPH varied largely. Table 3.6 shows a 5-variable lidar-only model for the mid-rotation age group (n = 70), with an R^2 of 0.62. Models from the best subsets analysis with more variables than 5 showed an increase in R^2 and $R^2_{adj'}$ but not significant enough to consider the addition of another variable. This model had three common variables with the model from all plots (n = 110) and those were d_5, d_9 and Cd-1, but the variable that contributed the most was All_{90th} (0.17). The lidar-only model developed for the end-of-rotation group of sites was able to explain 96% of the variation of number of trees in these plots (fig. 3.6), and had a CV-RSME of 6 trees per plot (table 3.6). None of the variables included in this model (I_{stdv}, I_{cv}, d_7, and Cd+4_{stdv}, and Cd-2), were also part of the mid-rotation and all plots models. In fact, this model has no similarities with any of the lidar and ground data models reported in table 3.7 either. All the variables in these three models (*n* = 78, 70, and 40) had VIF and CI values less than 5.

Best subsets were also evaluated for mid-rotation and end-of-rotation set of plots using the combination of lidar and ground data. For mid-rotation plots, a model of 4 variables was developed (table 3.7). In this case, a couple of lidar metrics (All_{90th} and Cd-1) from the model of lidar metrics only were included, and LPI, which was recurrent in all the lidar and ground data models. This model explained 97% of the variation in number of trees per plot for mid-rotation age stands; the CV-RMSE was 9; and the VIF and CI were < 5 (fig. 3.6). For the end-of-rotation group of plots, the models obtained from the best subset analysis, after including ground variables, did not perform better than the lidar-only models. R^2 values were consistently lower than those from the lidar-only model and collinearity problems arose frequently. Therefore, a model to predict N_{trees} at the end of the rotation using lidar and ground data was not reported.

The 90th percentile for all returns (All_{90}) had the highest correlation (0.98) with mean tree height (ht) and mean height to live crown (hlc). Estimated ht and hlc variables using 1-variable lidar metric model are shown in figures 2.8 and 2.9, respectively. For mean tree height, 1-variable model explained 97% of the variation and had an RMSE and a CV-RMSE of 0.6 m. Meanwhile, for mean height to live crown an R^2 of 0.96 was obtained with an RMSE and CV-RMSE of 0.8 m. There was no pattern observed regarding overestimation or underestimation for a particular group of plots or sites.

3.5 Discussion

In many aspects, variability was part of the sampled dataset; it included the intrinsic characteristics of each site, such as soil type, topography, and geographic location, and also the stand characteristics that resulted from forest management, such as number of trees per hectare, fertilization rates, and vegetation control. Plot size and stand age varied as well.

Laser penetration index (LPI) and the 90th percentile (All_{90th}) for all lidar returns (hag > 0.2 m) correlated negatively and significantly with number of trees (Barilotti et al. 2005; Woods et al. 2008). This was expected for LPI, since it is associated with the canopy interception, the higher the number of trees the less pulses would reach the ground level. In the case of the 90th percentile, an increase in the number of trees decreases the value of the 90th percentile (height above the ground in m) (Naesset 2002), which suggests that a large amount of the returns was coming from lower levels of tree crowns. The relationships of these two variables and number of trees became stronger for the mid-rotation and end-of-rotation group of plots. Dispersion statistics for intensity values of lidar returns, such as standard deviation and coefficient of variation, were included in all models. These variables appeared either together or by themselves. Both statistics had negative correlations with number of trees (except for I_{stdv} with 70 plots), which indicates that the less variation within the intensity values in a given plot, the greater the number of trees found in that plot. Intensity values vary by the reflectance and reflectivity of targets. If the ground is primarily covered by tree crowns, the returns obtained will be mostly from the leaves and branches within the canopy; if only a few trees are present, other targets such as ground and understory vegetation might be responsible for the variability of intensity values. Although, in the past, metrics derived from intensity values were used in the estimation of forest biomass (van Aardt et al. 2006), researchers have recommended caution when using lidar intensity values because such values are not usually calibrated (Bater et al. 2011). Nonetheless, the variability of the dataset used in this study resulted not only from the lidar data acquisition (i.e., different acquisition dates) but also from the inherent condition of the targets (i.e., topography, soil type, stand age, stem density, fertilization regime).

Although several density metrics (Naesset 2002) were significantly correlated with number of trees, most of them were part of the models using lidar metrics only, except for d_6 which was included in the best model for $n = 78$ plots. These variables relate to the crowns of the trees (with d_{10} as the section at the top of the trees). As the proportion of number of returns to the total number of returns, these variables are also physically related to the amount of targets (branches and leaves) that the laser could encounter. The low (d_1, d_2, and d_3) and high (d_8, d_9, and d_{10}) densities had a negative correlation with number of trees, while the mid-level densities (d_4, d_5, d_6, and d_7) were positively correlated. This suggests that the proportion of returns classified at the mid-level height above the ground relates to the tree crown density, which can also be explained by the fact that these mid-level densities were strongly correlated with mean height to live crown ($d_4 = -0.21$, $d_5 = -0.54$, $d_6 = -0.68$, and $d_7 = -0.60$); as the hlc was lower the values for those metrics were higher. Similar situation was observed among the crown density slices proportion of returns, since the 4th and 5th meters above and below the mode were negatively correlated with number of trees, while the rest of the sections from Cd+3 to Cd-3 (refer to fig. 3.2) correlated positively. These new metrics, although not the largest contributors, were always included in the best models, adding enough weight to increase the R^2 to a level of accuracy that can benefit forest management.

Initial number of trees ($Tree_0$) was expected to be highly correlated with number of trees. Although this variable is listed as ground based data along with tree height, diameter at breast height, and height to live crown, it is in fact the only one that requires no additional measurement or monitoring throughout the rotation. Forest managers usually keep this information from the moment the stands are planted. Since this information is known, the model reported in this study using this particular ground data can be considered as lidar data only. Meanwhile, by using this variable, the accuracy of predicting the number of trees for a given area increased to 92% without incurring in additional costs.

Separating the data set in groups of sites based on uniformity of tree spacing, mid-rotation age and end-of-rotation age stands allowed a comparison of these lidar-ground models to the ones developed using all sites. Clearly, there is a little gain in R^2 values and in accuracy between using more uniformed tree planting spacing (without RW19) plots and using all sites. However, such gain might not be completely related to the uniform tree spacing, perhaps it might be related to reducing the stem density variability within the dataset. When evaluating mid-rotation age plots, an increase in R^2 was obtained compared to using all plots even with the inclusion of fewer variables in the model. The major gain was observed among the lidar metrics only models. Since the end-of-rotation plots had a much higher R^2 than any other lidar metrics only model, this suggests that robust and accurate models to estimate stem density using lidar metrics can be developed, but only under the condition that forest stands should be homogeneous in at least age and tree planting spacing.

The results of this study have been consistent with those of previously published research. A study in Norwegian forest stands modeling groups of 19 to 37 plots, reported relative standard errors of predicted residuals (difference between observed values and predicted) ranging from 14% to 29%, or 97 to 466 trees ha^{-1} by modeling the natural log of stem density and lidar metrics (Naesset 2004). A subsequent study in Ontario Canada using 28 plots of plantation conifers showed predicted stem density results with a relative RMSE of 25%, or 257 trees ha^{-1} (Woods et al. 2008). Another study in Oregon, USA, used 29 plots from a mixed forest stand; modeling natural log of stem density with lidar-derived variables, it reported relative standard errors ranging from 27.2% to 39.3% or 128 to 185 trees ha^{-1} (Goerndt et al. 2011). In comparison, in this study the relative standard error of predicted residuals for the 5-variable model with lidar and ground data (110 plots) ranged from 14% to 16% (10 to 11 trees per plot, 162 to 178 trees ha^{-1}). For the mid-rotation age model using 70 plots the error range was between 10% and 11% (7 to 8 trees per plot, 108 to 123 trees ha^{-1}), and for the end-of-rotation model using 40 plots it was between 6% and 7% (4 to 5 trees per plot, 64 to 79 trees ha^{-1}). The results from previous work (McCombs et al. 2003) and from this study suggest that when the number of plots was reduced the R^2 from the models improved, and a similar relationship was observed when reducing the variability in stem density and plantation age. It is good news that lidar can accurately estimate stem density for uniform stands, however from the forest management point of view this might not be practical, since it will require the use of a different model based on the stand characteristics. For this reason, the model developed in this study using a dataset that includes a large variability in stem density and stand age represents a promising tool that has potential for use for forest managers regardless of the stand conditions.

Researchers have used lidar data to derive other biometric attribute estimations besides stem density, such as dominant height, mean tree height, and crown height. Several studies have estimated tree height by delineating individual trees (Holmgren and Persson 2004; Popescu and Zhao 2008), while others used regression models based on a combination of lidar derived metrics; their reported RMSE values were between 0.59 m to 1.5 m (Dean et al. 2009; Maltamo et al. 2010; Woods et al. 2008). The RMSE (0.6 m) obtained from the 1-variable model for mean height in this study is therefore in agreement with previous work. As also seen in Breidenbach et al (2008), the highest correlated variable with mean tree height was the 90th

percentile of lidar returns. The estimation of mean height to live crown from a 1-variable model showed an RMSE of 0.8 m, which is considerably lower than comparable published results; this might be attributed to the fact that most of the published work has been done in natural forest stands (Dean et al. 2009; Popescu and Zhao 2008; Vauhkonen 2010). The level of accuracy for predicting mean height and mean height to live crown models was 97% and 96%, respectively; such a high performance could be attributable to both the characteristics of lidar and their multiple returns, and to the uniform distribution and growth of trees in pine plantations.

Models of stem density have been developed in the past to estimate number of trees per hectare; however, the models reported in this study are based on the plot sampling area. In other words, the lidar metrics used in the model were estimated based on the lidar returns acquired per plot area, and the dependent variable used was the current number of trees for that given area or plot. Given this condition, such models can be used for estimating number of trees per area of lidar acquisition. For example if a lidar flight line (i.e. a strip of returns) is used to generate the metrics needed to utilize the model, the number of trees estimated will be associated with the area covered by such flight line. Furthermore, the slow rate at which forest managers in the United States have adopted the use of lidar technology is in principle related to the high cost associated with lidar. However, lidar data do not need to be acquired over the entire management area; just as with traditional inventories, a sampling of the forest stand area could be sufficient for evaluation purposes. Number of trees, mean height, and mean height to live crown estimations from lidar strips, distributed according to established inventory sampling protocols (i.e. systematic, random, stratified) across the entire managed land, will give forest managers the possibility of extrapolating to stand scales while maintaining higher accuracy, lower costs and fewer man-hours work than ground-based inventories.

Forest attributes such as height and height to live crown in intensively managed pine plantations depend on the type of silviculture applied. Thus, the uniqueness of the dataset used in this study, composed of plots with a variety of stem densities, fertilization regimes, etc., contributed to the development of robust models for mean tree height and mean height to live crown that are ready to use in forest plantations, regardless of management history or objectives. Moreover, a predictive model to estimate mean tree height from lidar in pine plantations gives forest managers the flexibility to use such estimates for calculating dbh and tree standing volume by using their own allometric equations.

The fusion of optical data and lidar data represents a good tool for estimating biometric attributes per individual basis since the geographic location of each tree is assessed. But a couple of disadvantages using fused data arise; the predictive error associated with it has been reported larger than the results found in this study, and there is an increase not only in the acquisition cost, but also in the processing time of such data.

The models developed in this study offer a more accurate, affordable, and simple approach to estimate key forest attributes using lidar data alone, and can be considered a practical tool to use for forest management decisions.

3.6 Literature cited

Akaike, H. 1969. Fitting autoregressive models for prediction. Ann. Inst. Stat. Math. 21:243-247.

Allen, D. 1971. The prediction sum of squares as a criterion for selection of predictor variables. Univ. of Ky. Dept. of Statistics, Tech. Report 23.

Anderson, E.S., J.A. Thompson, D.A. Crouse, and R.E. Austin. 2006. Horizontal resolution and data density effects on remotely sensed LIDAR-based DEM. Geoderma 132(3-4):406-415.

Bater, C.W., M.A. Wulder, N.C. Coops, R.F. Nelson, T. Hilker, and E. Naesset. 2011. Stability of sample-based scanning-LiDAR-derived vegetation metrics for forest monitoring. IEEE Trans. Geosci. Remote Sens. 49(6):2385-2392.

Barilotti, A., S. Turco, R. Napolitano, and E. Bressan. 2005. La tecnologia LiDAR per lo studio della biomassa negli ecosistemi forestali. in 15th Meeting of the Italian Society of Ecology, Torino, Italy.

Belsley, D.A. 1984. Demeaning conditioning diagnostics through centering (with discussion). Amer. Statistician 38:73-77.

Bortolot, Z.J., and R.H. Wynne. 2005. Estimating forest biomass using small footprint LiDAR data: An individual tree-based approach that incorporates training data. Photogramm. Eng. Rem. Sens. 59:342-360.

Breidenbach, J., B. Koch, G. Kändler, and A. Kleusberg. 2008. Quantifying the influence of slope, aspect, crown shape and stem density on the estimation of tree height at plot level using lidar and InSAR data. Internat. J. of Rem. Sens. 29(5):1511-1536.

Carlson, C.A., T.R. Fox, J. Creighton, P.M. Dougherty, and J.R. Johnson. 2009. Nine-year growth responses to planting density manipulation and repeated early fertilization in a loblolly pine stand in the Virginia Piedmont. South. J. Appl. For. 33(3):109-114.

Dalponte, M., N.C. Coops, L. Bruzzone, and D. Gianelle. 2009. Analysis on the use of multiple returns LiDAR data for the estimation of tree stems volume. IEEE J. Sel. Top. Appl. Earth Observ. Remote Sens. 2(4):310-318.

Dean, T.J., Q.V. Cao, S.D. Roberts, and D.L. Evans. 2009. Measuring heights to crown base and crown median with LiDAR in a mature, even-aged loblolly pine stand. Forest Ecol. Manag. 257(1):126-133.

FPC. 2011. Forest Productivity Cooperative. Shaping the future of plantation forestry (http://www.forestnutrition.org/, August 2009). Raleigh, NC.

Goerndt, M.E., V.J. Monleon, and H. Temesgen. 2011. A comparison of small-area estimation techniques to estimate selected stand attributes using LiDAR-derived auxiliary variables. Can. J. For. Res.-Rev. Can. Rech. For. 41(6):1189-1201.

Goodwin, N.R., N.C. Coops, and D.S. Culvenor. 2006. Assessment of forest structure with airborne LiDAR and the effects of platform altitude. Remote Sens. Environ. 103(2):140-152.

Harding, D.J., M.A. Lefsky, G.C. Parker, and J.B. Blair. 2001. Laser altimeter canopy height profiles: methods and validation for closed-canopy, broadleaf forests. Remote Sens. Environ. 76:283-297.

Hocking, R. 1976. The analysis and selection of variables in linear regression. Biometrics. 32:1-49

Holmgren, J., and A. Persson. 2004. Identifying species of individual trees using airborne laser scanner. Remote Sens. Environ. 90:415-423.

Holmgren, J. 2004. Prediction of tree height, basal area and stem volume in forest stands using airborne laser scanning. Scand. J. Forest Res. 19(6):543-553.

Jupp, D.L.B., D. Culvenor, J.L. Lovell, and G. Newnham. 2005. Evaluation and validation of canopy laser radar (LiDAR) systems for native and plantation forest inventory. CSIRO. 157 pp.

Lee, A.C., and R.M. Lucas. 2007. A LiDAR-derived canopy density model for tree stem and crown mapping in Australian forests. Remote Sens. Environ. 111(4):493-518.

Lefsky, M.A., W.B. Cohen, D.J. Harding, G.C. Parker, S.A. Acker, and S.T. Gower. 2002. Lidar remote sensing of above-ground biomass in three biomes. Global Ecol. Biogeogr. 11:393-399.

Magnussen, S., and P. Boudewyn. 1998. Derivations of stand heights from airborne laser scanner data with canopy-based quantile estimators. Can. J. Forest Res. 28(7):1016-1031.

Maltamo, M., O.M. Bollandsas, J. Vauhkonen, J. Breidenbach, T. Gobakken, and E. Naesset. 2010. Comparing different methods for prediction of mean crown height in Norway spruce stands using airborne laser scanner data. Forestry 83(3):257-268.

Marquart, D.W. 1980. Comment: you should standarize the predictor variables in your regression models. J. Amer. Stat. Assoc. 75:87-91.

McCombs, J.W., S.D. Roberts, and D.L. Evans. 2003. Influence of fusing lidar and multispectral imagery on remotely sensed estimates of stand density and mean tree height in a managed loblolly pine plantation. For. Sci. 49(3):457-466.

Morsdorf, F., E. Meier, B. Kötz, K.I. Itten, M. Dobbertin, and B. Allgöwer. 2004. LIDAR-based geometric reconstruction of boreal type forest stands at single tree level for forest and wildland fire management. Remote Sens. Environ. 92(3):353-362.

Naesset, E. 2002. Predicting forest stand characteristics with airborne scanning laser using a practical two-stage procedure and field data. Remote Sens. Environ. 80:88-99.

Naesset, E. 2004. Practical large-scale forest stand inventory using a small-footprint airborne scanning laser. Scand. J. Forest Res. 19(2):164-179.

Persson, A., J. Holmgren, and U. Soderman. 2002. Detecting and measuring individual trees using an airborne laser scanner. Photogramm. Eng. Rem. Sens. 68(9):925-932.

Popescu, S.C., R.H. Wynne, and R. Nelson. 2002. Estimating plot-level tree heights with lidar: local filtering with a canopy-height based variable window size. Comput. Electron. Agr. 37:71-95.

Popescu, S.C., and K. Zhao. 2008. A voxel-based lidar method for estimating crown base height for deciduous and pine trees. Remote Sens. Environ. 112:767-781.

Rawlings, J.O., S.G. Pantula, and D.A. Dickey. 2001. Applied Regression Analysis: A Research Tool. Springer.

SAS. 2010. The SAS System for Windows Release 9.1.3. SAS Institute Inc., Cary, NC USA.

Schwarz, G. 1978. Estimating the dimension of a model. Annals of Statistics. 6:461-464.

van Aardt, J., R.H. Wynne, and R.G. Oderwald. 2006. Forest volume and biomass estimation using small-footprint lidar-distributional parameters on a per-segment basis. For. Sci. 52(6):636-649.

Vauhkonen, J. 2010. Estimating crown base height for scots pine by means of the 3D geometry of airborne laser scanning data. Internat. J. Rem. Sens. 31(5):1213-1226.

Vitousek, P.M., and P.A. Matson. 1985. Disturbance, nitrogen availability, and nitrogen losses in an intensively managed loblolly-pine plantation. Ecology 66(4):1360-1376.

Woods, M., K. Lim, and P. Treitz. 2008. Predicting forest stand variables from LiDAR data in the Great Lakes - St. Lawrence forest of Ontario. For. Chron. 84(6):827-839.

Xiaoye Liu. 2008. Airborne LiDAR for DEM generation: some critical issues. Prog. Phys. Geog. 32(1):31-49.

Figure 3.1 Geographic location of the study sites in North Carolina and Virginia, USA.

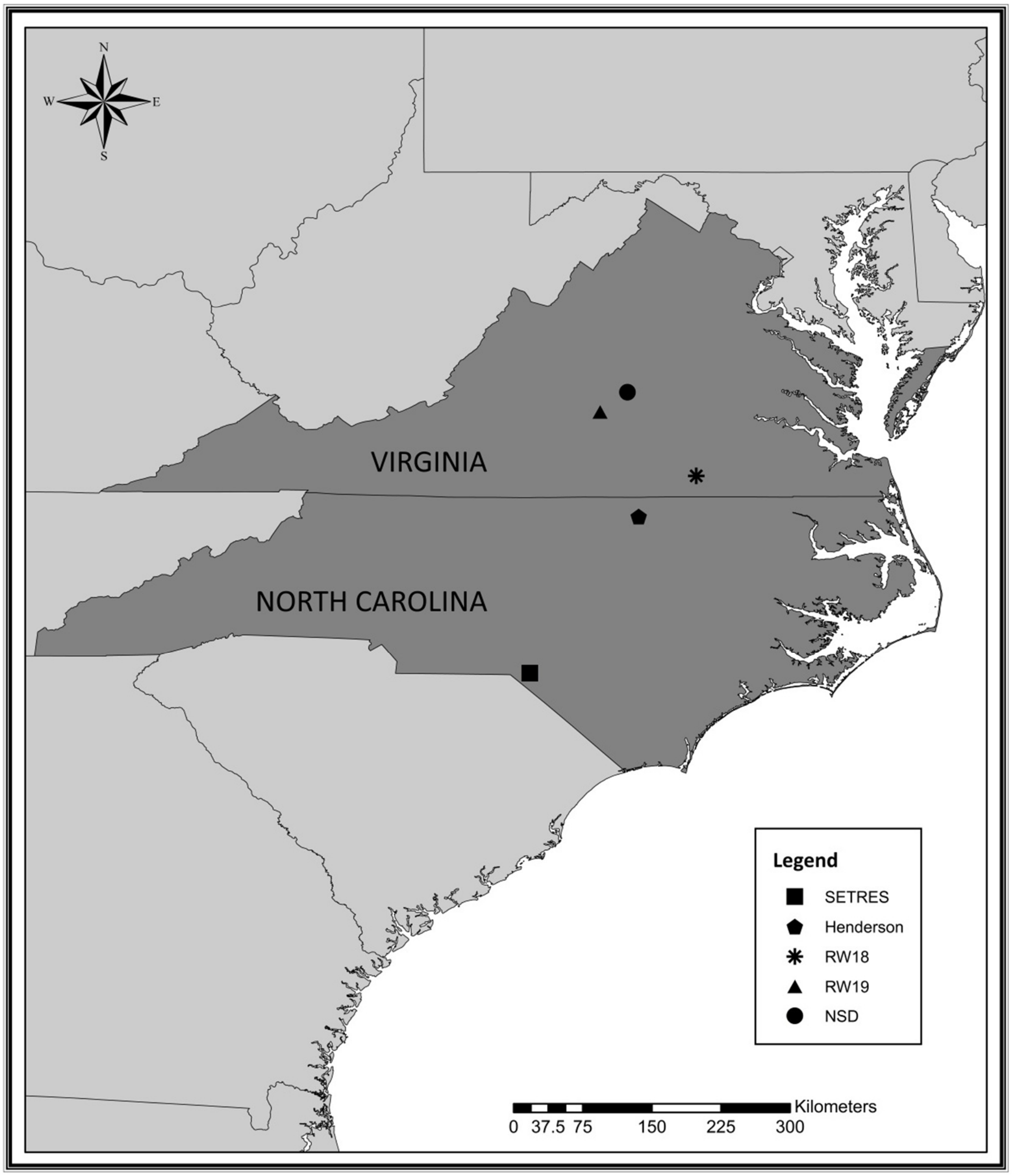

Figure 3.2 Crown density slices derived from the vegetation lidar returns mode (Veg_{mode}) value. Mid-crown height value per plot was calculated as: Tree total height – (crown length/2), and was significantly correlated (0.92) with Veg_{mode}. Five 1 m sections above and below the mode were defined, and the descriptive statistics (i.e., proportion of returns to the total number of returns, mean, standard deviation, and coefficient of variation) from the returns within each section were obtained. See table 3.1 for variable names and how they were calculated. (a) Crown density values for a fertilized unthinned plot from the RW18 site.

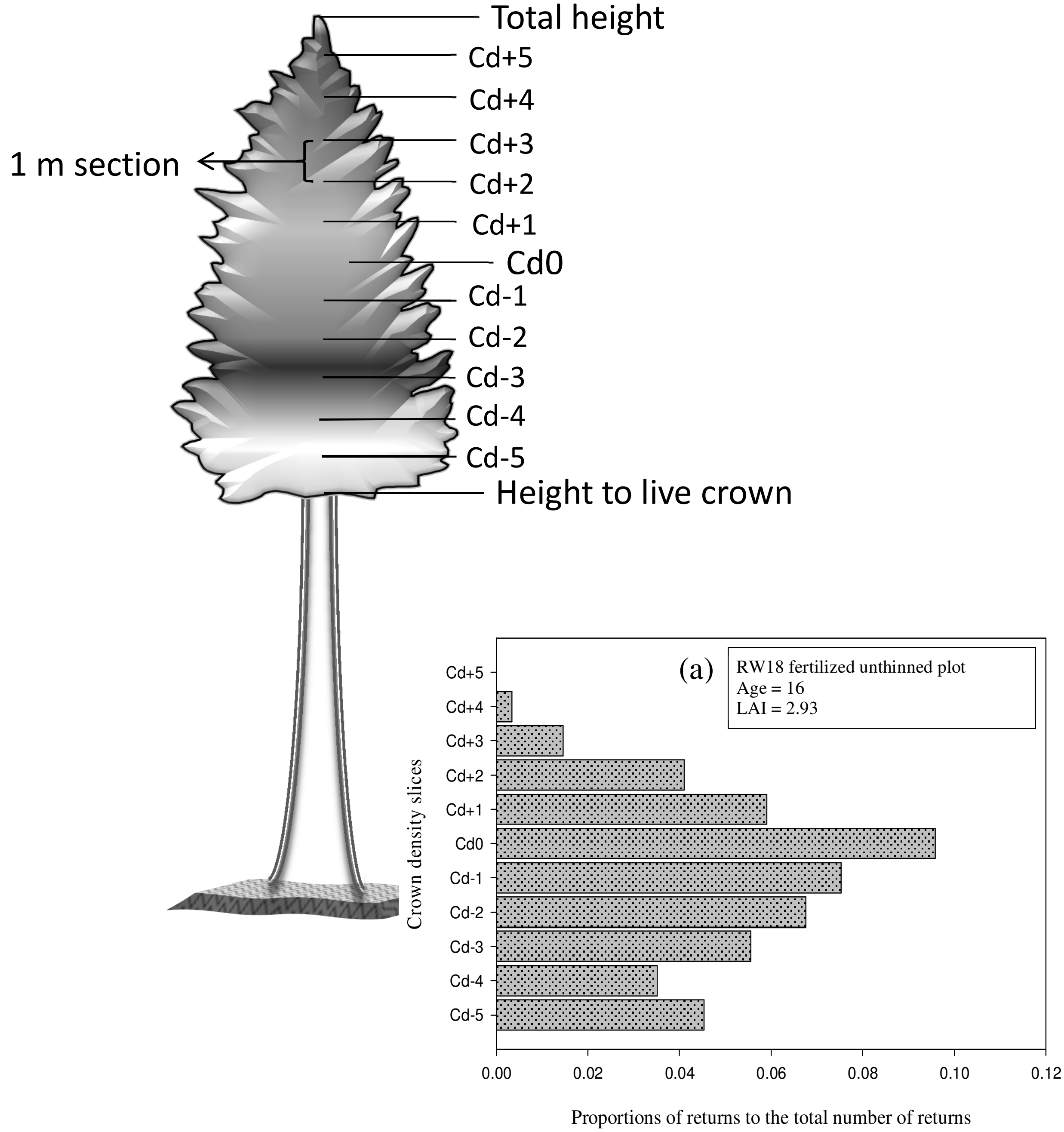

Figure 3.3 Relationship between estimated and measured number of trees (N_{trees}) using a 5-variable model with lidar metrics and ground data (n = 110). Plots were classified by stem density.

Model (refer to table 3.1 for variable names):

N_{trees} = 73.373 + 0.911 ($Tree_0$) – 1.373 (All_{10th}) – 129.548 (LPI) – 305.065 (Cd+2) – 736.945 (Cd-4)

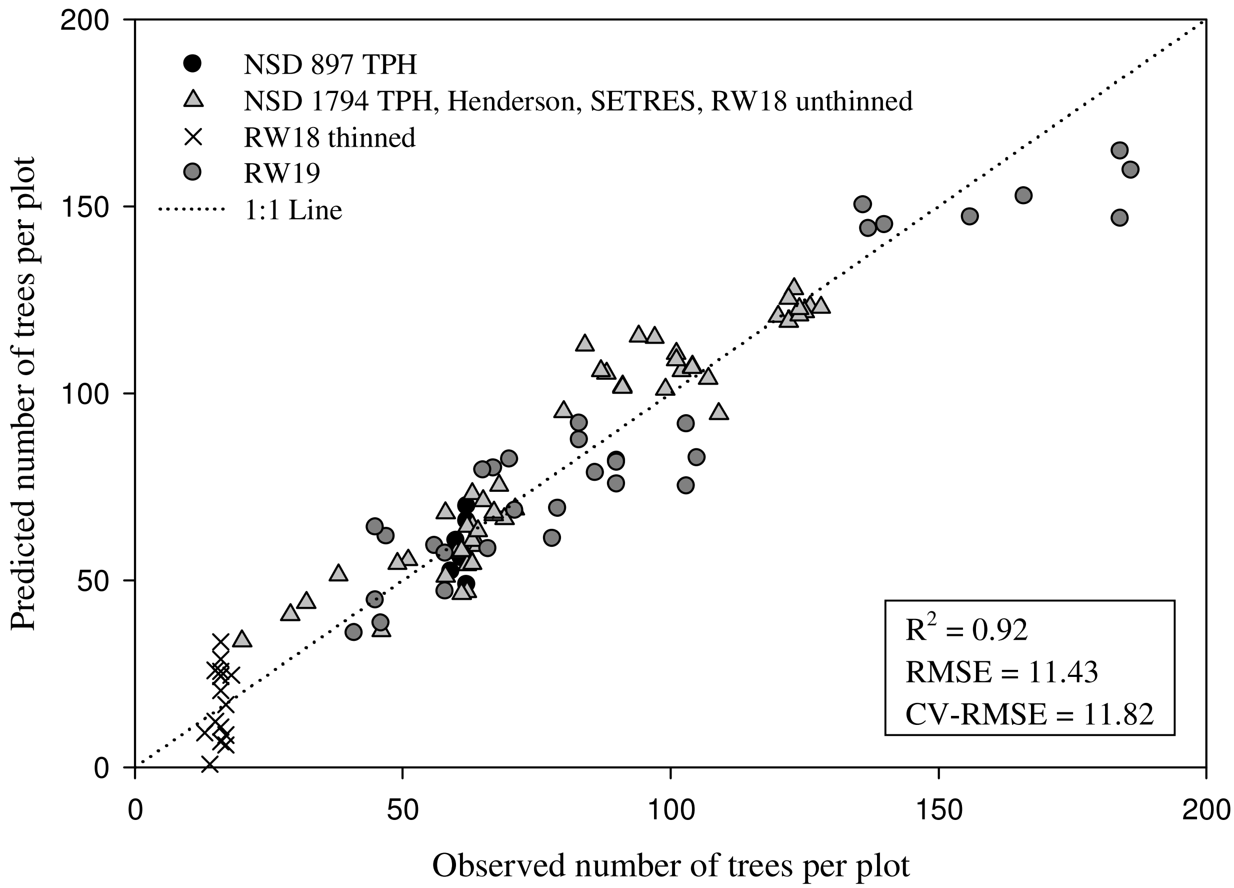

Figure 3.4 Subsets of aerial photos per study site, where straightness of plantation rows can be observed. From left to right: (a) RW19, (b) NSD, (c) RW18, unthinned (left) and thinned plots (right), (d) SETRES, and (e) Henderson, each study has 32, 18, 40 (only 20 used in this research), 16, and 24 plots, respectively. Aerial photography was acquired at the same time as lidar data. Plot boundaries are represented as white squares and rectangles.

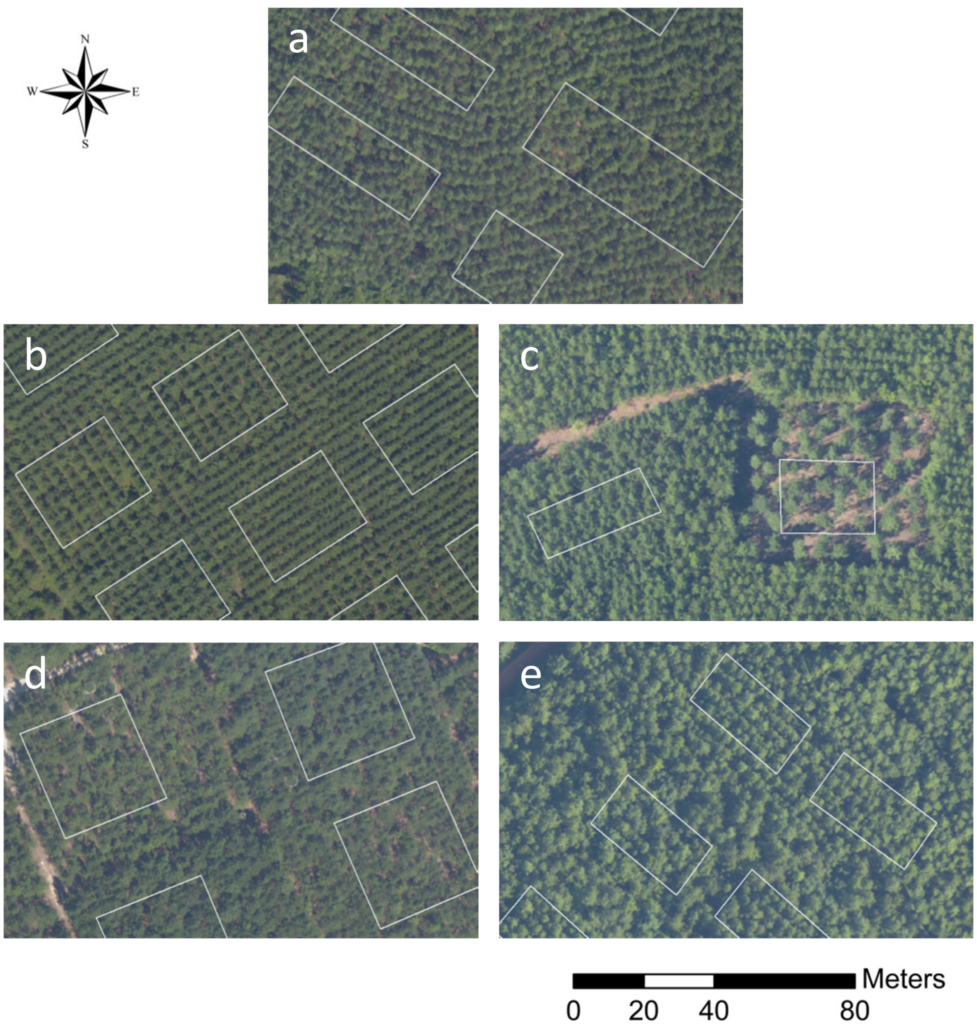

Figure 3.5 Relationship between estimated and measured number of trees (N_{trees}) using a 6-variable model with lidar variables and ground data (n = 78). Plots were classified by stem density.

Model (refer to table 3.1 for variable names):

$$N_{trees} = 68.686 + 0.689\ (Tree_0) - 143.229\ (LPI) + 48.499\ (d_6) - 368.642\ (Cd{+}2) - 737.816\ (Cd{-}4)$$

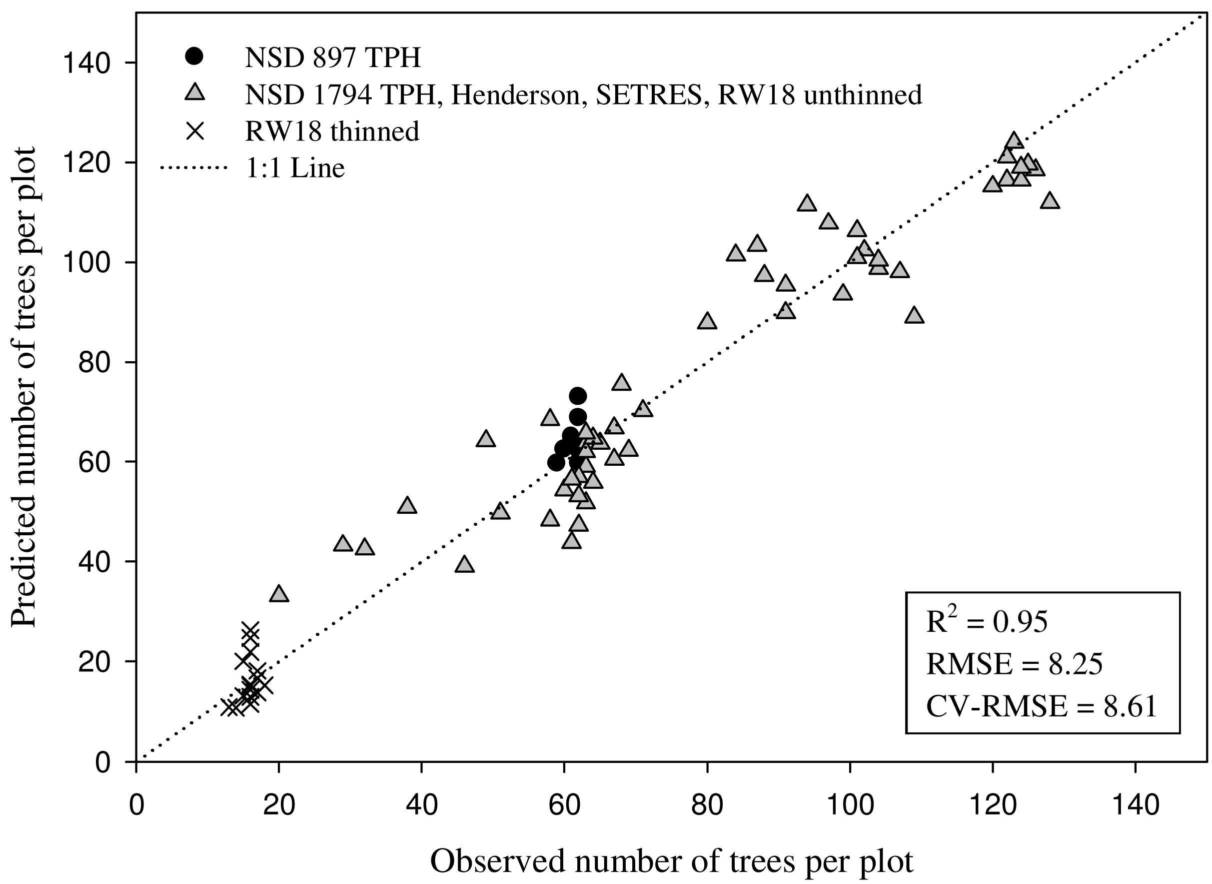

Figure 3.6 Relationship between estimated and measured number of trees (N_{trees}) per plot using a 5-variable model with lidar metrics only for end-of-rotation age plots (n = 40). Plots have same number of trees per hectare based on initial tree planting spacing. Plot size in Henderson is 450 m^2 and in SETRES is 900 m^2.

Model (refer to table 3.2 for variable names):

$$N_{trees} = 73.315 - 6.245\,(I_{stdv}) - 0.976\,(I_{cv}) + 42.287\,(d_7) + 48.911\,(Cd{+}4_{stdv}) + 114.877\,(Cd\text{-}2)$$

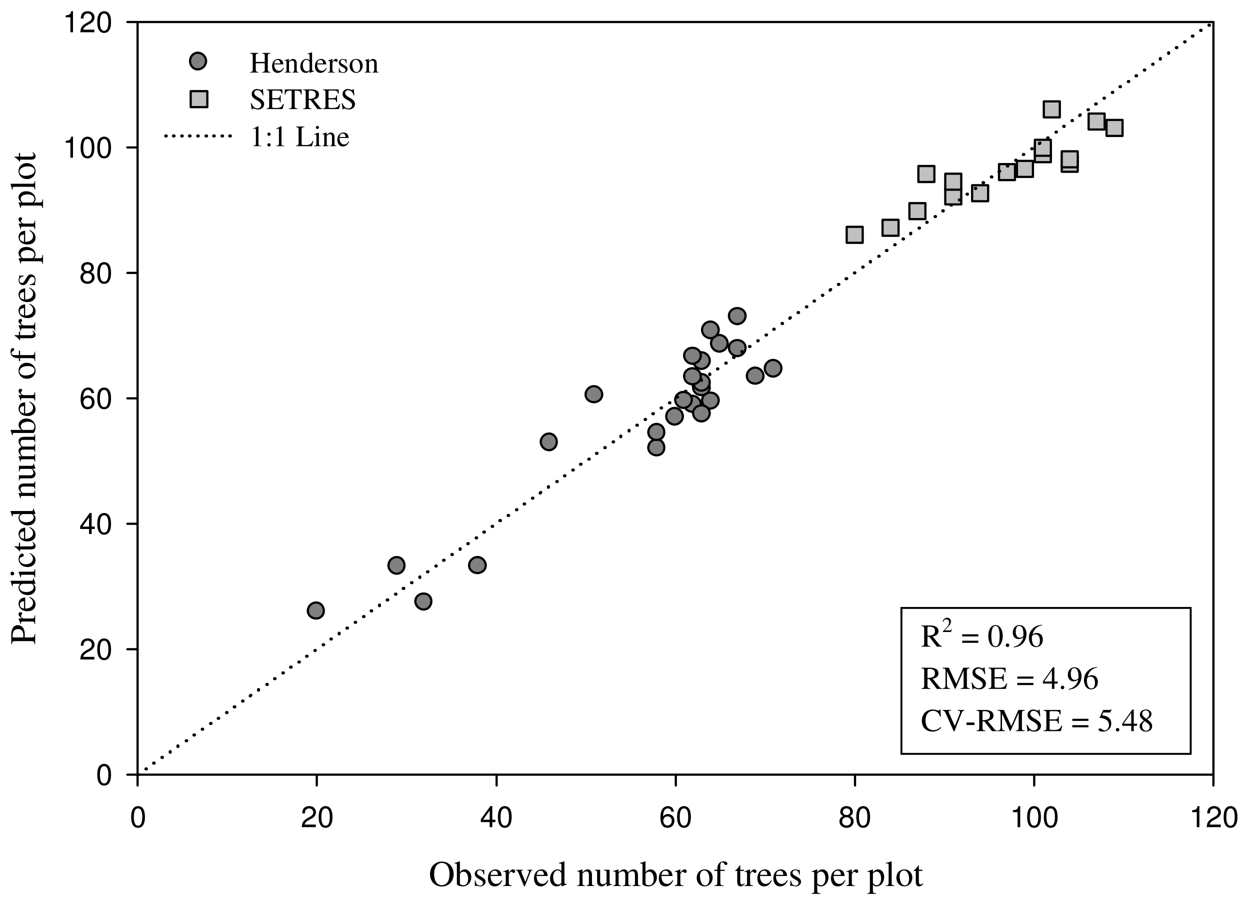

Figure 3.7 Relationship between estimated and measured number of trees (N_{trees}) using a 5-variable model with lidar metrics and ground data for mid-rotation age plots (n = 70).

Model (refer to table 3.1 for variable names):

$N_{trees} = 73.167 + 0.954\ (Tree_0) - 3.299\ (All_{90th}) - 83.305\ (LPI) + 205.669\ (Cd\text{-}1)$

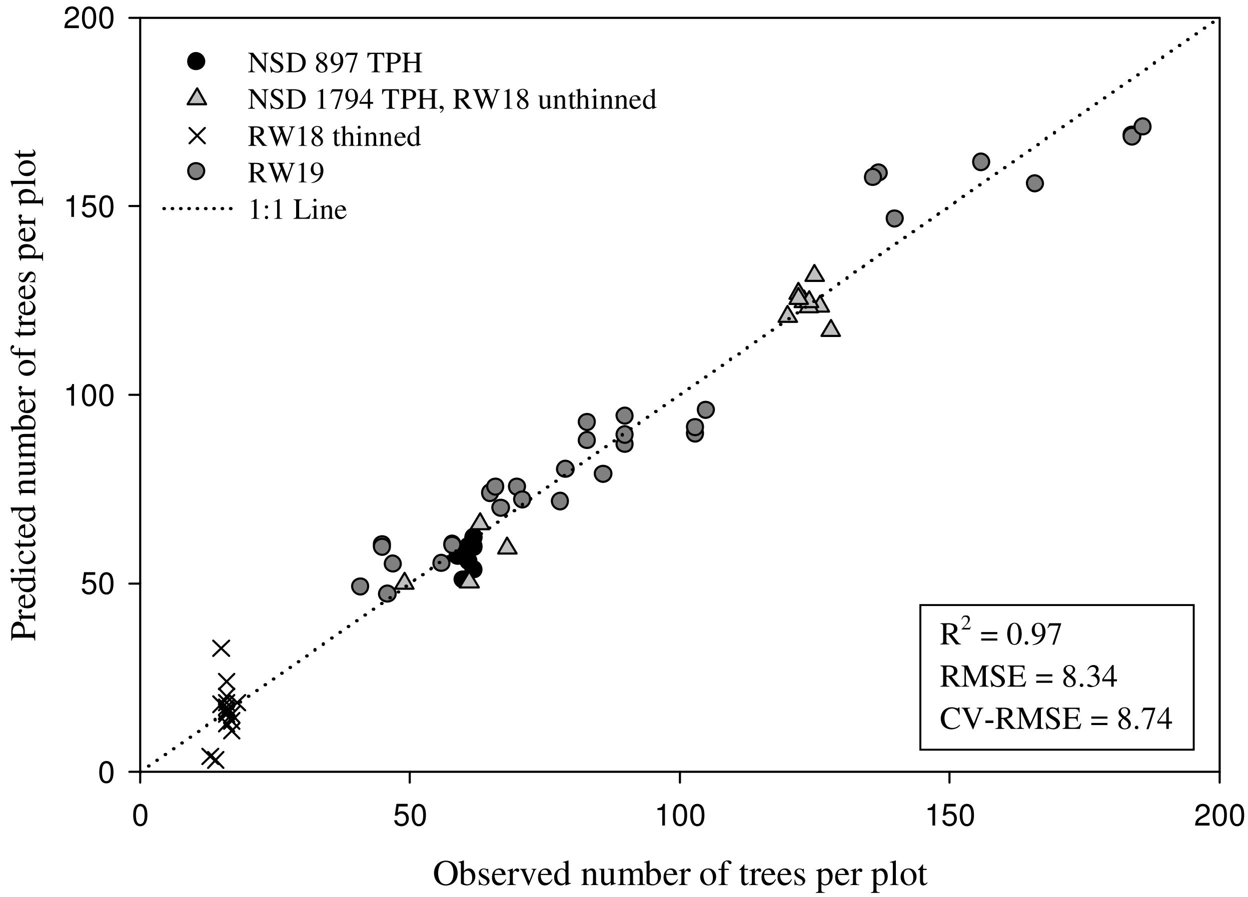

Figure 3.8 Relationship between estimated mean tree height and measured mean tree height (ht) using a 1-variable (90[th] percentile for all returns with height above ground > 0.2 m, All_{90th}) model, (n =110).

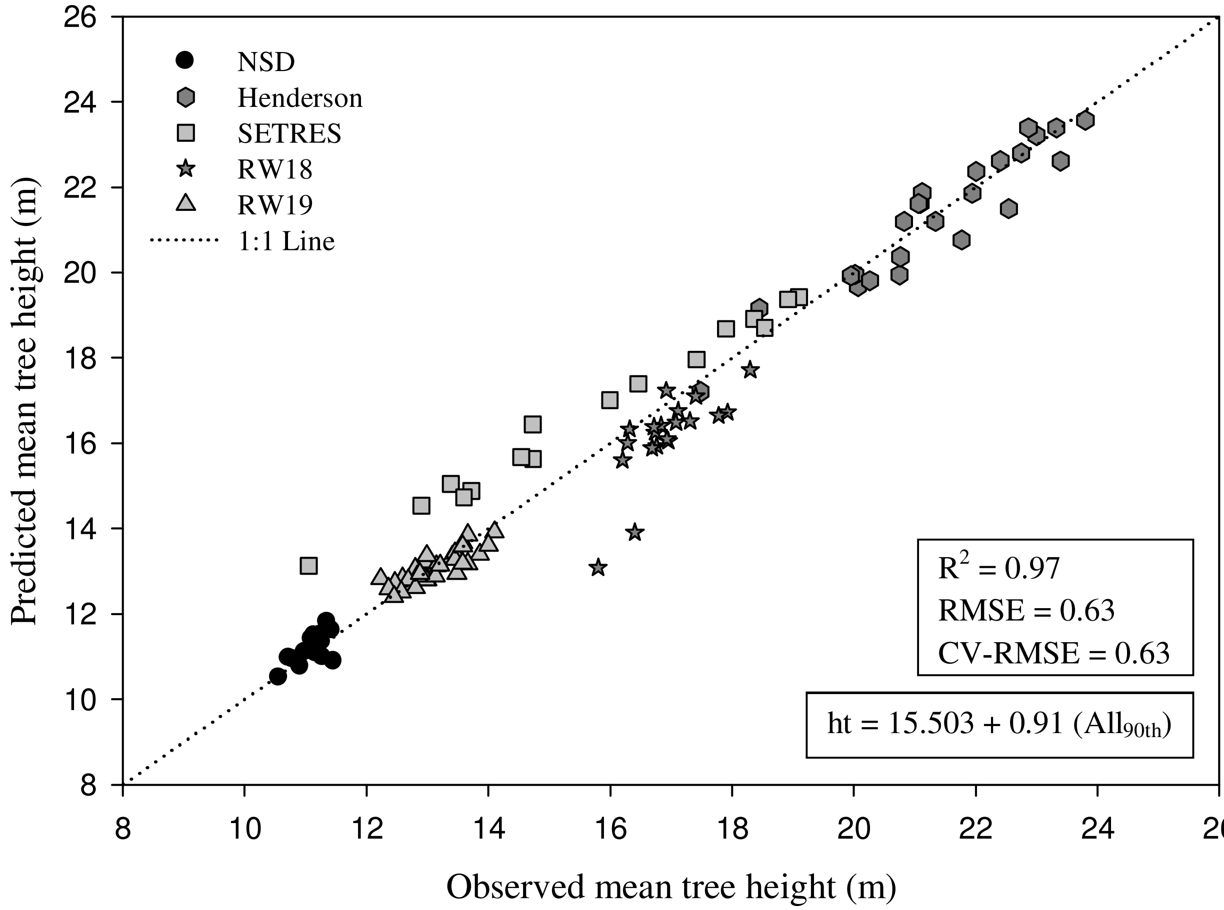

Figure 3.9 Relationship between estimated mean height to live crown (hlc) and measured mean hlc using a 1-variable (90th percentile for all returns with height above ground > 0.2 m, All_{90th}) model, (n =110).

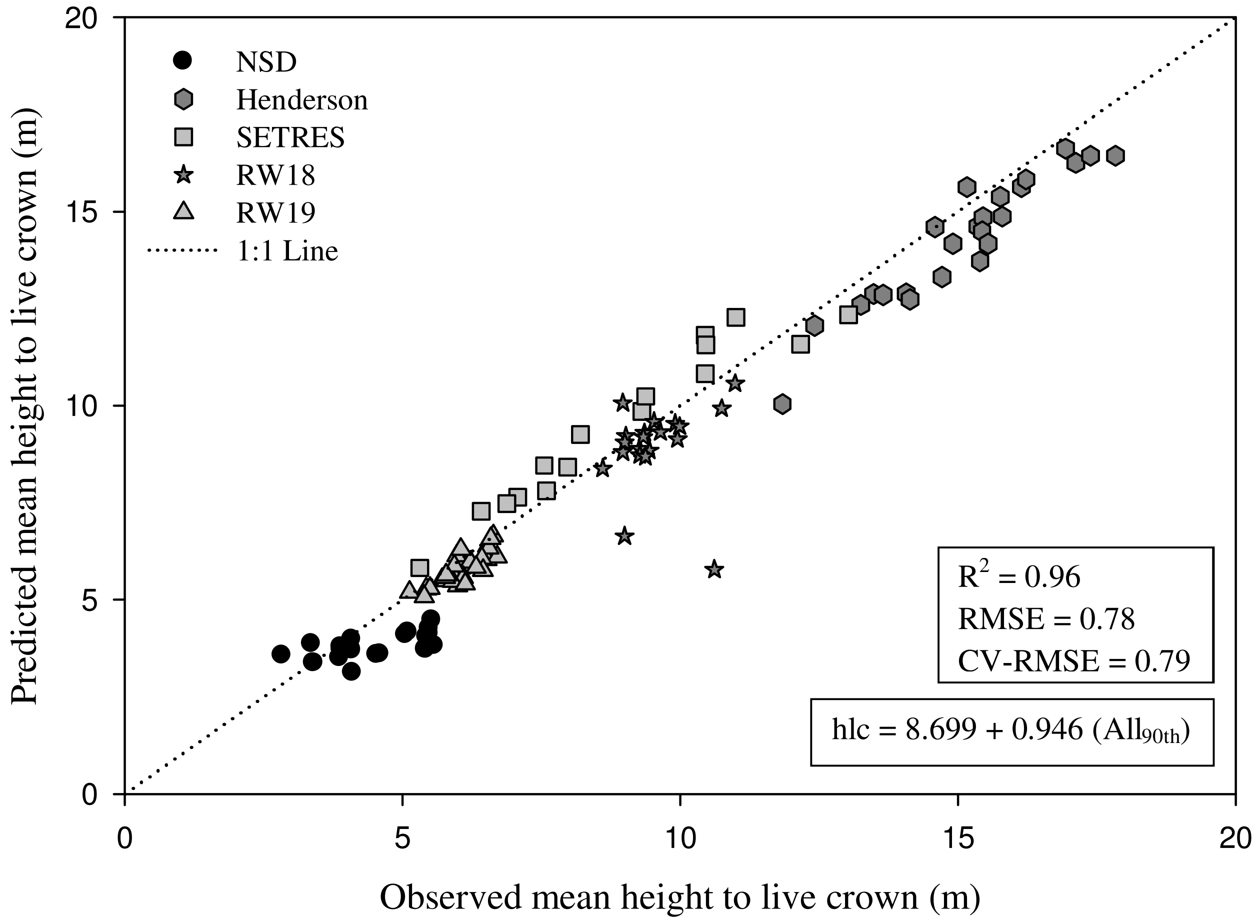

Table 3.1 Explanatory variables derived from lidar. Return hag refers to the return height above the ground. Statistics in subscripts were as follows: frequency (total), mean, mode, standard deviation (stdv), coefficient of variation (cv), minimum (min), maximum (max), and height percentiles (10^{th}, 20^{th} … 90^{th}). The metrics Gr_{total}, All_{total}, Veg_{total}, Gr_{pulses}, All_{pulses}, and Veg_{pulses} were determined for calculation of other metrics (i.e. proportions of returns), but were not used for model development.

Lidar metrics	**Symbol**
Total number of ground returns	Gr_{total}
All returns (return hag > 0.2 m) *Units are meters for all metrics except for* All_{total} *and* All_{cv}.	All_{total}, All_{mean}, All_{stdv}, All_{cv}, All_{min}, All_{max}, All_{10th},…, All_{90th}
Vegetation returns (return hag > 1 m) *Units are meters for all metrics except for* Veg_{total} *and* Veg_{cv}.	Veg_{total}, Veg_{mean}, Veg_{mode}, Veg_{stdv}, Veg_{cv}, Veg_{min}, Veg_{max}, Veg_{10th},...,Veg_{90th}
Pulses (number of lidar pulses per return class)	Gr_{pulses}, All_{pulses}
Laser penetration index (LPI)	$LPI = Gr_{pulses}/(Gr_{pulses} + All_{pulses})$
Intensity values (returns hag > 1 m) *Units are watts for all metrics except for* I_{cv}.	I_{mean}, I_{min}, I_{max}, I_{stdv}, I_{cv}
Proportion of 1^{st}, 2^{nd}, 3^{rd} and 4^{th} returns R*i is a proportion of returns*	R_i = total number of i returns/ Veg_{total} $i = 1^{st}$, 2^{nd}, 3^{rd}, and 4^{th}
Density d*i is a proportion of returns*	$d_i = [x + (Veg_{max} - Veg_{min})/10]/Veg_{total}$ $x = Veg_{min}$,1,..,10 i= 1, 2, …,10
Crown density slices around Veg_{mode} Refer to fig. 3.2 for a graphic representation of the slices *Units are meters for* Cdi_{mean}, Cdi_{stdv}, *and* Cdi_{cv}. Cd*i is a proportion of returns*	Cdi, Cdi_{mean}, Cdi_{stdv}, Cdi_{cv} Cd_i = [number of returns in i / (All_{total} + Gr_{total})] (i=+1,+ 2,+3,+4,+5, 0, -1, -2, -3, -4, and -5) i=+1,…,+ 5 at i meters above Veg_{mode} i = 0 at Veg_{mode} i = -1,…,-5 at i meters below Veg_{mode}

Table 3.2 Summary statistics for dbh and number of trees (N_{trees}) per group of plots (control and fertilized) within each site. Statistics for the total were calculated based on the plot means. Columns annotation: n (number of observations or plots), TPH (trees per hectare), N_{trees} (number of trees per plot), and Stdv (standard deviation).

Study	**Treatment**	***n***	**Age (yr)**	**TPH**	**Plot area (m^2)**	**N_{trees} (mean)**	**dbh (cm)**			
							Mean	**Stdv**	**Range**	
NSD	Control	3	11	897	676	61	17.4	1.9	11.2	23.9
		3		1794		125	14.3	1.9	6.6	18.8
	Fertilized	6		897		61	18.5	2.0	6.6	23.6
		6		1794		123	15.2	1.9	5.8	21.3
RW19	Fertilized	32	13	1176	(400-1280)	94	18.1	3.1	4.6	27.9
RW18	Control and thinned	2	16	(346 - 395)	(400-470)	16	20.5	2.2	17.5	28.7
	Fertilized unthinned	4	16	1678		60	19.8	3.5	9.7	29.9
	Fertilized and thinned	14	16	(313 - 470)		16	21.8	2.2	16.3	28.2
SETRES	Control	4	24	1665	900	100	16.6	3.9	6.5	29.3
	Fertilized, irrigated or both	12		1665		95	20.9	4.7	5.7	35.2
Henderson	Control	12	26	1665	450	63	20.3	4.6	9.1	35.9
	Vegetation control	12		1665		51	21.8	3.9	10.4	32.8
Total	----------	110	---	-----	642	73	19.6	2.2	13.6	24.7

Table 3.3 Summary statistics for height (ht) and height to live crown (hlc) for groups of control and fertilized plots. Statistics for the total were calculated based on the plot means. Column annotation: n (number of observations or plots), and Stdv (standard deviation).

Study	Treatment	*n*	Age (yr)	ht (m)				hlc (m)			
				Mean	Stdv	Range		Mean	Stdv	Range	
NSD	Control	3	11	11.0	0.9	7.1	12.9	3.8	0.7	2.0	5.6
		3		11.1	0.9	6.5	13.2	5.4	0.7	2.1	7.1
	Fertilized	6		11.1	1.0	5.7	13.3	3.8	0.9	1.5	6.6
		6		11.2	0.9	6.7	14.6	5.3	0.8	1.9	8.6
RW19	Fertilized	32	13	13.1	1.3	5.0	18.8	6.1	0.9	2.6	9.1
RW18	Control and thinned	2	16	16.7	0.8	15.5	18.0	9.0	0.9	7.1	11.3
	Fertilized unthinned	4	16	16.9	1.8	10.5	20.6	10.6	1.0	7.0	13.3
	Fertilized and thinned	14	16	16.9	0.8	13.8	19.4	9.3	0.9	6.4	11.8
SETRES	Control	4	24	12.9	2.1	4.8	17.8	6.7	1.3	2.7	9.7
	Fertilized, irrigated or both	12		16.6	2.5	6.0	22.1	9.7	2.1	3.8	15.5
Henderson	Control	12	26	21.1	2.4	13.4	27.9	14.8	1.7	8.9	20.8
	Vegetation control	12		21.9	2.2	14.0	26.9	15.8	1.8	6.2	20.9
Total		110		15.8	3.7	10.6	23.8	8.8	3.9	13.6	24.7

Table 3.4 Summary statistics for lidar ground and all returns (hag > 0.2 m), and the intensity values for the vegetation returns (hag > 1m). Intensity minimum values were 1 for all groups of plots. Column annotation: n (number of observations or plots), Gr_{total} (total number of ground returns), All_{total} (total number of all returns), Stdv (standard deviation), and Max (maximum value).

Study	**Treatment**	***n***	**Gr_{total} (mean)**	**All_{total} (mean)**	**Return heights (m)**			**Intensity (watts)**		
					Mean	**Stdv**	**Max**	**Mean**	**Stdv**	**Max**
NSD	Control	3	592	1992	6.2	2.6	11.5	34	14	93
		3	719	2882	7.2	2.4	12.1	37	14	75
	Fertilized	6	589	2685	6.7	2.5	12.1	39	15	91
		6	660	3095	7.5	2.4	12.1	41	15	80
RW19	Fertilized	32	1042	2460	8.3	3.4	15.2	37	16	115
RW18	Control and thinned	2	461	510	11.8	3.5	16.7	29	15	66
	Fertilized unthinned	4	223	1139	11.3	5.0	18.6	35	13	71
	Fertilized and thinned	14	430	740	10.9	4.7	19.4	31	15	87
SETRES	Control	4	814	2986	9.8	3.2	18.1	29	13	69
	Fertilized, irrigated or both	12	757	2589	13.3	4.0	21.2	34	15	80
Henderson	Control	12	131	1628	14.9	5.4	24.7	32	19	103
	Vegetation control	12	297	1487	16.1	6.7	25.7	30	16	105

Table 3.5 Pearson correlation coefficients for the independent variables used to predict number of trees, for each subset of plots (*n* = 110, 78, 70, and 40). The first row of each variable corresponds to the coefficients of determination when using all the plots (*n* = 110). Statistically significant correlations at $\alpha = 0.05$ are in bold. Field based variables are N_{trees} (number of trees per plot) and $Tree_0$ (initial number of trees per plot); lidar variables are described in table 3.1.

	N_{trees}	$Tree_0$	LPI	All_{10th}	All_{90th}	I_{stdv}	I_{cv}	d_5	d_6	d_7	d_9	Cd-1	Cd-2	Cd-4	Cd-5	Cd+2	$Cd{+}4_{stdv}$
N_{trees}		**0.856**	**-0.384**	-0.050	**-0.338**	-0.170	**-0.441**	0.111	**0.326**	**0.359**	**-0.432**	**0.348**	0.175	-0.089	**-0.297**	0.049	**0.193**
(*n* = 78)	1	**0.775**	**-0.637**	0.171	**-0.278**	**-0.460**	**-0.598**	**0.417**	**0.462**	**0.349**	**-0.416**	**0.539**	**0.315**	-0.056	**-0.286**	-0.005	0.146
(*n* = 70)		**0.904**	**-0.494**	-0.182	**-0.572**	0.090	**-0.403**	0.024	0.216	**0.359**	**-0.496**	**0.405**	0.219	-0.171	**-0.313**	0.053	0.169
(*n* = 40)		**0.859**	**0.641**	**0.417**	**-0.608**	**-0.841**	**-0.792**	**0.511**	**0.783**	**0.744**	**-0.741**	0.143	0.065	0.094	**-0.388**	0.063	**0.336**
Tree0			-0.090	0.168	**-0.233**	-0.142	**-0.308**	0.026	**0.325**	**0.382**	**-0.389**	**0.197**	0.105	0.097	-0.108	0.117	**0.290**
(*n* = 78)		1	**-0.268**	**0.481**	-0.183	**-0.374**	**-0.447**	**0.328**	**0.420**	**0.400**	**-0.394**	**0.335**	0.218	0.209	-0.043	0.137	**0.320**
(*n* = 70)			-0.136	-0.172	**-0.318**	**0.235**	-0.108	-0.144	0.056	**0.261**	**-0.337**	0.200	0.069	-0.114	-0.226	0.062	0.120
(*n* = 40)			**0.746**	**0.692**	**-0.796**	**-0.559**	**-0.837**	**0.542**	**0.816**	**0.747**	**-0.732**	0.095	0.092	0.289	-0.052	0.178	**0.585**
LPI				-0.029	-0.108	0.091	**0.250**	-0.170	0.029	0.099	0.014	**-0.528**	**-0.397**	-0.159	-0.074	-0.126	**-0.245**
(*n* = 78)			1	-0.032	-0.153	0.099	**0.234**	-0.101	0.009	0.117	-0.005	**-0.565**	**-0.437**	-0.162	-0.081	-0.119	**-0.276**
(*n* = 70)				0.192	**0.665**	0.178	**0.662**	**-0.453**	-0.271	**-0.283**	**0.549**	**-0.498**	**-0.371**	0.016	0.130	-0.109	**-0.335**
(*n* = 40)				0.274	**-0.759**	**-0.520**	**-0.488**	**0.707**	**0.772**	**0.370**	**-0.571**	-0.101	-0.015	0.211	-0.095	0.084	**0.507**
All_{10th}					**0.309**	**-0.216**	**-0.229**	-0.160	-0.007	-0.005	0.157	**0.324**	**0.306**	**0.290**	**0.264**	0.099	0.071
(*n* = 78)				1	0.164	-0.064	**-0.230**	-0.101	-0.028	0.116	0.010	**0.260**	**0.269**	**0.286**	**0.235**	0.167	**0.223**
(*n* = 70)					**0.288**	**-0.389**	**-0.349**	-0.104	-0.046	-0.161	**0.268**	**0.287**	0.232	-0.030	0.022	-0.085	**-0.292**
(*n* = 40)					**-0.423**	0.001	**-0.608**	0.092	**0.355**	**0.526**	**-0.361**	0.062	0.163	**0.317**	0.294	0.255	**0.576**
All_{90th}						0.031	**0.558**	**-0.552**	**-0.658**	**-0.561**	**0.730**	0.175	**0.212**	**0.392**	**0.413**	-0.015	**-0.199**
(*n* = 78)					1	0.218	**0.616**	**-0.677**	**-0.780**	**-0.527**	**0.683**	0.122	0.185	**0.414**	**0.381**	0.100	-0.076
(*n* = 70)						-0.061	**0.484**	**-0.455**	**-0.648**	**-0.374**	**0.686**	-0.125	0.013	**0.328**	**0.406**	-0.172	**-0.329**
(*n* = 40)						**0.355**	**0.480**	**-0.720**	**-0.775**	**-0.422**	**0.640**	-0.113	-0.104	-0.168	-0.011	-0.235	**-0.619**
I_{stdv}							**0.418**	-0.128	**-0.378**	**-0.257**	**0.274**	**-0.199**	-0.118	0.019	0.150	0.140	0.104
(*n* = 78)						1	**0.468**	**-0.305**	**-0.401**	**-0.372**	**0.466**	-0.164	-0.107	0.044	**0.238**	0.147	0.030
(*n* = 70)							**0.457**	0.004	**-0.251**	-0.059	0.076	**-0.274**	-0.206	0.113	-0.155	0.180	0.186
(*n* = 40)							**0.542**	**-0.416**	**-0.563**	**-0.468**	**0.539**	-0.061	0.045	0.042	**0.577**	0.140	0.049
I_{cv}								**-0.282**	**-0.518**	**-0.541**	**0.506**	**-0.385**	-0.187	0.171	**0.296**	0.083	0.009
(*n* = 78)							1	**-0.395**	**-0.574**	**-0.572**	**0.543**	**-0.390**	-0.186	0.192	**0.304**	0.150	0.034
(*n* = 70)								-0.190	**-0.370**	-0.171	**0.289**	**-0.672**	**-0.461**	0.149	0.165	0.129	0.113
(*n* = 40)								-0.220	**-0.578**	**-0.715**	**0.541**	**-0.317**	-0.067	-0.157	0.222	-0.106	-0.265
d_5									**0.543**	**0.270**	**-0.628**	-0.107	-0.153	-0.167	**-0.247**	0.173	**0.307**
(*n* = 78)								1	**0.818**	**0.292**	**-0.821**	-0.050	-0.114	-0.203	**-0.242**	0.086	**0.310**
(*n* = 70)									**0.325**	0.048	**-0.479**	0.000	-0.058	-0.048	-0.142	**0.240**	**0.318**
(*n* = 40)									**0.820**	**0.323**	**-0.808**	-0.095	-0.112	-0.029	-0.185	0.203	**0.443**
d_6										**0.660**	**-0.802**	-0.052	-0.086	-0.153	**-0.277**	-0.024	**0.235**
(*n* = 78)									1	**0.702**	**-0.899**	-0.040	-0.086	-0.175	**-0.312**	-0.001	**0.267**
(*n* = 70)										**0.469**	**-0.631**	0.071	-0.005	**-0.250**	-0.224	-0.096	0.076
(*n* = 40)										**0.724**	**-0.903**	-0.009	0.010	0.185	-0.151	0.152	**0.541**
d_7											**-0.714**	0.027	-0.002	-0.148	**-0.326**	-0.075	0.136
(*n* = 78)										1	**-0.688**	0.074	0.053	-0.120	**-0.292**	-0.175	0.036
(*n* = 70)											**-0.376**	**0.278**	0.225	-0.164	**-0.345**	-0.083	0.100
(*n* = 40)											**-0.757**	0.184	0.114	0.191	-0.116	0.029	0.313
d_9												0.099	0.100	0.163	**0.247**	-0.058	**-0.337**
(*n* = 78)											1	0.040	0.050	0.141	0.198	0.034	**-0.242**
(*n* = 70)												-0.078	-0.067	-0.058	-0.036	-0.160	**-0.532**
(*n* = 40)												-0.043	-0.033	-0.072	0.204	-0.133	**-0.393**
Cd-1													**0.738**	0.146	-0.026	**-0.268**	**-0.252**
(*n* = 78)												1	**0.746**	0.120	-0.067	**-0.296**	-0.207
(*n* = 70)													**0.780**	0.009	-0.179	**-0.357**	**-0.310**
(*n* = 40)													**0.471**	0.006	-0.126	-0.305	-0.314
Cd-2														**0.561**	**0.302**	**-0.543**	**-0.250**
(*n* = 78)													1	**0.531**	**0.269**	**-0.543**	-0.170
(*n* = 70)														**0.448**	0.120	**-0.606**	**-0.361**
(*n* = 40)														**0.635**	**0.425**	**-0.659**	-0.155
Cd-4															**0.754**	**-0.321**	0.069
(*n* = 78)														1	**0.772**	**-0.251**	0.198
(*n* = 70)															**0.696**	**-0.362**	-0.050
(*n* = 40)															**0.732**	**-0.534**	0.123
Cd-5																-0.162	0.152
(*n* = 78)															1	-0.089	**0.274**
(*n* = 70)																-0.206	0.102
(*n* = 40)																-0.275	0.155
Cd+2																	**0.652**
(*n* = 78)																1	**0.631**
(*n* = 70)																	**0.699**
(*n* = 40)																	**0.560**

Table 3.6 Best predictive models to estimate number of trees (N_{trees}) using lidar metrics only for the entire dataset (*n* = 110), mid-rotation age plots (*n* = 70), and end-of-rotation age plots (*n* = 40). The explanatory variables were centered. CV-RMSE refers to RMSE from the cross validation analyses, $R^2_{adj'}$ is the adjusted R^2 from the model, SSCC is the squared semipartial correlation coefficient from partial sum of squares, VIF is the variance inflation factor, and CI is the condition index. All coefficients were significant at $p < 0.05$. Variable names are described in table 3.1.

n	**# var.**	**R^2**	**$R^2_{adj'}$**	**RMSE**	**CV-RMSE**	**Variables**	**Coefficient**	**SSCC**	**VIF**	**CI**
110	5	0.51	0.48	28.65	29.28	Intercept	73.373	-----	-----	-----
						LPI	-131.721	0.09	1.56	1.09
						d_5	-170.974	0.83	1.85	1.34
						d_9	-219.750	0.23	1.70	1.42
						Cd-5	-946.509	0.06	1.12	1.96
						Cd-1	280.712	0.02	1.50	2.42
70	5	0.62	0.59	29.91	31.44	Intercept	41.053	-----	-----	-----
						All_{90th}	-13.902	0.17	2.33	1.68
						d_5	-177.600	0.09	1.36	1.97
						d_6	-295.245	0.08	1.95	2.23
						d_9	-285.096	0.09	2.28	3.40
						Cd-1	581.975	0.10	1.02	4.89
40	5	0.96	0.95	4.96	5.48	Intercept	73.315	-----	-----	-----
						I_{stdv}	-6.245	0.26	1.61	1.32
						I_{cv}	-0.976	0.02	2.37	1.50
						d_7	42.287	0.01	2.26	1.76
						$Cd+4_{stdv}$	48.911	0.06	1.28	3.14
						Cd-2	114.877	0.01	1.09	3.25

Table 3.7 Best predictive models to estimate number of trees (N_{trees}) using lidar and ground data for the entire dataset (*n* = 110), for a subset without the RW19 study (*n* = 78), and for mid-rotation age plots (*n* = 70). The explanatory variables were centered. CV-RMSE refers to RMSE from the cross validation analyses, R^2_{adj}, is the adjusted R^2 from the model, SSCC is the squared semipartial correlation coefficient from partial sum of squares, VIF is the variance inflation factor, and CI is the condition index. $Tree_0$ is the initial number of trees at the moment of planting. All coefficients were significant at $p < 0.005$. Variables in the models are described in table 3.1.

n	# var.	R^2	R^2_{adj},	RMSE	CV-RMSE	Variables	Coefficient	SSCC	VIF	CI
110	2	0.83	0.82	16.69	16.94	Intercept	73.373	-----	-----	-----
						$Tree_0$	0.850	0.68	1.01	1.04
						LPI	-108.503	0.10	1.01	1.10
110	5	0.92	0.92	11.43	11.82	Intercept	73.373	-----	-----	-----
						$Tree_0$	0.911	0.75	1.05	1.06
						All_{10th}	-1.373	0.01	1.16	1.20
						LPI	-129.548	0.13	1.07	1.22
						Cd+2	-305.065	0.02	1.23	1.32
						Cd-4	-736.945	0.05	1.34	1.77
78	5	0.95	0.94	8.25	8.61	Intercept	68.686	-----	-----	-----
						$Tree_0$	0.689	0.30	1.53	1.09
						LPI	-143.229	0.26	1.12	1.17
						d_6	48.499	0.01	1.38	1.31
						Cd+2	-368.642	0.05	1.16	1.53
						Cd-4	-737.816	0.08	1.30	2.09
70	4	0.97	0.97	8.34	8.74	Intercept	73.167	-----	-----	-----
						$Tree_0$	0.954	0.53	1.22	1.07
						All_{90th}	-3.299	0.01	2.33	1.45
						LPI	-83.305	0.02	2.78	1.85
						Cd-1	205.669	0.01	1.60	4.70

4. COMBINED USE OF AIRBORNE LASER SCANNING DATA AND DUAL-BAND, SINGLE-PASS INTERFEROMETRIC SYNTHETIC APERTURE RADAR DATA TO ESTIMATE LEAF AREA INDEX IN TEMPERATE MIXED FORESTS

4.1 Abstract

The objective of this study was to determine whether leaf area index in temperate mixed forests is best estimated using multiple-return airborne laser scanning (lidar) data or dual-band, single-pass interferometric synthetic aperture radar data (from GeoSAR) alone or both in combination. In situ measurements of LAI were made using the LiCor LAI-2000 Plant Canopy Analyzer on 61 plots (21 hardwood, 36 pine, 4 mixed pine hardwood; stand age ranging from 12-164 years; mean height ranging from 0.4 to 41.2 m) in the Appomattox-Buckingham State Forest, Virginia, USA. Lidar distributional metrics were calculated for all returns and for ten one meter deep crown density slices (a new metric), five above and five below the mode of the vegetation returns for each plot. GeoSAR metrics were calculated from the X-band backscatter coefficients (four looks) as well as both X- and P-band interferometric heights and magnitudes for each plot. Lidar and GeoSAR metrics were used as independent variables in best subsets regressions with LAI (measured in situ) as the dependent variable. Lidar metrics alone explained 69% of the variability in LAI, while GeoSAR metrics alone explained 52%. However, combining the lidar and GeoSAR metrics increased the R^2 to 0.77 with a CV-RMSE of 0.42. The most important metrics in the combined model were the 50th percentile of the X-band interferometric height and the 50th percentile of the lidar returns above 0.2 m. This study indicates the clear potential for X-band backscatter and interferometric height (both now

available from spaceborne sensors), when combined with small-footprint lidar data, to improve LAI estimation in temperate mixed forests.

4.2 Introduction

Leaf area index (LAI) is an important canopy descriptor used to estimate growth and productivity in forest ecosystems. Watson (1947) stated one of the early definitions of LAI as the total one-sided area of leaf tissue per unit of ground surface area. Thus, LAI is a dimensionless index that represents an important method to quantify the amount of photosynthesizing tissue in forests. Leaves are radiation receivers (depending on the amount of productive leaves and their specific surface area, they absorb between 80 to 90% of the light assimilated by forests), they are the main photosynthesizing organ in forest stands, thus variations in leaf production and light interception are directly related to forests growth and development. Accordingly, LAI is a key variable that can be used to monitor current forest stand growth and has become a key explanatory variable for ecosystem process models.

Remote sensing estimation of LAI has been mostly based on empirical modeling, using vegetation indices, generally developed with the spectral reflectance from the near-infrared and red wavelengths, and their correlations with ground-truth estimates. However, the use of optical imagery carries some disadvantages: It is only suitable to evaluate horizontal variation, optical sensors are unable to obtain data from the ground under a cloud cover, and most importantly, vegetation indices calculated using optical imagery tend to reach a saturation point when LAI values are between 3 to 5; this limitation can be particularly important when estimating LAI in the eastern US hardwood and mixed forests where reported estimations have ranged from 3.9 to 7.3 (Vose et al. 1995) and from 3.5 to 5.1 (Sampson et al. 1997).

Two fairly recent technologies could potentially improve the estimate of LAI in these forests where canopies can vary greatly not only horizontally but also vertically, and the likelihood of reaching a reflectance saturation point is high. Light detection and ranging (lidar) sensors measure the time between the emission and reception of laser pulses to estimate the location and height of the target feature. They thus acquire information in three dimensions (x, y, and z coordinates) and provide the means to evaluate variation across a vertical profile. Previous studies in which LAI was estimated in mixed forests using lidar data report the following results: (1) an R^2 of 0.89 (RMSE = 1.53) using eighteen 400 m^2 plots (14 coniferous, 6 hardwoods) (Barilotti et al. 2005), in which the laser penetration index (LPI, taking into account the transmission of the laser beams through the canopy) was used; (2) an R^2 of 0.86 (RMSE = 0.09) using 10 plots (400 m^2) in a hardwood forest (Kwak et al. 2007), using the LPI and an interception index (LII) that uses the vegetation returns; (3) an adjusted R^2 of 0.80 (RMSE = 0.23) using 17 plots with areas ranging from 60 m^2 - 400 m^2 distributed in a broad-leaved forest (Sasaki et al. 2008), and (4) an R^2 of 0.84 (RMSE = 0.29) for 53 plots of 491 m^2, 14 mixed hardwoods and 39 coniferous (18 in young pine plantations and 21 in mature pine stands) (Zhao and Popescu 2009). No prior study has reported a maximum LAI or saturation problem using lidar (Jensen et al. 2008; Morsdorf et al. 2006).

Dual-band interferometric synthetic aperture radar (DBInSAR) can now be collected using the geographic synthetic aperture radar (GeoSAR) airborne radar mapping system. GeoSAR acquires X-band (VV, 9.7 GHz and P-band (HH, 0.35 GHz) simultaneously over 11 km swaths (Williams et al. 2009). GeoSAR has emerged as a potential instrument to be used to estimate forest attributes, such as canopy height (Sexton et al., 2009) and biomass (Williams et al. 2009; Williams et al. 2010). Long wavelengths from the P-band (0.85 m) penetrate the upper canopy and can reach the ground; short wavelengths (0.03 m) from the X-band are scattered at the top of the canopy. This technology has been widely used in tropical regions where forest canopies are usually under clouds most of the year (Carson 2008; Williams and Jenkins 2009).

Previous attempts to estimate LAI using SAR (Synthetic Aperture Radar) data have found low correlations between ERS-2 (European Remote Sensing Satellite-2) SAR backscatter and LAI or biomass, but significant correlations between a green leaf biomass index (calculated using ERS-2 SAR backscatter) and LAI, in Mediterranean vegetation (Svoray et al. 2001). Other researchers have found saturation problems for the C-band (radar band that operates at a wavelength of 4-8 cm) backscatter with high values of LAI in tundra ecosystems and plantation forests (Durden et al. 1995; Paloscia 1998). Manninen et al. (2005) used a C-band backscatter ratio from ENVISAT (ENVIroment SATellite)/ASAR (Advanced Synthetic Aperture Radar) in a mixed forest obtaining an RMSE of 0.27. While these and other studies have used radar backscatter to estimate LAI, none to date has assessed the potential utility of interferometric heights for LAI estimation. Given that lidar data have been shown to enable robust LAI estimation, and both lidar and DBInSAR can be used to estimate canopy heights, we posited that the DBInSAR data from GeoSAR could be useful for remote sensing of LAI. As such, the objective of this study was to determine whether leaf area index in temperate mixed forests is best estimated using multiple-return airborne laser scanning (lidar) data or dual-band, single-pass interferometric synthetic aperture radar data (from GeoSAR) alone or both in combination.

4.3 Methods

4.3.1 Study site

The study area is located in Appomattox Buckingham State Forest in Virginia, at 37º25'9" N and 78º40'30" W (fig. 4.1). The elevation range is between 180 to 200 meters. This forest is composed of coniferous, hardwoods, and mixed stands. Three pine species are found: loblolly pine (*Pinus taeda* L.), shortleaf pine (*Pinus echinata* Mill.), and Virginia pine (*Pinus virginiana* Mill.); and among the deciduous trees are: northern red oak (*Quercus rubra* L.), white oak (*Quercus alba* L.), red maple (*Acer rubrum* L.), yellow poplar (*Liriodendron tulipifera* L.), blackgum (*Nyssa sylvatica* Marsh.), and american beech (*Fagus grandifolia* Ehrh.). Measurement plots are of two types: fixed radius plots and variable radius plots, the latter based on basal area guidelines. The fixed radius plots were installed in 1999 following U.S. National Forest Inventory and Analysis (FIA) guidelines. The plots are composed of 4 circular sub-plots (one in the center and three in a triangle shape around the center); each sub-plot has a radius of 7.32 meters (for tree measurement), and they are 36.58 meters apart from each other. 219 variable radius plots installed in 2002 using a basal area factor of 10 (BAF) and following a grid of 201.17 meters (10 chains) (van Aardt et al. 2006). For more details about this study design see Popescu et al. (2002).

4.3.2 ***Field data collection and analysis***

4.3.2.1 Inventory data

All plots were measured during the 2008 dormant season. Total tree height (ht) and diameter at breast height (dbh) were assessed for every individual with a dbh > 2.54 cm within the measurement plots using a Haglöf Vertex hypsometer and diameter tape.

4.3.2.2 Leaf area measured with an optical sensor

Leaf area index data were collected during late summer (September, 2008), using the LiCor LAI-2000 Plant Canopy Analyzer. Above-canopy readings were recorded remotely every 15 seconds by placing an instrument in an open field adjacent to the stand during the same date and time that measurements were taken inside the stand. The measurements inside the stand, below-canopy readings, were made holding the instrument at the height of 1 m facing upwards. This same procedure was repeated in every plot regardless of the presence of understory or mid-story vegetation. Due to the instrument design, measurements were taken under diffuse sky conditions to ensure that the sensor used indirect light only. Thus, measurements were taken during the dawn and predusk periods, with the above instrument facing north and using a 90º view cap. Sampling points were distributed in the following manner: one reading at the center of the plot, and one reading at 5 meters away from the center in each cardinal direction (north, south, east and west), for a total of 5 readings per plot. The calculation of LAI was accomplished using the FV-2000 software which averaged all the readings per plot. The canopy model used to calculate LAI was Horizontal (LI-COR 2010); the ring number 5 was masked to reduce the error introduced by the stem and branches of trees; and the option of skipping records with transmittance > 1 was used in order to avoid bad readings that can alter the mean values of LAI per plot. The above and below canopy records were matched by time (Welles and Norman 1991).

The center of the plots was found using GPS navigation, only 51 fixed radius plots were measured since 12 of them had been clear cut. Additionally, 30 variable radius plots were measured, distributed mainly near the access roads (fig. 4.1).

4.3.2.3 Lidar data

Small footprint lidar data were acquired in late August 2008. The system was an Optech ATLM 3100 with an integrated Applanix DSS 4K x 4K DSS camera. The data have multiple returns with a sampling density of 5 pulses per square meter, with 4 or fewer returns per pulse. The scan angle was less than 15 degrees. Instrument vertical accuracy over bare ground is 15 cm, and horizontal accuracy is 0.5 m.

The inverse distance weighted interpolation method was used to generate a digital elevation model (DEM) with the data classified as ground returns (Popescu 2002). Next, all data points ≥ 1 m of height above the ground (hag) were classified as vegetation returns; this threshold was selected to match the height at which the instrument was used to estimate LAI on the ground. Another set classified as "all returns" was defined using a threshold of ≥ 0.2 m hag. Next, lidar data points per plot were separated in three classes: "ground returns" (hag = 0 m), "all returns" (hag > 0.2 m), and "vegetation returns" (hag > 1 m). Vegetation returns were classified using a 1 m threshold because the instrument used to estimate LAI in situ was held at approximately 1 m above the ground. The metrics derived from the ground returns class (Gr) were: frequency (count) of returns and frequency (count) of pulses (table 4.1). The metrics derived from the all returns class (All) were: frequency (count), mean height, standard deviation, coefficient of variation, minimum, maximum, percentiles (10, 20, 25, 40, 50, 75, and 90), and frequency (count) of pulses (Holmgren 2004; Popescu 2002). The metrics derived from the vegetation returns class (Veg) were the same described for the all returns class with the addition of the mode. The distribution of intensity values (I) were described using the mean, minimum, maximum, standard deviation, and coefficient of variation. First, second, third and fourth returns were classified as such and divided by the total number of "vegetation returns" (R). The Laser Penetration Index (LPI) (Barilotti et al. 2005) was calculated per plot as the proportion of ground pulses to the total pulses (ground pulses + all pulses). Density metrics (d) were calculated following Naesset (2002), as the proportion of returns found on each of 10 sections equally divided within the range of heights of vegetation returns for each plot. Additionally, another set of metrics, crown density slices (Cd), was calculated using the mode value of vegetation returns. Ten 1-meter sections of vegetation returns (5 above and 5 below the mode value, based on the maximum value of crown length observed) were classified and proportion of returns to the total number of returns, mean, standard deviation, and coefficient of variation were calculated (fig. 4.2). Frequency of returns (count), calculated from each of the lidar data point classes, were used only to estimate other metrics, such as proportions of returns, but they were not used in the development of the models (table 4.1).

Ground plots were overlaid on digital orthophotographs acquired at the same time as the lidar data. Sixteen plots partially encompassed roads or herbaceous areas. These plots were eliminated from the dataset.

4.3.2.4 GeoSAR data

GeoSAR data were acquired in late summer 2008. The system recorded data from two microwave bands, X (VV, 9.7 GHz) with a 0.03 m wavelength and P (HH, 0.35 GHz) with a 0.85 m wavelength, in single passes. Postings from the X-band were 3 m; those from the P-band were 5 m. GeoSAR X-band interferometry yields a digital surface model (DSM) and P-band interferometry is used to create a digital elevation model (DEM). Previous research has used the difference between the DSM and DEM to create a canopy height model used to estimate forest biomass (Williams et al. 2009). The provider (Fugro EarthData, Inc.) performed the preprocessing, including both the interferometry and generation of two orthorectified magnitude images: (1) the magnitude from bands X and P, expressed as the squared root of the intensity values and (2) the sigma-0 (σ_0) or backscatter coefficient from all four looks (North, South, East, West), defined as the backscatter power per unit area on the ground.

Analogous to those used with lidar-derived heights and intensities, GeoSAR metrics were developed using the following approach (see also table 4.1):

- In order to evaluate the vegetation height, the difference between X-band (mostly backscattered from the vegetation/canopy surface) and P-band (mostly from the ground and lower tree branches) interferometric heights was calculated. In addition, the X-band was divided by the P-band with the purpose of evaluating any other relationship between the two layers.
- The high resolution DEM created from the lidar data were used to generate the heights above ground for the X and P bands.
- No changes were made to the magnitude layers or the σ_0 layers.

- The cell values from all the layers (10 in total) were extracted and the frequency, mean, standard deviation, coefficient of variation, minimum, maximum, and percentiles (10^{th} to 90^{th}) were calculated for all plots.

4.3.2.5 Statistical analysis

Based on the sampling distance and the conical view of the Licor LAI-2000 sensor (which radius is three times the canopy height), a buffer of 20 m was used from the center of each plot, generating circular plots of 1256.6 m^2 of size. A dataset of 81 plots was compiled for all lidar-derived, GeoSAR-derived and ground-truth metrics. However, after deleting plots for proximity to roads and for being outliers (but not influential), the number of plots was reduced to 61. Pearson correlation coefficients were used to evaluate relationships among lidar metrics, GeoSAR metrics and measured LAI. Multiple regressions were used to fit the dataset. Best subset regression models were examined using the RSQUARE method for best subsets model identification (SAS 2010). This method generates a set of best models for each number of variables (1, 2, …, 6, etc.). The criterion to choose the models with the best group of variables was a combination of several conditions, as follows:

- High coefficient of determination (R^2) value.
- Low residual mean square (RMSE).
- Similarity between the adjusted coefficients of determination $R^2_{adj'}$ and R^2 values. The $R^2_{adj'}$ is a rescaling of R^2 by degrees of freedom, hence involves the ratio of mean squares instead of sum of squares.
- Mallows' C_p statistic values (Hocking 1976). When the model is correct, the C_p is close to the number of variables in the model.

- Low values from two information criteria, the Akaike (1969) Information Criterion (AIC) and Schwarz (1978) Bayesian Criterion (SBC). The AIC is known for its tendency to select larger subset sizes than the true model; hence the SBC was used for comparison, since it penalizes models with larger number of explanatory variables heavier than AIC.

The best models chosen per each subset size (based on number of variables in the models) were evaluated for collinearity issues. Near-linear dependencies between the explanatory variables were evaluated using computational stability diagnostics. In order to make independent variables orthogonal to the intercept and therefore remove any collinearity that involves the intercept, independent variables were centered by subtracting their mean values (Belsley 1984; Marquart 1980). The variance inflation factor (VIF) with a threshold of 10 was used to quantify how much the variance of an estimated regression coefficient was inflated. However, condition index (CI) was also evaluated for all variables within the models since VIF neither detects multiple near-singularities nor identifies the source of singularities (Rawlings et al. 2001). Condition index is the square root of the ratio of the largest eigenvalue to the corresponding eigenvalue from the dataset matrix. Similar to VIF, the CI indicates weak dependencies when higher than 10 but lower than 30, and severe dependencies when higher than 30.

Additional data to test the models were not available, thus cross-validation analysis was performed using the prediction sum of squares (PRESS), which is the sum of squares of the difference between each observation and its prediction when that observation was not used in the prediction equation (Allen 1971). The root mean square error from the cross validation analysis (CV-RMSE) was then calculated as the square root of the ratio between the PRESS statistic and the number of observations. The CV-RMSE is an indicator of the predictive power of the model.

The significance level used for all the statistical tests was $\alpha = 0.05$ (p-value < 0.05). This p-value was used to evaluate if the variables included in the model were statistically significant as well. The squared semipartial correlation coefficients (SSCC) were calculated using partial sum of squares to determine the contribution from each variable to the models, while controlling the effects of other independent variables within the model. These coefficients represent the proportion of the variance of the dependent variable associated uniquely with the independent variable.

Although the statistical analyses applied to the dataset of 61 plots did not show the presence of outliers, three of these plots with measured low LAI values (1.34 to 1.43) could potentially be influencing the dependent versus independent variable relationships. Therefore, best subset analyses were also applied to the dataset after removing these three observations (n = 58).

4.4 Results

4.4.1 Summary statistics from ground measurements and lidar metrics

The 61 plots were distributed within the different forest types as follows: 3 in bottomland hardwoods, 18 in upland hardwoods, 4 in mixed pine-hardwoods, 24 in loblolly pine, 6 in shortleaf pine, and 6 in Virginia pine. For all forest types, stand age ranged between 10 and 164 years. Mean tree height ranged from 13 m to 16 m, and mean dbh from 13 cm to 24 cm. Leaf area index values estimated on the ground were between 3.4 to 4.1 (table 4.2). For all groups of forest types, the mean number of lidar ground returns ranged between 222 and 555, and for all returns (hag > 0.2 cm) from 4343 to 5278. Mean lidar heights above ground were between 9.9 m to 13.2 m, with standard deviations ranging from 4.5 m to 6.8 m (table 4.3). Minimum heights were set to 0.2 m, and maximum values ranged from 25.3 m to 37.6 m. Intensity mean values from vegetation returns (hag > 1 m) were observed between 37 to 51 watts. Standard deviations from the intensity values were over 20 watts for all groups of plots. Laser penetration index (LPI) was lowest (0.003) for the pine-hardwoods and shortleaf pine group of plots, and highest (0.039) for the upland hardwood plots.

The mean number of cells per plot from the GeoSAR P-band was 49, and for the X-band was 138. Mean heights from the P-band ranged from 5.46 m to 10.48 m, while for the X-band they ranged from 10.84 m to 16.06 m (table 4.4). Mean heights from the X-band were always higher than lidar returns, except for the upland hardwood plots. However, maximum values from the lidar returns were as much as 10 m higher than the maximum values from the X-band. P-band mean height values were high (up to 18 m) from the ground, which made the difference of X and P bands to be low, sometimes as low as half the mean height observed from the lidar returns. A comparison between lidar returns and GeoSAR heights for an upland hardwood plot can be visualized in figure 4.3. The range of magnitude values from the P-bands was larger than from the X-band, as shown by the standard deviation.

The vertical profile (distribution of heights vs. frequency) from lidar returns (fig. 4.4) showed two peaks, one at the mode value (13 m) and a second one at lower height. The latter might be related to a well-defined understory stratum in the forest stands. Also, a graph was obtained from the distribution of GeoSAR X-band heights, showing two peaks at similar heights to the lidar (fig. 4.4).

4.4.2 Variable selection and modeling

Pearson correlation coefficients were summarized for the variables included in the best models (table 4.5). Laser penetration index (LPI) had the highest correlation with LAI (-0.698), followed by All_{10th} (0.638) and X_{50th} (0.609). Also, d_2 (-0.347) and X_{cv} (-0.485) were statistically significant. The 10th and 20th percentiles (height values) were the only percentiles of any type significantly correlated with LAI.

The best models from lidar metrics had R^2 values up to 0.69 with 4 variables in the model. Adding more variables increased the R^2 and resulted in no collinearity problems. However, there was always at least one variable not contributing significantly to the model. Hence, only models with 2 and 4-variables were reported (table 4.6). Common variables in these models were LPI and All_{10th}, the increase in R^2 (from 0.58 to 0.69) was given by the d_{10} and Cd-3 metrics. The largest contribution in both models was from the LPI (0.174 and 0.202), and in the 4-variable model the other three variables (All_{10th}, d_{10}, and Cd-3) had a similar contribution (0.053, 0.064, and 0.059). Predicted values from the 4-variable model were plotted against the measured LAI (fig. 4.5). The results from the best subset analyses for GeoSAR metrics showed that although the R^2 values increased when adding more variables to the model, the R^2_{adj}, did not, therefore only a 4-variable model with an R^2 of 0.52 is shown in table 4.6. The variable that contributed the most was X_{50th} (0.127), followed by X_{cv} (0.098), $sn01xl_{cv}$ (0.047), and $Xmag_{stdv}$ (0.035). All variables included in the lidar only and GeoSAR only models had a VIF and CI lower than 5.

The best-performing models from the best subsets regressions using the metrics from lidar and GeoSAR combined are reported in table 4.7. The R^2 values ranged from 0.66 from a 2-variable model to 0.77 from a 6-variable model. The All_{50th} and X_{50th} variables were included in all models; the latter was the only variable from GeoSAR that was included. Other variables included in these models from lidar were LPI, d_2, and two crown density metrics (Cd-1, and Cd-3_{stdv}). The largest contributions (always higher than 0.1) were from the All_{50th} and X_{50th} variables. Between the 5 and 6-variable model, the R^2 and R^2_{adj}, increased and the RSME decreased with an extra variable, but the CV-RMSE stayed the same. There were no collinearity issues flagged by the VIF and CI, which were under 5 for all variables. Predicted values from the 4-variable model and 6-variable model are shown in figures 4.6 and 4.7 for comparison. The difference in R^2 values between these two is only 0.04, but the observations from the 6-variable model are distributed closer to the 1:1 line, suggesting a better fit.

The best models obtained from the best subset regression analyses applied to the dataset without the low LAI plots (*n* = 58), consistently included the same variables than the best models obtained when using the dataset of 61 plots. The R^2 values were lower (0.1 lower) than the R^2 values observed when using the 61 plots (fig. 4.8), however, this reduction of the R^2 values can be attributed to the reduced number of plots representing the low levels of the LAI range. In addition, the fact that the best models included the exact same variables than the models from the 61 plots, and that the reduction of the R^2 values is only 0.1 confirms that such plots are not influential enough to drive the relationship in the models. Therefore, since the exclusion of these three plots did not affect the relationship of measured LAI with the lidar and GeoSAR metrics, most of the results reported in this research used the dataset with 61 plots.

Crown density metrics were included in the best models using 5 or more variables. These were removed as independent variables, and the data re-analyzed. The results from these analyses are shown in table 4.8. It was noticeable than in the absence of the crown metrics from lidar, more variables from GeoSAR were included in the models, to the point of obtaining R^2 and

RMSE values comparable to the models in table 4.7. The additional metrics from GeoSAR were $Pmag_{stdv}$ and $Pmag_{max}$. The VIF values from these two models increased to 7.6 compared to the models with the crown metrics, due to the high correlation between $Pmag_{stdv}$ and $Pmag_{max}$ (0.931).

4.5 Discussion

The LAI range of values, among all plots, was large enough to develop a relationship with lidar metrics. There were few representatives (3) at the low range of LAI. These three plots were influential, and therefore, were not deleted from the dataset. Previous research has shown success estimating LAI in mixed forest using lidar metrics.

The high correlation of LPI with leaf area index was expected (Barilotti et al. 2006). Laser penetration index, defined as the proportion of ground pulses to the total number of pulses, is directly related to the amount of leaves and canopy thickness. The more open the canopy the more pulses reach the ground, and vice versa. This variable was included in the models that were developed with either lidar metrics alone or with the combination of lidar and GeoSAR metrics. There were two models where LPI was not included, in which the 50th percentile of lidar returns took its place.

Lidar return percentiles are height values calculated based on the vertical density of returns (Naesset 2002). They describe the height of the vegetation density across the stand vertical profiles. In other words, such heights relate to the target heights on the ground, as more targets (i.e. branches, leaves, etc.) the laser encounters at certain height or section from the ground, more returns are obtained from that section of the stand. For example, the 50th percentile value means that 50% of the return heights are above or below that height. In addition, the 10th

percentile was included in the lidar only models, this metric ranged from 0.40 m to 8.08 m, with a mean of 3.54 m for all 61 plots. At this height (of the vertical profile) in the measured forest stands, mostly understory was present, making this stratum an important contributor to the LAI value of the plot.

Similar to the 10^{th} percentile of the lidar returns, the density metric d_{10}, defined as the proportion of returns found at the top of the canopy with respect to the total number of returns from the vegetation, was included in the lidar metric models only (Naesset 2002),. The top of the canopy is directly related to tree crowns, and hence LAI. Almost opposite to d_{10}, the density metric d_2 was selected in the models using lidar and GeoSAR metrics together. This variable relates to the low section of the vertical profile of the stand.

Crown density slice metrics are descriptors of tree crowns, and metrics related with the proportions of returns and standard deviation of the return heights at 1 and 3 meters below the mode value were included in the models. These variables contributed as much as the density metrics. Interestingly, the combination of all returns percentiles, densities, and crown density metrics in the models managed to describe the vegetation at the top, medium, and low level of the vertical profile. For instance, d_{10}, Cd-3, and All_{10th} were together in the 4-variable model for lidar metrics only.

The interferometric heights from the X-band, after corrected by the DEM developed from lidar data, showed the largest correlations with LAI. The 50^{th} percentile of the height values per plot was positively correlated with LAI. The coefficient of variation from all the height values within a plot correlated negatively, suggesting more variability among the height values in plots with low LAI values. In addition, the metrics of the layer generated from the difference between X-band and P-band (X- minus P-band), and the metrics from the P-band interferometry showed significant correlations with LAI but they were not included in the best models. Moreover, the coefficient of variation obtained from the values of one of the σ_0 layers contributed significantly to the model when only GeoSAR data were used.

In the past, models for LAI prediction in mixed hardwood and coniferous forests using only lidar data have reported R^2 values ranging from 0.8 to 0.9, using either very few plots (between 10 to 18) or small plot sizes (400 m^2 to 500 m^2) (Barilotti et al. 2005; Kwak et al. 2007; Sasaki et al. 2008; Zhao and Popescu 2009). The results reported in this research, using 61 plots of 1257 m^2 size, reveal an R^2 of 0.69 (CV-RMSE = 0.48) for lidar only models, and an increased R^2 value of 0.77 (CV-RMSE = 0.42) when using lidar and GeoSAR data together. Considering the variability observed, from the set of plots used in this study, in stand age (10 to 164), forest type (21 plots of hardwoods, 36 plots of pure pine, and 4 plots of pine-hardwood), and also in measured LAI values (1.3 to 4.9), the models developed represent a robust and accurate way to estimate LAI in temperate mixed forests. Importantly, given that the most important metric in the combined model was the 50th percentile of the X-band interferometric height, X-band interferometry – currently possible using spaceborne sensors – shows clear utility for LAI estimation at landscape to regional scales.

At present, a rising hardwood utilization industry, and the current diversity in land ownership and in management plans and goals, requires decision support tools that can aid management, planning, and policy making under these conditions. Leaf area index is a key variable for the estimation of wood production and carbon storage when using such tools. Consequently, robust and accurate models to remotely estimate this variable are essential. The results from this research provide a suite of models in line with these needs.

4.6 Literature cited

Akaike, H. 1969. Fitting autoregressive models for prediction. Ann. Inst. Stat. Math. 21:243-247.

Allen, D. 1971. The prediction sum of squares as a criterion for selection of predictor variables. Univ. of Ky. Dept. of Statistics, Tech. Report 23.

Barilotti, A., S. Turco, and G. Alberti. 2006. LAI determination in forestry ecosystem by lidar data analysis. P. 248-252 *in* Proceedings of Workshop on 3D Remote Sensing in Forestry, Vienna, Austria.

Barilotti, A., S. Turco, R. Napolitano, and E. Bressan. 2005. La tecnologia LiDAR per lo studio della biomassa negli ecosistemi forestali. in 15th Meeting of the Italian Society of Ecology, Torino, Italy.

Belsley, D.A. 1984. Demeaning conditioning diagnostics through centering (with discussion). Amer. Statistician 38:73-77.

Carson, T.M. 2008. Topographic mapping in the equatorial belt using dual-frequency airborne IFSAR (GeoSAR). Photogramm. Eng. Remote Sens. 74(8):939-944.

Durden, S.L., L.A. Morrissey, and G.P. Livingston. 1995. Microwave backscatter and attenuation dependence on leaf area index for flooded rice fields. IEEE Trans. Geosci. Remote Sens. 33(3):807-810.

Jensen, J.L.R., K.S. Humes, L.A. Vierling, and A.T. Hudak. 2008. Discrete return lidar-based prediction of leaf area index in two conifer forests. Remote Sens. Environ. 112(10):3947-3957.

Hocking, R. 1976. The analysis and selection of variables in linear regression. Biometrics. 32:1-49.

Holmgren, J. 2004. Prediction of tree height, basal area and stem volume in forest stands using airborne laser scanning. Scandinavian Journal of Forest Research 19(6):543-553.

Kwak, D.-A., W.-K. Lee, and H.-K. Cho. 2007. Estimation of LAI using lidar remote sensing in forest. P. 248-252 in ISPRS Workshop on Laser Scanning and SilviLaser, Espoo, Finland.

LI-COR. 2010. FV2000 the LAI-2000 data file viewer. P. 73. LI-COR Biosciences, Lincoln, NE USA.

Manninen, T., P. Stenberg, M. Rautiainen, P. Voipio, and H. Smolander. 2005. Leaf area index estimation of boreal forest using ENVISAT ASAR. IEEE Trans. Geosci. Remote Sens. 43(11):2627-2635.

Marquart, D.W. 1980. Comment: you should standarize the predictor variables in your regression models. J. Amer. Stat. Assoc. 75:87-91.

Morsdorf, F., B. Kötz, E. Meier, K.I. Itten, and B. Allgöwer. 2006. Estimation of LAI and fractional cover from small footprint airborne laser scanning data based on gap fraction. Remote Sens. Environ. 104(1):50-61.

Naesset, E. 2002. Predicting forest stand characteristics with airborne scanning laser using a practical two-stage procedure and field data. Remote Sens. Environ. 80:88-99.

Paloscia, S. 1998. An empirical approach to estimating leaf area index from multifrequency SAR data. Internat. J. of Rem. Sens. 19(2):361-366.

Popescu, S.C., R.H. Wynne, and R. Nelson. 2002. Estimating plot-level tree heights with lidar: local filtering with a canopy-height based variable window size. Comput. Electron. Agr. 37:71-95.

Rawlings, J.O., S.G. Pantula, and D.A. Dickey. 2001. Applied Regression Analysis: A Research Tool. Springer.

Sampson, D.A., J.M. Vose, and H.L. Allen. 1997. A conceptual approach to stand management using leaf area index as the integral of site structure, physiological function, and resource supply. P. 447-451 in Proceedings Ninth Biennial Southern Silvicultural Research Conference. U. S. Department of Agriculture, Forest Service, Southern Research Station., Clemson, SC.

SAS. 2010. The SAS System for Windows Release 9.1.3. SAS Institute Inc., Cary, NC USA.

Schwarz, G. 1978. Estimating the dimension of a model. Annals of Statistics. 6:461-464.

Sasaki, T., J. Imanishi, K. Ioki, Y. Morimoto, and K. Kitada. 2008. Estimation of leaf area index and canopy openness in broad leaved forest using an airborne laser scanner in comparison with high-reslution near-infrared digital photography. Landscape Ecol. Eng. 4:47-55.

Svoray, T., M. Shoshany, P.J. Curran, G.M. Foody, and A. Perevolotsky. 2001. Relationship between green leaf biomass volumetric density and ERS-2 SAR backscatter of four vegetation formations in the semi-arid zone of Israel. Int. J. Remote Sens. 22(8):1601-1607.

van Aardt, J., R.H. Wynne, and R.G. Oderwald. 2006. Forest volume and biomass estimation using small-footprint lidar-distributional parameters on a per-segment basis. For. Sci. 52(6):636-649.

Vose, J.M., N.H. Sullivan, B.D. Clinton, and P.V. Bolstad. 1995. Vertical leaf area distribution, light transmittance, and application of the Beer-Lambert law in four mature hardwood stands in the southern Appalachians. Can. J. For. Res. 25:1036-1043.

Watson, D.J. 1947. Comparative physiological studies in the growth of field crops. I. Variation in net assimilation rate and leaf area between species and varieties, and within and between years. Ann. Bot-London(11):41-76.

Welles, J.M., and J.M. Norman. 1991. Instrument for indirect measurement of canopy architecture. Agron. J. 83(5):818-825.

Williams, M.L., and L.G. Jenkins. 2009. GeoSAR and DBInSAR: Combining "X" With "P" for Tropical Forest "C". Photogramm. Eng. Remote Sens. 75(7):738-743.

Williams, M.L., T. Milne, I. Tapley, J.J. Reis, M. Sanford, B. Kofman, and S. Hensley. 2009. Tropical forest biomass recovery using GeoSAR observations. P. IV-173-IV-176 *in* Geoscience and Remote Sensing Symposium,2009 IEEE International,IGARSS 2009.

Williams, M.L., M. Silman, S. Saatchi, S. Hensley, M. Sanford, A. Yohannan, B. Kofman, J. Reis, and B. Kampes. 2010. Analysis of GeoSAR dual-band InSAR data for peruvian forest. P. 1398-1401 *in* Geoscience and Remote Sensing Symposium (IGARSS), 2010 IEEE International.

Zhao, K., and S. Popescu. 2009. Lidar-based mapping of leaf area index and its use for validating GLOBCARBON satellite LAI product in a temperate forest of the southern USA. Remote Sens. Environ. 113(8):1628-1645.

Figure 4.1 Geographic distribution of plots in Appomattox Buckingham State Forest, VA, USA.

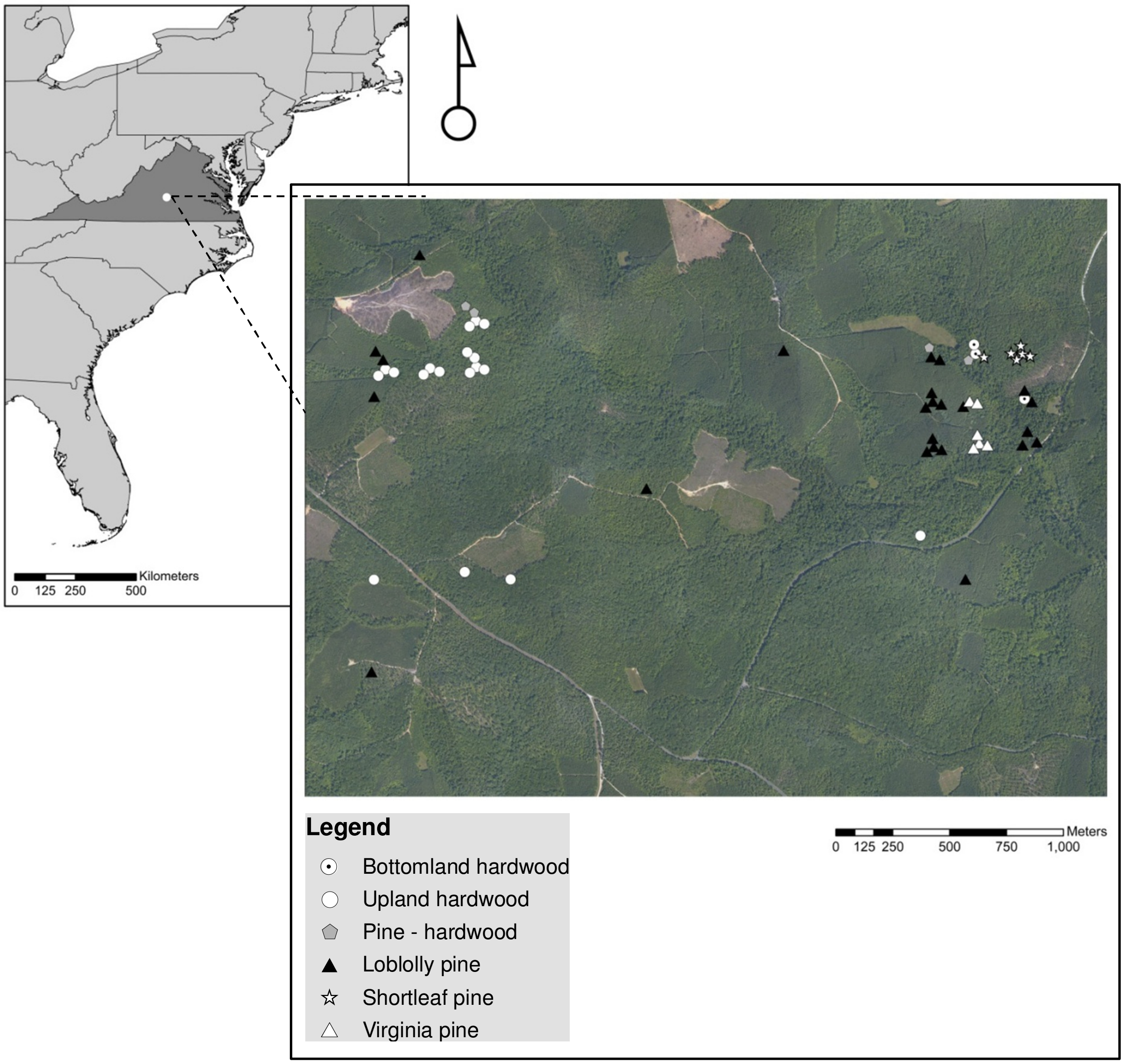

Figure 4.2 Hypothetical representation of crown density slices derived from lidar Veg_{mode} value, height to live crown was not measured on the ground. Five 1 m sections above and below the mode were defined, and the descriptive statistics (i.e., frequency, mean, standard deviation, and coefficient of variation) from the returns within each section were obtained. See table 4.1 for variable names and how they were calculated. (a) Crown density values for an upland hardwood plot.

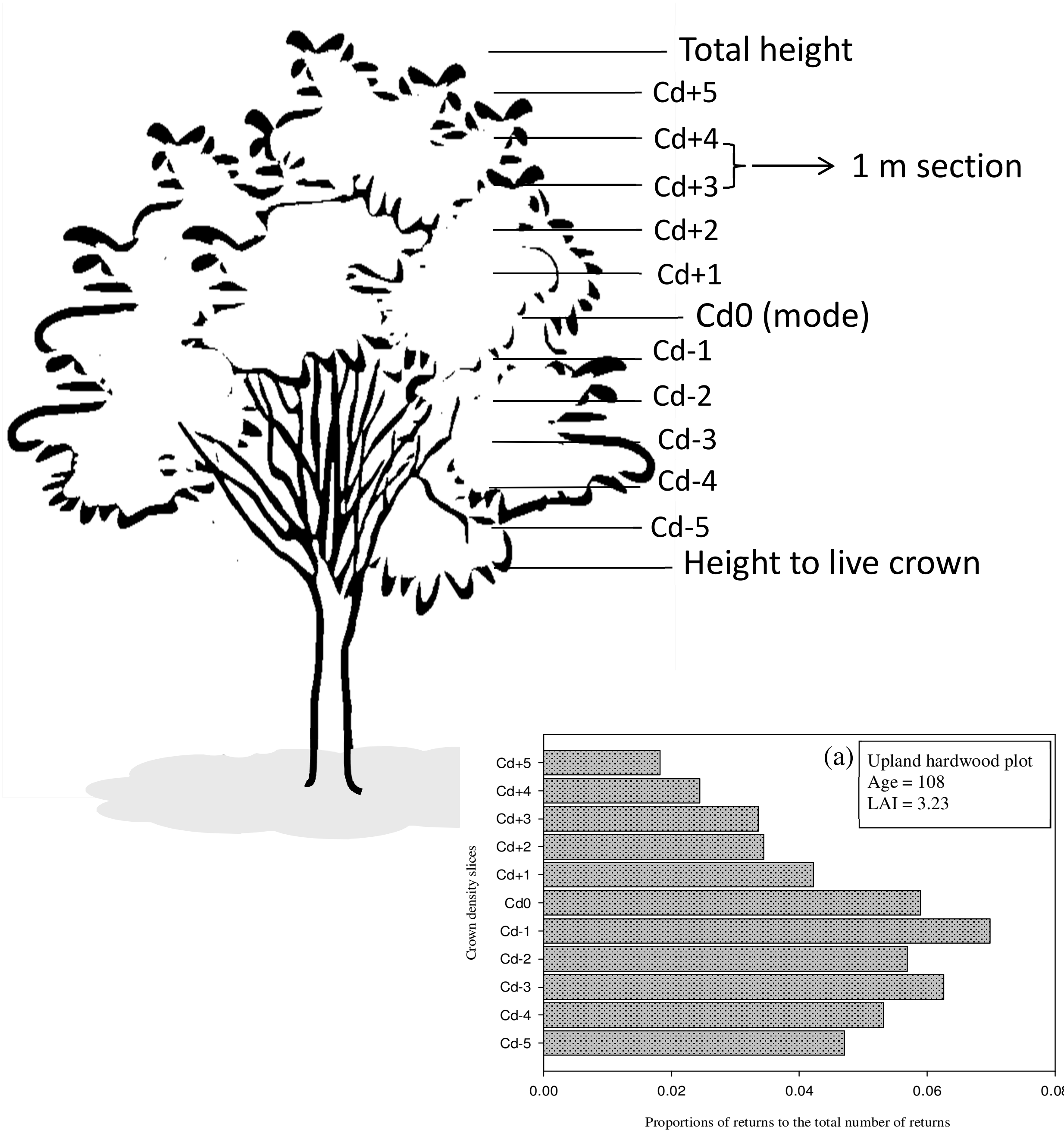

Figure 4.3 Lidar returns and GeoSAR X- and P-band heights from an upland hardwood plot of 108 yr-old and LAI = 3.23. Three-dimensional plots are: (a) Lidar returns (from ground and vegetation), and (b) GeoSAR interferometric heights from bands X and P, after subtracted from a DEM created from lidar. Ground returns are drawn for reference.

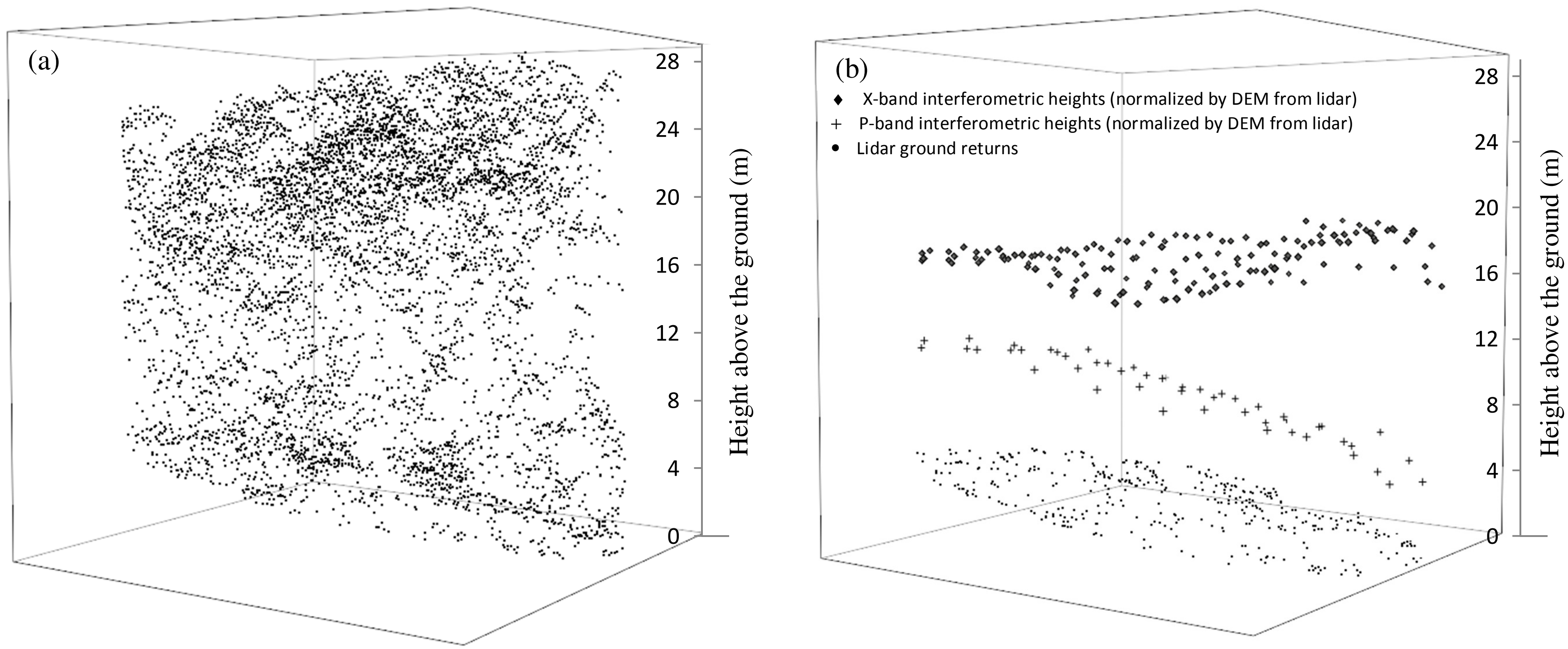

Figure 4.4 Vertical profiles for all plots: (a) lidar vegetation returns (hag > 1 m) and (b) heights generated from GeoSAR X-band (cells), after corrected by a DEM generated from lidar returns. The mode calculated from the lidar vegetation returns is circled on the *y* axis: (a) black, (b) gray, drawn as a reference for visual comparison.

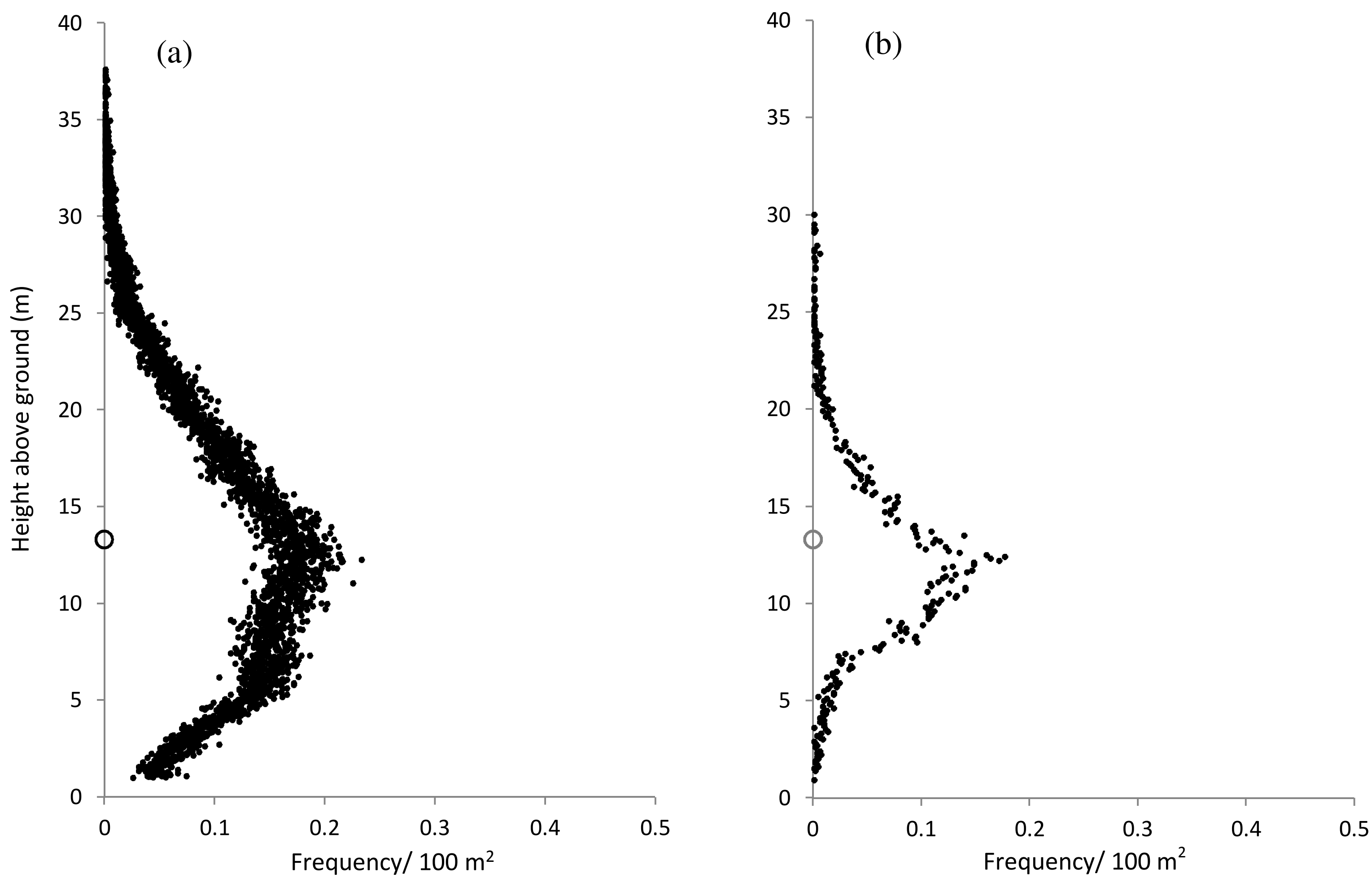

Figure 4.5 Relationship between estimated LAI and measured LAI using the 4-variable model with lidar metrics only (n = 61). Plots were classified by forest type.

Model (refer to table 4.1 for variable names):

$$LAI = 3.405 - 7.480\,(LPI) + 0.134\,(All_{10th}) - 12.498\,(d_{10}) - 15.113\,(Cd\text{-}3)$$

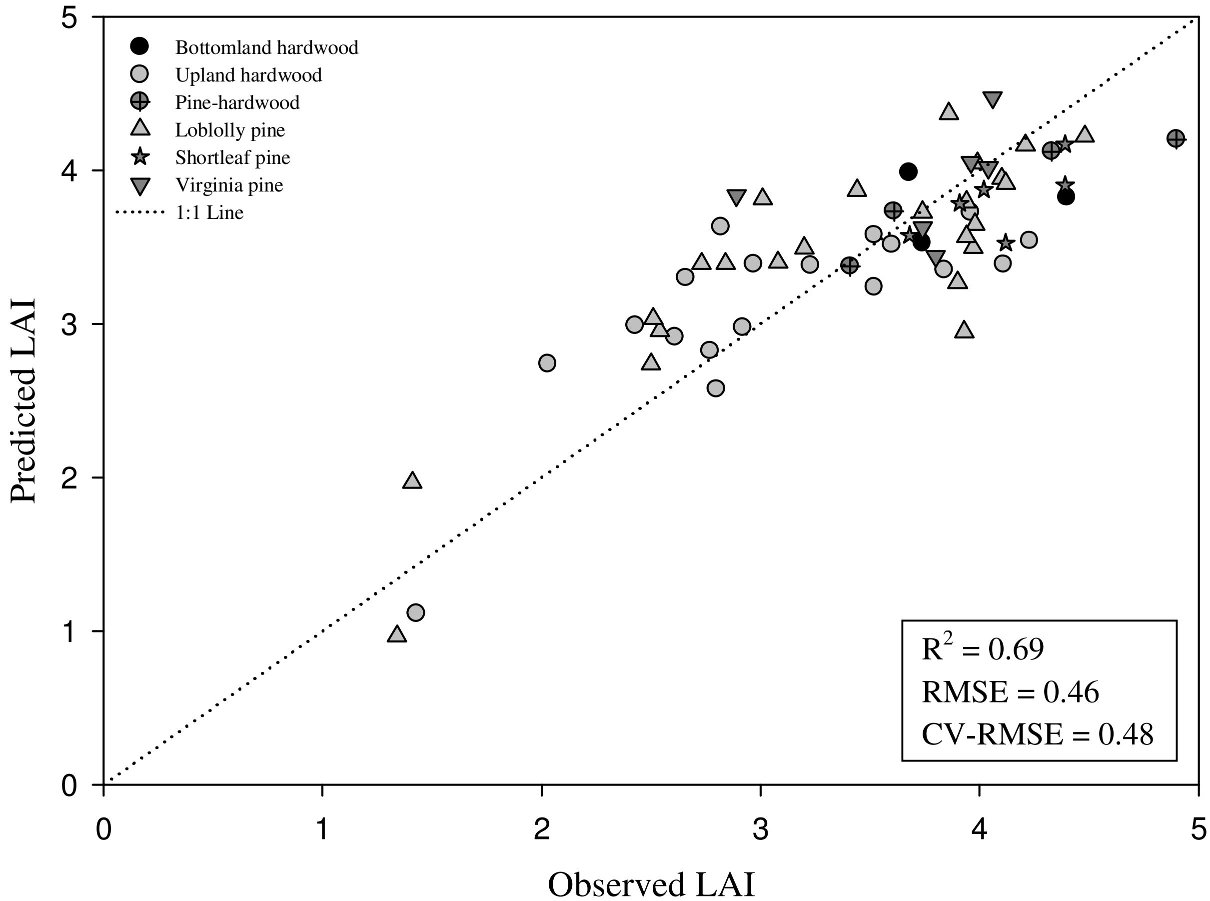

Figure 4.6 Relationship between estimated LAI and measured LAI using the 4-variable model with lidar and GeoSAR metrics (n = 61). Plots were classified by forest type.

Model (refer to table 4.1 for variable names):

$$LAI = 3.391 - 3.044\ (LPI) - 0.147\ (All_{50th}) - 3.027\ (d_2) + 0.201\ (X_{50th})$$

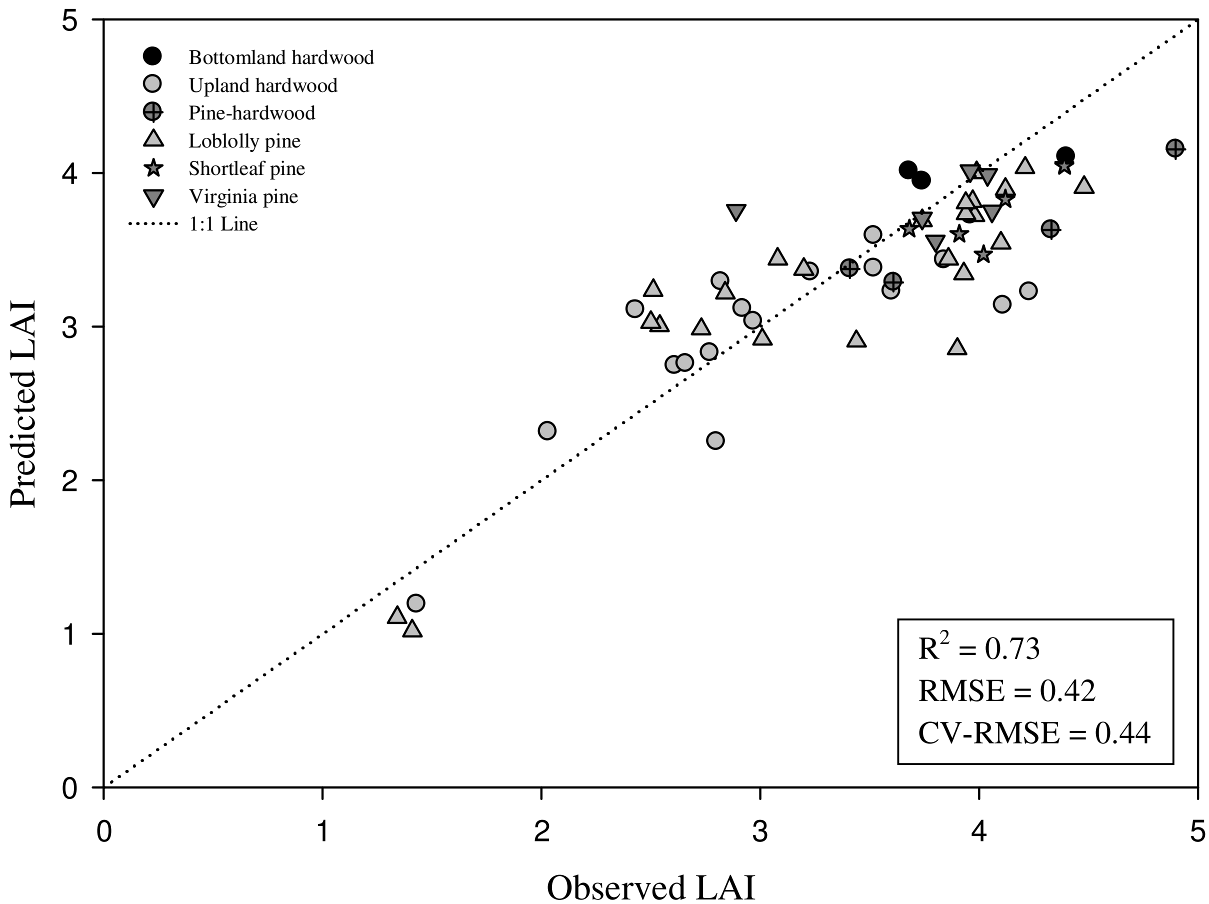

Figure 4.7 Relationship between estimated LAI and measured LAI using the 6-variable model with lidar and GeoSAR metrics (n = 61). Plots were classified by forest type.

Model (refer to table 4.1 for variable names):

$$LAI = 3.475 - 4.246\ (LPI) - 0.185\ (All_{50th}) - 4.979\ (d_2) + 0.208\ (X_{50th}) - 14.977\ (Cd\text{-}3_{stdv}) - 7.805\ (Cd\text{-}1)$$

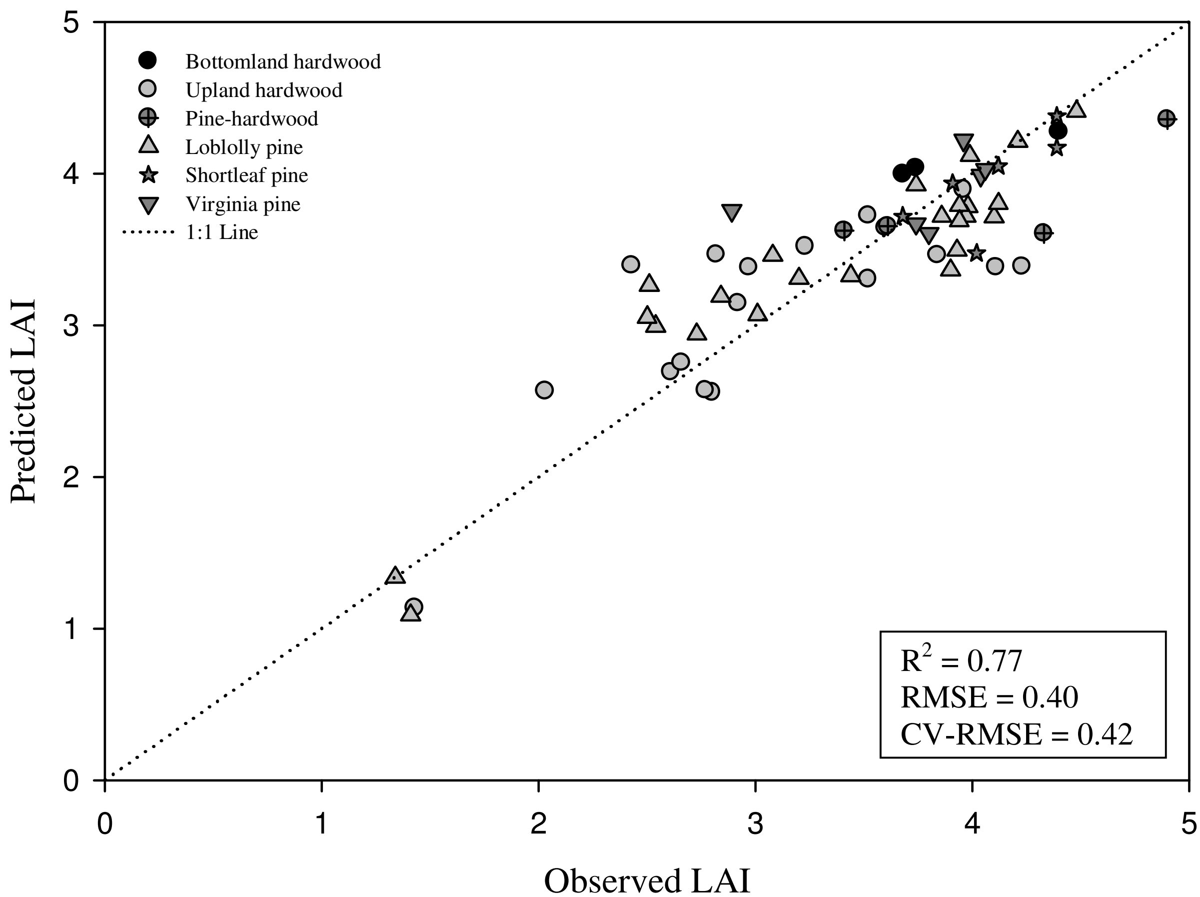

Figure 4.8 Relationship between estimated LAI and measured LAI using the 6-variable model with lidar and GeoSAR metrics and excluding the three plots of low LAI values from the dataset (n = 58). Plots were classified by forest type.

Model (refer to table 4.1 for variable names):

$$LAI = 3.658 - 8.933\ (LPI) - 0.193\ (All_{50th}) - 4.800\ (d_2) + 0.211\ (X_{50th}) - 18.042\ (Cd\text{-}3_{stdv}) - 8.531\ (Cd\text{-}1)$$

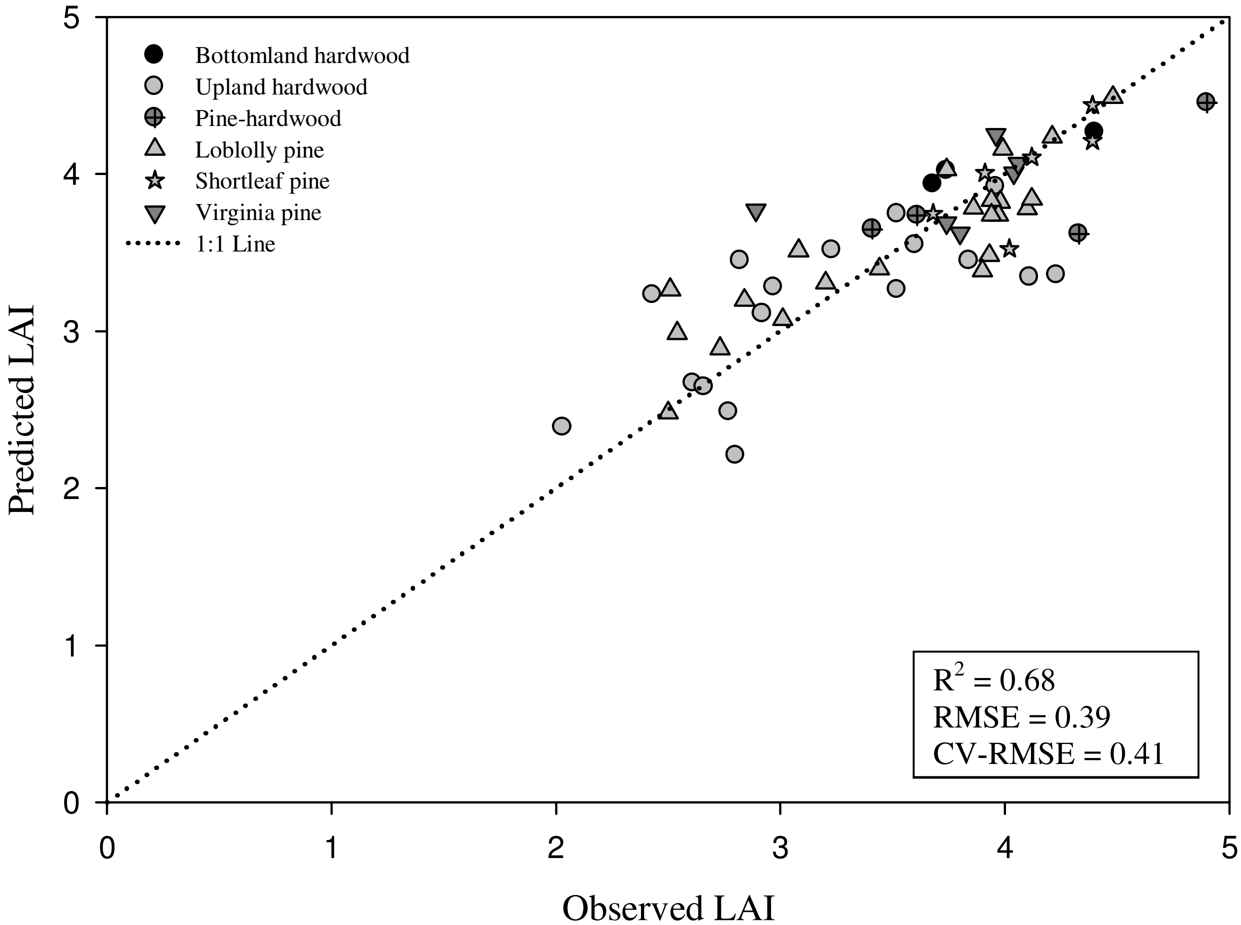

Table 4.1 Explanatory variables derived from lidar and GeoSAR. Return hag refers to the return height above the ground. Statistics in subscripts were as follows: frequency (total), mean, mode, standard deviation (stdv), coefficient of variation (cv), minimum (min), maximum (max), and height percentiles (10^{th}, 20^{th}, …, 90^{th}). The metrics Gr_{total}, All_{total}, Veg_{total}, Gr_{pulses}, All_{pulses}, and Veg_{pulses} were determined for calculation of other metrics (i.e. proportions of returns), but were not used for model development.

Lidar metrics	**Symbol**
Total number of ground returns	Gr_{total}
All returns (return hag > 0.2 m) *Units are meters for all metrics except for* All_{total} *and* All_{cv}.	All_{total}, All_{mean}, All_{stdv}, All_{cv}, All_{min}, All_{max}, All_{10th},…, All_{90th}
Vegetation returns (return hag > 1 m) *Units are meters for all metrics except for* Veg_{total} *and* Veg_{cv}.	Veg_{total}, Veg_{mean}, Veg_{mode}, Veg_{stdv}, Veg_{cv}, Veg_{min}, Veg_{max}, Veg_{10th},...,Veg_{90th}
Pulses (number of lidar pulses per return class)	Gr_{pulses}, All_{pulses}
Laser penetration index (LPI)	$LPI = Gr_{pulses}/(Gr_{pulses} + All_{pulses})$
Intensity values (returns hag > 1 m) *Units are watts for all metrics except for* I_{cv}.	I_{mean}, I_{min}, I_{max}, I_{stdv}, I_{cv}
Proportion of 1^{st}, 2^{nd}, 3^{rd} and 4^{th} returns R*i is a proportion of returns*	R_i = total number of i returns/ Veg_{total} $i = 1^{st}, 2^{nd}, 3^{rd}$, and 4^{th}
Density d*i is a proportion of returns*	$d_i = [x + (Veg_{max} - Veg_{min})/10]/Veg_{total}$ $x = Veg_{min}, 1,..,10$ $i= 1, 2, …,10$
Crown density slices around Veg_{mode} Refer to fig. 4.2 for a graphic explanation of the slices *Units are meters for* Cdi_{mean}, Cdi_{stdv}, *and* Cdi_{cv}. Cd*i is a proportion of returns*	Cdi, Cdi_{mean}, Cdi_{stdv}, Cdi_{cv} Cd_i = [number of returns in i / ($All_{total} + Gr_{total}$)] (i=+1,+ 2,+3,+4,+5, 0, -1, -2, -3, -4, and -5) i=+1,…,+ 5 at i meters above Veg_{mode} i = 0 at Veg_{mode} i = -1,…,-5 at i meters below Veg_{mode}
GeoSAR metrics	
Values from all cells per plot *Units are meters for all metrics (except for* i_{total} *and* i_{cv}*) obtained from the interferometric height bands.* *Units from magnitude bands are* $\sqrt{\text{watts/m}^2}$ *Units for* σ_0 *are* dB/m^2 (dB=decibels)	i_{total}, i_{mean}, i_{stdv}, i_{cv}, i_{min}, i_{max}, i_{10th}, i_{20th}, i_{25th}, i_{40th}, i_{50th}, i_{60th}, i_{75th}, i_{80th}, and i_{90th} i = P (P-band interferometric heights), X (X-band interferometric heights), X-P (X minus P), Pmag (P-band magnitude), Xmag (X-band magnitude), sn01xl (σ_0 for flight line 1), sn02xl (σ_0 for flight line 2), sn03xl (σ_0 for flight line 3), sn04xl (σ_0 for flight line 4)

Table 4.2 Descriptive statistics for tree height, tree dbh, and leaf area index (LAI) at plots per forest type classes. Statistics for total were calculated based on plot means. Column annotation: *n* (number of observations or plots), ht (mean tree height), dbh (diameter at breast height), and Stdv (standard deviation).

Forest type	***n***	**Stand age**	**ht (m)**				**dbh (cm)**				**LAI**			
			Mean	**Stdv**	**Range**		**Mean**	**Stdv**	**Range**		**Mean**	**Stdv**	**Range**	
Bottomland hardwood	3	89	14.0	6.4	0.4	26.8	18.7	11.2	3.1	43.7	3.94	0.40	3.68	4.40
Upland hardwood	18	12 - 164	16.3	6.3	2.7	41.2	23.7	11.9	2.5	55.1	3.08	0.74	1.43	4.23
Pine-hardwood	4	45 - 118	14.9	5.9	2.4	35.4	17.0	9.0	2.5	50.0	4.06	0.68	3.41	4.90
Loblolly pine	24	10 - 63	13.3	3.8	0.9	33.8	16.3	6.9	2.5	86.1	3.37	0.86	1.34	4.48
Shortleaf pine	6	30 - 38	12.9	3.8	4.0	24.1	14.1	7.4	2.5	42.7	4.09	0.28	3.68	4.39
Virginia pine	6	60	14.1	3.6	4.3	33.5	12.4	8.0	2.8	73.7	3.75	0.44	2.89	4.06
Total	61	10 – 164	14.2	3.2	0.4	41.2	17.0	5.9	2.5	86.1	3.71	0.57	1.34	4.90

Table 4.3 Means of lidar returns per forest type. Minimum values for all returns heights above ground were set at 0.2 m. Intensity minimum value was 1 for all plots (n = 61). Column annotation: n (number of observations or plots), Gr_{total} (total number of ground returns), All_{total} (total number of all returns), Stdv (standard deviation), Max (maximum value), and LPI (Laser Penetration Index).

Forest type	n	**Gr_{total} (mean)**	**All_{total} (mean)**	**Return heights (m)**			**Intensity (watts)**			**LPI**
				Mean	**Stdv**	**Max**	**Mean**	**Stdv**	**Max**	
Bottomland hardwood	3	222	4343	12.7	6.8	36.6	51	29	136	0.019
Upland hardwood	18	537	5278	13.2	6.8	31.0	44	28	150	0.039
Pine-hardwood	4	264	5009	12.7	5.9	34.9	49	28	126	0.003
Loblolly pine	24	534	4436	10.2	4.8	32.7	41	24	149	0.034
Shortleaf pine	6	353	5165	9.9	4.5	25.3	43	27	137	0.003
Virginia pine	6	555	4617	13.2	5.1	37.6	37	22	125	0.005
Total	61	411	4808	12.0	5.7	37.6	44	26	150	0.017

Table 4.4 Means of GeoSAR cell values per forest type. P and X band heights were calculated by subtracting the values from a DEM created from the lidar returns (n = 61). Column annotation: X – P (X-band minus P-band), P_{mag} (P-band magnitude values), X_{mag} (X-band magnitude values), n (number of observations or plots), Stdv (standard deviation), and Max (maximum value).

Forest type	***n***	**P-band heights (m)**			**X-band heights (m)**			**(X – P) heights (m)**			**Pmag (watts/m^2)**			**Xmag (watts/m^2)**		
		Mean	**Stdv**	**Max**	**Mean**	**Stdv**	**Max**	**Mean**	**Stdv**	**Max**	**Mean**	**Stdv**	**Max**	**Mean**	**Stdv**	**Max**
Bottomland hardwood	3	10.48	1.70	14.71	16.06	2.35	25.30	5.57	1.85	11.78	0.24	0.05	0.45	0.13	0.04	0.31
Upland hardwood	18	6.65	1.35	13.53	11.96	1.81	20.91	5.20	1.99	13.40	0.26	0.05	0.62	0.11	0.03	0.25
Pine-hardwood	4	8.03	1.52	16.27	13.72	1.66	24.77	5.47	1.71	11.74	0.23	0.05	0.48	0.12	0.04	0.41
Loblolly pine	24	5.46	1.30	13.26	10.84	1.22	22.55	5.46	1.70	15.40	0.36	0.08	0.99	0.07	0.02	0.27
Shortleaf pine	6	6.89	1.45	11.77	11.78	1.44	18.83	4.98	1.55	12.95	0.30	0.06	0.55	0.09	0.03	0.21
Virginia pine	6	6.83	1.94	18.38	15.04	1.71	30.02	8.15	1.86	15.46	0.41	0.09	0.88	0.08	0.03	0.25
Total	61	7.39	1.54	18.38	13.23	1.70	30.02	5.80	1.78	15.46	0.30	0.06	0.99	0.10	0.03	0.41

Table 4.5 Pearson correlation coefficients for the independent variables used to predict leaf area index (LAI) (n = 61). For a description of the variable names refer to table 4.1. LAI was measured on the ground. Bold values were significant at $\alpha = 0.05$.

	LAI	**LPI**	**$\mathbf{All_{10th}}$**	**$\mathbf{All_{50th}}$**	**$\mathbf{d_2}$**	**$\mathbf{d_{10}}$**	**Cd-1**	**Cd-3**	**$\mathbf{Cd\text{-}3_{stdv}}$**	**$\mathbf{X_{cv}}$**	**$\mathbf{X_{50th}}$**	**$\mathbf{Xmag_{stdv}}$**	**$\mathbf{Pmag_{stdv}}$**	**$\mathbf{Pmag_{max}}$**	**$\mathbf{sn01xl_{cv}}$**
LAI	1	**-0.698**	**0.638**	-0.116	0.085	**-0.347**	0.030	-0.084	0.223	**-0.485**	**0.609**	0.241	-0.013	-0.092	-0.124
LPI		1	**-0.546**	0.063	-0.054	0.160	-0.237	-0.242	**-0.262**	**0.693**	**-0.520**	-0.065	0.181	0.187	0.071
$\mathbf{All_{10th}}$			1	0.163	-0.091	-0.148	0.106	-0.031	0.168	**-0.451**	**0.685**	**0.269**	0.072	0.054	-0.075
$\mathbf{All_{50th}}$				1	**-0.292**	**0.508**	**-0.438**	-0.168	0.013	0.087	**0.550**	0.168	-0.116	-0.112	**0.252**
$\mathbf{d_2}$					1	-0.083	**-0.286**	**-0.290**	0.085	0.050	0.086	**0.331**	0.078	0.031	0.105
$\mathbf{d_{10}}$						1	-0.242	-0.181	0.199	0.039	0.080	-0.041	-0.190	-0.146	**0.286**
Cd-1							1	**0.562**	**-0.269**	**-0.429**	**-0.285**	**-0.421**	0.136	0.216	-0.251
Cd-3								1	-0.062	-0.326	-0.176	-0.413	0.024	0.131	-0.083
$\mathbf{Cd\text{-}3_{stdv}}$									1	-0.127	**0.316**	0.176	**-0.408**	**-0.430**	0.105
$\mathbf{X_{cv}}$										1	**-0.363**	0.222	-0.074	-0.109	0.044
$\mathbf{X_{50th}}$											1	**0.345**	-0.096	-0.111	0.159
$\mathbf{Xmag_{stdv}}$												1	-0.225	**-0.358**	0.210
$\mathbf{Pmag_{stdv}}$													1	**0.931**	-0.196
$\mathbf{Pmag_{max}}$														1	-0.185
$\mathbf{sn01xl_{cv}}$															1

Table 4.6 Best predictive models of LAI using lidar metrics only and GeoSAR metrics only, *n* = 61. The statistics R^2_{adj}', CV-RMSE, SSCC, VIF, and CI are the adjusted coefficient of determination, the RMSE from the cross validation analysis, the squared semipartial correlation coefficient from partial sum of squares, the variance inflation factor and the condition index, respectively. For a description of the variable names refer to table 4.1. All variables in the models were highly significant at a p-value < 0.001.

Sensor	# var.	R^2	R^2_{adj}'	RMSE	CV-RMSE	Variable	Coefficient	SSCC	VIF	CI
Lidar	2	0.58	0.57	0.52	0.53	Intercept	3.363	----	----	----
						LPI	-6.602	0.17	1.43	1.28
						All_{10th}	0.173	0.09	1.43	1.94
	4	0.69	0.67	0.46	0.48	Intercept	3.405	----	----	----
						LPI	-7.480	0.20	1.58	1.24
						All_{10th}	0.134	0.05	1.50	1.28
						d_{10}	-12.498	0.06	1.06	1.56
						Cd-3	-15.113	0.06	1.14	2.16
GeoSAR	4	0.52	0.49	0.56	0.58	Intercept	3.407	----	----	----
						X_{cv}	-0.032	0.10	1.37	1.08
						X_{50th}	0.104	0.13	1.49	1.20
						$Xmag_{stdv}$	16.887	0.04	1.37	1.38
						$sn01xl_{cv}$	-0.002	0.05	1.06	2.00

Table 4.7 Best predictive models of LAI using lidar metrics (including crown density slices) and GeoSAR metrics, n = 61. The statistics $R^2_{adj'}$, CV-RMSE, SSCC, VIF, and CI are the adjusted coefficient of determination, the RMSE from the cross validation analysis, the squared semipartial correlation coefficient from partial sum of squares, the variance inflation factor and the condition index, respectively. All variables in the models were highly significant at a p-value < 0.0001. For a description of the variable names refer to table 4.1.

# var.	R^2	$R^2_{adj'}$	RMSE	CV-RMSE	Variable	Coefficient	SSCC	VIF	CI
2	0.66	0.65	0.47	0.47	Intercept	3.439	----	----	----
					All_{50th}	-0.153	0.29	1.43	1.27
					X_{50th}	0.229	0.65	1.43	1.88
3	0.71	0.69	0.44	0.45	Intercept	3.393	----	----	----
					LPI	-3.732	0.04	1.80	1.27
					All_{50th}	-0.120	0.14	1.88	1.43
					X_{50th}	0.176	0.21	2.57	2.97
4	0.73	0.71	0.42	0.44	Intercept	3.391	----	----	----
					LPI	-3.044	0.03	1.91	1.20
					All_{50th}	-0.147	0.16	2.39	1.33
					d_2	-3.027	0.03	1.28	1.58
					X_{50th}	0.201	0.24	3.00	3.34
5	0.76	0.74	0.40	0.42	Intercept	3.401	----	----	----
					LPI	-4.253	0.05	2.19	1.11
					All_{50th}	-0.148	0.16	2.39	1.20
					d_2	-3.996	0.04	1.39	1.46
					X_{50th}	0.183	0.18	3.20	2.00
					Cd-3	-11.703	0.03	1.36	3.41
6	0.77	0.75	0.40	0.42	Intercept	3.475	----	----	----
					LPI	-4.246	0.05	2.13	1.19
					All_{50th}	-0.185	0.20	3.00	1.33
					d_2	-4.979	0.05	1.65	1.41
					X_{50th}	0.208	0.24	3.22	2.31
					$Cd\text{-}3_{stdv}$	-14.977	0.02	1.34	2.98
					Cd-1	-7.805	0.04	2.07	3.92

Table 4.8 Best predictive models of LAI using lidar metrics (excluding crown density slices) and GeoSAR metrics, *n* = 61. The statistics $R^2_{adj'}$, CV-RMSE, SSCC, VIF, and CI are the adjusted coefficient of determination, the RMSE from the cross validation analysis, the squared semipartial correlation coefficient from partial sum of squares, the variance inflation factor and the condition index, respectively. All variables in the models were highly significant at a p-value < 0.0001. For a description of the variable names refer to table 4.1.

# var.	R^2	$R^2_{adj'}$	RMSE	CV-RMSE	Variable	Coefficient	SSCC	VIF	CI
5	0.74	0.72	0.42	0.44	Intercept	3.442	----	----	----
					All_{50th}	-0.180	0.34	1.72	1.16
					d_2	-4.187	0.05	1.23	1.38
					X_{50th}	0.247	0.68	1.59	1.47
					$Pmag_{stdv}$	16.079	0.04	7.63	2.47
					$Pmag_{max}$	-2.731	0.04	7.61	5.50
6	0.77	0.74	0.40	0.42	Intercept	3.406	----	----	----
					LPI	-3.110	0.03	2.00	1.17
					All_{50th}	-0.147	0.16	2.45	1.31
					d_2	-3.455	0.03	1.30	1.45
					X_{50th}	0.199	0.23	3.04	1.75
					$Pmag_{stdv}$	16.643	0.04	7.64	3.71
					$Pmag_{max}$	-2.632	0.04	7.63	0.07

5. CONCLUSIONS

This study provided a set of robust models that accurately explained the variation of leaf area index, stem density, mean tree height, and mean height to live crown on loblolly pine plantations across a wide range of site conditions, stand ages, and silvicultural regimes, as well as a model to estimate LAI on different forest types in a mixed temperate forest. Wall-to-wall estimates of these important biophysical parameters are becoming increasingly essential to forest management.

Previous attempts to estimate forest attributes (stand tree height, biomass, stand volume, and leaf area index) using lidar data reported the utility of a number of metrics that were also found to be useful in this study. The laser penetration index (LPI), a measure of stand canopy closure or amount of leaves and branches, was one of the most consistent contributors in the models (Barilotti et al. 2006). In company of LPI, vegetation return percentiles and density metrics improved estimations of the dependent variables (Naesset 2002; Popescu et al. 2002). Fewer results have been reported using GeoSAR data to estimate stand height or any other forest parameter, however, the percentile metrics as well as the bands' descriptive statistics were important variables.

Other major contributions of this research to forestry remote sensing are as follows:

1. The development of a new set of lidar metrics that increase the potential utilization of lidar data for estimating forest parameters. Crown density slices of one meter depth, five above and five below the mode value of the vegetation lidar returns, showed significant correlations and significant contributions to the estimation of leaf area index and stem density, and were also responsible for increasing model accuracy, even when GeoSAR metrics were included.

2. The use of intensity values. Descriptive statistics for intensity values from lidar data were found to be useful estimating leaf area index and stem density in pine plantations. The variability in intensity values is a result of the variability in reflectance and reflectivity of the ground targets. Previous research has used absolute values of intensity with caution, particularly because most of the times lidar instruments are not calibrated for intensity prior to data acquisition; however, the use of the dispersion measures of these values is an effective way to utilize these data.
3. The use of a ground variable (initial number of trees) as a resource to increase accuracy (up to 92%) to estimate stem density from lidar returns. Previous attempts to estimate number of trees in pine plantations using remote sensed data have used optical data, lidar, or the fusion between optical and lidar data. Nonetheless, this important ground-based variable has not been taken into account. The number of trees planted at the beginning of the rotation, for each of the stands, is information recorded and archived by forest managers; and unlike other ground-based variables (i.e., tree height, dbh, etc.), this value does not require monitoring. Therefore, even when this variable is considered as ground based data, the models in which it is included can still be considered lidar only models.
4. The use of X-band interferometric heights from GeoSAR to estimate leaf area index. The X-band height percentiles were shown to be useful, particularly when combined with lidar data, for estimating leaf area index in mixed temperate forests in the eastern U.S. Previous research has assessed the potential utility of high frequency radar backscatter to quantify LAI. However, these same studies have shown that backscatter tends to saturate at high LAI values. Although follow-up studies to confirm these results are necessary, X-band interferometry – currently possible using spaceborne sensors – shows strong

promise for enabling robust wall-to-wall mapping of LAI at the landscape- to regional-scale.

The models developed in this study highlight the eventual promise of accurate, affordable, and straightforward mapping of key forest attributes using active remote sensing to improve forest resource management.

5.1 Literature cited

Barilotti, A., S. Turco, and G. Alberti. 2006. LAI determination in forestry ecosystem by lidar data analysis. P. 248-252 *in* Proceedings of Workshop on 3D Remote Sensing in Forestry, Vienna, Austria.

Fassnacht, K.S., S.T. Gower, J.M. Norman, and R.E. McMurtric. 1994. A comparison of optical and direct methods for estimating foliage surface area index in forests. Agr. Forest Meteorol. 71(1-2):183-207.

Huete, A.R., H.Q. Liu, K. Batchily, and W. Leeuwen van. 1997. A comparison of vegetation indices over a global set of TM images for EOS-MODIS. Remote Sens. Environ. 59(3):440-451.

Jensen, J.R., X. Huang, and H.E. Mackey Jr. 1997. Remote sensing of successional changes in wetland vegetation as monitored during a four-year drawdown of a former cooling lake. Applied Geographic Studies 1(1):31-44.

le Maire, G., C. Francois, K. Soudani, H. Davi, V. Le Dantec, B. Saugier, and E. Dufrene. 2006. Forest leaf area index determination: A multiyear satellite-independent method based on within-stand normalized difference vegetation index spatial variability. J. Geophys. Res.-Biogeosci. 111(G2).

Lefsky, M.A., W.B. Cohen, G.G. Parker, and D.J. Harding. 2002. Lidar remote sensing for ecosystem studies. BioScience 52(1):19-30.

Naesset, E. 2002. Predicting forest stand characteristics with airborne scanning laser using a practical two-stage procedure and field data. Remote Sens. Environ. 80:88-99.

Popescu, S.C., R.H. Wynne, and R. Nelson. 2002. Estimating plot-level tree heights with lidar: local filtering with a canopy-height based variable window size. Comput. Electron. Agr. 37:71-95.

Smith, J.L., M. Clutter, B. Keefer, and Z. Ma. 2003. Special commentary: the future of digital remote sensing for production forestry organizations. For. Sci. 49:455-456.

Stanturf, J.A., R.C. Kellison, F.S. Broerman, and S.B. Jones. 2003. Innovation and forest industry: domesticating the pine forests of the southern United States, 1920-1999. Forest Policy Econ. 5(4):407-419.

Zheng, G., and L.M. Moskal. 2009. Retrieving leaf area index (LAI) using remote sensing: theories, methods and sensors. Sensors 9(4):2719-2745.

APPENDICES

Appendix A: Ground-based variables and lidar metrics used for the LAI models (Chapter 2)*

Site	Plot	TPH/ block	Treatment	LAI	ht_{mean}	$Crown_{length}$	dbh_{mean}	Gr_{total}	Veg_{total}	Veg_{mean}	Veg_{stdv}	Veg_{cv}
NSD	1	1794	fertilized	2.84	11.43	5.94	15.11	745	2378	8.098	1.518	18.741
NSD	2	897	fertilized	3.13	11.12	7.23	18.43	790	2543	7.258	1.730	23.838
NSD	3	1794	fertilized	3.92	11.14	5.66	15.21	575	1377	8.103	1.440	17.766
NSD	4	897	control	2.38	10.56	6.46	17.01	474	1191	6.841	1.581	23.106
NSD	5	897	fertilized	3.97	11.17	7.08	18.76	395	1413	7.434	1.567	21.074
NSD	6	897	fertilized	3.18	10.78	7.95	18.82	486	1499	7.030	1.728	24.579
NSD	7	897	control	2.78	10.91	7.51	17.88	629	1529	6.898	1.676	24.299
NSD	8	1794	control	4.13	10.98	5.57	13.60	595	1265	7.526	1.526	20.282
NSD	9	897	control	2.56	11.46	7.59	17.42	673	1139	6.940	1.705	24.573
NSD	10	897	fertilized	3.04	11.27	7.18	18.60	630	1617	7.488	1.755	23.443
NSD	11	1794	fertilized	2.98	11.10	5.67	14.74	789	2395	7.942	1.425	17.948
NSD	12	1794	fertilized	3.53	11.25	6.16	15.34	544	2340	8.129	1.382	17.006
NSD	13	1794	fertilized	4.03	11.35	5.82	15.70	566	2383	8.407	1.365	16.236
NSD	14	1794	control	3.68	11.14	6.09	14.74	730	2204	7.853	1.545	19.676
NSD	15	1794	fertilized	3.67	10.72	6.18	14.96	739	2432	7.466	1.438	19.257
NSD	16	897	fertilized	3.4	11.19	7.83	18.63	622	2223	7.404	1.678	22.660
NSD	17	1794	control	3.35	11.20	5.62	14.64	832	2428	7.836	1.309	16.704
NSD	18	897	fertilized	2.51	11.28	6.69	17.99	608	2175	7.050	1.777	25.200
Henderson	3	-----	vegetation control	4.36	22.40	6.26	21.83	83	1612	17.225	4.941	28.685
Henderson	4	-----	control	4.69	23.00	5.88	22.94	143	1569	16.753	6.598	39.386
Henderson	5	-----	vegetation control	4.6	21.09	5.73	20.21	186	1477	16.274	4.802	29.507
Henderson	6	-----	control	4.71	20.83	5.91	19.65	152	1640	15.179	5.560	36.631
Henderson	9	-----	vegetation control	2.85	21.12	5.32	20.87	422	1276	18.430	3.686	19.999
Henderson	10	-----	control	4.8	20.75	7.27	19.92	76	1570	14.851	3.838	25.845
Henderson	11	-----	vegetation control	2.75	21.06	6.48	22.82	256	1310	17.478	4.533	25.933
Henderson	12	-----	control	3.09	21.95	6.49	21.61	242	1376	17.023	5.459	32.069
Henderson	13	-----	control	4.65	20.07	6.81	19.77	82	1528	14.475	3.885	26.841
Henderson	14	-----	vegetation control	2.43	22.54	7.11	21.78	369	1255	16.598	5.107	30.769
Henderson	15	-----	control	4.02	21.77	6.37	19.39	204	1347	14.900	5.818	39.042
Henderson	16	-----	vegetation control	2.08	20.02	5.95	20.76	331	1403	15.182	5.225	34.416
Henderson	17	-----	vegetation control	4.43	18.45	6.03	19.25	92	1362	14.279	3.748	26.247
Henderson	18	-----	control	4.57	21.34	5.79	20.00	169	1782	15.165	5.369	35.407
Henderson	19	-----	vegetation control	2.69	23.33	5.94	22.24	317	1264	19.554	4.239	21.677
Henderson	20	-----	control	3.84	20.26	6.13	19.37	188	1703	14.206	5.098	35.883
Henderson	24	-----	vegetation control	2.18	20.76	6.05	20.13	497	1585	16.786	3.752	22.353
Henderson	25	-----	control	3.52	22.87	5.03	22.20	317	1320	19.003	5.516	29.026
Henderson	26	-----	control	2.85	19.95	6.30	21.24	216	1603	14.261	5.923	41.529
Henderson	27	-----	vegetation control	4.3	17.48	5.64	17.66	126	1708	12.415	3.374	27.175
Henderson	28	-----	control	4.91	22.01	6.24	20.64	81	1760	15.895	5.887	37.038
Henderson	29	-----	vegetation control	3.22	22.75	6.51	21.75	295	1255	17.532	6.280	35.822

* Site = study site (refer to fig. 2.1), TPH/block = trees per hectare or block, for other variable names refer to table 2.1

Site	Plot	TPH/ block	Treatment	LAI	ht_{mean}	$Crown_{length}$	dbh_{mean}	Gr_{total}	Veg_{total}	Veg_{mean}	Veg_{stdv}	Veg_{cv}
Henderson	30	-----	vegetation control	4.49	23.40	8.23	24.25	131	1724	16.808	5.200	30.938
Henderson	31	-----	control	4.53	23.80	6.87	22.93	154	1526	17.079	7.067	41.380
RW18	3	-----	fertilized thinned	1.27	16.00	7.39	21.61	374	1501	11.150	4.467	40.064
RW18	12	-----	fertilized unthinned	3.94	16.35	7.55	18.96	235	1318	14.135	1.700	12.027
RW18	14	-----	fertilized thinned	1.52	16.87	7.67	21.88	498	762	13.366	2.213	16.557
RW18	15	-----	fertilized unthinned	2.93	15.05	7.20	18.94	216	889	7.097	3.637	51.247
RW18	16	-----	fertilized thinned	0.82	16.14	6.98	21.26	498	681	13.137	2.114	16.093
RW18	20	-----	fertilized thinned	0.92	15.67	6.80	20.27	406	424	12.672	1.989	15.695
RW18	21	-----	fertilized thinned	0.84	15.87	7.27	20.15	399	470	12.714	1.763	13.870
RW18	22	-----	fertilized thinned	0.57	15.77	7.19	20.92	434	566	12.446	1.852	14.883
RW18	23	-----	fertilized unthinned	3.87	15.27	7.02	19.12	216	943	13.115	1.793	13.668
RW18	26	-----	fertilized thinned	0.92	16.50	7.34	20.89	315	333	13.407	1.813	13.523
RW18	27	-----	fertilized thinned	1.09	16.19	7.53	21.17	319	402	13.092	1.766	13.486
RW18	28	-----	control and thinned	1.00	16.55	7.89	20.78	453	586	12.901	1.952	15.131
RW18	29	-----	fertilized thinned	0.8	15.87	7.10	19.34	589	729	11.446	3.447	30.117
RW18	30	-----	fertilized thinned	1.32	16.19	7.37	21.65	516	703	12.775	2.023	15.837
RW18	31	-----	fertilized thinned	1.06	15.77	7.56	21.52	390	1256	9.050	3.851	42.553
RW18	45	-----	fertilized thinned	0.96	16.70	7.02	20.83	287	308	13.418	1.827	13.619
RW18	46	-----	control and thinned	0.57	15.42	7.20	18.76	469	369	12.148	1.672	13.762
RW18	47	-----	fertilized unthinned	4.85	16.74	7.56	19.94	223	975	14.483	2.094	14.460
RW18	48	-----	fertilized thinned	0.45	16.06	7.30	21.07	530	579	13.023	1.888	14.498
RW19	1	-----	fertilized	2.34	14.10	7.47	19.01	394	1398	10.163	1.979	19.478
RW19	2	-----	fertilized	2.53	13.00	7.01	18.59	496	1072	9.311	2.027	21.766
RW19	3	-----	fertilized	2.20	12.95	6.71	17.93	2090	2901	9.449	1.926	20.388
RW19	4	-----	fertilized	2.48	12.59	6.87	19.14	1098	2315	8.982	2.135	23.769
RW19	5	-----	fertilized	2.39	12.23	6.15	17.78	1006	1417	9.062	1.843	20.334
RW19	6	-----	fertilized	2.09	13.41	6.89	18.19	721	1215	9.576	1.869	19.513
RW19	8	-----	fertilized	2.76	12.99	7.20	19.50	1875	3101	9.020	1.827	20.259
RW19	9	-----	fertilized	2.39	12.98	6.94	18.44	1077	1829	9.005	1.900	21.103
RW19	10	-----	fertilized	2.49	13.15	7.10	19.21	1073	1547	9.202	2.150	23.361
RW19	11	-----	fertilized	2.54	13.86	7.15	17.68	864	1624	9.681	1.869	19.303
RW19	12	-----	fertilized	2.85	13.58	7.05	18.78	1252	4089	10.057	1.753	17.432
RW19	13	-----	fertilized	2.87	12.68	6.69	17.29	2137	3663	8.889	2.088	23.495
RW19	14	-----	fertilized	2.99	14.00	7.45	18.18	1249	2404	9.733	1.979	20.335
RW19	15	-----	fertilized	2.69	13.66	7.45	18.40	1114	1776	9.326	1.998	21.426
RW19	17	-----	fertilized	3.05	13.45	7.47	20.26	386	1545	9.570	2.015	21.054
RW19	18	-----	fertilized	2.90	13.48	7.57	17.68	1844	3945	9.233	1.946	21.073
RW19	19	-----	fertilized	2.86	13.45	7.23	19.70	587	1904	9.314	2.129	22.861
RW19	20	-----	fertilized	2.97	12.99	6.56	18.97	854	2263	9.681	1.847	19.078
RW19	21	-----	fertilized	2.34	12.80	6.35	16.90	632	1580	9.237	2.167	23.459
RW19	22	-----	fertilized	2.29	12.83	6.74	16.53	1687	4134	8.932	2.258	25.282
RW19	23	-----	fertilized	2.55	12.68	6.78	17.34	969	2123	9.009	2.012	22.329
RW19	24	-----	fertilized	2.52	13.66	7.07	18.36	593	2074	10.202	1.812	17.757
RW19	25	-----	fertilized	2.63	12.47	6.33	16.70	944	1876	8.807	2.209	25.087
RW19	26	-----	fertilized	2.54	13.13	7.37	19.12	755	1323	9.080	2.004	22.067
RW19	27	-----	fertilized	2.55	12.36	6.93	18.58	1720	3295	8.464	2.357	27.847
RW19	28	-----	fertilized	2.69	12.81	7.31	17.99	930	2025	8.137	2.631	32.335
RW19	29	-----	fertilized	2.90	12.57	7.44	18.27	868	1621	8.621	2.201	25.525

Site	Plot	TPH/ block	Treatment	LAI	ht_{mean}	$Crown_{length}$	dbh_{mean}	Gr_{total}	Veg_{total}	Veg_{mean}	Veg_{stdv}	Veg_{cv}
RW19	30	-----	fertilized	2.43	13.58	7.52	19.27	576	1629	9.726	1.960	20.151
RW19	31	-----	fertilized	2.34	13.58	7.65	18.81	493	1072	9.278	1.878	20.238
RW19	32	-----	fertilized	1.93	12.88	7.09	17.26	1586	3830	9.040	2.001	22.139
RW19	33	-----	fertilized	2.44	12.45	7.06	17.62	772	1857	8.504	1.909	22.442
RW19	34	-----	fertilized	2.49	13.21	6.88	17.63	716	1983	9.462	1.729	18.268
Setres	1	1	control	2.4	13.72	6.64	16.76	887	3005	10.864	2.091	19.244
Setres	1	2	control	2.19	14.73	6.75	17.78	770	2143	11.724	2.043	17.422
Setres	1	3	control	2.6	15.99	6.69	20.76	779	2298	13.687	1.861	13.596
Setres	1	4	control	2.79	18.36	7.90	22.41	819	3777	15.302	2.367	15.470
Setres	2	1	fertilized, irrigated	2.32	13.38	5.79	17.30	770	2352	11.074	2.074	18.725
Setres	2	2	fertilized, irrigated	2.51	14.54	6.99	18.28	767	1313	11.816	2.058	17.415
Setres	2	3	fertilized, irrigated	3.27	18.54	6.37	23.21	614	2782	15.609	1.837	11.768
Setres	2	4	fertilized, irrigated	3.23	19.10	6.06	23.07	609	2666	15.878	2.209	13.911
Setres	3	1	fertilized, irrigated	1.55	11.05	5.73	15.71	906	2455	9.042	2.023	22.367
Setres	3	2	fertilized, irrigated	2.31	14.72	6.52	17.80	844	2788	12.380	2.192	17.704
Setres	3	3	fertilized, irrigated	2.96	17.42	6.97	22.61	826	2962	14.423	2.077	14.402
Setres	3	4	fertilized, irrigated	2.58	17.90	7.44	22.12	829	2985	14.926	2.540	17.019
Setres	4	1	fertilized, irrigated	2.08	12.90	6.48	16.57	905	2556	10.577	2.051	19.393
Setres	4	2	fertilized, irrigated	1.87	13.60	6.72	18.03	783	2505	10.815	2.030	18.771
Setres	4	3	fertilized, irrigated	2.74	16.47	7.09	21.53	636	2741	14.008	1.916	13.678
Setres	4	4	fertilized, irrigated	2.86	18.92	7.91	24.67	597	1365	15.987	2.104	13.161

Appendix A: Continued[*].

Site	Plot	TPH/ block	Treatment	Veg_{20th}	I_{mean}	I_{max}	I_{stdv}	I_{cv}	$Cd{+}4_{cv}$	$Cd{+}1_{stdv}$	Cd+1	Cd-4	LPI
NSD	1	1794	fertilized	6.830	35.633	100	15.675	43.990	0.000	0.289	0.101	0.007	0.027
NSD	2	897	fertilized	5.750	37.487	84	16.322	43.539	1.933	0.284	0.104	0.012	0.030
NSD	3	1794	fertilized	6.920	39.054	104	15.587	39.911	0.000	0.273	0.108	0.005	0.033
NSD	4	897	control	5.460	31.826	106	16.348	51.365	0.698	0.294	0.080	0.015	0.023
NSD	5	897	fertilized	6.070	41.085	99	16.325	39.735	0.000	0.308	0.071	0.033	0.047
NSD	6	897	fertilized	5.490	40.021	115	16.679	41.675	1.303	0.278	0.107	0.017	0.052
NSD	7	897	control	5.440	34.785	109	16.854	48.451	2.734	0.282	0.103	0.001	0.050
NSD	8	1794	control	6.275	33.441	106	15.975	47.771	2.019	0.275	0.106	0.000	0.071
NSD	9	897	control	5.450	30.902	101	15.647	50.634	2.927	0.285	0.094	0.001	0.072
NSD	10	897	fertilized	6.020	34.923	97	15.745	45.085	2.115	0.288	0.111	0.007	0.047
NSD	11	1794	fertilized	6.730	35.996	99	15.844	44.015	0.000	0.286	0.090	0.006	0.011
NSD	12	1794	fertilized	7.010	42.909	80	16.647	38.796	0.000	0.287	0.120	0.005	0.050
NSD	13	1794	fertilized	7.140	42.791	91	16.000	37.391	0.000	0.266	0.069	0.021	0.018
NSD	14	1794	control	6.530	35.432	92	15.519	43.800	0.294	0.287	0.089	0.011	0.037
NSD	15	1794	fertilized	6.210	37.627	107	16.412	43.618	0.000	0.285	0.070	0.014	0.054
NSD	16	897	fertilized	5.910	38.762	102	16.713	43.116	2.330	0.280	0.100	0.009	0.020
NSD	17	1794	control	6.670	35.512	99	15.426	43.439	0.000	0.268	0.078	0.006	0.045
NSD	18	897	fertilized	5.530	34.242	99	17.109	49.965	2.394	0.292	0.088	0.008	0.025
Henderson	3	-----	vegetation control	12.494	30.946	97	17.988	58.128	0.934	0.282	0.114	0.027	0.023
Henderson	4	-----	control	9.417	29.259	92	16.504	56.408	0.000	0.294	0.099	0.034	0.002
Henderson	5	-----	vegetation control	12.057	31.912	89	18.560	58.162	1.173	0.275	0.111	0.012	0.019
Henderson	6	-----	control	8.326	29.067	84	17.517	60.264	1.147	0.287	0.120	0.014	0.001
Henderson	9	-----	vegetation control	17.715	31.067	94	16.078	51.754	0.000	0.276	0.143	0.015	0.008
Henderson	10	-----	control	11.444	38.393	98	22.845	59.503	1.523	0.286	0.101	0.038	0.001
Henderson	11	-----	vegetation control	16.671	33.367	82	17.289	51.816	0.000	0.289	0.125	0.026	0.009
Henderson	12	-----	control	16.537	31.709	73	16.653	52.518	0.000	0.289	0.142	0.011	0.005
Henderson	13	-----	control	10.219	34.759	103	21.304	61.291	1.166	0.286	0.113	0.018	0.008
Henderson	14	-----	vegetation control	14.507	28.654	95	16.657	58.133	0.824	0.288	0.104	0.039	0.027
Henderson	15	-----	control	7.685	28.154	86	16.389	58.213	0.077	0.276	0.059	0.032	0.002
Henderson	16	-----	vegetation control	14.724	26.989	83	15.150	56.135	0.000	0.296	0.129	0.010	0.009
Henderson	17	-----	vegetation control	11.525	41.809	94	23.444	56.073	1.212	0.295	0.103	0.051	0.004
Henderson	18	-----	control	9.253	27.867	94	17.204	61.737	0.000	0.282	0.082	0.022	0.001
Henderson	19	-----	vegetation control	18.542	29.877	91	16.985	56.850	0.000	0.295	0.055	0.061	0.051
Henderson	20	-----	control	7.657	25.524	72	14.673	57.487	0.000	0.273	0.062	0.030	0.012
Henderson	24	-----	vegetation control	15.970	27.166	96	14.990	55.179	0.000	0.271	0.095	0.025	0.017
Henderson	25	-----	control	18.602	31.217	105	16.607	53.200	0.000	0.304	0.113	0.028	0.002
Henderson	26	-----	control	10.918	26.570	84	15.261	57.437	0.438	0.291	0.123	0.015	0.010
Henderson	27	-----	vegetation control	9.503	36.635	97	22.637	61.792	1.253	0.284	0.091	0.042	0.021
Henderson	28	-----	control	8.427	27.882	93	16.831	60.365	1.103	0.281	0.092	0.036	0.002
Henderson	29	-----	vegetation control	16.785	29.961	78	16.171	53.973	0.529	0.293	0.132	0.017	0.036
Henderson	30	-----	vegetation control	11.604	28.649	85	17.093	59.664	0.000	0.299	0.052	0.063	0.010
Henderson	31	-----	control	7.028	30.506	89	17.213	56.426	0.785	0.279	0.112	0.020	0.002
RW18	3	-----	fertilized thinned	5.824	26.153	74	14.887	56.924	1.688	0.294	0.080	0.029	0.183

[*] Site = study site (refer to fig. 2.1), TPH/block = trees per hectare or block, for other variable names refer to table 2.1

Site	Plot	TPH/ block	Treatment	Veg_{20th}	I_{mean}	I_{max}	I_{stdv}	I_{cv}	$Cd+4_{cv}$	$Cd+1_{stdv}$	Cd+1	Cd-4	LPI
RW18	12	-----	fertilized unthinned	12.963	27.965	78	13.179	47.128	0.000	0.266	0.067	0.027	0.008
RW18	14	-----	fertilized thinned	11.819	35.512	97	21.676	61.039	0.000	0.306	0.065	0.033	0.255
RW18	15	-----	fertilized unthinned	3.055	30.276	71	13.392	44.232	1.025	0.296	0.059	0.035	0.011
RW18	16	-----	fertilized thinned	11.897	31.233	83	16.997	54.420	0.000	0.302	0.107	0.012	0.319
RW18	20	-----	fertilized thinned	11.459	31.541	80	16.965	53.789	0.000	0.291	0.085	0.015	0.399
RW18	21	-----	fertilized thinned	11.067	30.074	83	17.208	57.220	0.000	0.292	0.080	0.030	0.359
RW18	22	-----	fertilized thinned	10.890	28.450	77	15.578	54.756	0.000	0.309	0.084	0.035	0.322
RW18	23	-----	fertilized unthinned	11.985	35.950	62	13.739	38.217	0.000	0.260	0.077	0.036	0.011
RW18	26	-----	fertilized thinned	11.952	34.128	97	18.857	55.252	0.000	0.310	0.073	0.022	0.369
RW18	27	-----	fertilized thinned	11.579	29.366	72	15.610	53.155	0.000	0.276	0.104	0.020	0.334
RW18	28	-----	control and thinned	11.425	27.885	74	15.127	54.249	0.000	0.289	0.064	0.031	0.358
RW18	29	-----	fertilized thinned	10.254	30.995	88	17.988	58.036	0.000	0.287	0.064	0.011	0.404
RW18	30	-----	fertilized thinned	11.368	32.453	83	17.196	52.988	0.000	0.288	0.096	0.018	0.327
RW18	31	-----	fertilized thinned	5.692	27.686	87	14.731	53.208	2.218	0.279	0.071	0.036	0.199
RW18	45	-----	fertilized thinned	12.188	34.092	75	17.647	51.764	0.000	0.281	0.137	0.007	0.405
RW18	46	-----	control and thinned	10.882	29.349	80	16.312	55.580	0.000	0.298	0.066	0.007	0.474
RW18	47	-----	fertilized unthinned	13.361	38.776	68	15.513	40.008	0.000	0.271	0.118	0.015	0.009
RW18	48	-----	fertilized thinned	11.670	29.647	78	16.079	54.237	0.648	0.289	0.094	0.001	0.373
RW19	1	-----	fertilized	8.560	34.632	104	16.796	48.499	1.981	0.291	0.140	0.025	0.015
RW19	2	-----	fertilized	7.823	33.820	82	17.220	50.916	1.896	0.292	0.113	0.019	0.044
RW19	3	-----	fertilized	7.860	33.440	128	18.493	55.303	1.964	0.290	0.098	0.011	0.230
RW19	4	-----	fertilized	7.359	31.708	117	17.879	56.388	2.199	0.293	0.108	0.023	0.044
RW19	5	-----	fertilized	7.581	34.718	105	17.207	49.561	1.915	0.286	0.098	0.015	0.058
RW19	6	-----	fertilized	8.007	32.340	108	16.371	50.621	1.964	0.294	0.108	0.011	0.034
RW19	8	-----	fertilized	7.527	39.159	119	18.027	46.035	1.915	0.288	0.104	0.020	0.164
RW19	9	-----	fertilized	7.475	33.712	127	17.553	52.068	1.989	0.292	0.092	0.018	0.103
RW19	10	-----	fertilized	7.666	35.690	114	18.293	51.255	2.172	0.293	0.101	0.016	0.045
RW19	11	-----	fertilized	8.167	34.217	98	17.334	50.659	0.000	0.273	0.091	0.023	0.067
RW19	12	-----	fertilized	8.575	38.507	112	17.128	44.481	1.626	0.291	0.128	0.023	0.090
RW19	13	-----	fertilized	7.471	33.884	116	17.453	51.508	1.430	0.287	0.096	0.014	0.186
RW19	14	-----	fertilized	8.180	35.439	106	17.115	48.294	0.906	0.266	0.093	0.030	0.085
RW19	15	-----	fertilized	7.730	34.840	103	16.922	48.570	1.742	0.290	0.072	0.042	0.061
RW19	17	-----	fertilized	8.122	37.540	118	17.421	46.407	1.666	0.298	0.102	0.029	0.027
RW19	18	-----	fertilized	7.878	34.698	116	16.712	48.165	1.772	0.291	0.116	0.013	0.062
RW19	19	-----	fertilized	7.799	35.510	104	16.940	47.705	2.188	0.298	0.149	0.019	0.031
RW19	20	-----	fertilized	8.331	35.570	122	16.834	47.328	1.887	0.283	0.139	0.008	0.072
RW19	21	-----	fertilized	7.847	37.634	100	19.129	50.828	0.000	0.281	0.092	0.033	0.055
RW19	22	-----	fertilized	7.522	37.395	114	18.994	50.794	0.000	0.286	0.070	0.038	0.067
RW19	23	-----	fertilized	7.591	38.421	109	18.947	49.313	1.622	0.281	0.108	0.014	0.088
RW19	24	-----	fertilized	8.710	35.003	91	16.506	47.156	1.420	0.285	0.142	0.017	0.026
RW19	25	-----	fertilized	7.423	38.746	121	19.333	49.896	1.832	0.287	0.107	0.014	0.042
RW19	26	-----	fertilized	7.636	35.453	109	17.316	48.842	0.000	0.288	0.064	0.032	0.029
RW19	27	-----	fertilized	6.875	33.603	110	18.689	55.617	1.625	0.287	0.082	0.023	0.163
RW19	28	-----	fertilized	6.274	35.982	115	18.638	51.797	2.091	0.306	0.087	0.030	0.097
RW19	29	-----	fertilized	7.094	33.525	111	18.101	53.991	2.040	0.301	0.091	0.020	0.069
RW19	30	-----	fertilized	8.038	36.915	120	17.387	47.100	1.273	0.289	0.106	0.035	0.052
RW19	31	-----	fertilized	7.686	34.413	100	16.918	49.161	1.623	0.259	0.114	0.024	0.023
RW19	32	-----	fertilized	7.495	33.865	117	18.359	54.212	1.921	0.291	0.103	0.020	0.158

Site	Plot	TPH/ block	Treatment	Veg_{20th}	I_{mean}	I_{max}	I_{stdv}	I_{cv}	$Cd+4_{cv}$	$Cd+1_{stdv}$	Cd+1	Cd-4	LPI
RW19	33	-----	fertilized	6.912	36.535	112	17.835	48.817	1.785	0.301	0.122	0.021	0.088
RW19	34	-----	fertilized	8.057	35.577	116	17.098	48.059	2.131	0.301	0.132	0.013	0.045
Setres	1	1	control	9.075	27.298	88	13.581	49.749	1.779	0.287	0.103	0.041	0.053
Setres	1	2	control	10.010	27.733	101	13.922	50.202	1.758	0.292	0.084	0.038	0.055
Setres	1	3	control	12.230	35.395	90	15.924	44.991	1.396	0.287	0.121	0.031	0.044
Setres	1	4	control	13.620	32.084	97	15.195	47.362	1.421	0.286	0.143	0.026	0.035
Setres	2	1	fertilized, irrigated	9.410	28.440	63	14.088	49.536	1.823	0.293	0.110	0.036	0.053
Setres	2	2	fertilized, irrigated	10.050	29.125	72	14.288	49.058	1.785	0.278	0.092	0.032	0.074
Setres	2	3	fertilized, irrigated	14.210	36.579	72	15.467	42.283	0.452	0.289	0.124	0.033	0.026
Setres	2	4	fertilized, irrigated	14.250	33.546	75	15.428	45.992	1.458	0.291	0.122	0.039	0.020
Setres	3	1	fertilized, irrigated	7.420	27.466	88	14.676	53.434	2.616	0.296	0.126	0.012	0.090
Setres	3	2	fertilized, irrigated	10.560	29.806	80	14.630	49.084	1.775	0.292	0.079	0.059	0.037
Setres	3	3	fertilized, irrigated	12.810	35.613	69	15.751	44.229	0.928	0.293	0.103	0.049	0.029
Setres	3	4	fertilized, irrigated	13.040	31.957	80	15.629	48.906	0.781	0.272	0.104	0.063	0.040
Setres	4	1	fertilized, irrigated	8.820	28.462	86	13.934	48.958	1.757	0.302	0.093	0.040	0.077
Setres	4	2	fertilized, irrigated	9.075	27.560	71	14.416	52.308	1.966	0.289	0.106	0.037	0.066
Setres	4	3	fertilized, irrigated	12.510	35.971	78	15.574	43.295	1.433	0.287	0.136	0.027	0.022
Setres	4	4	fertilized, irrigated	14.365	36.929	76	16.191	43.845	1.290	0.294	0.126	0.029	0.046

Appendix B: Normal quantiles vs. Studentized residuals plot (top) and predicted vs. residuals plot (bottom) for the LAI 2-variable model with lidar metrics only, n = 109 (Chapter 2). Refer to table 2.1 for variable names.

$$\text{Model LAI} = 2.767 - 7.518\ (\text{LPI}) - 0.237\ (\text{Cd+4}_{cv})$$

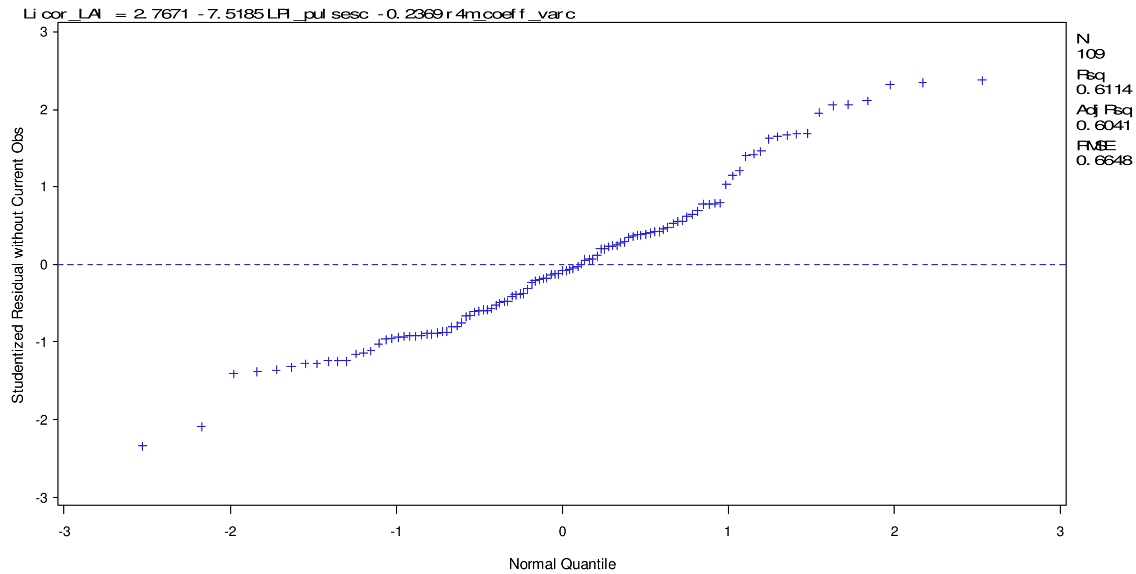

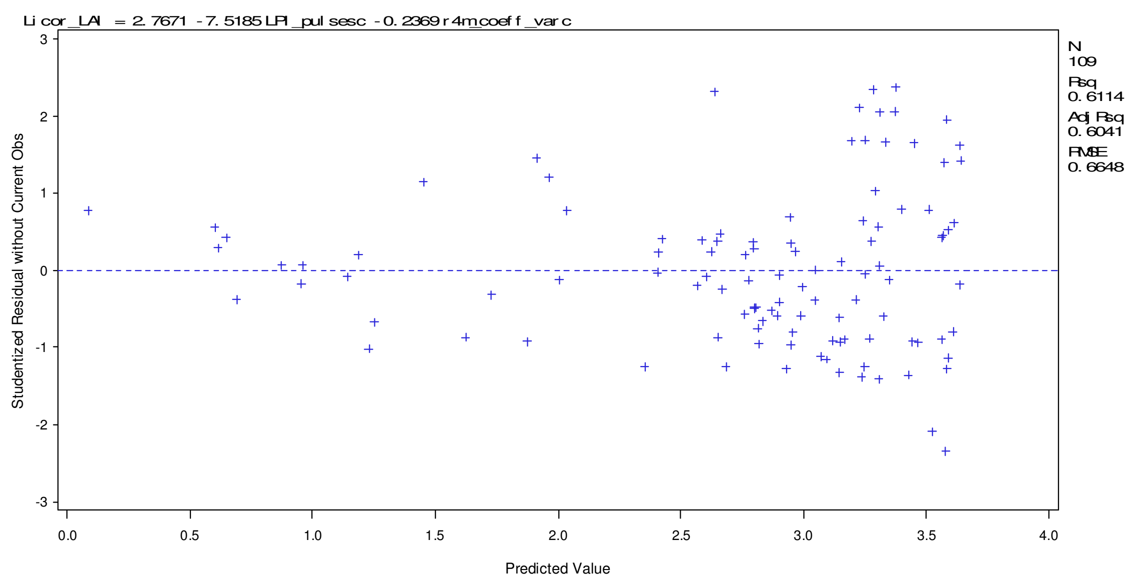

Appendix C: Normal quantiles vs. Studentized residuals plot (top) and predicted vs. residuals plot (bottom) for the LAI 3-variable model with lidar metrics only, *n* = 109 (Chapter 2). Refer to table 2.1 for variable names.

$$\text{LAI} = 2.767 + 0.318\ (\text{Veg}_{\text{stdv}}) - 5.393\ (\text{LPI}) + 0.099\ (\text{I}_{\text{mean}})$$

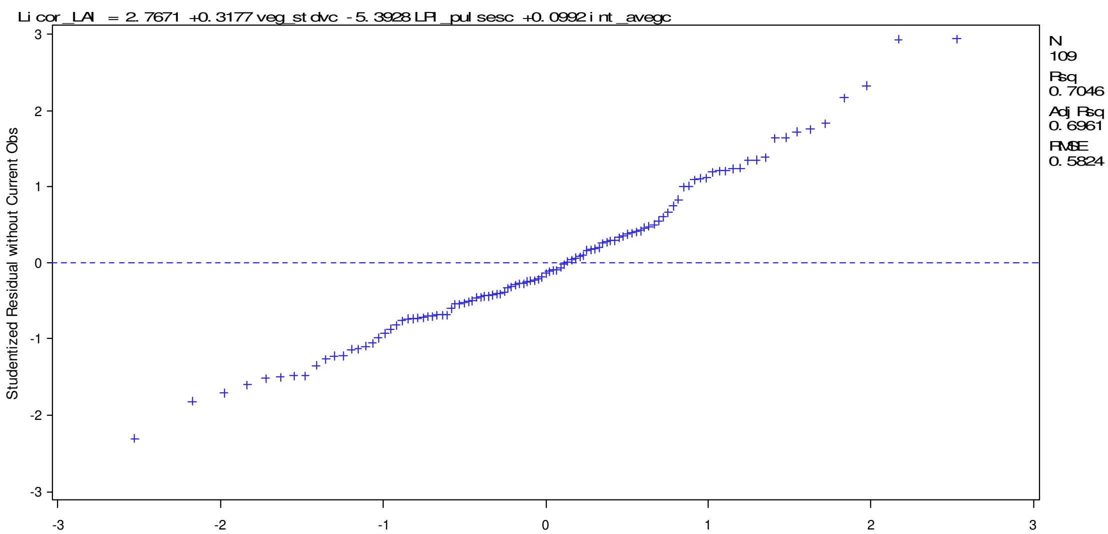

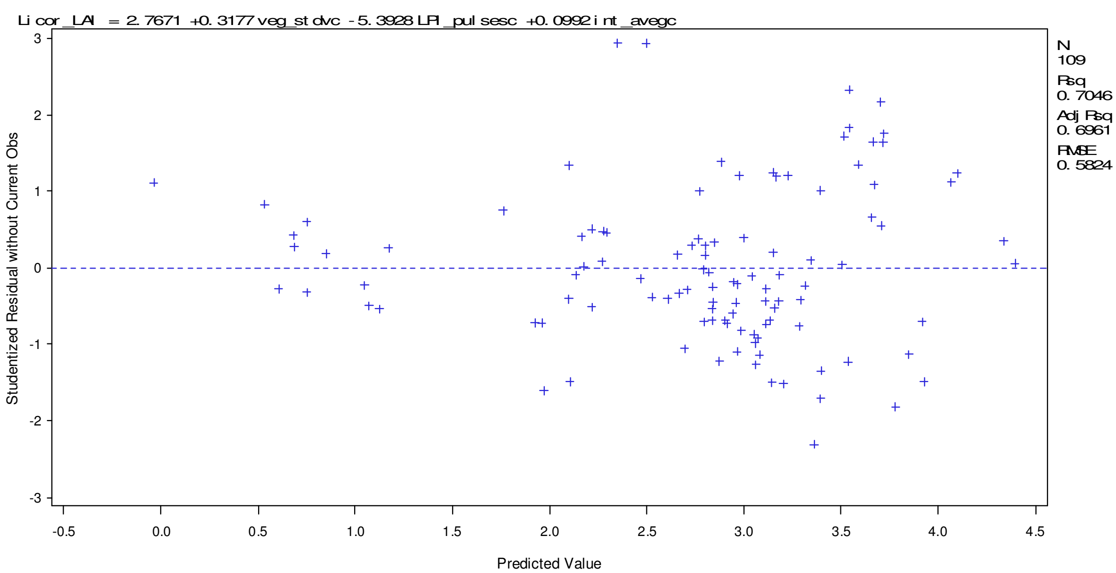

Appendix D: Normal quantiles vs. Studentized residuals plot (top) and predicted vs. residuals plot (bottom) for the LAI 4-variable model with lidar metrics only, n = 109 (Chapter 2). Refer to table 2.1 for variable names.

$$LAI = 2.767 + 0.330\ (Veg_{mean}) - 0.268\ (Veg_{20th}) - 5.522\ (LPI) + 0.106\ (I_{mean})$$

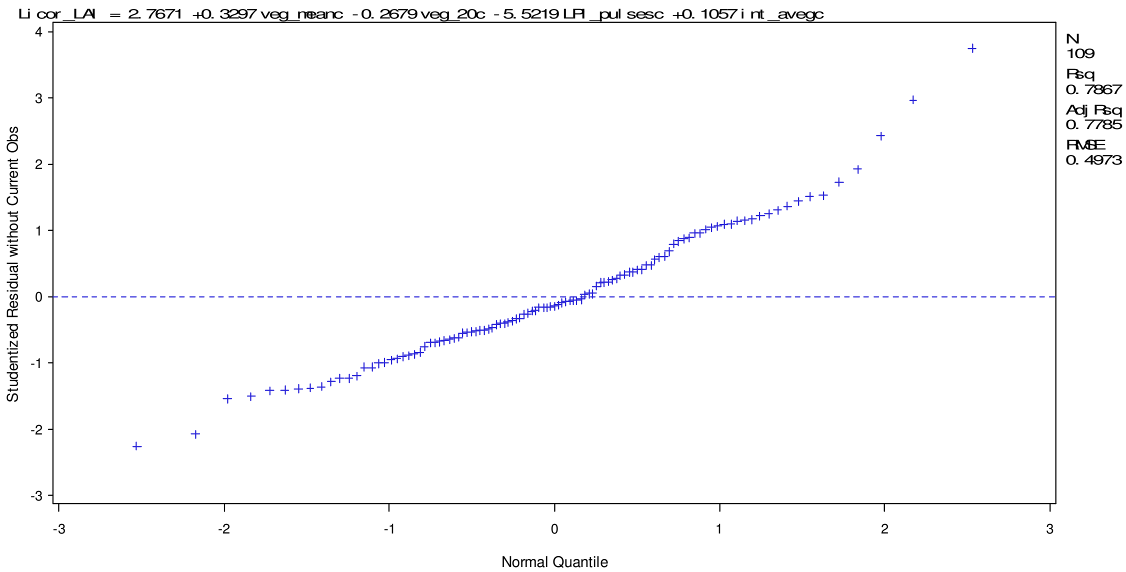

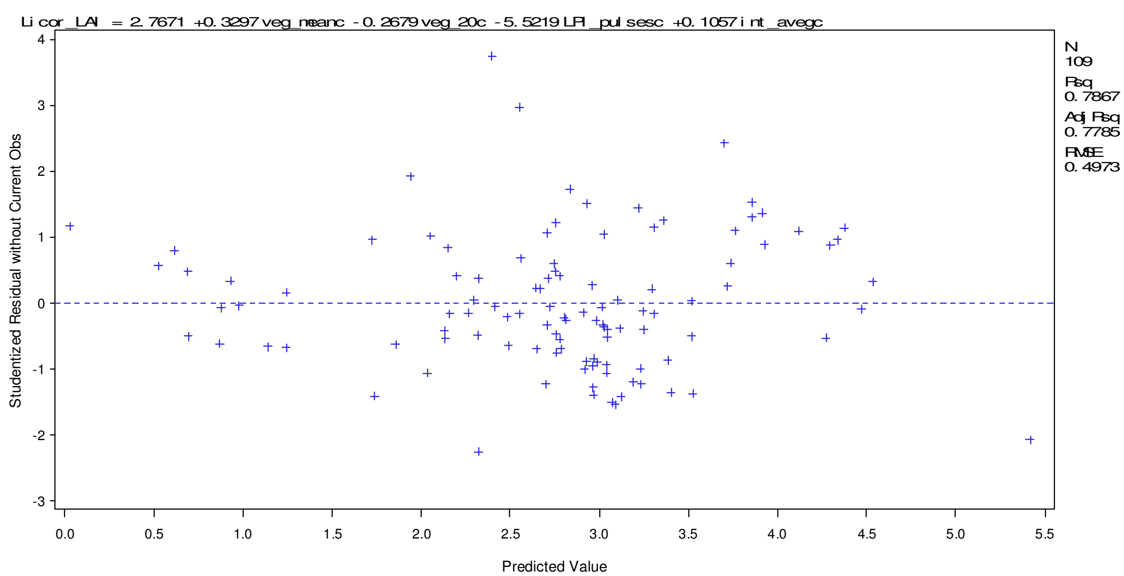

Appendix E: Normal quantiles vs. Studentized residuals plot (top) and predicted vs. residuals plot (bottom) for the LAI 5-variable model with lidar metrics only, *n* = 109 (Chapter 2). Refer to table 2.1 for variable names.

$$LAI = 2.767 + 0.324\ (Veg_{mean}) - 0.262\ (Veg_{20th}) - 5.275\ (LPI) + 0.104\ (I_{mean}) - 13.046\ (Cd{+}1_{stdv})$$

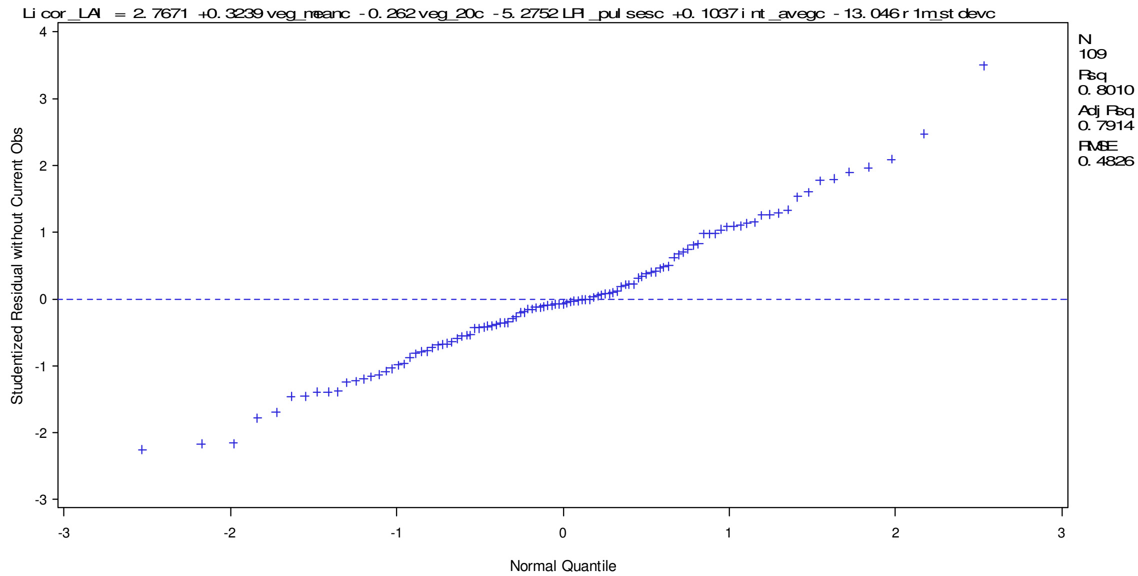

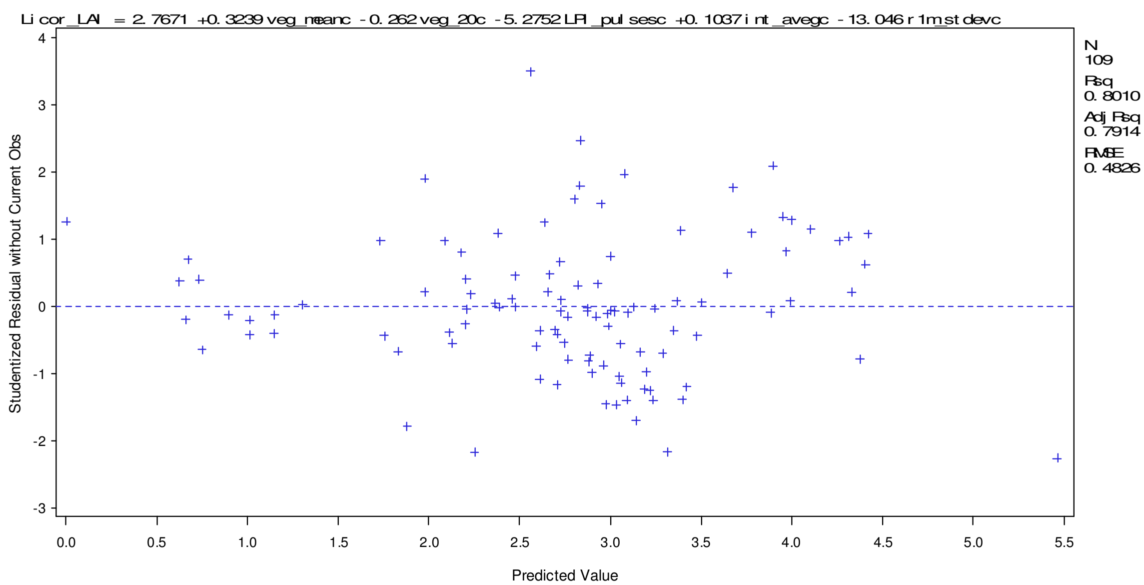

Appendix F: Normal quantiles vs. Studentized residuals plot (top) and predicted vs. residuals plot (bottom) for the LAI 6-variable model with lidar metrics only, n = 109 (Chapter 2). Refer to table 2.1 for variable names.

$$LAI = 2.767 + 0.345\ (Veg_{mean}) - 0.236\ (Veg_{20th}) - 6.475\ (LPI) + 0.113\ (I_{mean}) - 10.772\ (Cd+1) - 18.581\ (Cd\text{-}4)$$

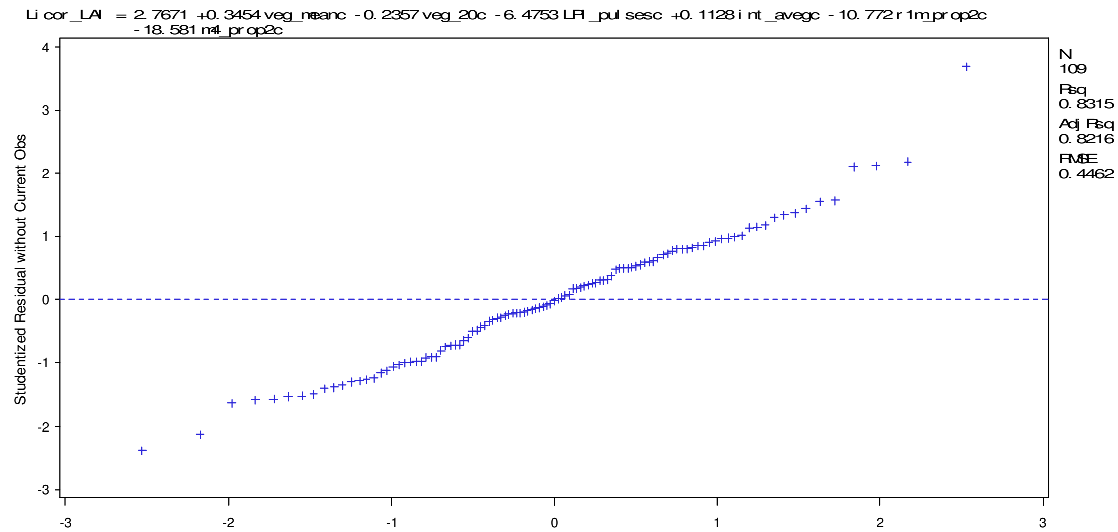

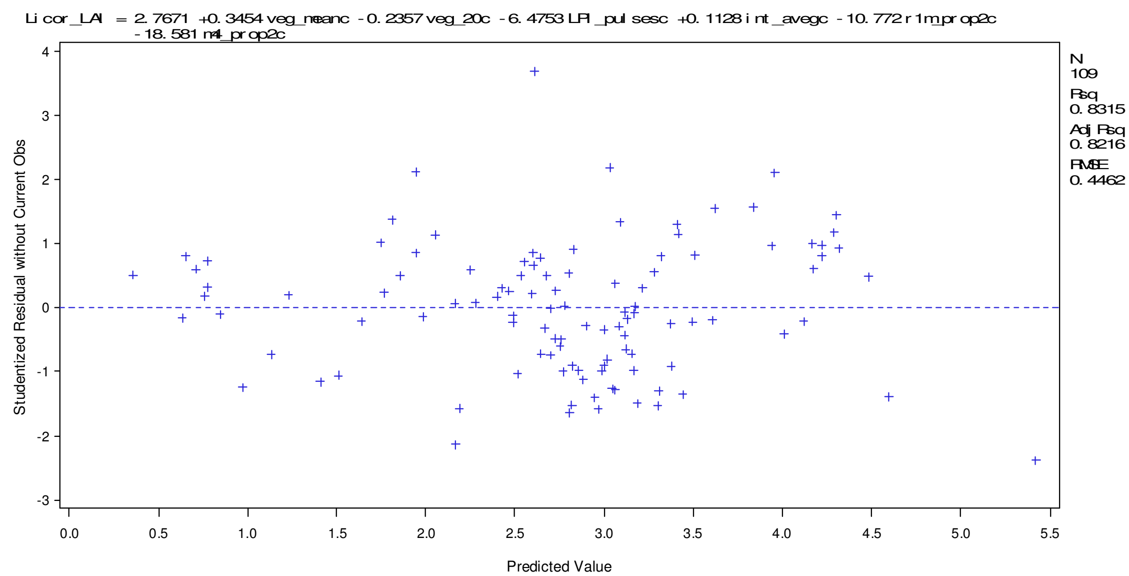

Appendix G: Ground-based variables and lidar metrics used for the number of trees models (chapter 3)*

Site	Plot	TPH/ block	Treatment	N_{trees}	$Tree_0$	ht_{mean}	$htlc_{mean}$	dbh_{mean}	Gr_{total}	LPI	All_{total}	All_{mean}	All_{stdv}	All_{cv}	All_{10th}	All_{90th}
NSD	1	1794	fertilized	120	128	11.43	5.48	15.11	745	0.027	3399	7.484	2.556	34.155	5.050	9.970
NSD	2	897	fertilized	62	64	11.12	3.89	18.43	790	0.030	3528	6.760	2.450	36.240	4.060	9.460
NSD	3	1794	fertilized	126	128	11.14	5.48	15.21	575	0.033	1844	7.639	2.317	30.329	5.800	9.830
NSD	4	897	control	62	64	10.56	4.10	17.01	474	0.023	1938	5.940	2.681	45.124	0.410	8.770
NSD	5	897	fertilized	62	64	11.17	4.09	18.76	395	0.047	1899	7.026	2.249	32.011	4.760	9.390
NSD	6	897	fertilized	59	64	10.78	2.83	18.82	486	0.052	2052	6.629	2.314	34.903	4.080	9.240
NSD	7	897	control	61	64	10.91	3.40	17.88	629	0.050	2316	6.347	2.423	38.183	3.585	9.045
NSD	8	1794	control	128	128	10.98	5.42	13.60	595	0.071	1912	6.651	2.759	41.474	0.360	9.410
NSD	9	897	control	60	64	11.46	3.86	17.42	673	0.072	1724	6.291	2.551	40.546	1.080	9.180
NSD	10	897	fertilized	62	64	11.27	4.09	18.60	630	0.047	2263	6.903	2.585	37.451	3.990	9.670
NSD	11	1794	fertilized	123	128	11.10	5.44	14.74	789	0.011	3552	7.247	2.583	35.641	4.590	9.750
NSD	12	1794	fertilized	122	128	11.25	5.10	15.34	544	0.050	3138	7.768	2.128	27.398	5.920	9.860
NSD	13	1794	fertilized	125	128	11.35	5.53	15.70	566	0.018	3147	8.020	2.184	27.232	6.220	10.190
NSD	14	1794	control	124	128	11.14	5.05	14.74	730	0.037	3159	7.399	2.339	31.606	5.260	9.800
NSD	15	1794	fertilized	124	128	10.72	4.54	14.96	739	0.054	3490	6.976	2.280	32.683	4.985	9.265
NSD	16	897	fertilized	61	64	11.19	3.36	18.63	622	0.020	3131	6.966	2.357	33.838	4.540	9.560
NSD	17	1794	control	122	128	11.20	5.57	14.64	832	0.045	3576	7.307	2.303	31.521	5.600	9.500
NSD	18	897	fertilized	62	64	11.28	4.59	17.99	608	0.025	3239	6.171	2.806	45.476	0.390	9.280
Henderson	3	-----	vegetation control	62	75	22.40	16.14	21.83	83	0.023	1627	17.069	5.178	30.335	8.887	21.945
Henderson	4	-----	control	64	75	23.00	17.12	22.94	143	0.002	1604	16.397	6.948	42.376	4.027	22.594
Henderson	5	-----	vegetation control	58	75	21.09	15.36	20.21	186	0.019	1506	15.967	5.234	32.780	7.524	20.867
Henderson	6	-----	control	63	75	20.83	14.92	19.65	152	0.001	1665	14.956	5.805	38.814	5.814	20.400
Henderson	9	-----	vegetation control	63	75	21.12	15.80	20.87	422	0.008	1357	17.352	5.576	32.135	6.988	21.136
Henderson	10	-----	control	29	75	20.75	13.48	19.92	76	0.001	1581	14.750	4.012	27.200	8.731	19.036
Henderson	11	-----	vegetation control	60	75	21.06	14.59	22.82	256	0.009	1391	16.483	5.947	36.078	4.548	20.857
Henderson	12	-----	control	69	75	21.95	15.45	21.61	242	0.005	1432	16.372	6.249	38.168	4.001	21.117
Henderson	13	-----	control	38	75	20.07	13.26	19.77	82	0.008	1546	14.310	4.152	29.018	8.195	18.741
Henderson	14	-----	vegetation control	51	75	22.54	15.44	21.78	369	0.027	1344	15.526	6.370	41.031	2.875	20.729

* Site = study site (refer to fig. 2.1), TPH/block = trees per hectare or block, for other variable names refer to table 3.1

Site	Plot	TPH/ block	Treatment	N_{trees}	$Tree_0$	ht_{mean}	$htlc_{mean}$	dbh_{mean}	Gr_{total}	LPI	All_{total}	All_{mean}	All_{stdv}	All_{cv}	All_{10th}	All_{90th}
Henderson	15	-----	control	71	75	21.77	15.40	19.39	204	0.002	1379	14.563	6.153	42.252	4.078	19.929
Henderson	16	-----	vegetation control	63	75	20.02	14.07	20.76	331	0.009	1551	13.777	6.588	47.815	1.050	19.044
Henderson	17	-----	vegetation control	20	75	18.45	12.42	19.25	92	0.004	1390	13.997	4.197	29.983	7.753	18.178
Henderson	18	-----	control	58	75	21.34	15.55	20.00	169	0.001	1823	14.831	5.746	38.746	5.618	20.399
Henderson	19	-----	vegetation control	61	75	23.33	17.39	22.24	317	0.051	1392	17.793	6.851	38.506	2.214	22.792
Henderson	20	-----	control	67	75	20.26	14.13	19.37	188	0.012	1754	13.804	5.534	40.092	5.087	18.892
Henderson	24	-----	vegetation control	65	75	20.76	14.72	20.13	497	0.017	1752	15.222	5.997	39.398	1.165	19.499
Henderson	25	-----	control	63	75	22.87	17.84	22.20	317	0.002	1406	17.867	6.957	38.938	2.456	22.789
Henderson	26	-----	control	67	75	19.95	13.65	21.24	216	0.010	1739	13.182	6.789	51.499	1.302	19.013
Henderson	27	-----	vegetation control	32	75	17.48	11.84	17.66	126	0.021	1750	12.125	3.812	31.441	6.314	16.055
Henderson	28	-----	control	62	75	22.01	15.77	20.64	81	0.002	1779	15.729	6.071	38.597	6.300	21.674
Henderson	29	-----	vegetation control	62	75	22.75	16.23	21.75	295	0.036	1320	16.685	7.166	42.945	2.488	22.148
Henderson	30	-----	vegetation control	46	75	23.40	15.16	24.25	131	0.010	1746	16.601	5.484	33.037	7.927	21.938
Henderson	31	-----	control	64	75	23.80	16.94	22.93	154	0.002	1560	16.717	7.400	44.264	3.867	22.982
RW18	3	-----	fertilized thinned	16	61	16.00	8.62	21.61	374	0.183	1505	11.122	4.494	40.409	4.056	16.084
RW18	12	-----	fertilized unthinned	68	71	16.35	8.80	18.96	235	0.008	1594	11.743	5.453	46.436	0.318	15.937
RW18	14	-----	fertilized thinned	16	68	16.87	9.20	21.88	498	0.255	1094	9.402	6.286	66.862	0.249	15.529
RW18	15	-----	fertilized unthinned	61	70	15.05	7.85	18.94	216	0.011	953	6.660	3.874	58.167	1.268	11.567
RW18	16	-----	fertilized thinned	16	67	16.14	9.16	21.26	498	0.319	786	11.419	4.800	42.036	0.299	15.301
RW18	20	-----	fertilized thinned	16	69	15.67	8.87	20.27	406	0.399	455	11.827	3.668	31.011	9.359	14.800
RW18	21	-----	fertilized thinned	16	74	15.87	8.60	20.15	399	0.359	567	10.585	4.958	46.838	0.267	14.846
RW18	22	-----	fertilized thinned	16	66	15.77	8.58	20.92	434	0.322	607	11.624	3.543	30.483	8.944	14.748
RW18	23	-----	fertilized unthinned	63	70	15.27	8.25	19.12	216	0.011	993	12.468	3.309	26.542	9.606	15.104
RW18	26	-----	fertilized thinned	16	75	16.50	9.16	20.89	315	0.369	374	11.972	4.439	37.076	0.564	15.576
RW18	27	-----	fertilized thinned	17	66	16.19	8.66	21.17	319	0.334	437	12.065	3.874	32.112	9.145	15.189
RW18	28	-----	control and thinned	17	66	16.55	8.66	20.78	453	0.358	625	12.115	3.588	29.621	9.124	15.277
RW18	29	-----	fertilized thinned	15	71	15.87	8.78	19.34	589	0.404	762	10.965	4.062	37.045	3.401	14.675
RW18	30	-----	fertilized thinned	18	69	16.19	8.82	21.65	516	0.327	781	11.536	4.188	36.304	1.039	15.016
RW18	31	-----	fertilized thinned	17	61	15.77	8.22	21.52	390	0.199	1296	8.786	4.070	46.327	3.181	14.625
RW18	45	-----	fertilized thinned	13	66	16.70	9.68	20.83	287	0.405	327	12.656	3.548	28.036	10.462	15.449
RW18	46	-----	control and thinned	14	64	15.42	8.22	18.76	469	0.474	395	11.365	3.365	29.605	9.336	14.311
RW18	47	-----	fertilized unthinned	49	63	16.74	9.18	19.94	223	0.009	1017	13.896	3.492	25.130	11.191	16.611
RW18	48	-----	fertilized thinned	16	86	16.06	8.76	21.07	530	0.373	634	11.922	4.005	33.593	7.417	15.164

Site	Plot	TPH/ block	Treatment	N_{trees}	$Tree_0$	ht_{mean}	$htlc_{mean}$	dbh_{mean}	Gr_{total}	LPI	All_{total}	All_{mean}	All_{stdv}	All_{cv}	All_{10th}	All_{90th}
RW18	7	-----	fertilized thinned	15	73	16.40	9.00	19.57	471	0.274	1156	8.593	3.440	40.027	3.383	12.471
RW19	1	-----	fertilized	45	71	14.10	6.63	19.01	394	0.015	1496	9.516	3.103	32.607	6.326	12.481
RW19	2	-----	fertilized	46	60	13.00	5.99	18.59	496	0.044	1179	8.497	3.222	37.922	3.806	11.677
RW19	3	-----	fertilized	140	187	12.95	6.24	17.93	2090	0.230	3364	8.191	3.623	44.230	0.343	11.718
RW19	4	-----	fertilized	83	108	12.59	5.72	19.14	1098	0.044	2814	7.449	3.828	51.386	0.316	11.296
RW19	5	-----	fertilized	70	90	12.23	6.08	17.78	1006	0.058	1582	8.147	3.198	39.248	0.585	11.282
RW19	6	-----	fertilized	47	71	13.41	6.52	18.19	721	0.034	1378	8.480	3.470	40.918	0.392	11.845
RW19	8	-----	fertilized	137	187	12.99	5.78	19.50	1875	0.164	3284	8.534	2.673	31.326	5.921	11.261
RW19	9	-----	fertilized	83	108	12.98	6.04	18.44	1077	0.103	2105	7.864	3.431	43.622	0.337	11.259
RW19	10	-----	fertilized	67	90	13.15	6.05	19.21	1073	0.045	1738	8.225	3.443	41.858	0.458	11.614
RW19	11	-----	fertilized	56	71	13.86	6.71	17.68	864	0.067	1844	8.562	3.510	40.997	0.375	11.903
RW19	12	-----	fertilized	184	188	13.58	6.53	18.78	1252	0.090	4366	9.438	2.920	30.939	6.861	12.196
RW19	13	-----	fertilized	166	187	12.68	5.99	17.29	2137	0.186	4331	7.570	3.637	48.041	0.339	11.136
RW19	14	-----	fertilized	103	108	14.00	6.56	18.18	1249	0.085	2563	9.147	2.978	32.557	6.272	12.145
RW19	15	-----	fertilized	78	90	13.66	6.21	18.40	1114	0.061	1920	8.649	3.056	35.333	5.473	11.670
RW19	17	-----	fertilized	58	67	13.45	5.98	20.26	386	0.027	1657	8.945	3.030	33.868	5.435	11.939
RW19	18	-----	fertilized	184	187	13.48	5.92	17.68	1844	0.062	4397	8.315	3.280	39.448	0.612	11.424
RW19	19	-----	fertilized	90	108	13.45	6.22	19.70	587	0.031	2059	8.637	3.135	36.301	4.332	11.775
RW19	20	-----	fertilized	71	90	12.99	6.43	18.97	854	0.072	2495	8.809	3.243	36.814	3.729	11.876
RW19	21	-----	fertilized	58	71	12.80	6.45	16.90	632	0.055	1803	8.140	3.557	43.702	0.497	11.541
RW19	22	-----	fertilized	186	187	12.83	6.09	16.53	1687	0.067	4658	7.970	3.440	43.158	0.615	11.350
RW19	23	-----	fertilized	103	108	12.68	5.90	17.34	969	0.088	2366	8.118	3.253	40.071	0.826	11.257
RW19	24	-----	fertilized	105	108	13.66	6.59	18.36	593	0.026	2207	9.605	2.940	30.614	7.039	12.405
RW19	25	-----	fertilized	86	90	12.47	6.13	16.70	944	0.042	2015	8.221	3.030	36.852	2.879	11.178
RW19	26	-----	fertilized	45	71	13.13	5.76	19.12	755	0.029	1499	8.051	3.391	42.120	0.431	11.358
RW19	27	-----	fertilized	136	187	12.36	5.43	18.58	1720	0.163	4007	7.024	3.763	53.579	0.330	11.036
RW19	28	-----	fertilized	90	108	12.81	5.50	17.99	930	0.097	2246	7.372	3.408	46.232	1.070	11.062
RW19	29	-----	fertilized	65	90	12.57	5.13	18.27	868	0.069	1987	7.095	3.778	53.256	0.302	10.951
RW19	30	-----	fertilized	66	90	13.58	6.05	19.27	576	0.052	1751	9.069	3.054	33.678	5.968	12.116
RW19	31	-----	fertilized	41	60	13.58	5.93	18.81	493	0.023	1149	8.677	2.886	33.265	5.835	11.673
RW19	32	-----	fertilized	156	187	12.88	5.79	17.26	1586	0.158	4251	8.179	3.218	39.347	1.115	11.423
RW19	33	-----	fertilized	90	108	12.45	5.39	17.62	772	0.088	2046	7.750	2.982	38.477	3.698	10.830
RW19	34	-----	fertilized	79	90	13.21	6.33	17.63	716	0.045	2185	8.617	3.118	36.188	5.248	11.627

Site	Plot	TPH/ block	Treatment	N_{trees}	$Tree_0$	ht_{mean}	$htlc_{mean}$	dbh_{mean}	Gr_{total}	LPI	All_{total}	All_{mean}	All_{stdv}	All_{cv}	All_{10th}	All_{90th}
Setres	1	1	control	107	150	13.72	7.07	16.76	887	0.053	3209	10.192	3.280	32.184	7.270	13.530
Setres	1	2	control	102	150	14.73	7.98	17.78	770	0.055	2274	11.064	3.324	30.042	8.370	14.340
Setres	1	3	control	97	150	15.99	9.31	20.76	779	0.044	2424	12.990	3.486	26.836	10.640	15.850
Setres	1	4	control	91	150	18.36	10.46	22.41	819	0.035	4039	14.327	4.353	30.382	10.870	17.920
Setres	2	1	fertilized, irrigated	104	150	13.38	7.59	17.30	770	0.053	2489	10.480	3.183	30.371	7.590	13.700
Setres	2	2	fertilized, irrigated	101	150	14.54	7.55	18.28	767	0.074	1373	11.312	3.101	27.415	8.550	14.390
Setres	2	3	fertilized, irrigated	94	150	18.54	12.17	23.21	614	0.026	2923	14.869	3.746	25.190	12.460	17.680
Setres	2	4	fertilized, irrigated	99	150	19.10	13.03	23.07	609	0.020	2800	15.132	3.967	26.219	12.215	18.470
Setres	3	1	fertilized, irrigated	84	150	11.05	5.32	15.71	906	0.090	2618	8.496	2.888	33.994	5.680	11.610
Setres	3	2	fertilized, irrigated	109	150	14.72	8.21	17.80	844	0.037	2998	11.532	3.746	32.488	8.410	15.230
Setres	3	3	fertilized, irrigated	91	150	17.42	10.45	22.61	826	0.029	3115	13.729	3.667	26.712	10.920	16.880
Setres	3	4	fertilized, irrigated	80	150	17.90	10.46	22.12	829	0.040	3143	14.189	4.048	28.525	10.550	17.660
Setres	4	1	fertilized, irrigated	104	150	12.90	6.42	16.57	905	0.077	2690	10.063	3.006	29.871	7.185	13.150
Setres	4	2	fertilized, irrigated	88	150	13.60	6.88	18.03	783	0.066	2643	10.264	3.070	29.909	7.470	13.360
Setres	4	3	fertilized, irrigated	101	150	16.47	9.38	21.53	636	0.022	2861	13.431	3.332	24.804	11.000	16.260
Setres	4	4	fertilized, irrigated	87	150	18.92	11.01	24.67	597	0.046	1426	15.315	3.787	24.728	12.360	18.410

Appendix G: Continued*.

Site	Plot	TPH/ block	Treatment	I_{stdv}	I_{cv}	d_5	d_6	d_7	d_9	$Cd{+}4_{stdv}$	Cd+2	Cd-1	Cd-2	Cd-4	Cd-5
NSD	1	1794	fertilized	15.675	43.990	0.108	0.213	0.274	0.121	0.000	0.051	0.130	0.088	0.007	0.002
NSD	2	897	fertilized	16.322	43.539	0.095	0.233	0.283	0.127	0.219	0.067	0.121	0.087	0.012	0.003
NSD	3	1794	fertilized	15.587	39.911	0.084	0.195	0.284	0.132	0.000	0.042	0.143	0.086	0.005	0.000
NSD	4	897	control	16.348	51.365	0.104	0.202	0.292	0.120	0.078	0.032	0.119	0.094	0.015	0.000
NSD	5	897	fertilized	16.325	39.735	0.153	0.240	0.267	0.083	0.000	0.027	0.140	0.128	0.033	0.004
NSD	6	897	fertilized	16.679	41.675	0.168	0.224	0.238	0.094	0.146	0.056	0.115	0.092	0.017	0.003
NSD	7	897	control	16.854	48.451	0.195	0.242	0.213	0.067	0.285	0.079	0.105	0.048	0.001	0.003
NSD	8	1794	control	15.975	47.771	0.114	0.255	0.304	0.081	0.227	0.063	0.120	0.053	0.000	0.002
NSD	9	897	control	15.647	50.634	0.207	0.223	0.188	0.067	0.304	0.072	0.092	0.043	0.001	0.002
NSD	10	897	fertilized	15.745	45.085	0.185	0.230	0.217	0.071	0.239	0.071	0.102	0.067	0.007	0.000
NSD	11	1794	fertilized	15.844	44.015	0.092	0.232	0.280	0.102	0.000	0.038	0.139	0.102	0.006	0.000
NSD	12	1794	fertilized	16.647	38.796	0.196	0.244	0.193	0.059	0.000	0.048	0.167	0.086	0.005	0.001
NSD	13	1794	fertilized	16.000	37.391	0.183	0.195	0.188	0.063	0.000	0.014	0.182	0.136	0.021	0.002
NSD	14	1794	control	15.519	43.800	0.179	0.209	0.216	0.074	0.035	0.038	0.143	0.102	0.011	0.004
NSD	15	1794	fertilized	16.412	43.618	0.216	0.212	0.207	0.054	0.000	0.017	0.148	0.124	0.014	0.003
NSD	16	897	fertilized	16.713	43.116	0.164	0.262	0.242	0.064	0.265	0.075	0.120	0.084	0.009	0.001
NSD	17	1794	control	15.426	43.439	0.208	0.193	0.212	0.084	0.000	0.028	0.153	0.112	0.006	0.000
NSD	18	897	fertilized	17.109	49.965	0.186	0.237	0.220	0.072	0.272	0.061	0.117	0.096	0.008	0.002
Henderson	3	-----	vegetation control	17.988	58.128	0.005	0.005	0.038	0.451	0.226	0.072	0.136	0.125	0.027	0.015
Henderson	4	-----	control	16.504	56.408	0.034	0.026	0.101	0.245	0.000	0.046	0.128	0.108	0.034	0.025
Henderson	5	-----	vegetation control	18.560	58.162	0.012	0.020	0.062	0.343	0.263	0.103	0.112	0.072	0.012	0.016
Henderson	6	-----	control	17.517	60.264	0.064	0.065	0.124	0.260	0.256	0.101	0.119	0.060	0.014	0.010
Henderson	9	-----	vegetation control	16.078	51.754	0.018	0.016	0.055	0.355	0.000	0.072	0.155	0.080	0.015	0.006
Henderson	10	-----	control	22.845	59.503	0.073	0.052	0.073	0.284	0.326	0.075	0.124	0.121	0.038	0.040
Henderson	11	-----	vegetation control	17.289	51.816	0.023	0.047	0.076	0.297	0.000	0.066	0.145	0.098	0.026	0.012
Henderson	12	-----	control	16.653	52.518	0.059	0.052	0.173	0.202	0.000	0.076	0.141	0.090	0.011	0.009
Henderson	13	-----	control	21.304	61.291	0.035	0.021	0.054	0.304	0.237	0.087	0.130	0.098	0.018	0.026
Henderson	14	-----	vegetation control	16.657	58.133	0.004	0.013	0.036	0.491	0.191	0.041	0.114	0.082	0.039	0.028
Henderson	15	-----	control	16.389	58.213	0.088	0.085	0.182	0.217	0.018	0.019	0.147	0.124	0.032	0.016

* Site = study site (refer to fig. 2.1), TPH/block = trees per hectare or block, for other variable names refer to table 3.1

Site	Plot	TPH/ block	Treatment	I_{stdv}	I_{cv}	d_5	d_6	d_7	d_9	$Cd+4_{stdv}$	Cd+2	Cd-1	Cd-2	Cd-4	Cd-5
Henderson	16	-----	vegetation control	15.150	56.135	0.007	0.021	0.050	0.440	0.000	0.069	0.139	0.075	0.010	0.003
Henderson	17	-----	vegetation control	23.444	56.073	0.006	0.009	0.031	0.414	0.247	0.070	0.140	0.111	0.051	0.035
Henderson	18	-----	control	17.204	61.737	0.082	0.050	0.192	0.188	0.000	0.039	0.140	0.113	0.022	0.019
Henderson	19	-----	vegetation control	16.985	56.850	0.015	0.061	0.111	0.348	0.000	0.009	0.138	0.135	0.061	0.026
Henderson	20	-----	control	14.673	57.487	0.023	0.019	0.090	0.275	0.000	0.020	0.148	0.139	0.030	0.009
Henderson	24	-----	vegetation control	14.990	55.179	0.004	0.010	0.048	0.381	0.000	0.034	0.152	0.113	0.025	0.010
Henderson	25	-----	control	16.607	53.200	0.051	0.093	0.190	0.189	0.000	0.050	0.140	0.109	0.028	0.006
Henderson	26	-----	control	15.261	57.437	0.053	0.051	0.061	0.273	0.093	0.070	0.127	0.097	0.015	0.008
Henderson	27	-----	vegetation control	22.637	61.792	0.022	0.023	0.073	0.412	0.229	0.059	0.156	0.120	0.042	0.047
Henderson	28	-----	control	16.831	60.365	0.030	0.015	0.043	0.323	0.269	0.047	0.122	0.099	0.036	0.016
Henderson	29	-----	vegetation control	16.171	53.973	0.004	0.017	0.085	0.408	0.128	0.061	0.132	0.082	0.017	0.007
Henderson	30	-----	vegetation control	17.093	59.664	0.007	0.021	0.096	0.312	0.000	0.029	0.108	0.111	0.063	0.044
Henderson	31	-----	control	17.213	56.426	0.092	0.161	0.321	0.060	0.199	0.068	0.135	0.078	0.020	0.013
RW18	3	-----	fertilized thinned	14.887	56.924	0.047	0.100	0.219	0.101	0.311	0.048	0.104	0.086	0.029	0.027
RW18	12	-----	fertilized unthinned	13.179	47.128	0.010	0.142	0.307	0.137	0.000	0.012	0.183	0.160	0.027	0.010
RW18	14	-----	fertilized thinned	21.676	61.039	0.022	0.085	0.189	0.297	0.000	0.035	0.086	0.073	0.033	0.011
RW18	15	-----	fertilized unthinned	13.392	44.232	0.087	0.119	0.144	0.070	0.147	0.041	0.075	0.068	0.035	0.045
RW18	16	-----	fertilized thinned	16.997	54.420	0.010	0.051	0.132	0.308	0.000	0.070	0.107	0.049	0.012	0.004
RW18	20	-----	fertilized thinned	16.965	53.789	0.005	0.038	0.163	0.316	0.000	0.039	0.107	0.094	0.015	0.001
RW18	21	-----	fertilized thinned	17.208	57.220	0.115	0.187	0.206	0.134	0.000	0.045	0.102	0.063	0.030	0.006
RW18	22	-----	fertilized thinned	15.578	54.756	0.062	0.141	0.237	0.201	0.000	0.031	0.101	0.104	0.035	0.016
RW18	23	-----	fertilized unthinned	13.739	38.217	0.050	0.106	0.242	0.168	0.000	0.012	0.207	0.162	0.036	0.029
RW18	26	-----	fertilized thinned	18.857	55.252	0.027	0.081	0.261	0.246	0.000	0.019	0.096	0.093	0.022	0.012
RW18	27	-----	fertilized thinned	15.610	53.155	0.139	0.189	0.162	0.077	0.000	0.063	0.091	0.077	0.020	0.009
RW18	28	-----	control and thinned	15.127	54.249	0.063	0.172	0.213	0.160	0.000	0.019	0.115	0.105	0.031	0.035
RW18	29	-----	fertilized thinned	17.988	58.036	0.021	0.069	0.214	0.188	0.000	0.030	0.122	0.079	0.011	0.009
RW18	30	-----	fertilized thinned	17.196	52.988	0.024	0.064	0.185	0.284	0.000	0.056	0.108	0.086	0.018	0.015
RW18	31	-----	fertilized thinned	14.731	53.208	0.180	0.130	0.112	0.075	0.278	0.059	0.072	0.063	0.036	0.041
RW18	45	-----	fertilized thinned	17.647	51.764	0.013	0.026	0.153	0.338	0.000	0.049	0.091	0.047	0.007	0.005
RW18	46	-----	control and thinned	16.312	55.580	0.068	0.233	0.282	0.130	0.000	0.045	0.105	0.065	0.007	0.002
RW18	47	-----	fertilized unthinned	15.513	40.008	0.011	0.029	0.146	0.332	0.000	0.037	0.186	0.124	0.015	0.015
RW18	48	-----	fertilized thinned	16.079	54.237	0.002	0.041	0.162	0.294	0.105	0.100	0.077	0.031	0.001	0.003
RW18	7	-----	fertilized thinned	18.869	50.948	0.146	0.217	0.192	0.033	0.287	0.058	0.097	0.071	0.044	0.045
RW19	1	-----	fertilized	16.796	48.499	0.259	0.094	0.228	0.102	0.284	0.087	0.134	0.112	0.025	0.015

Site	Plot	TPH/ block	Treatment	I_{stdv}	I_{cv}	d_5	d_6	d_7	d_9	$Cd+4_{stdv}$	Cd+2	Cd-1	Cd-2	Cd-4	Cd-5
RW19	2	-----	fertilized	17.220	50.916	0.216	0.107	0.197	0.133	0.253	0.088	0.122	0.066	0.019	0.010
RW19	3	-----	fertilized	18.493	55.303	0.060	0.133	0.226	0.104	0.262	0.072	0.094	0.067	0.011	0.003
RW19	4	-----	fertilized	17.879	56.388	0.226	0.142	0.251	0.060	0.294	0.063	0.113	0.074	0.023	0.009
RW19	5	-----	fertilized	17.207	49.561	0.272	0.127	0.236	0.085	0.254	0.054	0.117	0.066	0.015	0.012
RW19	6	-----	fertilized	16.371	50.621	0.270	0.106	0.221	0.130	0.262	0.084	0.107	0.071	0.011	0.006
RW19	8	-----	fertilized	18.027	46.035	0.058	0.151	0.254	0.064	0.255	0.058	0.118	0.091	0.020	0.006
RW19	9	-----	fertilized	17.553	52.068	0.134	0.134	0.237	0.081	0.265	0.064	0.113	0.083	0.018	0.007
RW19	10	-----	fertilized	18.293	51.255	0.303	0.123	0.215	0.080	0.290	0.065	0.090	0.059	0.016	0.004
RW19	11	-----	fertilized	17.334	50.659	0.079	0.068	0.172	0.171	0.000	0.048	0.122	0.100	0.023	0.009
RW19	12	-----	fertilized	17.128	44.481	0.032	0.089	0.213	0.104	0.233	0.071	0.148	0.105	0.023	0.006
RW19	13	-----	fertilized	17.453	51.508	0.052	0.106	0.216	0.102	0.189	0.059	0.111	0.077	0.014	0.007
RW19	14	-----	fertilized	17.115	48.294	0.115	0.098	0.214	0.115	0.129	0.055	0.129	0.103	0.030	0.009
RW19	15	-----	fertilized	16.922	48.570	0.133	0.156	0.228	0.073	0.250	0.034	0.105	0.099	0.042	0.011
RW19	17	-----	fertilized	17.421	46.407	0.071	0.113	0.227	0.089	0.238	0.056	0.150	0.132	0.029	0.017
RW19	18	-----	fertilized	16.712	48.165	0.099	0.133	0.280	0.049	0.236	0.074	0.127	0.076	0.013	0.005
RW19	19	-----	fertilized	16.940	47.705	0.131	0.122	0.229	0.072	0.292	0.092	0.124	0.071	0.019	0.012
RW19	20	-----	fertilized	16.834	47.328	0.048	0.103	0.238	0.086	0.252	0.094	0.116	0.062	0.008	0.005
RW19	21	-----	fertilized	19.129	50.828	0.132	0.069	0.161	0.175	0.000	0.035	0.135	0.110	0.033	0.009
RW19	22	-----	fertilized	18.994	50.794	0.106	0.106	0.220	0.101	0.000	0.029	0.140	0.118	0.038	0.013
RW19	23	-----	fertilized	18.947	49.313	0.082	0.118	0.222	0.092	0.215	0.064	0.124	0.091	0.014	0.007
RW19	24	-----	fertilized	16.506	47.156	0.093	0.072	0.200	0.128	0.203	0.084	0.139	0.104	0.017	0.009
RW19	25	-----	fertilized	19.333	49.896	0.272	0.111	0.216	0.085	0.243	0.064	0.125	0.089	0.014	0.006
RW19	26	-----	fertilized	17.316	48.842	0.200	0.132	0.249	0.077	0.000	0.027	0.120	0.108	0.032	0.014
RW19	27	-----	fertilized	18.689	55.617	0.062	0.155	0.242	0.066	0.214	0.055	0.109	0.085	0.023	0.013
RW19	28	-----	fertilized	18.638	51.797	0.072	0.130	0.193	0.086	0.278	0.054	0.103	0.098	0.030	0.025
RW19	29	-----	fertilized	18.101	53.991	0.071	0.126	0.224	0.082	0.272	0.047	0.108	0.085	0.020	0.015
RW19	30	-----	fertilized	17.387	47.100	0.091	0.118	0.205	0.109	0.181	0.061	0.128	0.108	0.035	0.015
RW19	31	-----	fertilized	16.918	49.161	0.584	0.135	0.230	0.111	0.216	0.083	0.122	0.093	0.024	0.004
RW19	32	-----	fertilized	18.359	54.212	0.058	0.163	0.259	0.070	0.256	0.071	0.132	0.095	0.020	0.005
RW19	33	-----	fertilized	17.835	48.817	0.132	0.132	0.218	0.099	0.219	0.088	0.107	0.070	0.021	0.006
RW19	34	-----	fertilized	17.098	48.059	0.117	0.113	0.256	0.093	0.286	0.086	0.140	0.080	0.013	0.002
Setres	1	1	control	13.581	49.749	0.177	0.273	0.250	0.048	0.274	0.071	0.139	0.109	0.041	0.016
Setres	1	2	control	13.922	50.202	0.119	0.280	0.324	0.061	0.288	0.063	0.142	0.115	0.038	0.013
Setres	1	3	control	15.924	44.991	0.025	0.120	0.290	0.181	0.255	0.048	0.145	0.120	0.031	0.012

Site	Plot	TPH/ block	Treatment	I_{stdv}	I_{cv}	d_5	d_6	d_7	d_9	$Cd{+}4_{stdv}$	Cd+2	Cd-1	Cd-2	Cd-4	Cd-5
Setres	1	4	control	15.195	47.362	0.021	0.084	0.223	0.243	0.275	0.105	0.116	0.083	0.026	0.014
Setres	2	1	fertilized, irrigated	14.088	49.536	0.243	0.210	0.157	0.023	0.281	0.071	0.141	0.107	0.036	0.014
Setres	2	2	fertilized, irrigated	14.288	49.058	0.166	0.254	0.241	0.056	0.294	0.054	0.115	0.091	0.032	0.016
Setres	2	3	fertilized, irrigated	15.467	42.283	0.041	0.122	0.265	0.170	0.091	0.040	0.170	0.121	0.033	0.019
Setres	2	4	fertilized, irrigated	15.428	45.992	0.022	0.096	0.249	0.199	0.298	0.076	0.148	0.102	0.039	0.017
Setres	3	1	fertilized, irrigated	14.676	53.434	0.295	0.255	0.175	0.022	0.325	0.102	0.123	0.058	0.012	0.002
Setres	3	2	fertilized, irrigated	14.630	49.084	0.080	0.229	0.288	0.127	0.309	0.059	0.125	0.123	0.059	0.026
Setres	3	3	fertilized, irrigated	15.751	44.229	0.030	0.132	0.291	0.159	0.180	0.051	0.153	0.122	0.049	0.026
Setres	3	4	fertilized, irrigated	15.629	48.906	0.037	0.107	0.229	0.225	0.158	0.038	0.135	0.113	0.063	0.035
Setres	4	1	fertilized, irrigated	13.934	48.958	0.260	0.246	0.138	0.008	0.270	0.053	0.139	0.112	0.040	0.020
Setres	4	2	fertilized, irrigated	14.416	52.308	0.207	0.224	0.174	0.028	0.303	0.067	0.135	0.119	0.037	0.018
Setres	4	3	fertilized, irrigated	15.574	43.295	0.032	0.131	0.302	0.155	0.262	0.084	0.144	0.112	0.027	0.012
Setres	4	4	fertilized, irrigated	16.191	43.845	0.104	0.196	0.262	0.104	0.262	0.073	0.124	0.078	0.029	0.017

Appendix H: Normal quantiles vs. Studentized residuals plot (top) and predicted vs. residuals plot (bottom) for the number of trees 5-variable model with lidar metrics only, n = 110 (Chapter 3). Refer to table 3.1 for variable names.

$$N_{trees} = 73.373 - 131.721\ (LPI) - 170.974\ (d_5) - 219.750\ (d_9) - 946.509\ (Cd\text{-}5) + 280.712\ (Cd\text{-}1)$$

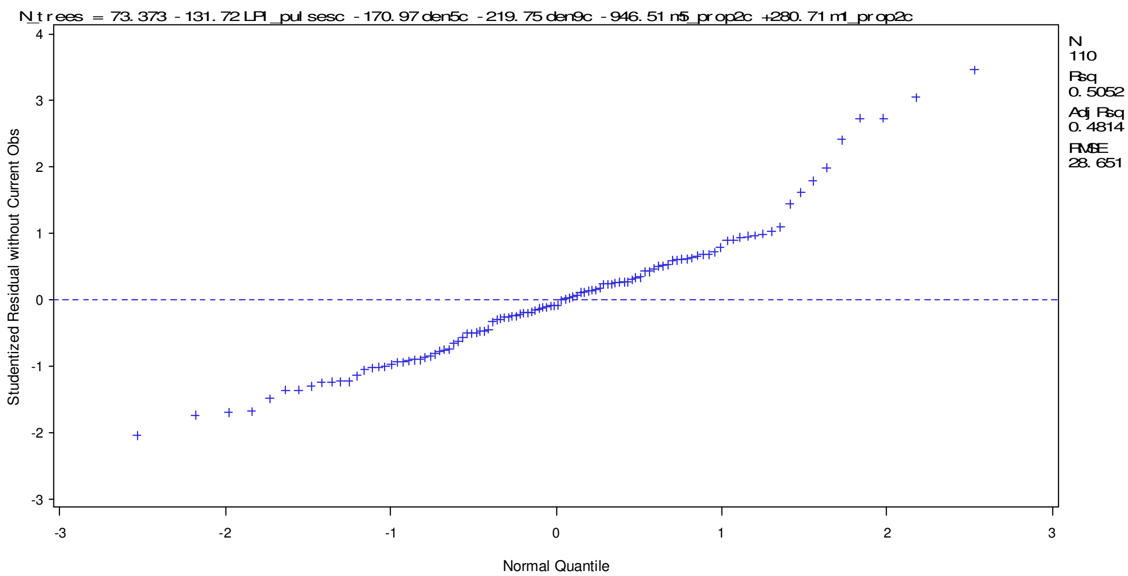

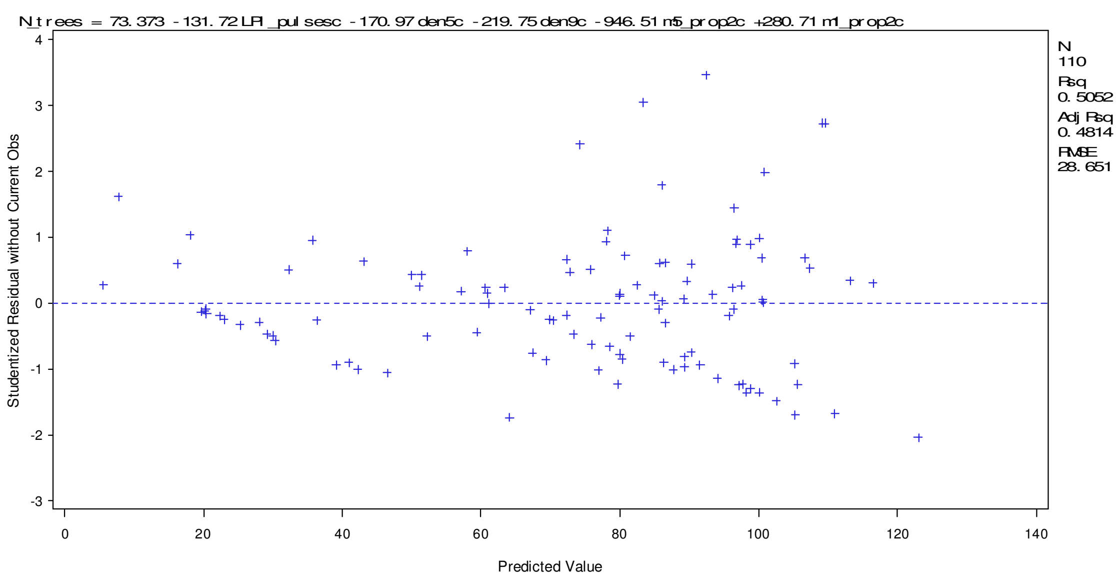

Appendix I: Normal quantiles vs. Studentized residuals plot (top) and predicted vs. residuals plot (bottom) for the number of trees 5-variable model with lidar metrics only, n = 70 (Chapter 3). Refer to table 3.1 for variable names.

$$N_{trees} = 41.053 - 13.902\ (All_{90th}) - 177.600\ (d_5) - 295.\ 245\ (d_6) - 285.096\ (d_9) + 581.975\ (Cd\text{-}1)$$

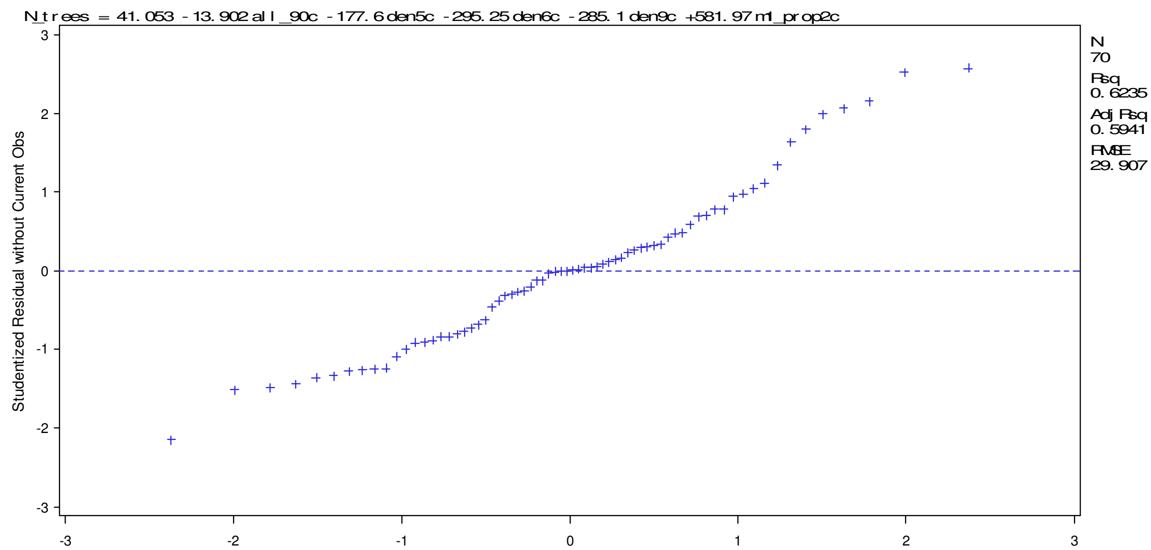

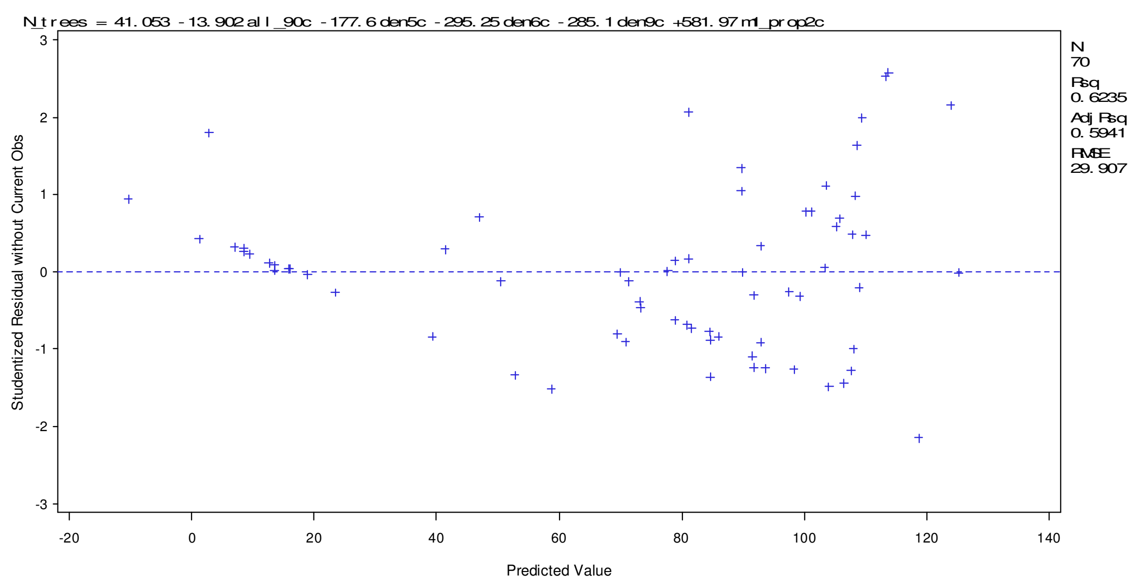

Appendix J: Normal quantiles vs. Studentized residuals plot (top) and predicted vs. residuals plot (bottom) for the number of trees 5-variable model with lidar metrics only, n = 40 (Chapter 3). Refer to table 3.1 for variable names.

$$N_{trees} = 73.315 - 6.245\ (I_{stdv}) - 0.976\ (I_{cv}) + 42.287\ (d_7) + 48.911\ (Cd{+}4_{stdv}) + 114.877\ (Cd\text{-}2)$$

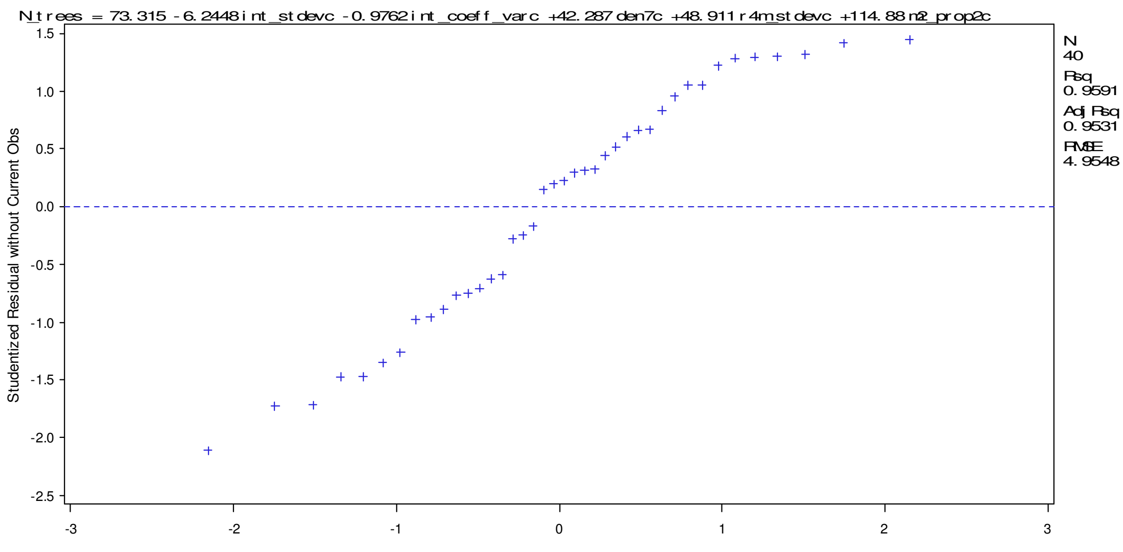

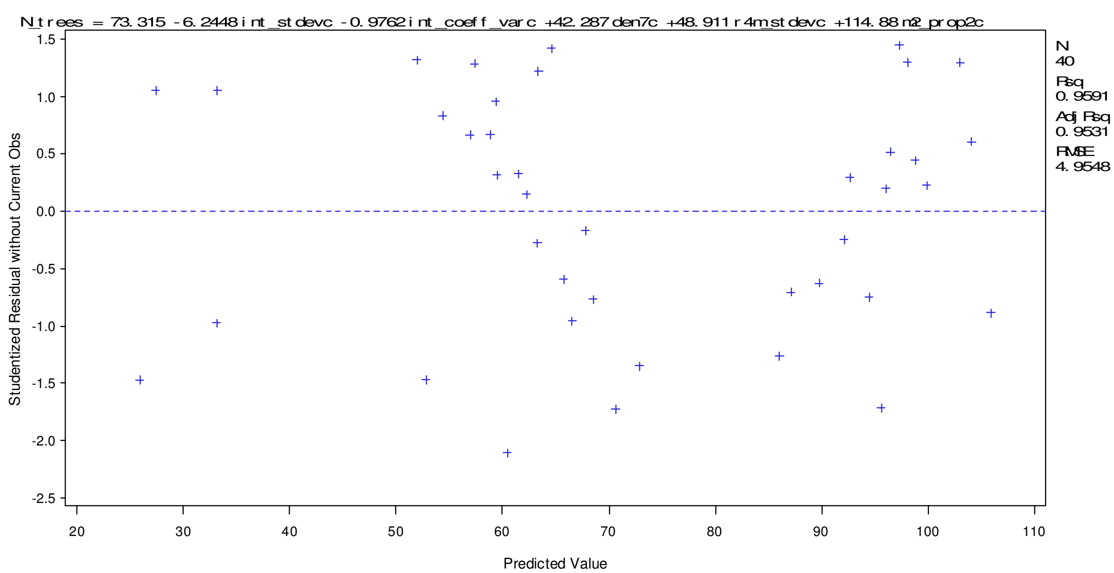

Appendix K: Normal quantiles vs. Studentized residuals plot (top) and predicted vs. residuals plot (bottom) for the number of trees 2-variable model with lidar metrics and ground data, n = 110 (Chapter 3). Refer to table 3.1 for variable names.

$$N_{trees} = 73.373 + 0.850\ (Tree_0) - 108.503\ (LPI)$$

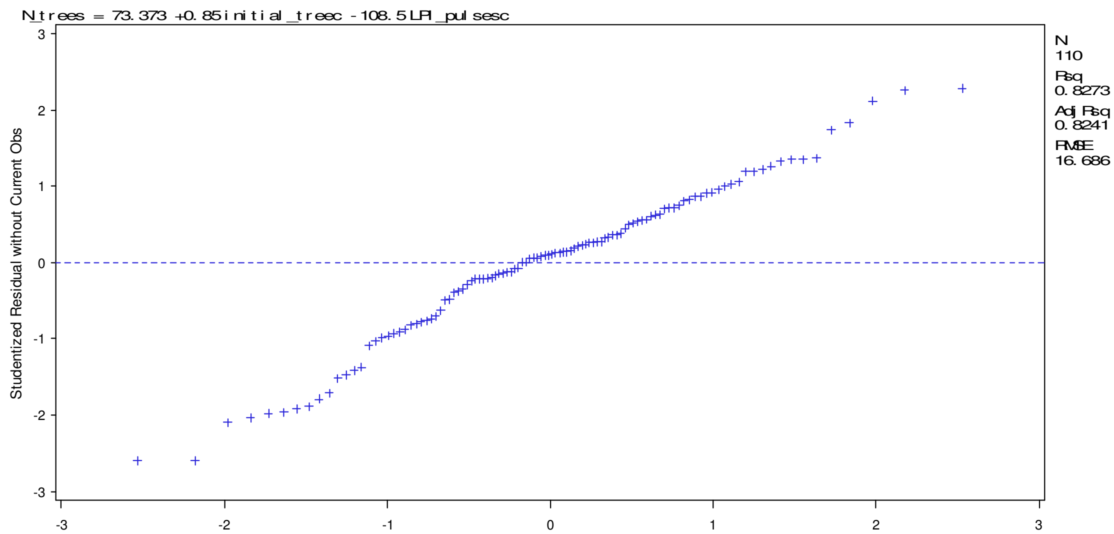

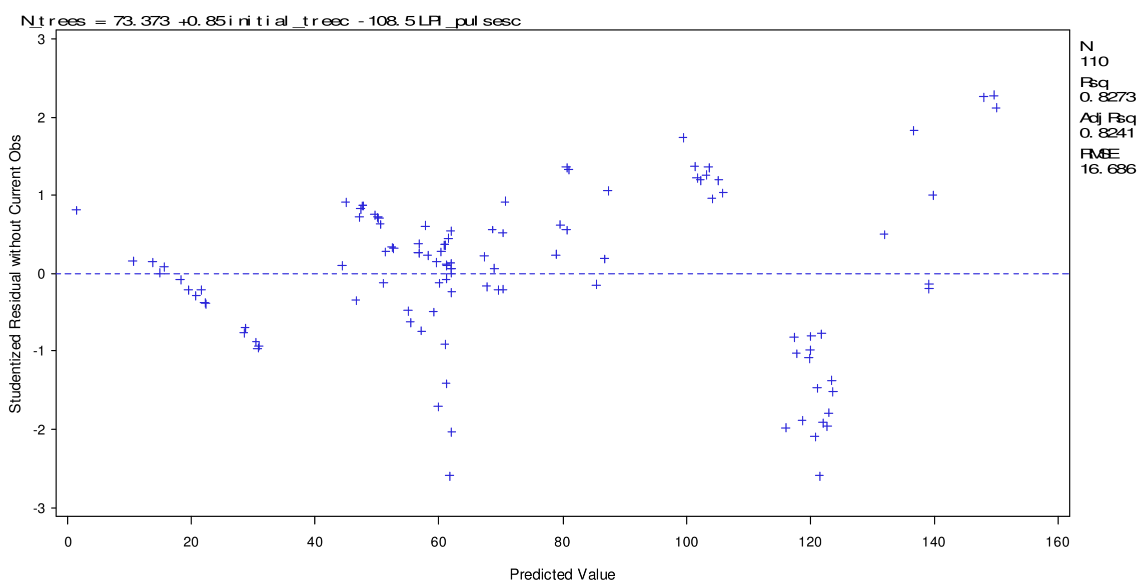

Appendix L: Normal quantiles vs. Studentized residuals plot (top) and predicted vs. residuals plot (bottom) for the number of trees 5-variable model with lidar metrics and ground data, n = 110 (Chapter 3). Refer to table 3.1 for variable names.

N_{trees} = 73.373 + 0.911 ($Tree_0$) – 1.373 (All_{10th}) – 129.548 (LPI) – 305.065 (Cd+2) – 736.945 (Cd-4)

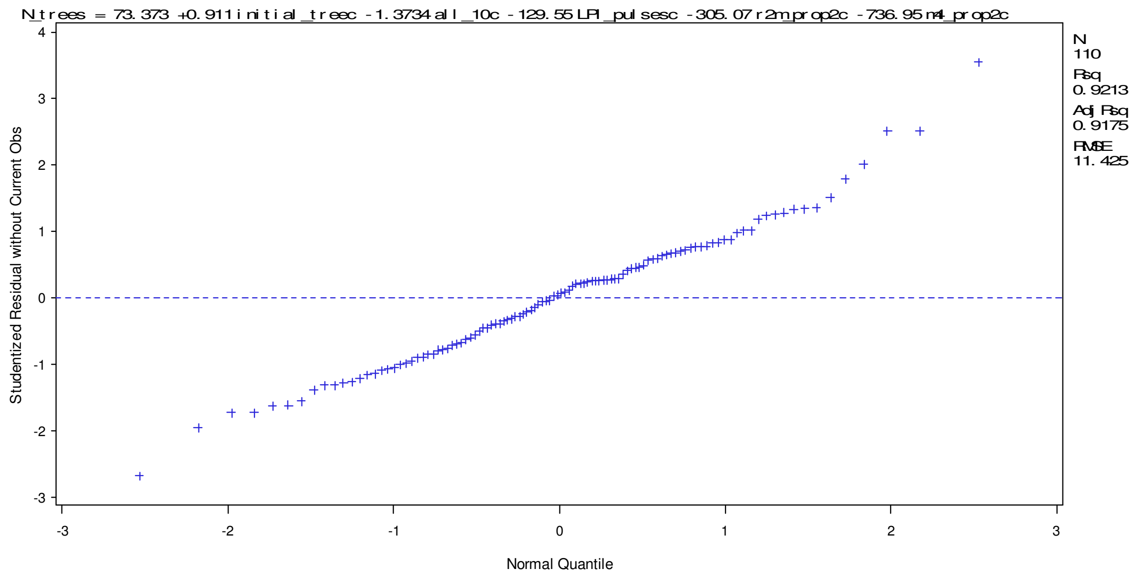

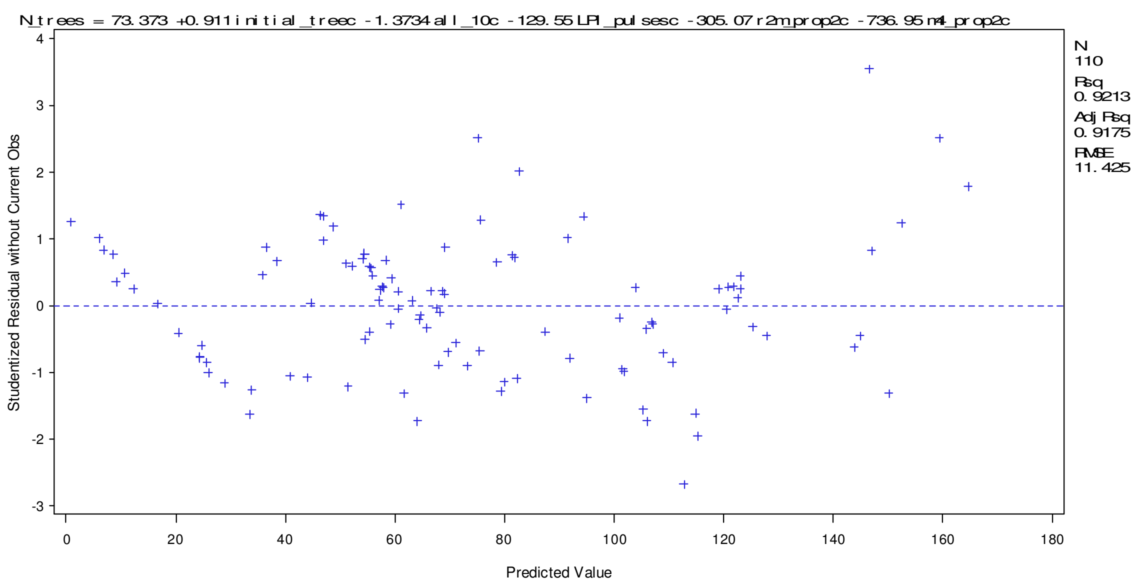

Appendix M: Normal quantiles vs. Studentized residuals plot (top) and predicted vs. residuals plot (bottom) for the number of trees 5-variable model with lidar metrics and ground data, n = 78 (Chapter 3). Refer to table 3.1 for variable names.

N_{trees} = 68.686 + 0.689 ($Tree_0$) – 143.229 (LPI) + 48.499 (d_6) – 368.642 (Cd+2) – 737.816 (Cd-4)

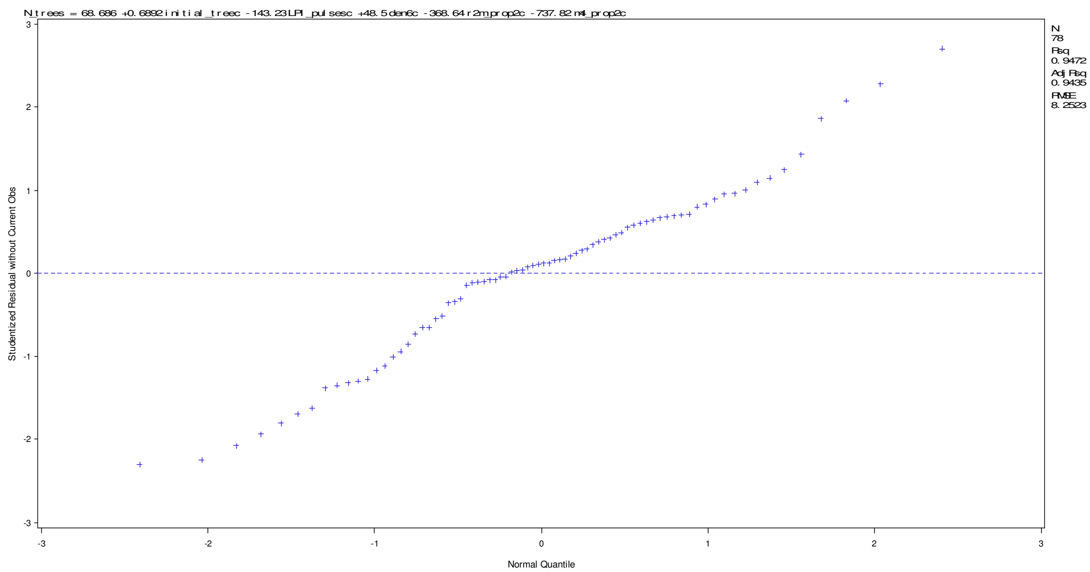

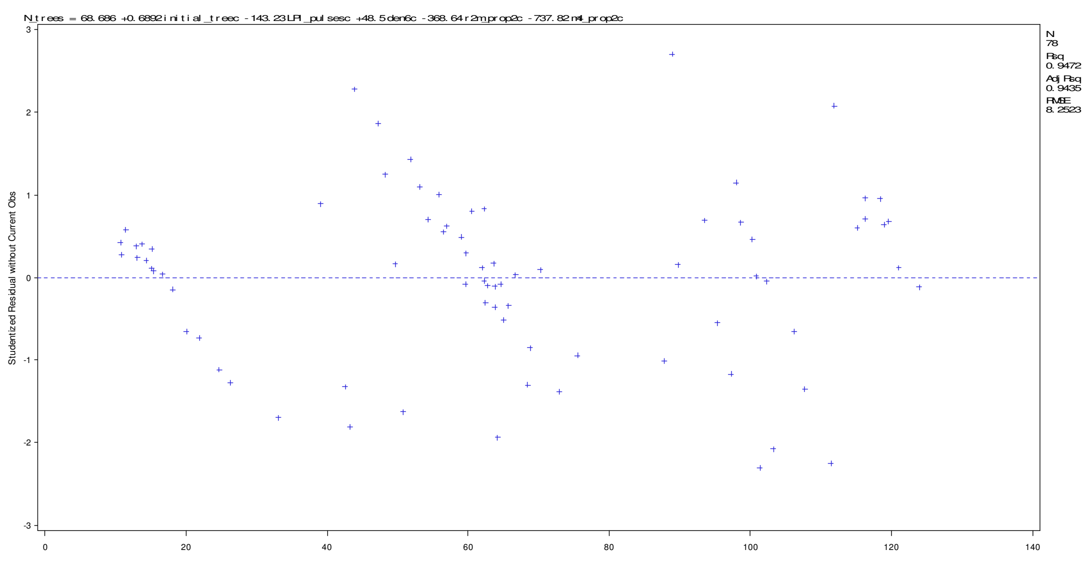

Appendix N: Normal quantiles vs. Studentized residuals plot (top) and predicted vs. residuals plot (bottom) for the number of trees 4-variable model with lidar metrics and ground data, n = 70 (Chapter 3). Refer to table 3.1 for variable names.

$$N_{trees} = 73.167 + 0.954\ (Tree_0) - 3.299\ (All_{90th}) - 83.305\ (LPI) + 205.669\ (Cd\text{-}1)$$

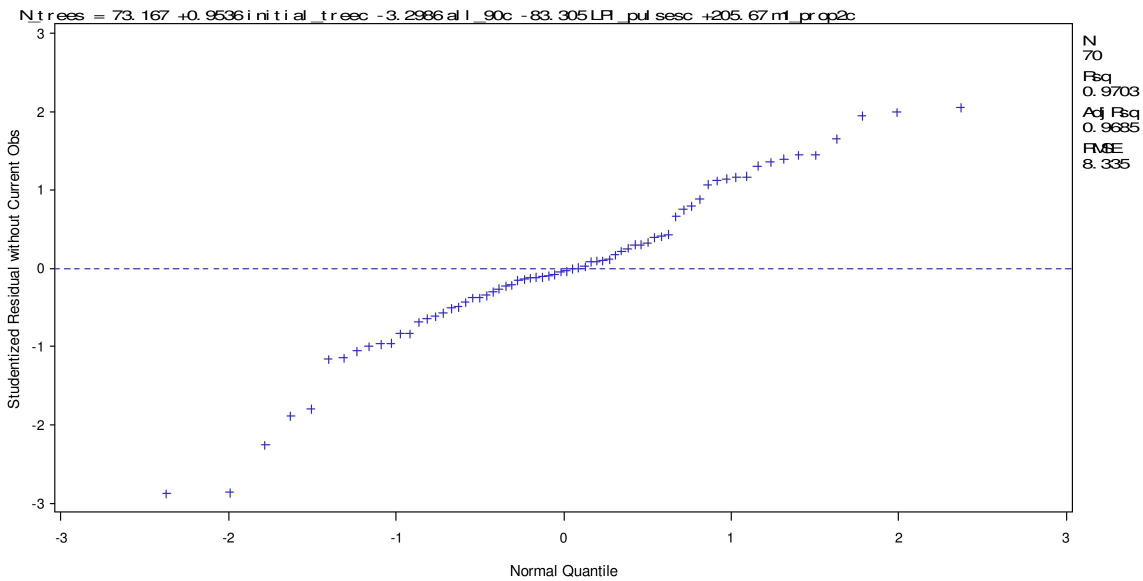

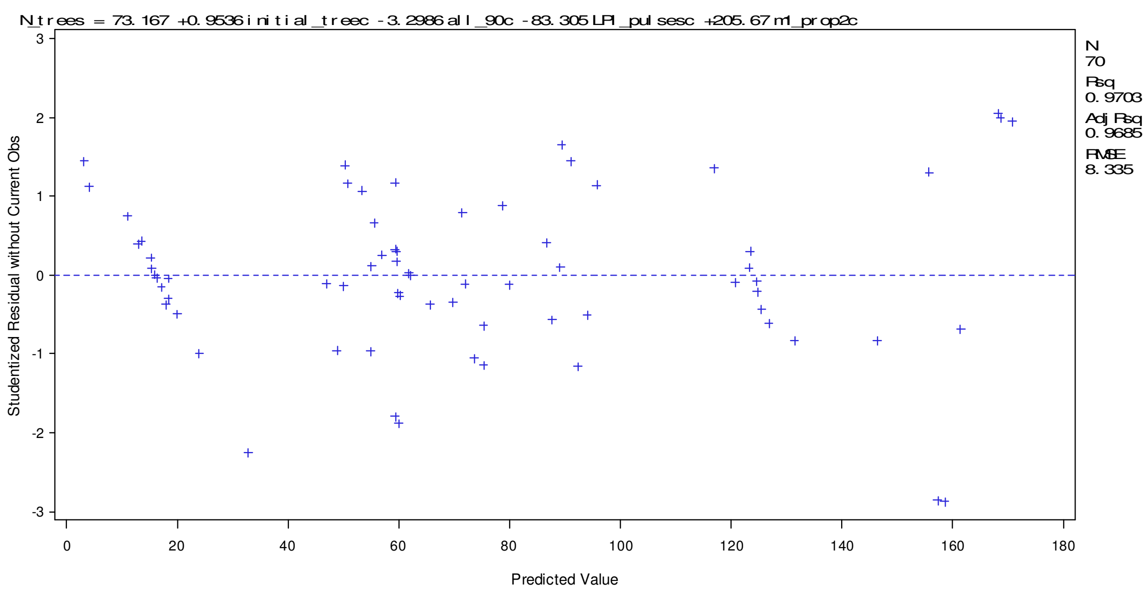

Appendix O: Normal quantiles vs. Studentized residuals plot (top) and predicted vs. residuals plot (bottom) for the mean tree height 1-variable model, *n* = 110 (Chapter 3). Refer to table 3.1 for variable names.

$$ht = 15.503 + 0.911\ (All_{90th})$$

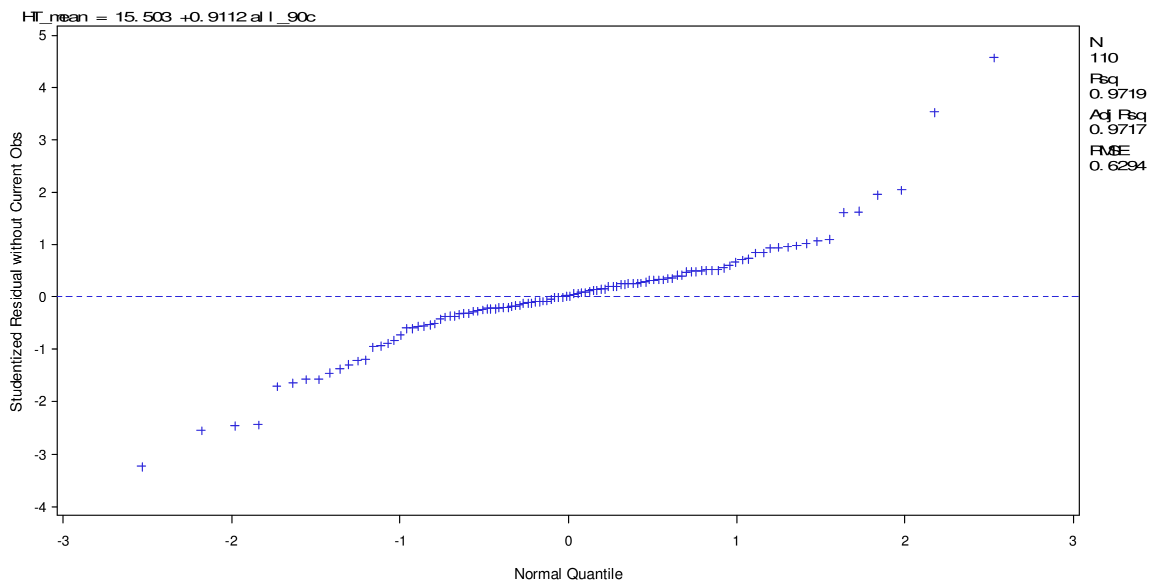

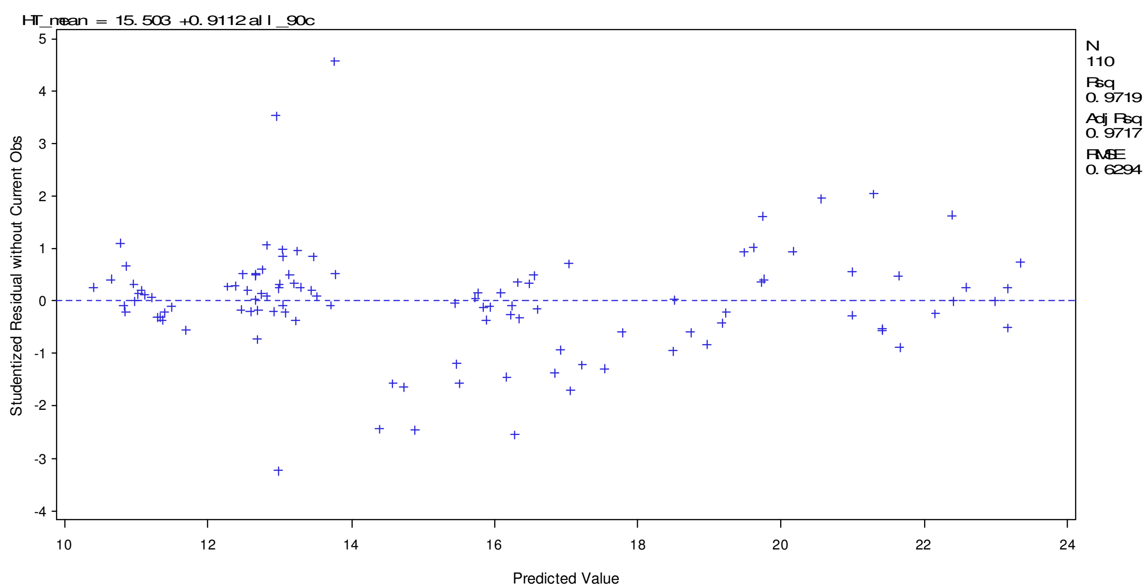

Appendix P: Normal quantiles vs. Studentized residuals plot (top) and predicted vs. residuals plot (bottom) for mean height to live crown 1-variable model, n = 110 (Chapter 3). Refer to table 3.1 for variable names.

$$hlc = 8.699 + 0.946\ (All_{90th})$$

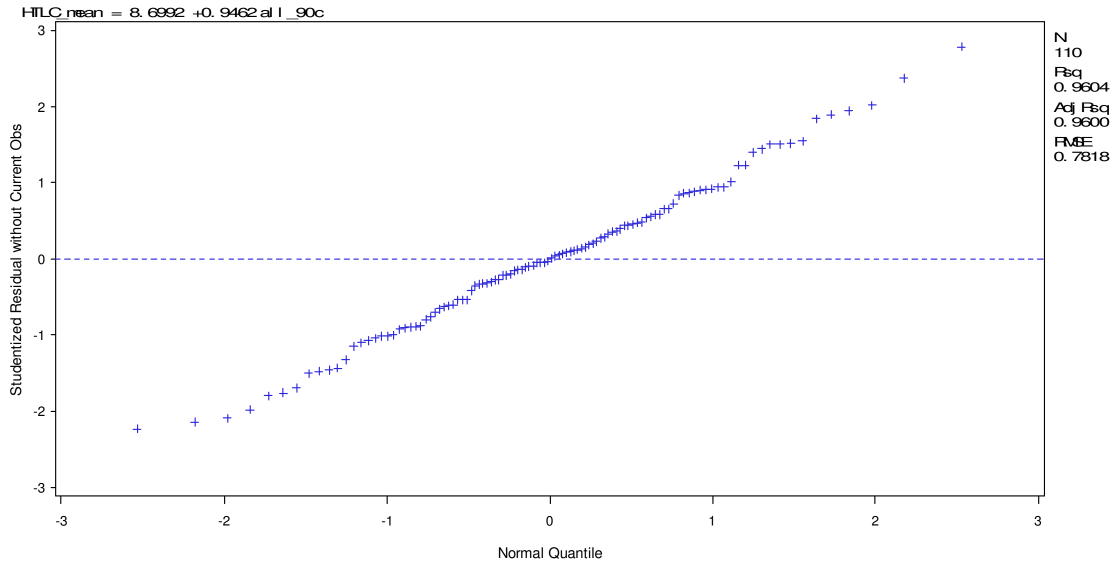

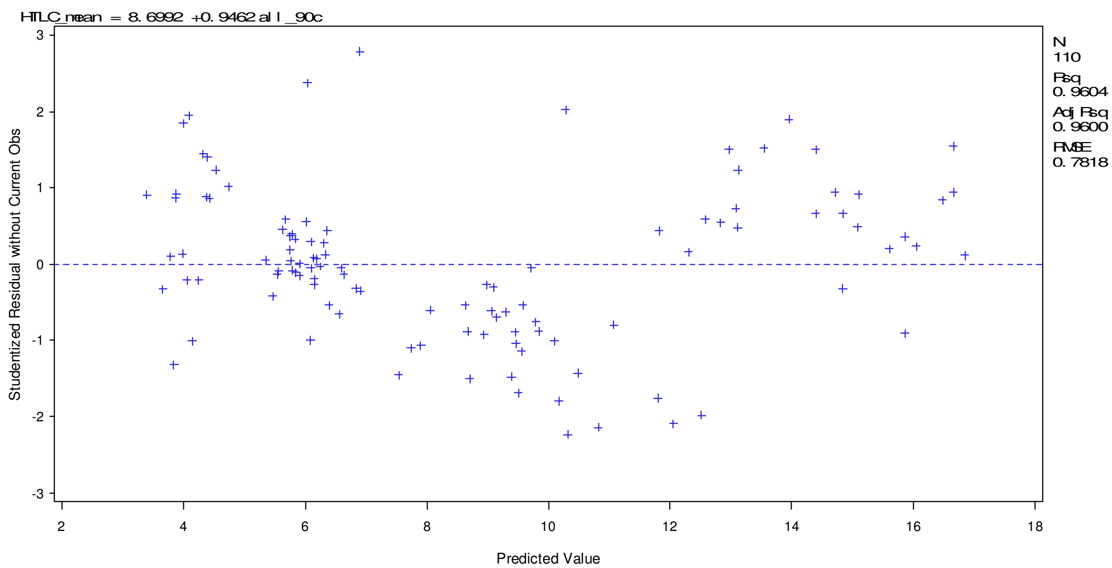

Appendix Q: Ground-based variables used for the LAI models (chapter 4)[*]

plot	radius	forest type	age	LAI	ht_{mean}	ht_{stdv}	ht_{min}	ht_{max}	dbh_{mean}	dbh_{stdv}	dbh_{min}	dbh_{max}
2	var	LP	17	3.01	14.57	2.45	10.36	18.29	18.85	2.87	13.72	25.40
19	var	PH	49	3.41	18.61	3.23	13.72	23.47	22.17	6.33	13.97	36.58
33	var	LP	20	2.54	16.73	1.63	14.33	20.12	18.19	2.18	14.22	24.64
35	var	UH	116	2.61	23.80	2.65	17.37	27.43	47.33	5.62	37.59	55.12
42	var	LP	16	3.93	14.42	1.50	11.89	16.46	19.72	1.82	15.49	22.86
47	var	SP	38	3.68	16.61	1.35	15.24	18.29	22.67	4.41	19.56	29.21
49	var	LP	18	3.9	16.15	1.25	14.33	18.59	19.94	2.48	16.51	23.62
87	var	LP	45	3.44	17.13	5.09	9.45	23.47	24.69	10.82	12.95	41.91
109	var	UH	164	3.52	27.26	7.28	11.28	41.15	39.28	10.42	14.48	50.80
113	var	UH	154	2.97	20.77	5.38	11.89	27.43	34.20	12.90	13.72	53.09
115	var	UH	58	1.43	18.55	2.71	14.02	22.86	25.99	6.77	13.46	36.83
116	var	UH	58	2.03	19.25	2.65	13.11	23.47	27.12	6.52	16.51	37.59
126	var	LP	15	2.51	11.25	2.36	7.01	13.41	17.19	2.75	12.70	22.86
145	var	LP	45	1.41	26.54	3.03	18.59	31.39	45.52	18.43	19.30	86.11
LDABFB31	fix	UH	108	3.23	19.13	9.09	7.32	30.18	27.27	17.47	6.60	49.28
LDABFB32	fix	PH	45	3.61	10.95	3.86	2.44	18.59	11.71	5.52	2.54	21.59
LDABFB33	fix	UH	108	3.96	13.06	9.00	3.96	24.38	23.37	16.69	6.35	48.01
LDABFB34	fix	UH	108	3.84	12.87	9.60	2.74	32.92	15.20	15.40	3.05	44.70
LDABFB41	fix	UH	12	3.52	13.38	6.70	5.79	26.21	17.98	14.02	2.79	46.74
LDABFB42	fix	LP	12	3.2	14.51	4.08	5.49	19.51	13.60	5.32	2.54	21.08
LDABFB43	fix	UH	12	4.23	14.99	5.81	6.40	21.95	24.17	13.76	8.13	48.26
LDABFB44	fix	UH	12	3.6	11.84	6.26	3.66	23.47	19.33	11.55	8.89	41.15
LDABFB51	fix	UH	108	2.66	14.06	7.36	3.66	23.16	18.51	12.28	2.54	36.32
LDABFB53	fix	UH	108	2.43	14.09	6.82	3.05	30.78	14.44	10.67	2.54	45.21
LDABFB54	fix	UH	12	2.8	16.64	6.65	7.01	24.38	21.95	10.62	6.60	42.67
LDABFB61	fix	UH	108	2.92	14.10	5.07	7.92	22.25	21.45	14.54	6.60	53.34
LDABFB62	fix	UH	108	2.77	12.78	8.33	2.74	25.30	17.21	14.32	2.79	50.04
LDABFB63	fix	UH	108	2.82	12.08	6.03	3.66	20.12	14.89	11.56	3.30	38.10

[*] Radius = variable and fix radius plots (see section 4.3.1 for description), forest type = BH (bottomland hardwood), UH (upland hardwood), PH (pine-hardwood), LP (loblolly pine), SP (shortleaf pine), and VP (Virginia pine), LAI = leaf area index, ht = total tree height, dbh (diameter at breast height). Subscripts mean (average), stdv (standard deviation), min (minimum), max (maximum).

plot	radius	forest type	age	LAI	ht_{mean}	ht_{stdv}	ht_{min}	ht_{max}	dbh_{mean}	dbh_{stdv}	dbh_{min}	dbh_{max}
LDABFB64	fix	UH	108	4.11	14.13	5.46	3.35	21.64	16.48	9.83	6.60	37.34
LDABFD11	fix	LP	10	3.86	10.01	3.91	3.66	15.85	10.93	6.53	3.05	20.57
LDABFD12	fix	PH	118	4.33	11.16	4.94	4.27	24.08	13.97	10.89	3.56	50.04
LDABFD13	fix	LP	10	4.1	11.07	4.01	4.57	17.37	11.24	6.37	2.79	28.45
LDABFD21	fix	BH	89	4.4	12.88	9.01	4.88	26.82	16.17	10.46	7.37	39.88
LDABFD22	fix	BH	89	3.74	17.27	4.20	13.41	23.77	26.33	10.52	15.49	43.69
LDABFD23	fix	SP	30	4.02	10.03	3.63	6.40	20.42	12.13	12.61	3.56	42.67
LDABFD24	fix	PH	118	4.9	18.94	11.38	8.23	35.36	20.17	13.19	8.13	38.61
LDABFD31	fix	SP	30	4.39	12.63	4.60	4.88	18.90	11.54	6.48	2.79	22.10
LDABFD32	fix	SP	30	3.91	12.74	3.40	7.32	19.51	12.20	5.43	6.60	24.38
LDABFD33	fix	SP	30	4.39	13.69	6.31	3.96	24.08	13.78	7.51	2.54	27.18
LDABFD34	fix	SP	30	4.12	11.38	3.41	6.40	16.15	12.47	8.00	4.06	25.91
LDABFD41	fix	LP	10	3.08	9.77	2.73	4.27	13.41	11.36	4.34	3.05	18.80
LDABFD42	fix	LP	10	3.98	10.84	2.77	5.79	14.33	10.79	4.90	2.54	17.27
LDABFD43	fix	LP	10	2.84	12.36	2.36	7.62	15.24	15.21	4.25	6.35	20.57
LDABFD44	fix	LP	10	2.5	8.64	2.35	4.27	11.28	11.18	3.12	7.62	15.24
LDABFD51	fix	VP	60	3.8	13.07	1.87	7.01	16.46	10.10	3.33	3.81	20.83
LDABFD53	fix	VP	60	3.74	13.15	2.64	6.71	17.68	10.69	3.58	2.79	19.81
LDABFD54	fix	LP	10	3.97	13.07	3.11	5.79	16.76	14.63	5.00	3.30	21.08
LDABFD61	fix	BH	89	3.68	11.87	5.84	0.40	22.56	13.68	12.65	3.05	37.59
LDABFD62	fix	LP	18	1.34	15.74	4.70	6.10	22.56	14.54	6.53	2.54	24.38
LDABFD63	fix	LP	63	4.21	14.48	7.11	4.88	31.39	15.32	14.19	3.05	53.85
LDABFD71	fix	LP	10	4.12	11.08	3.31	0.88	15.54	11.22	3.62	6.35	18.03
LDABFD72	fix	LP	10	3.99	11.01	3.46	5.49	15.85	10.86	5.87	2.79	19.81
LDABFD73	fix	LP	10	4.48	14.70	8.12	5.49	27.43	17.62	11.96	3.05	36.32
LDABFD74	fix	LP	10	3.94	12.38	3.04	5.18	15.85	13.16	5.12	2.79	19.56
LDABFD81	fix	VP	60	4.04	13.86	4.41	8.53	25.91	14.41	12.06	5.59	44.20
LDABFD82	fix	VP	60	2.89	14.54	1.86	10.97	18.29	10.48	2.26	6.35	18.29
LDABFD83	fix	VP	60	4.06	13.66	7.68	5.49	33.53	16.69	20.32	6.35	73.66
LDABFD84	fix	VP	60	3.96	16.22	3.08	4.27	25.91	12.17	6.16	7.11	43.43
LDABFD92	fix	LP	63	3.74	15.47	10.09	6.71	33.83	26.81	22.14	7.11	59.44
LDABFD93	fix	LP	63	2.73	9.38	4.82	3.66	28.35	10.25	10.15	3.05	40.39
LDABFD94	fix	LP	63	3.94	7.76	2.75	3.66	15.85	7.81	5.22	2.54	24.13

Appendix R: Lidar metrics used for the LAI models (chapter 4)*

plot	radius	forest type	Gr_{total}	All_{total}	LPI	All_{mean}	All_{stdv}	All_{cv}	All_{10th}	All_{50th}	I_{mean}	I_{stdv}	d_2	d_{10}	$Cd\text{-}3_{stdv}$	Cd-3	Cd-1
2	var	LP	252	3620	0.017	9.966	4.035	40.490	4.367	10.626	38.223	21.596	0.112	0.001	0.280	0.060	0.099
19	var	PH	409	5678	0.005	12.697	5.543	43.658	3.156	14.143	48.568	30.079	0.039	0.014	0.286	0.074	0.083
33	var	LP	809	3836	0.011	11.908	4.791	40.229	3.299	13.608	29.568	17.057	0.047	0.037	0.275	0.081	0.135
35	var	UH	447	6898	0.007	13.116	6.917	52.741	2.630	15.561	45.158	29.496	0.088	0.084	0.297	0.041	0.079
42	var	LP	942	5486	0.014	9.462	3.985	42.120	3.076	10.323	37.436	21.891	0.049	0.021	0.288	0.091	0.103
47	var	SP	329	5358	0.005	8.711	4.118	47.274	3.704	8.087	46.296	28.553	0.068	0.018	0.294	0.062	0.108
49	var	LP	824	3858	0.023	9.464	4.616	48.777	1.984	10.750	29.237	17.599	0.077	0.019	0.267	0.058	0.086
87	var	LP	410	4783	0.012	9.167	4.831	52.699	2.882	8.941	46.427	28.341	0.134	0.004	0.279	0.043	0.070
109	var	UH	392	5198	0.008	16.669	7.595	45.562	4.400	19.151	48.807	30.860	0.064	0.050	0.297	0.062	0.075
113	var	UH	714	8205	0.040	10.608	6.997	65.959	1.070	10.585	35.239	23.237	0.106	0.016	0.291	0.035	0.053
115	var	UH	1165	3081	0.279	9.409	7.107	75.529	0.400	10.164	54.686	35.257	0.090	0.042	0.301	0.040	0.050
116	var	UH	675	4500	0.051	12.009	6.231	51.886	0.834	13.999	44.968	29.593	0.042	0.011	0.276	0.075	0.089
126	var	LP	608	5287	0.011	7.023	3.275	46.626	1.844	7.604	39.970	21.644	0.072	0.007	0.292	0.087	0.118
145	var	LP	1141	3148	0.181	15.233	8.828	57.952	0.540	19.114	40.191	26.572	0.029	0.017	0.273	0.054	0.076
LDABFB31	fix	UH	376	5810	0.010	14.990	7.294	48.662	3.267	16.697	48.460	31.070	0.068	0.025	0.289	0.063	0.070
LDABFB32	fix	PH	285	5237	0.002	11.268	5.322	47.229	4.437	11.509	53.261	30.002	0.104	0.021	0.287	0.057	0.062
LDABFB33	fix	UH	362	5545	0.011	15.080	8.282	54.920	3.593	16.551	50.427	30.586	0.124	0.011	0.286	0.054	0.062
LDABFB34	fix	UH	309	5466	0.005	15.709	7.396	47.081	3.844	17.769	46.871	30.047	0.081	0.049	0.301	0.052	0.057
LDABFB41	fix	UH	382	4872	0.004	14.195	6.181	43.545	5.383	14.777	42.691	25.226	0.077	0.038	0.295	0.061	0.070
LDABFB42	fix	LP	519	4475	0.004	11.589	5.090	43.918	3.305	13.294	31.736	19.575	0.057	0.007	0.293	0.073	0.109
LDABFB43	fix	UH	261	4630	0.020	10.589	6.133	57.921	2.009	11.314	44.251	25.754	0.132	0.006	0.298	0.052	0.058
LDABFB44	fix	UH	536	4106	0.042	11.394	6.025	52.883	3.285	11.110	39.187	23.912	0.103	0.015	0.286	0.047	0.053
LDABFB51	fix	UH	511	4994	0.028	13.991	6.981	49.895	2.947	15.829	37.470	24.775	0.082	0.039	0.295	0.045	0.076
LDABFB53	fix	UH	683	4746	0.048	13.033	7.373	56.573	1.504	14.279	39.404	25.299	0.076	0.036	0.291	0.045	0.052
LDABFB54	fix	UH	859	4283	0.092	12.442	6.857	55.111	0.993	14.858	37.603	24.990	0.067	0.019	0.274	0.060	0.072
LDABFB61	fix	UH	470	5756	0.012	13.268	6.174	46.530	3.807	15.106	45.131	30.353	0.062	0.055	0.293	0.069	0.086

* Radius = variable and fix radius plots (see section 4.3.1 for description), forest type = BH (bottomland hardwood), UH (upland hardwood), PH (pine-hardwood), LP (loblolly pine), SP (shortleaf pine), and VP (Virginia pine). See table 4.1 for description of other variables.

plot	radius	forest type	Gr_{total}	All_{total}	LPI	All_{mean}	All_{stdv}	All_{cv}	All_{10th}	All_{50th}	I_{mean}	I_{stdv}	d_2	d_{10}	Cd-3_{stdv}	Cd-3	Cd-1
LDABFB62	fix	UH	491	6210	0.014	14.707	7.584	51.570	2.296	17.663	43.564	29.388	0.085	0.068	0.300	0.053	0.091
LDABFB63	fix	UH	497	5504	0.010	14.013	5.869	41.880	4.596	15.454	46.755	30.224	0.032	0.021	0.290	0.061	0.080
LDABFB64	fix	UH	544	5206	0.018	11.977	5.999	50.086	1.438	13.345	40.600	27.833	0.048	0.008	0.291	0.056	0.072
LDABFD11	fix	LP	290	4186	0.001	9.106	3.355	36.845	5.006	8.972	42.367	23.907	0.057	0.002	0.288	0.036	0.093
LDABFD12	fix	PH	245	3964	0.003	10.218	3.930	38.465	5.775	9.854	55.684	26.017	0.041	0.012	0.293	0.051	0.122
LDABFD13	fix	LP	408	4395	0.001	10.195	3.896	38.216	5.072	10.561	45.693	26.065	0.076	0.002	0.284	0.065	0.103
LDABFD21	fix	BH	160	4098	0.022	11.096	6.234	56.188	3.425	10.824	47.707	27.416	0.172	0.010	0.298	0.041	0.053
LDABFD22	fix	BH	169	4504	0.017	10.368	5.946	57.351	2.651	10.298	53.290	27.879	0.147	0.002	0.305	0.063	0.058
LDABFD23	fix	SP	295	3870	0.004	7.275	3.669	50.433	2.734	6.867	47.838	25.122	0.105	0.008	0.289	0.042	0.125
LDABFD24	fix	PH	116	5155	0.001	16.735	8.760	52.348	5.018	17.583	40.163	26.260	0.165	0.021	0.283	0.032	0.053
LDABFD31	fix	SP	391	5828	0.002	11.047	4.777	43.244	4.782	11.177	39.506	25.637	0.057	0.022	0.293	0.048	0.071
LDABFD32	fix	SP	439	5637	0.002	10.297	4.752	46.145	4.296	10.037	39.435	25.615	0.077	0.020	0.291	0.054	0.072
LDABFD33	fix	SP	334	5461	0.001	12.690	5.300	41.765	5.758	13.930	40.041	27.025	0.066	0.013	0.294	0.047	0.080
LDABFD34	fix	SP	328	4838	0.005	9.144	4.268	46.681	4.085	8.564	44.487	28.228	0.069	0.028	0.286	0.060	0.105
LDABFD41	fix	LP	353	4477	0.005	6.959	3.480	50.005	2.145	7.484	40.011	21.518	0.137	0.005	0.291	0.070	0.108
LDABFD42	fix	LP	515	5357	0.003	8.013	3.465	43.241	3.202	8.575	37.336	21.109	0.081	0.004	0.294	0.065	0.106
LDABFD43	fix	LP	403	4565	0.008	7.986	4.216	52.794	2.278	8.500	35.959	20.527	0.145	0.012	0.307	0.065	0.076
LDABFD44	fix	LP	912	3633	0.138	7.789	3.384	43.441	2.847	8.334	44.273	22.335	0.083	0.003	0.288	0.056	0.100
LDABFD51	fix	VP	533	4438	0.010	9.524	4.242	44.542	1.985	11.197	31.305	18.261	0.048	0.020	0.275	0.052	0.140
LDABFD53	fix	VP	536	4207	0.004	10.523	3.992	37.935	4.442	11.652	33.238	20.627	0.056	0.007	0.287	0.075	0.124
LDABFD54	fix	LP	302	4314	0.002	9.796	3.906	39.878	3.928	10.668	36.551	20.554	0.079	0.010	0.298	0.078	0.111
LDABFD61	fix	BH	337	4427	0.016	16.697	8.236	49.326	6.247	15.658	51.098	30.818	0.095	0.018	0.307	0.052	0.058
LDABFD62	fix	LP	1363	2396	0.318	11.035	6.909	62.608	0.447	14.012	43.738	30.481	0.054	0.034	0.267	0.038	0.065
LDABFD63	fix	LP	267	4799	0.005	15.612	8.255	52.876	4.811	14.958	43.288	27.898	0.114	0.027	0.304	0.025	0.038
LDABFD71	fix	LP	383	4967	0.001	10.026	3.417	34.079	4.893	10.602	43.654	23.735	0.044	0.004	0.285	0.064	0.145
LDABFD72	fix	LP	426	4772	0.001	10.453	3.803	36.382	4.970	11.069	40.245	23.504	0.048	0.011	0.293	0.050	0.101
LDABFD73	fix	LP	284	5156	0.005	13.466	5.973	44.357	5.684	13.580	50.267	28.571	0.069	0.010	0.281	0.044	0.057
LDABFD74	fix	LP	539	5225	0.002	10.321	3.837	37.180	4.478	11.130	37.760	21.661	0.064	0.009	0.287	0.078	0.114
LDABFD81	fix	VP	587	4693	0.002	13.335	4.429	33.214	7.291	13.738	42.309	24.059	0.034	0.018	0.288	0.066	0.116
LDABFD82	fix	VP	896	4633	0.007	11.579	4.193	36.209	4.728	12.631	33.077	18.997	0.038	0.012	0.279	0.058	0.137
LDABFD83	fix	VP	264	4961	0.003	19.462	7.918	40.684	8.076	20.262	42.789	26.783	0.071	0.017	0.286	0.043	0.048
LDABFD84	fix	VP	513	4771	0.007	14.717	5.712	38.814	6.171	15.119	40.876	24.562	0.051	0.007	0.283	0.061	0.090
LDABFD92	fix	LP	247	4822	0.006	13.175	8.577	65.102	3.299	10.238	45.413	29.817	0.208	0.015	0.285	0.051	0.064

plot	radius	forest type	Gr_{total}	All_{total}	LPI	All_{mean}	All_{stdv}	All_{cv}	All_{10th}	All_{50th}	I_{mean}	I_{stdv}	d_2	d_{10}	Cd-3$_{stdv}$	Cd-3	Cd-1
LDABFD93	fix	LP	354	4620	0.047	10.025	7.001	69.840	3.673	7.620	46.355	27.597	0.304	0.020	0.272	0.052	0.104
LDABFD94	fix	LP	265	4293	0.002	7.937	3.441	43.356	4.260	7.481	56.889	26.350	0.111	0.009	0.289	0.062	0.136

Appendix S: GeoSAR metrics used for the LAI models (chapter 4)*

plot	radius	forest type	P_{mean}	P_{min}	P_{max}	P_{stdv}	X_{mean}	X_{min}	X_{max}	X_{stdv}	X_{50th}	$X\text{-}P_{mean}$	$X\text{-}P_{min}$	$X\text{-}P_{max}$	$X\text{-}P_{stdv}$
2	var	LP	5.039	1.700	9.492	1.459	8.966	6.398	10.695	0.983	8.992	3.823	0.494	6.845	1.495
19	var	PH	7.883	5.434	9.616	1.097	12.711	10.813	15.569	0.936	12.550	4.489	2.135	9.708	1.585
33	var	LP	0.717	0.068	1.708	0.447	10.507	8.837	11.885	0.571	10.522	10.414	7.555	12.037	1.066
35	var	UH	6.325	3.493	8.960	1.610	11.169	9.383	13.260	1.019	11.215	4.211	1.764	6.731	1.229
42	var	LP	4.260	0.789	7.750	1.917	9.601	7.185	11.512	1.182	9.884	5.222	2.744	7.290	1.225
47	var	SP	6.269	3.502	8.472	1.029	9.639	8.234	10.698	0.714	9.856	3.571	1.608	5.663	1.057
49	var	LP	3.986	1.463	5.598	1.020	8.401	7.819	9.476	0.375	8.318	4.467	2.569	7.484	1.197
87	var	LP	4.298	1.953	6.888	1.356	7.953	7.191	8.660	0.319	7.949	3.395	0.891	6.185	1.467
109	var	UH	9.413	5.838	13.528	2.054	16.487	13.031	19.469	1.295	16.661	6.644	3.149	10.764	2.150
113	var	UH	8.210	5.005	11.062	1.596	9.101	1.970	14.244	2.992	9.798	1.140	-2.409	4.690	1.745
115	var	UH	2.178	0.884	4.774	0.979	4.012	0.939	8.066	1.660	3.703	1.869	-2.032	5.948	1.664
116	var	UH	2.916	0.570	4.944	1.012	7.867	2.022	11.457	2.426	7.912	5.024	-0.641	10.273	2.814
126	var	LP	6.162	4.836	7.571	0.750	7.686	5.632	11.580	1.099	7.665	1.683	-0.832	4.511	1.389
145	var	LP	5.236	2.960	8.607	1.170	7.777	3.278	14.060	3.004	6.982	2.721	-2.637	8.818	3.192
LDABFB31	fix	UH	6.874	4.856	8.562	1.008	15.057	11.742	18.946	1.956	14.823	8.238	4.119	13.397	2.690
LDABFB32	fix	PH	7.429	3.972	9.126	1.105	10.566	7.125	12.970	1.749	11.136	2.961	-0.611	6.745	1.956
LDABFB33	fix	UH	9.607	4.285	12.499	2.293	16.827	10.916	20.909	2.636	17.418	7.023	4.544	10.338	1.289
LDABFB34	fix	UH	7.476	4.133	9.433	1.270	16.183	13.000	18.908	1.153	16.130	8.598	5.896	11.782	1.178
LDABFB41	fix	UH	7.987	6.265	10.152	1.246	14.277	10.453	16.079	1.271	14.653	6.156	3.108	9.194	1.499
LDABFB42	fix	LP	6.336	4.510	7.619	0.692	12.273	11.087	14.324	0.671	12.178	6.162	5.090	8.314	0.771
LDABFB43	fix	UH	8.070	6.339	9.924	0.961	10.860	6.010	14.964	2.692	11.372	2.528	-0.947	5.814	2.094
LDABFB44	fix	UH	6.580	3.862	10.049	1.725	10.508	4.367	15.479	3.517	11.135	3.701	-0.047	8.206	2.253
LDABFB51	fix	UH	6.136	3.579	7.598	1.051	11.733	7.995	15.042	1.580	11.706	5.514	0.914	10.149	2.357
LDABFB53	fix	UH	6.209	3.126	8.030	1.386	11.940	5.829	15.917	2.930	12.539	5.555	0.393	10.415	2.871
LDABFB54	fix	UH	5.048	0.957	7.303	1.837	9.350	5.791	13.522	1.985	9.233	4.250	-1.291	12.372	3.661
LDABFB61	fix	UH	6.383	3.917	9.106	1.152	12.651	11.268	14.991	0.851	12.412	6.184	4.745	9.440	1.251
LDABFB62	fix	UH	7.525	5.385	9.681	1.152	13.080	10.748	15.251	1.107	13.244	5.282	1.532	9.370	2.159
LDABFB63	fix	UH	7.973	5.428	9.953	1.248	13.153	12.170	14.932	0.653	13.075	5.416	2.954	8.796	1.606

* Radius = variable and fix radius plots (see section 4.3.1 for description), forest type = BH (bottomland hardwood), UH (upland hardwood), PH (pine-hardwood), LP (loblolly pine), SP (shortleaf pine), and VP (Virginia pine). See table 4.1 for description of other variables.

plot	radius	forest type	P_{mean}	P_{min}	P_{max}	P_{stdv}	X_{mean}	X_{min}	X_{max}	X_{stdv}	X_{50th}	$X\text{-}P_{mean}$	$X\text{-}P_{min}$	$X\text{-}P_{max}$	$X\text{-}P_{stdv}$
LDABFB64	fix	UH	4.730	3.319	6.210	0.642	10.932	9.120	12.798	0.925	11.116	6.211	3.797	8.614	1.227
LDABFD11	fix	LP	4.319	1.959	7.529	1.348	9.539	7.160	12.864	0.893	9.315	5.105	0.872	8.781	1.832
LDABFD12	fix	PH	5.067	1.482	8.111	1.576	10.630	4.575	15.706	2.203	10.683	5.497	1.353	9.699	2.080
LDABFD13	fix	LP	5.356	2.663	7.909	1.691	11.344	9.185	14.007	1.008	11.273	5.983	2.637	10.285	1.699
LDABFD21	fix	BH	11.376	8.068	13.819	1.228	15.500	7.962	18.149	1.974	16.028	4.178	-1.695	7.965	2.092
LDABFD22	fix	BH	10.152	8.222	12.720	1.135	14.733	11.389	20.687	2.066	14.396	4.403	1.464	7.846	1.431
LDABFD23	fix	SP	5.843	2.802	9.593	1.429	8.698	4.828	11.679	1.385	8.679	2.859	-1.059	5.959	1.997
LDABFD24	fix	PH	11.744	7.772	16.273	2.284	20.952	17.696	24.773	1.753	20.761	8.949	6.816	11.744	1.211
LDABFD31	fix	SP	8.238	6.047	11.773	1.497	13.674	10.278	16.387	1.510	13.991	5.521	2.878	8.220	1.457
LDABFD32	fix	SP	6.092	3.470	11.189	2.010	11.826	9.201	15.589	1.813	11.207	5.793	4.109	8.955	1.015
LDABFD33	fix	SP	6.883	4.974	9.911	1.211	15.621	10.729	18.826	2.021	16.056	8.920	3.949	12.950	2.253
LDABFD34	fix	SP	8.002	4.088	10.315	1.531	11.197	8.712	14.136	1.198	11.191	3.201	0.922	6.336	1.524
LDABFD41	fix	LP	3.514	1.077	6.343	1.574	9.356	7.501	11.238	0.711	9.477	5.752	1.995	8.408	1.887
LDABFD42	fix	LP	3.975	1.281	6.964	1.232	10.827	9.424	11.809	0.502	10.803	7.017	4.386	9.800	1.073
LDABFD43	fix	LP	3.655	2.387	5.834	0.886	9.428	7.166	12.786	1.428	9.293	5.813	2.226	8.751	1.779
LDABFD44	fix	LP	7.128	4.504	8.328	0.863	9.150	6.829	11.468	0.839	9.254	2.152	-0.566	5.504	1.442
LDABFD51	fix	VP	5.366	3.091	6.918	1.209	11.200	8.852	12.461	0.904	11.514	5.681	3.289	8.693	1.054
LDABFD53	fix	VP	6.164	4.075	8.741	1.272	12.810	10.741	15.463	1.043	12.604	6.508	4.234	9.769	1.545
LDABFD54	fix	LP	5.527	2.592	9.337	1.998	12.624	10.131	14.610	1.088	12.748	6.875	2.117	10.114	2.207
LDABFD61	fix	BH	9.903	3.822	14.712	2.740	17.932	12.179	25.302	3.015	17.841	8.113	3.790	11.779	2.039
LDABFD62	fix	LP	5.405	1.938	10.035	1.792	7.664	3.432	14.678	3.023	6.128	2.735	-2.173	6.506	2.146
LDABFD63	fix	LP	10.983	8.892	13.258	1.125	17.779	15.046	22.551	1.439	17.544	6.654	2.917	10.511	1.659
LDABFD71	fix	LP	7.622	4.416	9.979	1.574	12.537	10.829	13.572	0.475	12.558	4.782	1.174	8.078	1.790
LDABFD72	fix	LP	4.318	2.364	7.138	1.259	13.291	11.532	14.628	0.752	13.501	9.009	5.659	11.277	1.138
LDABFD73	fix	LP	10.144	7.405	12.757	1.404	15.264	10.950	20.984	2.426	15.219	5.225	1.260	10.741	2.186
LDABFD74	fix	LP	4.790	0.710	8.611	2.065	12.404	10.235	13.618	0.654	12.463	7.823	3.376	11.010	1.960
LDABFD81	fix	VP	4.586	1.315	8.289	2.046	15.228	13.342	17.201	0.759	15.182	10.823	6.599	13.863	2.136
LDABFD82	fix	VP	4.931	0.913	7.230	1.431	13.509	11.277	15.805	1.183	13.353	8.442	5.281	11.319	1.734
LDABFD83	fix	VP	11.665	8.147	18.379	2.847	20.451	14.173	30.021	4.555	19.346	8.641	4.558	15.456	2.524
LDABFD84	fix	VP	8.262	2.962	14.166	2.817	17.021	14.653	22.266	1.785	16.642	8.814	5.211	12.756	2.164
LDABFD92	fix	LP	8.933	7.438	11.684	0.900	13.887	8.597	19.672	2.738	13.813	5.256	0.678	10.808	2.415
LDABFD93	fix	LP	6.405	4.240	8.517	1.201	10.763	8.588	14.023	1.215	10.466	4.544	1.923	6.379	1.046
LDABFD94	fix	LP	2.836	0.350	5.728	1.502	11.147	8.788	17.946	1.836	10.861	8.472	3.925	15.396	2.742

Appendix S: Continued[*].

plot	radius	forest type	$Pmag_{mean}$	$Pmag_{min}$	$Pmag_{max}$	$Pmag_{stdv}$	$Xmag_{mean}$	$Xmag_{min}$	$Xmag_{max}$	$Xmag_{stdv}$	$sn01xl_{cv}$
2	var	LP	0.439	0.319	0.685	0.074	0.071	0.033	0.214	0.030	111.342
19	var	PH	0.207	0.151	0.271	0.032	0.103	0.057	0.181	0.026	183.229
33	var	LP	0.493	0.349	0.624	0.071	0.040	0.024	0.066	0.009	270.541
35	var	UH	0.239	0.133	0.316	0.039	0.117	0.065	0.209	0.027	256.719
42	var	LP	0.326	0.198	0.459	0.057	0.049	0.028	0.128	0.017	158.966
47	var	SP	0.318	0.243	0.415	0.048	0.086	0.044	0.171	0.024	115.788
49	var	LP	0.657	0.354	0.917	0.149	0.040	0.027	0.065	0.007	131.048
87	var	LP	0.242	0.137	0.394	0.052	0.086	0.051	0.158	0.021	80.592
109	var	UH	0.246	0.151	0.406	0.056	0.119	0.058	0.254	0.036	145.414
113	var	UH	0.199	0.111	0.280	0.039	0.107	0.057	0.236	0.031	216.137
115	var	UH	0.211	0.124	0.350	0.047	0.100	0.043	0.173	0.024	243.696
116	var	UH	0.225	0.149	0.399	0.051	0.109	0.059	0.178	0.025	83.252
126	var	LP	0.459	0.287	0.700	0.099	0.053	0.033	0.127	0.016	131.342
145	var	LP	0.257	0.172	0.355	0.049	0.091	0.049	0.226	0.029	172.683
LDABFB31	fix	UH	0.261	0.180	0.352	0.036	0.134	0.066	0.252	0.040	250.640
LDABFB32	fix	PH	0.221	0.138	0.296	0.041	0.135	0.063	0.406	0.049	280.260
LDABFB33	fix	UH	0.270	0.140	0.349	0.050	0.132	0.062	0.233	0.038	170.710
LDABFB34	fix	UH	0.264	0.191	0.327	0.031	0.112	0.057	0.197	0.029	208.230
LDABFB41	fix	UH	0.266	0.159	0.421	0.049	0.117	0.065	0.223	0.033	249.900
LDABFB42	fix	LP	0.319	0.201	0.428	0.058	0.042	0.019	0.099	0.013	131.117
LDABFB43	fix	UH	0.241	0.146	0.378	0.049	0.122	0.061	0.230	0.034	118.706
LDABFB44	fix	UH	0.267	0.187	0.335	0.037	0.105	0.041	0.249	0.043	162.895
LDABFB51	fix	UH	0.281	0.195	0.387	0.048	0.097	0.056	0.168	0.021	276.021
LDABFB53	fix	UH	0.290	0.210	0.431	0.054	0.099	0.050	0.183	0.027	148.904
LDABFB54	fix	UH	0.291	0.173	0.438	0.063	0.095	0.043	0.223	0.031	293.076
LDABFB61	fix	UH	0.316	0.226	0.487	0.051	0.096	0.046	0.168	0.022	247.869
LDABFB62	fix	UH	0.235	0.145	0.327	0.040	0.119	0.045	0.224	0.029	94.000

[*] Radius = variable and fix radius plots (see section 4.3.1 for description), forest type = BH (bottomland hardwood), UH (upland hardwood), PH (pine-hardwood), LP (loblolly pine), SP (shortleaf pine), and VP (Virginia pine). See table 4.1 for description of other variables.

plot	radius	forest type	$Pmag_{mean}$	$Pmag_{min}$	$Pmag_{max}$	$Pmag_{stdv}$	$Xmag_{mean}$	$Xmag_{min}$	$Xmag_{max}$	$Xmag_{stdv}$	$sn01xl_{cv}$
LDABFB63	fix	UH	0.282	0.207	0.416	0.051	0.093	0.049	0.200	0.028	408.955
LDABFB64	fix	UH	0.349	0.204	0.615	0.088	0.087	0.045	0.173	0.025	175.082
LDABFD11	fix	LP	0.270	0.140	0.456	0.086	0.091	0.033	0.245	0.038	74.101
LDABFD12	fix	PH	0.211	0.138	0.309	0.043	0.125	0.048	0.328	0.045	70.532
LDABFD13	fix	LP	0.322	0.153	0.477	0.091	0.104	0.033	0.257	0.044	92.247
LDABFD21	fix	BH	0.301	0.190	0.448	0.071	0.123	0.055	0.314	0.046	236.164
LDABFD22	fix	BH	0.227	0.143	0.435	0.052	0.126	0.017	0.254	0.050	344.201
LDABFD23	fix	SP	0.221	0.139	0.363	0.052	0.111	0.048	0.205	0.029	237.079
LDABFD24	fix	PH	0.261	0.142	0.479	0.068	0.110	0.037	0.197	0.032	222.204
LDABFD31	fix	SP	0.286	0.204	0.393	0.048	0.075	0.033	0.163	0.026	131.259
LDABFD32	fix	SP	0.303	0.211	0.500	0.066	0.077	0.041	0.173	0.023	96.330
LDABFD33	fix	SP	0.311	0.206	0.424	0.051	0.088	0.038	0.184	0.029	147.752
LDABFD34	fix	SP	0.338	0.240	0.549	0.064	0.091	0.047	0.167	0.024	153.089
LDABFD41	fix	LP	0.462	0.294	0.686	0.078	0.059	0.031	0.124	0.017	130.744
LDABFD42	fix	LP	0.340	0.208	0.496	0.054	0.053	0.026	0.084	0.012	151.103
LDABFD43	fix	LP	0.330	0.182	0.482	0.059	0.050	0.033	0.096	0.011	67.776
LDABFD44	fix	LP	0.386	0.248	0.545	0.072	0.070	0.032	0.157	0.025	95.111
LDABFD51	fix	VP	0.417	0.286	0.562	0.064	0.065	0.033	0.133	0.018	85.486
LDABFD53	fix	VP	0.340	0.233	0.481	0.058	0.087	0.035	0.232	0.035	78.614
LDABFD54	fix	LP	0.402	0.236	0.645	0.103	0.051	0.029	0.082	0.010	143.437
LDABFD61	fix	BH	0.191	0.147	0.332	0.035	0.145	0.074	0.262	0.034	152.670
LDABFD62	fix	LP	0.383	0.194	0.991	0.138	0.076	0.028	0.128	0.019	162.273
LDABFD63	fix	LP	0.314	0.146	0.511	0.090	0.107	0.045	0.241	0.042	212.110
LDABFD71	fix	LP	0.328	0.204	0.439	0.049	0.068	0.036	0.159	0.025	243.892
LDABFD72	fix	LP	0.338	0.254	0.474	0.053	0.062	0.035	0.159	0.024	122.734
LDABFD73	fix	LP	0.201	0.129	0.357	0.045	0.120	0.050	0.211	0.031	86.386
LDABFD74	fix	LP	0.345	0.215	0.469	0.069	0.054	0.031	0.131	0.015	72.381
LDABFD81	fix	VP	0.418	0.219	0.811	0.121	0.080	0.042	0.162	0.025	176.298
LDABFD82	fix	VP	0.415	0.287	0.587	0.075	0.055	0.031	0.110	0.015	120.689
LDABFD83	fix	VP	0.543	0.274	0.881	0.126	0.115	0.045	0.247	0.037	136.815
LDABFD84	fix	VP	0.300	0.209	0.481	0.064	0.082	0.040	0.149	0.025	207.920
LDABFD92	fix	LP	0.339	0.212	0.477	0.066	0.096	0.037	0.205	0.027	260.643
LDABFD93	fix	LP	0.450	0.265	0.714	0.106	0.106	0.046	0.273	0.045	148.635

plot	radius	forest type	$Pmag_{mean}$	$Pmag_{min}$	$Pmag_{max}$	$Pmag_{stdv}$	$Xmag_{mean}$	$Xmag_{min}$	$Xmag_{max}$	$Xmag_{stdv}$	$sn01xl_{cv}$
LDABFD94	fix	LP	0.204	0.111	0.395	0.057	0.097	0.051	0.192	0.028	224.933

Appendix T: Normal quantiles vs. Studentized residuals plot (top) and predicted vs. residuals plot (bottom) for the LAI 2-variable model with lidar metrics only, n = 61 (Chapter 4)**.** Refer to table 4.1 for variable names.

$$LAI = 3.363 - 6.602\ (LPI) + 0.173\ (All_{10th})$$

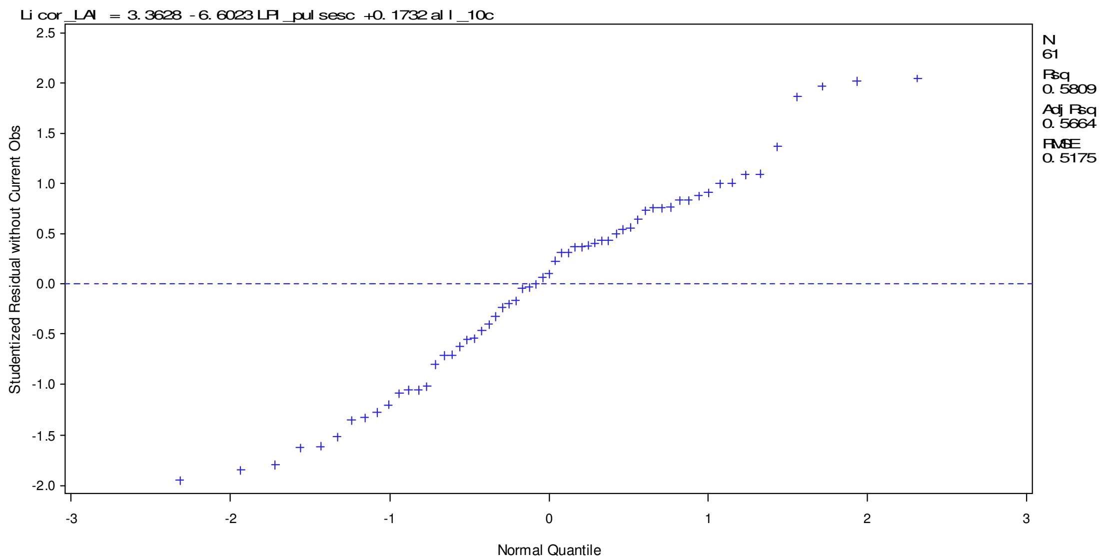

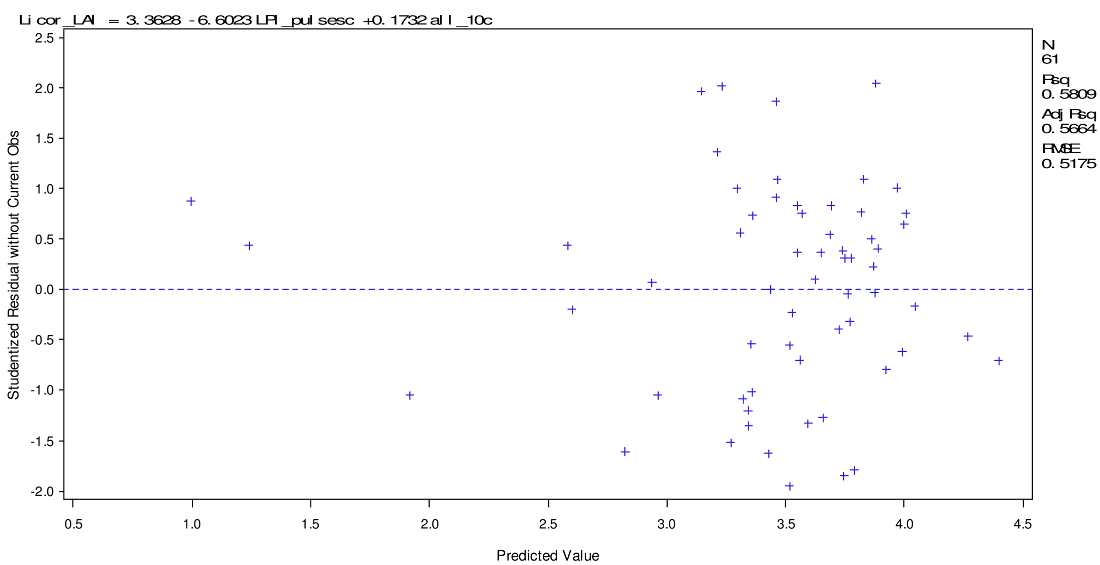

Appendix U: Normal quantiles vs. Studentized residuals plot (top) and predicted vs. residuals plot (bottom) for the LAI 4-variable model with lidar metrics only, n = 61 (Chapter 4). Refer to table 4.1 for variable names.

$$LAI = 3.405 - 7.480\ (LPI) + 0.134\ (All_{10th}) - 12.498\ (d_{10}) - 15.113\ (Cd\text{-}3)$$

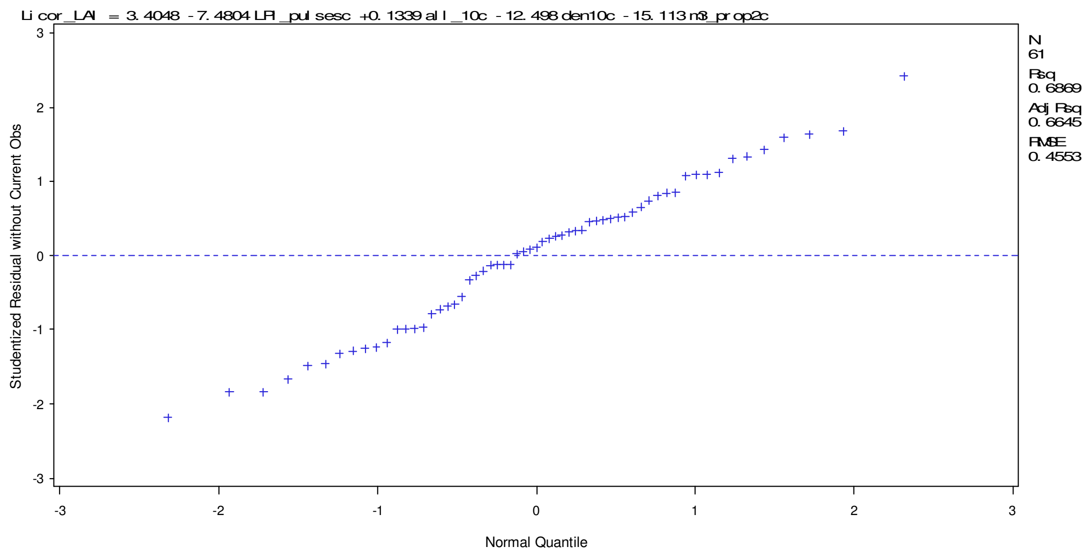

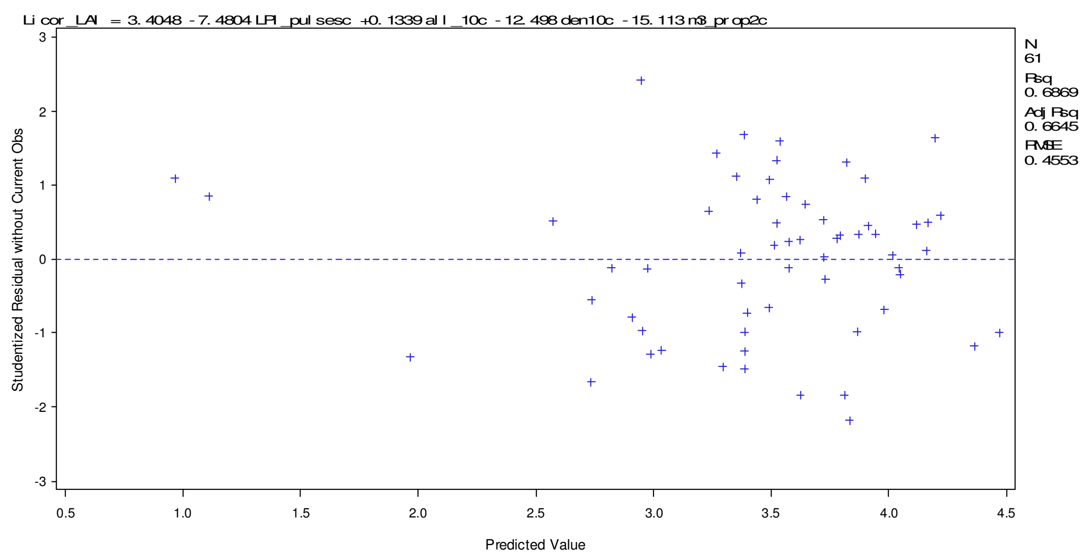

Appendix V: Normal quantiles vs. Studentized residuals plot (top) and predicted vs. residuals plot (bottom) for the LAI 4-variable model with GeoSAR metrics only, *n* = 61 (Chapter 4). Refer to table 4.1 for variable names.

$$LAI = 3.407 - 0.032\ (X_{cv}) + 0.104\ (X_{50th}) + 16.887\ (Xmag_{stdv}) - 0.002\ (sn01xl_{cv})$$

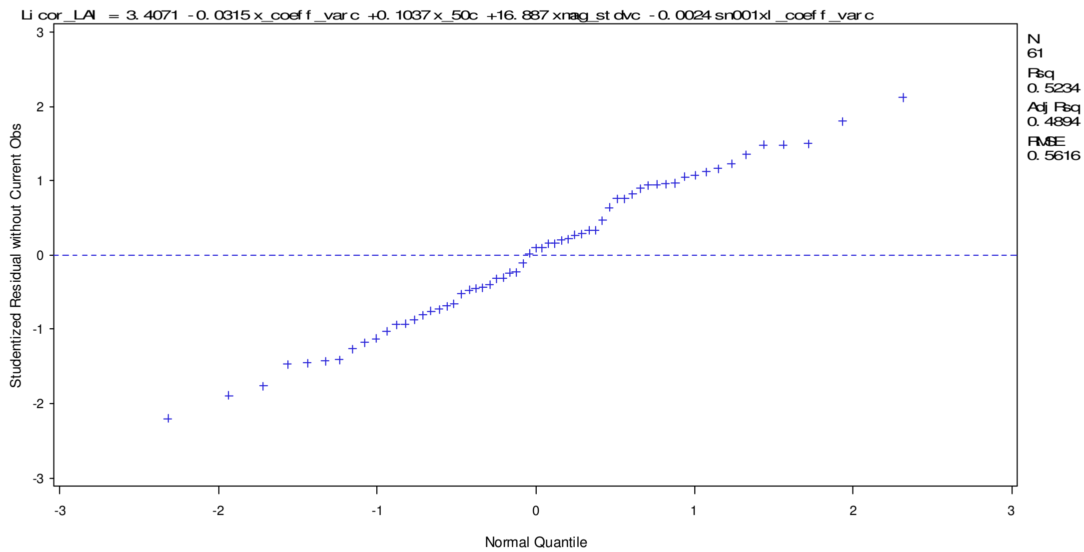

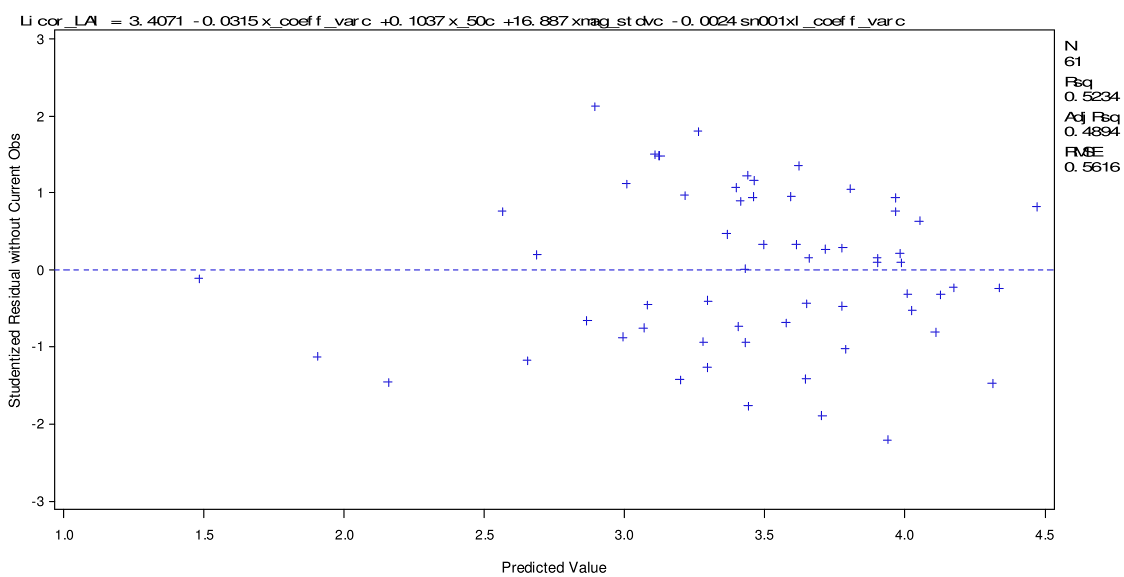

Appendix W: Normal quantiles vs. Studentized residuals plot (top) and predicted vs. residuals plot (bottom) for the LAI 2-variable model with lidar and GeoSAR metrics combined (including crown density slices), n = 61 (Chapter 4). Refer to table 4.1 for variable names.

$$LAI = 3.439 - 0.153\ (All_{50th}) + 0.229\ (X_{50th})$$

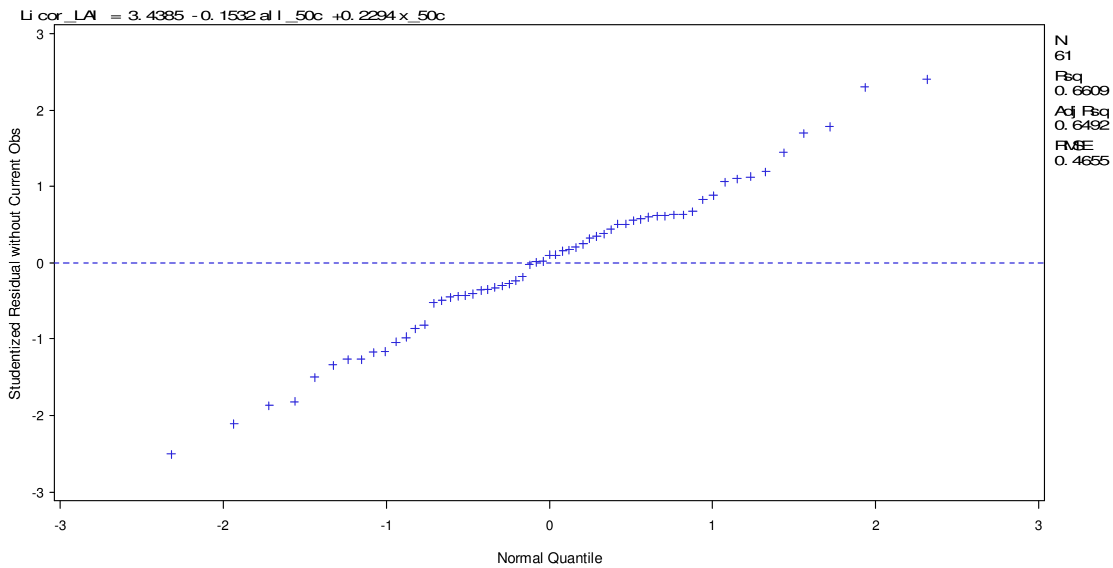

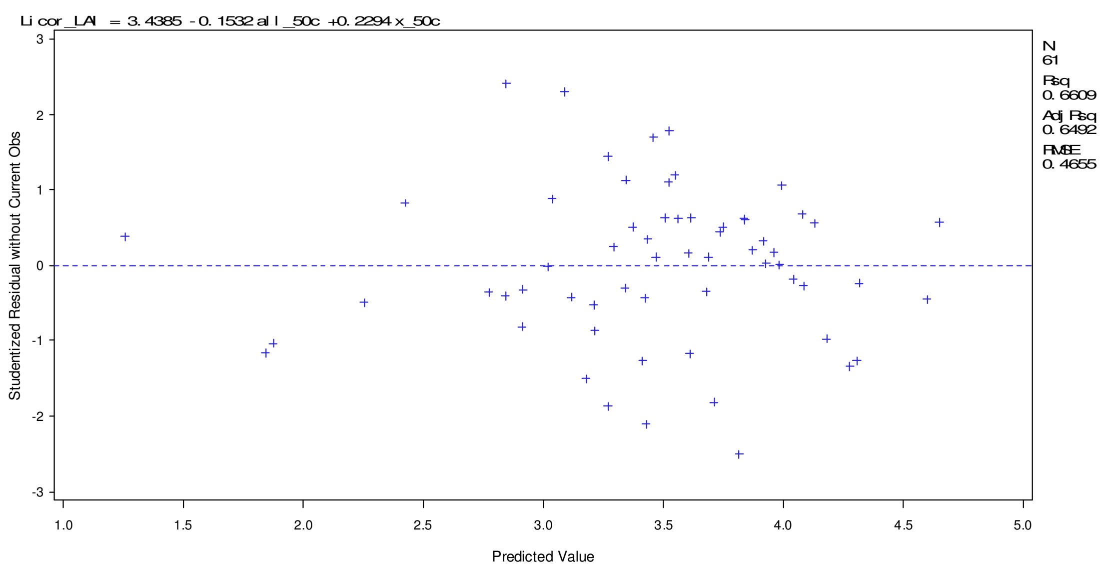

Appendix X: Normal quantiles vs. Studentized residuals plot (top) and predicted vs. residuals plot (bottom) for the LAI 3-variable model with lidar and GeoSAR metrics combined (including crown density slices), n = 61 (Chapter 4). Refer to table 4.1 for variable names.

$$LAI = 3.393 - 3.732\ (LPI) - 0.120\ (All_{50th}) + 0.176\ (X_{50th})$$

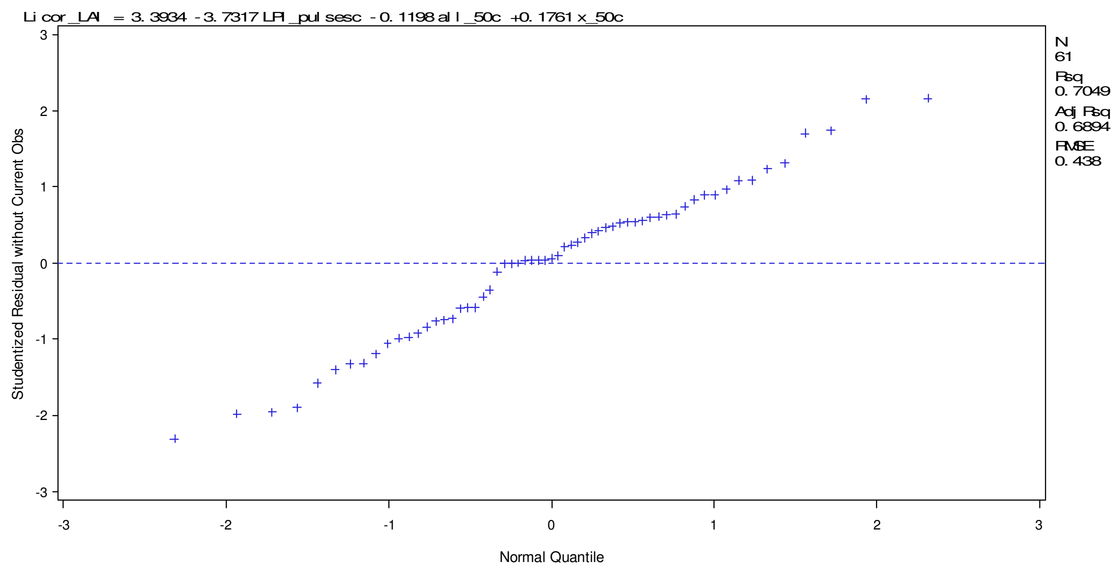

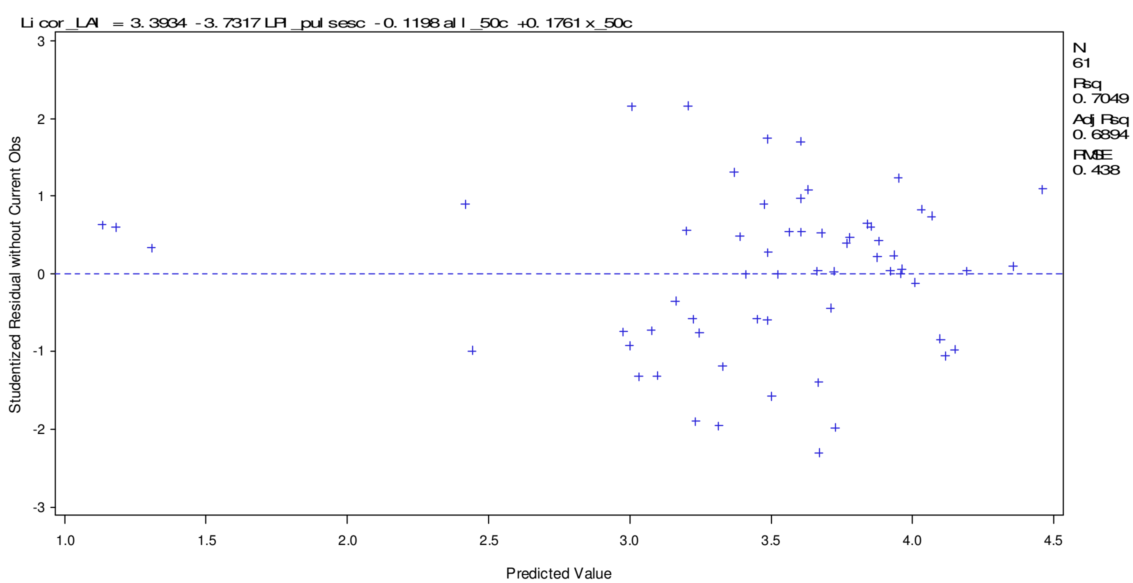

Appendix Y: Normal quantiles vs. Studentized residuals plot (top) and predicted vs. residuals plot (bottom) for the LAI 4-variable model with lidar and GeoSAR metrics combined (including crown density slices), n = 61 (Chapter 4). Refer to table 4.1 for variable names.

$$LAI = 3.391 - 3.044\ (LPI) - 0.147\ (All_{50th}) - 3.027\ (d_2) + 0.201\ (X_{50th})$$

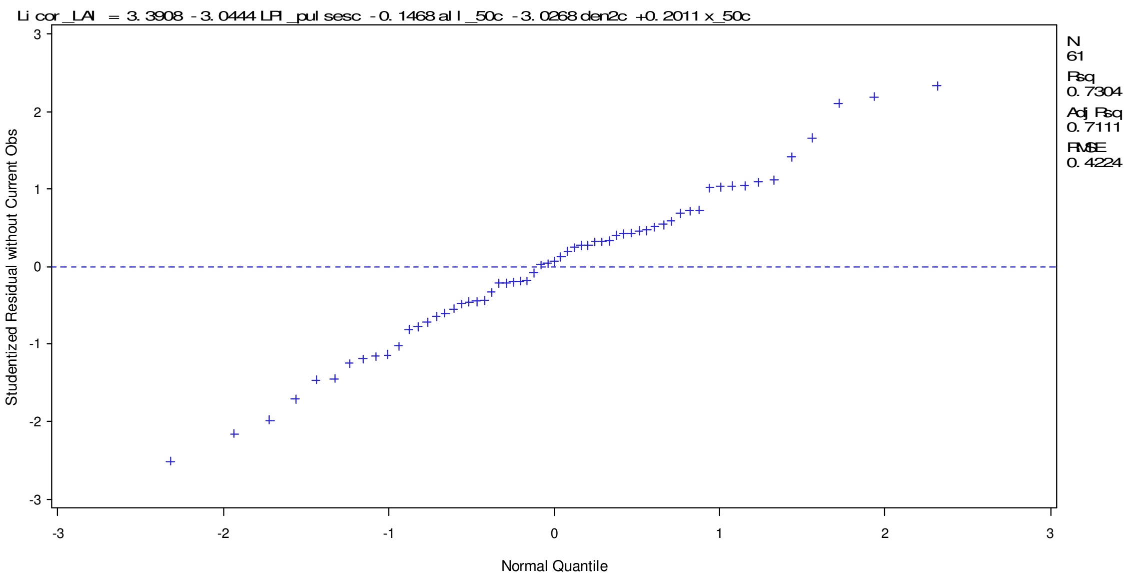

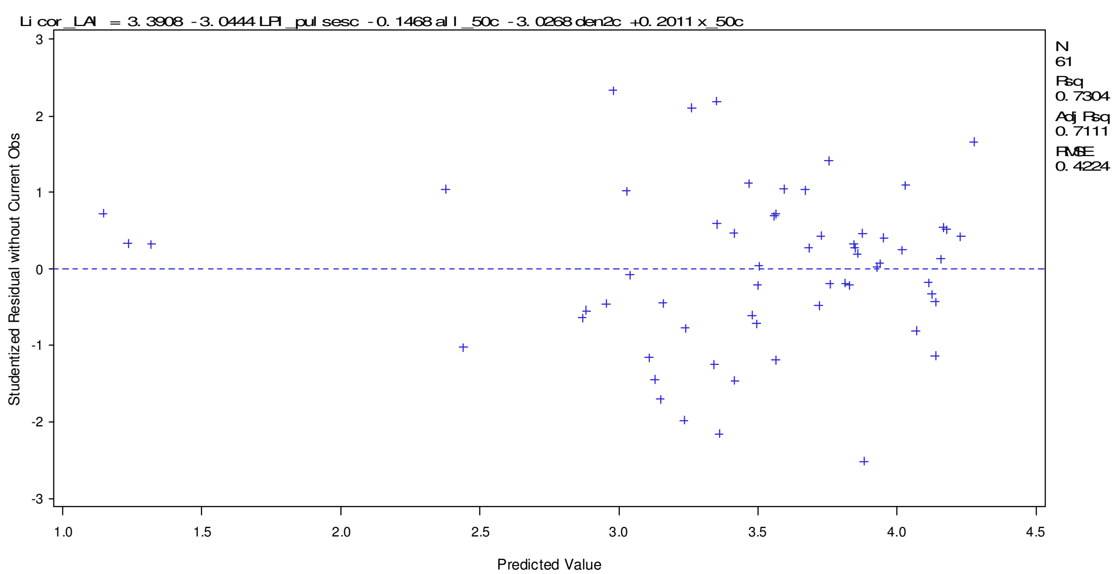

Appendix Z: Normal quantiles vs. Studentized residuals plot (top) and predicted vs. residuals plot (bottom) for the LAI 5-variable model with lidar and GeoSAR metrics combined (including crown density slices), *n* = 61 (Chapter 4). Refer to table 4.1 for variable names.

$$LAI = 3.401 - 4.253\ (LPI) - 0.148\ (All_{50th}) - 3.996\ (d_2) + 0.183\ (X_{50th}) - 11.703\ (Cd\text{-}3)$$

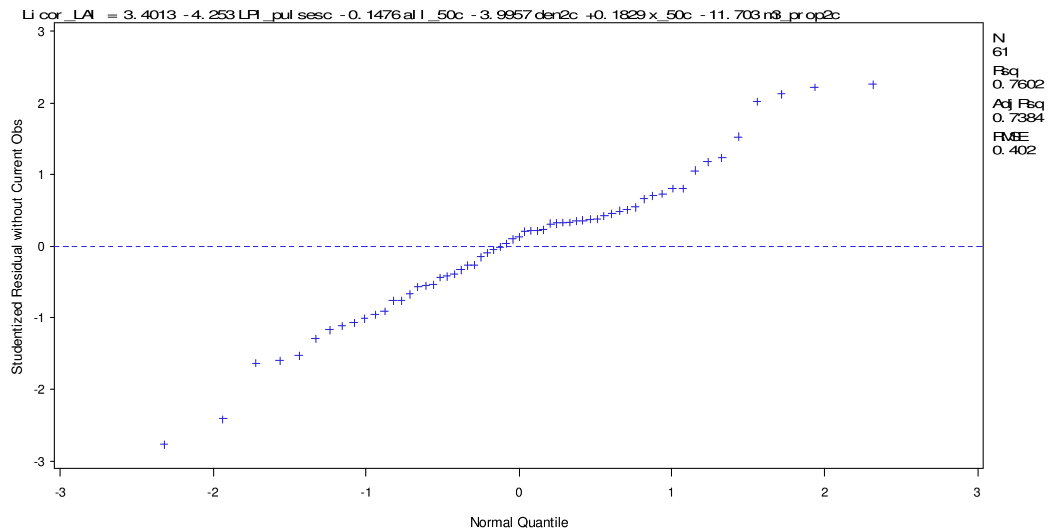

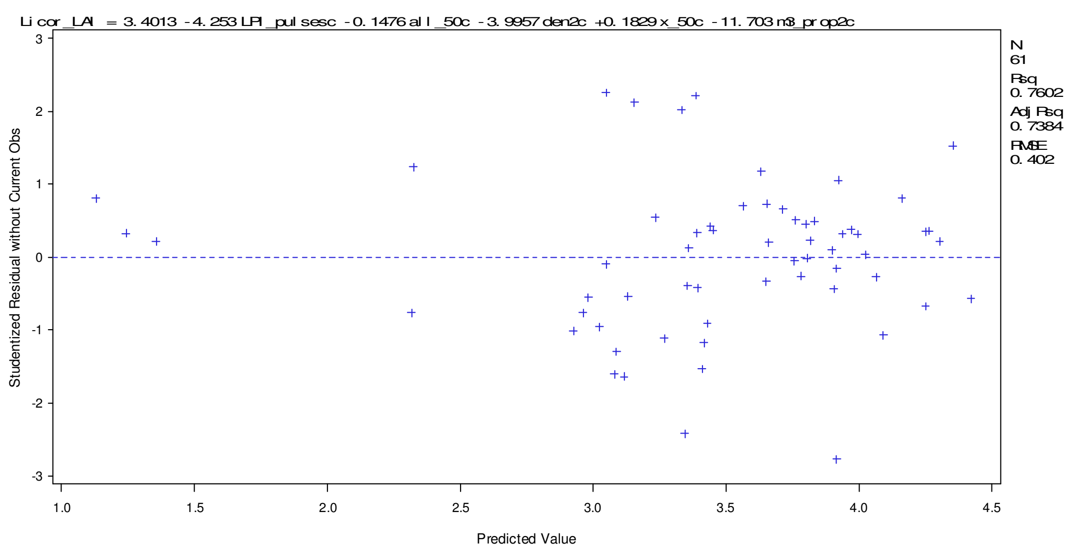

Appendix AA: Normal quantiles vs. Studentized residuals plot (top) and predicted vs. residuals plot (bottom) for the LAI 6-variable model with lidar and GeoSAR metrics combined (including crown density slices), *n* = 61 (Chapter 4). Refer to table 4.1 for variable names.

$$LAI = 3.475 - 4.246\ (LPI) - 0.185\ (All_{50th}) - 4.979\ (d_2) + 0.208\ (X_{50th}) - 14.977\ (Cd\text{-}3_{stdv}) - 7.805\ (Cd\text{-}1)$$

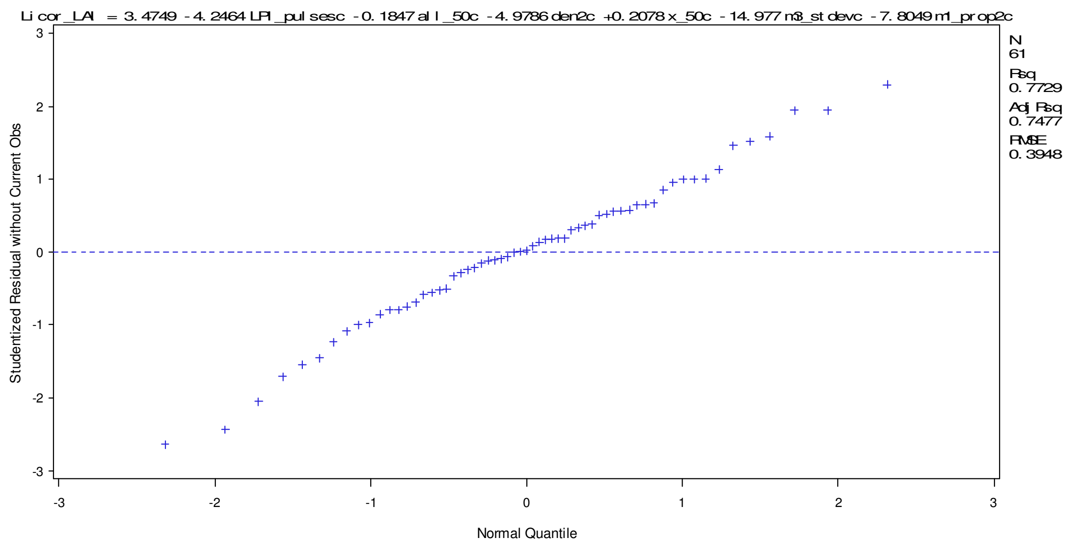

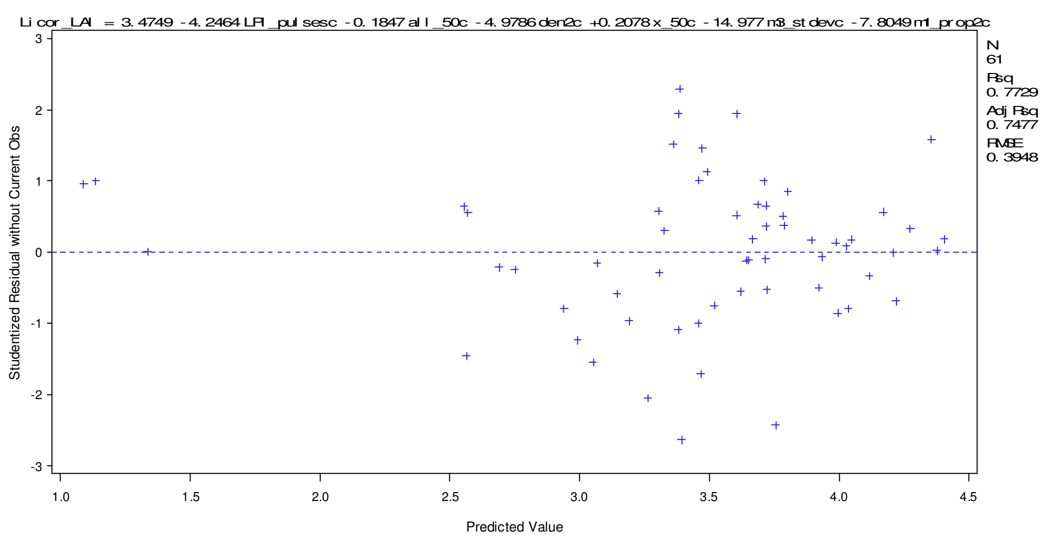

Appendix AB: Normal quantiles vs. Studentized residuals plot (top) and predicted vs. residuals plot (bottom) for the LAI 5-variable model with lidar and GeoSAR metrics combined (excluding crown density slices), n = 61 (Chapter 4). Refer to table 4.1 for variable names.

$$\text{LAI} = 3.442 - 0.180\ (\text{All}_{50th}) - 4.187\ (\text{d}_2) + 0.247\ (\text{X}_{50th}) + 16.079\ (\text{Pmag}_{stdv}) - 2.731\ (\text{Pmag}_{max})$$

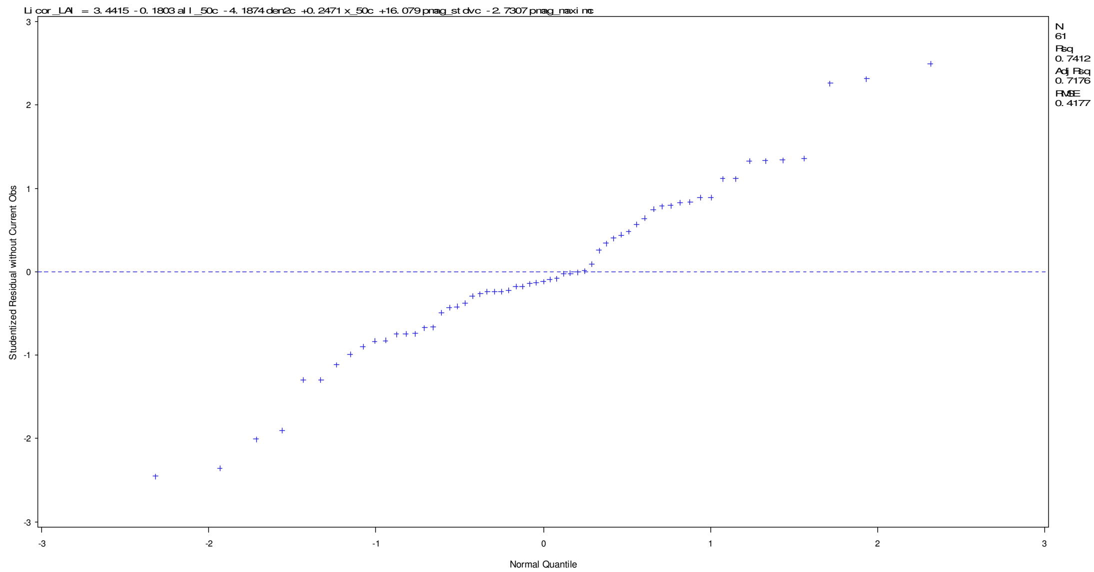

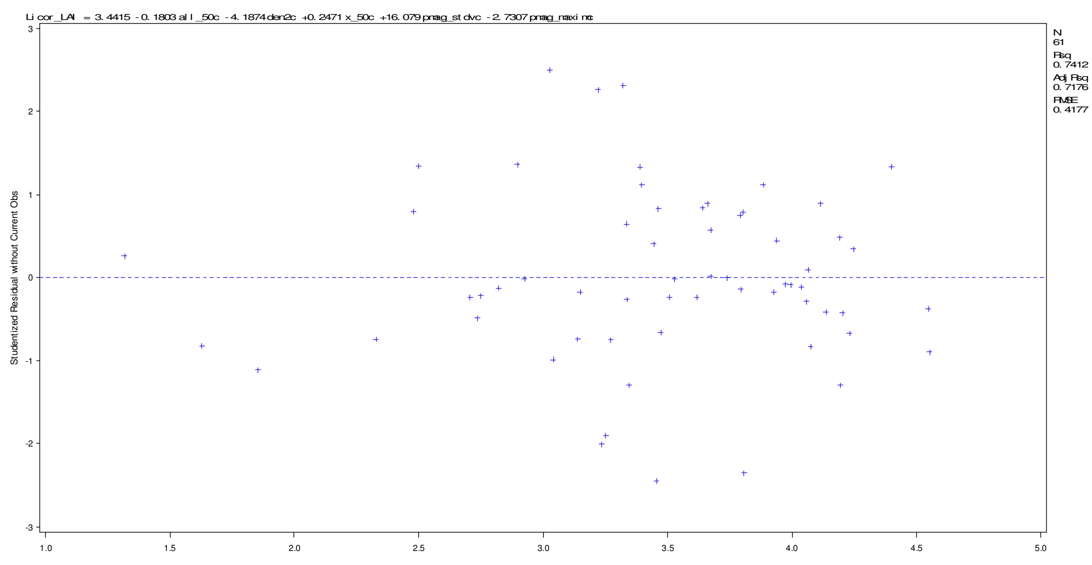

Appendix AC: Normal quantiles vs. Studentized residuals plot (top) and predicted vs. residuals plot (bottom) for the LAI 6-variable model with lidar and GeoSAR metrics combined (excluding crown density slices), *n* = 61 (Chapter 4). Refer to table 4.1 for variable names.

$$LAI = 3.406 - 3.110\ (LPI) - 0.147\ (All_{50th}) - 3.455\ (d_2) + 0.199\ (X_{50th}) + 16.643\ (Pmag_{stdv}) - 2.632\ (Pmag_{max})$$

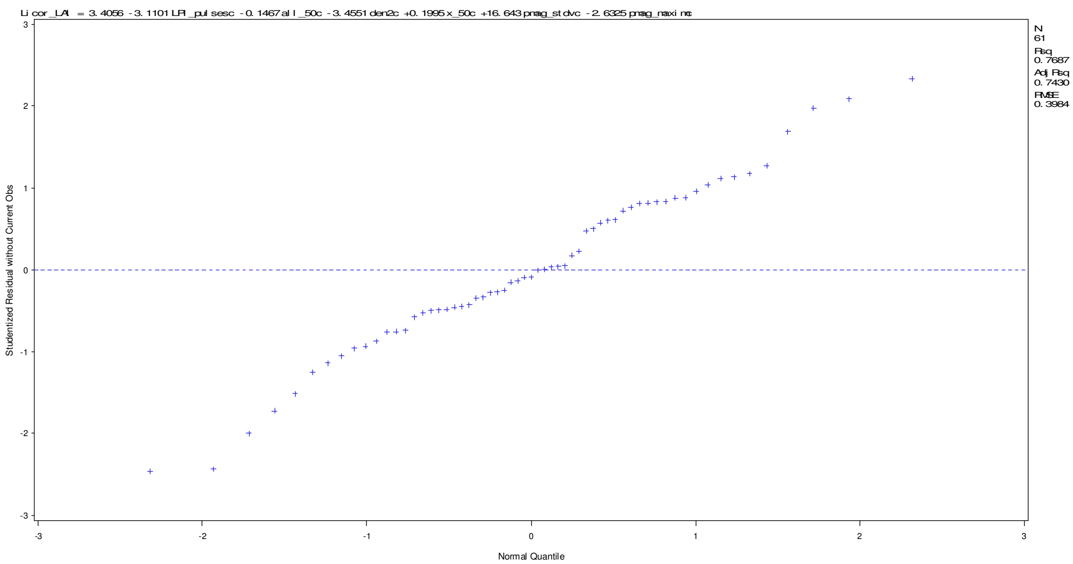

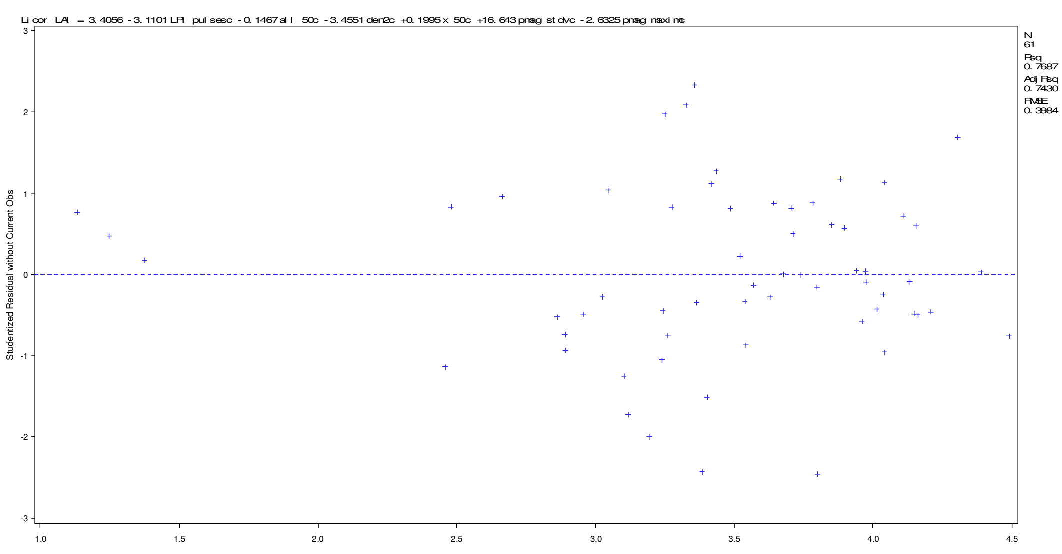

Appendix AD: Normal quantiles vs. Studentized residuals plot (top) and predicted vs. residuals plot (bottom) for the LAI 6-variable model with lidar and GeoSAR metrics combined (excluding three plots with low LAI values), *n* = 58 (Chapter 4). Refer to table 4.1 for variable names.

LAI = 3.658 – 8.933 (LPI) – 0.193 (All_{50th}) – 4.800 (d_2) + 0.211 (X_{50th}) – 18.042 ($Cd\text{-}3_{stdv}$) – 8.531 (Cd-1)

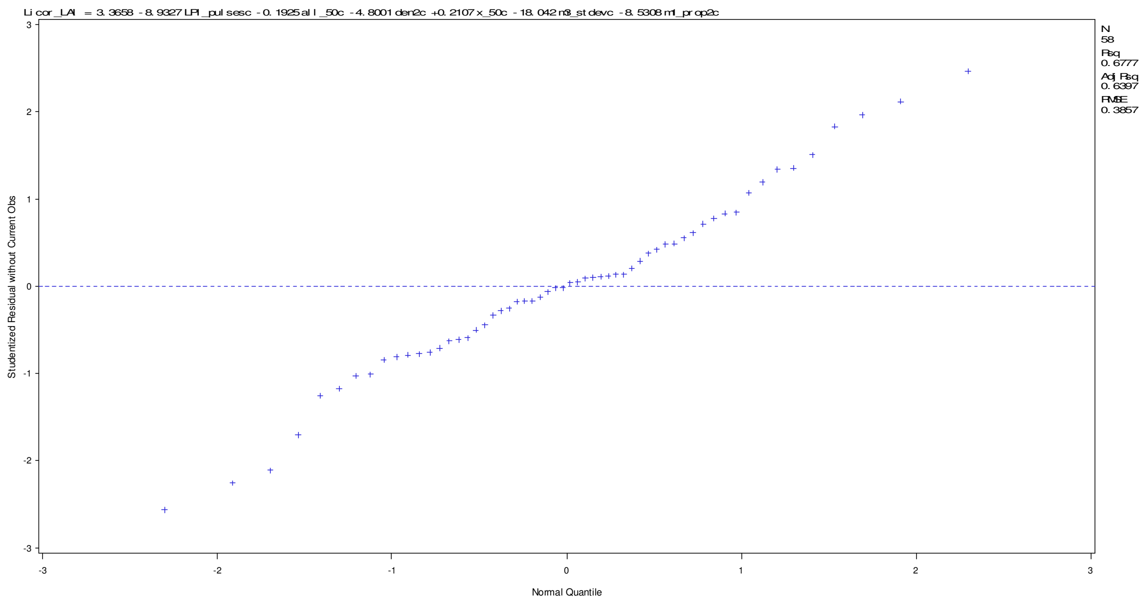

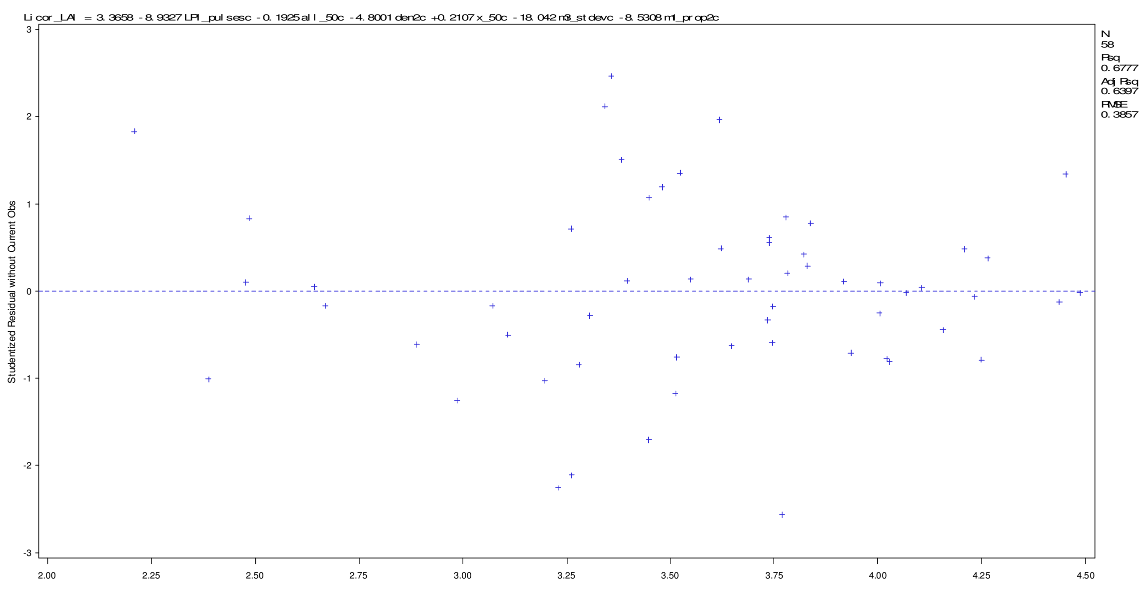

Appendix AE: Plot coordinates from the datasets used in chapters 2 and 3*.

Site	Plot	TPH/block	treatment	1		2		3		4	
				Northing	Easting	Northing	Easting	Northing	Easting	Northing	Easting
NSD	1	1794	fertilized	4162720.923	725447.8057	4162737.142	725472.7062	4162718.083	725486.0687	4162701.144	725460.8399
NSD	2	897	fertilized	4162679.508	725457.2795	4162695.956	725482.3117	4162676.258	725495.352	4162659.908	725470.156
NSD	3	1794	fertilized	4162646.219	725479.4612	4162662.342	725504.6247	4162643.008	725517.7958	4162626.527	725492.9274
NSD	4	897	control	4162612.389	725501.9651	4162629.495	725527.073	4162609.949	725540.6983	4162593.031	725515.6211
NSD	5	897	fertilized	4162579.635	725523.5296	4162595.984	725548.4963	4162576.266	725561.6022	4162559.95	725536.6355
NSD	6	897	fertilized	4162555.723	725485.8503	4162571.319	725510.9808	4162551.267	725524.0211	4162534.885	725498.7268
NSD	7	897	control	4162588.986	725465.2085	4162604.418	725488.7008	4162584.785	725502.2654	4162568.999	725478.5438
NSD	8	1794	control	4162622.877	725442.6664	4162638.637	725467.9608	4162619.044	725480.4769	4162602.629	725455.2153
NSD	9	897	control	4162656.062	725421.8281	4162671.658	725445.3859	4162651.35	725458.8194	4162635.656	725435.065
NSD	10	897	fertilized	4162697.564	725411.5672	4162712.628	725435.1034	4162693.117	725448.6732	4162677.286	725424.7153
NSD	11	1794	fertilized	4162673.394	725374.4504	4162689.672	725399.3188	4162670.314	725412.4902	4162653.965	725387.3924
NSD	12	1794	fertilized	4162632.165	725384.1683	4162647.87	725408.5842	4162627.571	725421.531	4162611.901	725397.2558
NSD	13	1794	fertilized	4162598.841	725406.1323	4162614.287	725429.9865	4162594.333	725443.1907	4162578.508	725419.4035
NSD	14	1794	control	4162565.336	725427.5947	4162580.801	725451.8406	4162560.749	725465.3724	4162544.563	725440.6023
NSD	15	1794	fertilized	4162531.553	725449.5369	4162547.604	725473.3997	4162527.355	725487.3575	4162511.231	725462.4985
NSD	16	897	fertilized	4162635.041	725329.3667	4162641.154	725358.494	4162617.891	725363.5398	4162611.665	725333.9533
NSD	17	1794	control	4162673.961	725320.7849	4162680.583	725348.894	4162657.058	725354.7916	4162650.397	725326.2638
NSD	18	897	fertilized	4162663.938	725280.0882	4162669.279	725304.1374	4162641.527	725311.2474	4162636.337	725286.913
Henderson	3	-----	vegetation control	4036979.642	727240.8283	4036997.349	727217.3057	4037010.809	727226.4533	4036992.775	727249.976
Henderson	4	-----	control	4037000.682	727205.4137	4037019.63	727179.0814	4037031.522	727188.2944	4037013.227	727214.3
Henderson	5	-----	vegetation control	4037036.587	727158.6299	4037052.591	727133.4052	4037065.025	727141.6151	4037048.902	727166.6614
Henderson	6	-----	control	4037057.707	727122.9345	4037076.923	727097.2339	4037090.011	727106.7527	4037071.212	727132.4533
Henderson	9	-----	vegetation control	4036943.901	727223.1863	4036960.889	727197.7035	4036974.088	727205.8711	4036956.903	727230.9618
Henderson	10	-----	control	4036965.136	727186.0729	4036982.125	727160.3287	4036994.866	727168.4309	4036978.466	727194.2404
Henderson	11	-----	vegetation control	4036998.81	727136.9747	4037016.003	727111.5715	4037029.389	727119.3055	4037012.433	727144.7682
Henderson	12	-----	control	4037019.156	727100.506	4037034.803	727075.4597	4037048.188	727082.8368	4037032.482	727108.24
Henderson	13	-----	control	4036565.33	726427.585	4036585.699	726403.9034	4036598.203	726413.8398	4036577.999	726437.0245

* Site = study site (refer to figs. 2.1 and 3.1), TPH/block = trees per hectare or block, for other variable names refer to tables 2.1 and 3.1. Projected coordinate system: NAD 1983 UTM Zone 17N

Site	Plot	TPH/block	treatment	1		2		3		4	
				Northing	Easting	Northing	Easting	Northing	Easting	Northing	Easting
Henderson	14	-----	vegetation control	4036539.247	726462.445	4036558.126	726436.6105	4036571.126	726445.9673	4036551.999	726471.3049
Henderson	15	-----	control	4036532.209	726400.1773	4036551.833	726376.8269	4036564.999	726386.9289	4036545.54	726410.0308
Henderson	16	-----	vegetation control	4036506.043	726433.6296	4036526.413	726410.6933	4036539.247	726420.7952	4036519.126	726443.566
Henderson	17	-----	vegetation control	4036501.323	726373.5976	4036522.521	726350.2472	4036534.776	726360.3492	4036513.827	726383.3683
Henderson	18	-----	control	4036473.75	726406.3047	4036493.788	726382.6231	4036506.292	726391.9798	4036485.922	726415.6614
Henderson	19	-----	vegetation control	4036469.858	726322.2599	4036491.47	726298.7439	4036503.145	726309.1771	4036481.699	726332.6102
Henderson	20	-----	control	4036443.444	726353.2281	4036463.731	726330.0434	4036475.406	726339.5657	4036455.451	726362.5848
Henderson	24	-----	vegetation control	4036402.615	725913.723	4036429.988	725896.6424	4036438.491	725909.3223	4036411.341	725926.4029
Henderson	25	-----	control	4036366.29	725938.1131	4036392.187	725920.627	4036401.197	725932.2953	4036375.092	725949.3759
Henderson	26	-----	control	4036351.224	725989.9515	4036379.567	725972.498	4036388.592	725985.4017	4036359.727	726002.7806
Henderson	27	-----	vegetation control	4036316.69	726010.0156	4036343.765	725994.2776	4036351.895	726007.1813	4036324.745	726023.2176
Henderson	28	-----	control	4036424.706	725810.4961	4036450.928	725795.0984	4036459.151	725808.0626	4036432.677	725823.2925
Henderson	29	-----	vegetation control	4036378.119	725825.8642	4036407.31	725808.2863	4036416.689	725821.4466	4036387.969	725838.3878
Henderson	30	-----	vegetation control	4036341.464	725872.1975	4036370.449	725856.5242	4036377.572	725869.4345	4036349.171	725884.9216
Henderson	31	-----	control	4036306.171	725894.6646	4036333.728	725876.9963	4036342.38	725889.7931	4036315.333	725907.4613
RW18	3	-----	fertilized thinned	4063294.957	769382.2434	4063316.36	769392.239	4063310.134	769409.2191	4063289.249	769398.465
RW18	12	-----	fertilized unthinned	4062766.303	768902.0001	4062779.658	768932.6723	4062767.548	768938.5577	4062754.758	768907.6592
RW18	14	-----	fertilized thinned	4062781.808	768970.9275	4062781.016	768996.8461	4062761.436	768997.1856	4062761.775	768971.4935
RW18	15	-----	fertilized unthinned	4063587.488	769145.4904	4063579.322	769176.583	4063564.392	769173.8183	4063572.346	769143.7465
RW18	16	-----	fertilized thinned	4062873.026	768875.088	4062878.904	768900.8913	4062863.96	768904.7768	4062857.983	768879.372
RW18	20	-----	fertilized thinned	4062852.204	768930.1816	4062855.591	768950.9039	4062836.164	768954.7894	4062833.375	768934.5652
RW18	21	-----	fertilized thinned	4064572.593	769666.0579	4064562.931	769689.8902	4064548.503	769681.5167	4064558.68	769658.0708
RW18	22	-----	fertilized thinned	4064621.417	769703.4167	4064609.823	769728.6661	4064596.94	769722.2249	4064609.179	769697.2332
RW18	23	-----	fertilized unthinned	4064749.198	769294.3413	4064749.748	769321.8775	4064731.712	769322.0152	4064731.781	769294.7543
RW18	26	-----	fertilized thinned	4064726.315	769614.4414	4064717.362	769634.5303	4064700.549	769626.1236	4064709.611	769605.3796
RW18	27	-----	fertilized thinned	4064610.725	769619.8103	4064598.486	769647.5073	4064588.567	769640.8085	4064600.161	769613.2403
RW18	28	-----	control and thinned	4064799.589	769418.1166	4064783.824	769433.7434	4064770.745	769420.3195	4064787.266	769404.0731
RW18	29	-----	fertilized thinned	4063194.002	769582.8687	4063181.082	769607.9597	4063166.804	769599.44	4063179.116	769574.3022
RW18	30	-----	fertilized thinned	4064887.532	769401.6604	4064881.997	769422.2189	4064862.173	769417.1357	4064865.957	769396.6338
RW18	31	-----	fertilized thinned	4063790.084	768991.6443	4063794.215	769022.1604	4063779.426	769022.9116	4063775.765	768992.0198
RW18	45	-----	fertilized thinned	4062967.838	768775.4871	4062983.583	768797.0918	4062974.01	768803.3094	4062958.042	768782.0177
RW18	46	-----	control and thinned	4062932.735	768809.1846	4062946.565	768830.6328	4062933.727	768840.0784	4062920.367	768818.3171

Site	Plot	TPH/block	treatment	1		2		3		4	
				Northing	Easting	Northing	Easting	Northing	Easting	Northing	Easting
RW18	47	-----	fertilized unthinned	4062867.872	768793.8021	4062878.298	768814.331	4062862.847	768825.4599	4062851.557	768805.2011
RW18	48	-----	fertilized thinned	4062751.568	769358.5148	4062740.07	769379.0126	4062722.238	769369.7636	4062732.904	769348.8492
RW18*	7	-----	fertilized thinned	4063525.859	769476.2053	4063515.985	769501.3055	4063502.855	769493.3617	4063513.061	769467.3236
RW19	1	-----	fertilized	4146597.453	706408.8282	4146615.784	706420.952	4146603.676	706439.2598	4146585.289	706427.0987
RW19	2	-----	fertilized	4146544.095	706421.5319	4146593.578	706454.4772	4146581.736	706472.2636	4146532.152	706439.4701
RW19	3	-----	fertilized	4146627.341	706436.6362	4146667.516	706463.2072	4146659.108	706475.921	4146618.932	706449.35
RW19	4	-----	fertilized	4146608.842	706464.6064	4146646.22	706489.3275	4146638.653	706500.7699	4146601.274	706476.0488
RW19	5	-----	fertilized	4146584.269	706544.6851	4146608.934	706560.9977	4146601.366	706572.4401	4146576.701	706556.1275
RW19	6	-----	fertilized	4146495.833	706481.3685	4146545.416	706514.1619	4146533.644	706531.9611	4146484.061	706499.1677
RW19	8	-----	fertilized	4146569.909	706490.5365	4146610.084	706517.1075	4146601.675	706529.8213	4146561.5	706503.2503
RW19	9	-----	fertilized	4146516.528	706456.1631	4146553.907	706480.8842	4146546.339	706492.3266	4146508.961	706467.6055
RW19	10	-----	fertilized	4146753.138	706944.1869	4146774.596	706964.5346	4146765.156	706974.489	4146743.699	706954.1413
RW19	11	-----	fertilized	4146757.852	706799.7382	4146779.184	706799.172	4146780.761	706858.598	4146759.429	706859.1642
RW19	12	-----	fertilized	4146759.914	706877.449	4146775.152	706877.0446	4146776.43	706925.1949	4146761.192	706925.5993
RW19	13	-----	fertilized	4146725.853	706800.5874	4146739.567	706800.2235	4146740.756	706845.0215	4146727.042	706845.3854
RW19	14	-----	fertilized	4146666.252	706759.7894	4146688.193	706759.2071	4146688.776	706781.149	4146666.834	706781.7314
RW19	15	-----	fertilized	4146646.596	706800.5662	4146667.929	706800	4146669.506	706859.4261	4146648.173	706859.9922
RW19	17	-----	fertilized	4146686.214	706799.5148	4146701.451	706799.1103	4146702.729	706847.2606	4146687.491	706847.665
RW19	18	-----	fertilized	4146633.646	706737.7826	4146647.36	706737.4186	4146648.549	706782.2166	4146634.835	706782.5806
RW19	19	-----	fertilized	4146423.359	706651.987	4146441.667	706664.0953	4146429.559	706682.4031	4146411.251	706670.2948
RW19	20	-----	fertilized	4146458.773	706671.3887	4146476.573	706683.1606	4146443.779	706732.7441	4146425.98	706720.9722
RW19	21	-----	fertilized	4146465.615	706600.2551	4146478.328	706608.6637	4146451.757	706648.839	4146439.044	706640.4303
RW19	22	-----	fertilized	4146493.585	706618.7539	4146505.027	706626.3216	4146480.306	706663.7	4146468.864	706656.1323
RW19	23	-----	fertilized	4146639.541	707030.7742	4146651.649	707040.0341	4146633.5	707063.765	4146621.392	707054.5052
RW19	24	-----	fertilized	4146551.812	706932.208	4146599.032	706968.3217	4146586.068	706985.2726	4146538.848	706949.1588
RW19	25	-----	fertilized	4146577.862	707002.0243	4146616.123	707031.2855	4146606.863	707043.3932	4146568.602	707014.1319
RW19	26	-----	fertilized	4146527.736	706963.6881	4146563.333	706990.9123	4146554.999	707001.809	4146519.403	706974.5849
RW19	27	-----	fertilized	4146426.894	706798.4283	4146445.202	706810.5366	4146433.094	706828.8444	4146414.786	706816.7361
RW19	28	-----	fertilized	4146434.636	706756.0397	4146484.219	706788.8331	4146472.448	706806.6322	4146422.864	706773.8388
RW19	29	-----	fertilized	4146360.167	706754.3409	4146400.343	706780.912	4146391.934	706793.6258	4146351.759	706767.0547

* This plot was not used in the analysis for chapter 2 (modeling LAI) due to its low LAI (0.12) measured with Licor LAI-2000.

Site	Plot	TPH/block	treatment	1		2		3		4	
				Northing	Easting	Northing	Easting	Northing	Easting	Northing	Easting
RW19	30	-----	fertilized	4146377.825	706727.626	4146415.203	706752.3472	4146407.636	706763.7897	4146370.257	706739.0685
RW19	31	-----	fertilized	4146516.701	706653.0212	4146535.008	706665.1295	4146522.9	706683.4373	4146504.592	706671.329
RW19	32	-----	fertilized	4146501.248	706691.2232	4146550.832	706724.0166	4146539.06	706741.8158	4146489.476	706709.0224
RW19	33	-----	fertilized	4146552.716	706672.1005	4146592.892	706698.6715	4146584.483	706711.3853	4146544.308	706684.8143
RW19	34	-----	fertilized	4146573.665	706739.0139	4146611.044	706763.7351	4146603.476	706775.1775	4146566.097	706750.4563
SETRES	1	1	control	3863613.257	638635.7558	3863583.655	638646.9036	3863574.233	638617.7916	3863603.636	638607.4959
SETRES	1	2	control	3863639.763	638560.8812	3863611.006	638572.1355	3863600.562	638544.3371	3863629.468	638532.9764
SETRES	1	3	control	3863594.789	638576.9638	3863565.748	638588.2891	3863554.955	638559.6032	3863584.671	638548.9169
SETRES	1	4	control	3863672.837	638615.5904	3863643.662	638626.5607	3863633.721	638597.6262	3863663.72	638586.9755
SETRES	2	1	fertilized, irrigated	3863533.654	638596.9517	3863505.252	638609.4485	3863494.14	638581.6502	3863522.826	638569.2953
SETRES	2	2	fertilized, irrigated	3863509.924	638683.4462	3863481.401	638696.156	3863469.451	638668.0381	3863498.35	638655.3993
SETRES	2	3	fertilized, irrigated	3863550.375	638665.1873	3863521.59	638677.5066	3863510.045	638648.2526	3863539.76	638636.4659
SETRES	2	4	fertilized, irrigated	3863484.114	638618.8318	3863454.931	638631.0801	3863443.57	638603.1753	3863472.475	638590.2297
SETRES	3	1	fertilized, irrigated	3863595.392	638450.6108	3863567.161	638463.0721	3863556.801	638436.1258	3863585.771	638424.41
SETRES	3	2	fertilized, irrigated	3863545.145	638469.8267	3863516.409	638481.4149	3863506.388	638452.3824	3863535.536	638440.753
SETRES	3	3	fertilized, irrigated	3863567.985	638523.2842	3863538.646	638532.4769	3863530.787	638503.5771	3863560.232	638493.8863
SETRES	3	4	fertilized, irrigated	3863617.759	638507.617	3863588.825	638518.1115	3863578.707	638490.7221	3863607.463	638478.3985
SETRES	4	1	fertilized, irrigated	3863464.183	638567.2007	3863436.342	638581.0466	3863423.561	638553.6388	3863451.934	638540.3964
SETRES	4	2	fertilized, irrigated	3863511.23	638545.1182	3863483.432	638559.2126	3863470.303	638532.3018	3863498.386	638519.2014
SETRES	4	3	fertilized, irrigated	3863486.656	638490.338	3863459.433	638504.7165	3863445.409	638478.2317	3863473.456	638463.4272
SETRES	4	4	fertilized, irrigated	3863438.82	638513.237	3863411.66	638527.509	3863398.51	638499.771	3863426.415	638485.783

Appendix AF: Plot coordinates from the dataset used in chapter 4*.

Plot	Radius	Forest type	Northing	Easting
2	var	LP	4145368.677	704451.1704
19	var	PH	4145145.247	704653.8658
33	var	LP	4144947.095	704257.2504
35	var	UH	4144942.365	704660.4566
42	var	LP	4144950.527	706051.411
47	var	SP	4144940.293	707051.8397
49	var	LP	4144749.414	704250.999
87	var	LP	4144347.402	705448.2132
109	var	UH	4144139.491	706653.1936
113	var	UH	4143947.71	704250.6498
115	var	UH	4143981.274	704649.6836
116	var	UH	4143949.032	704851.0641
126	var	LP	4143949.651	706850.9102
145	var	LP	4143546.386	704239.4942
LDABFB31	fix	UH	4145079	704698
LDABFB32	fix	PH	4145117.75	704691.0625
LDABFB33	fix	UH	4145066	704736.0625
LDABFB34	fix	UH	4145055	704670.5
LDABFB41	fix	UH	4144867	704300.75
LDABFB42	fix	LP	4144909.75	704290.0625
LDABFB43	fix	UH	4144854.5	704338.5
LDABFB44	fix	UH	4144839.25	704269.75
LDABFB51	fix	UH	4144872.25	704497
LDABFB53	fix	UH	4144857.5	704538.8125
LDABFB54	fix	UH	4144844.75	704468.4375
LDABFB61	fix	UH	4144877.5	704700.375
LDABFB62	fix	UH	4144918.25	704692.6875
LDABFB63	fix	UH	4144866.25	704736.0625
LDABFB64	fix	UH	4144852.75	704672.125
LDABFD11	fix	LP	4144922.5	706700.4375
LDABFD12	fix	PH	4144964	706692.125
LDABFD13	fix	LP	4144910	706738
LDABFD21	fix	BH	4144935.25	706896.0625
LDABFD22	fix	BH	4144975.75	706889.125
LDABFD23	fix	SP	4144923	706933.25
LDABFD24	fix	PH	4144909	706864.625
LDABFD31	fix	SP	4144936.5	707102.625
LDABFD32	fix	SP	4144973	707094.5
LDABFD33	fix	SP	4144927.75	707136.0625
LDABFD34	fix	SP	4144912.25	707076.1875
LDABFD41	fix	LP	4144728	706707.3125
LDABFD42	fix	LP	4144766	706702.375

* Radius = variable and fix radius plots (see section 4.3.1 for description), forest type = BH (bottomland hardwood), UH (upland hardwood), PH (pine-hardwood), LP (loblolly pine), SP (shortleaf pine), and VP (Virginia pine). See table 4.1 for description of other variables. Projected coordinate system: NAD 1983 UTM Zone 17N

Plot	Radius	Forest type	Northing	Easting
LDABFD43	fix	LP	4144715.5	706744.6875
LDABFD44	fix	LP	4144702.5	706676.5
LDABFD51	fix	VP	4144729.5	706869.4375
LDABFD53	fix	VP	4144720.75	706903
LDABFD54	fix	LP	4144706	706841.375
LDABFD61	fix	BH	4144738.75	707110.9375
LDABFD62	fix	LP	4144776	707110.8125
LDABFD63	fix	LP	4144726.5	707143.125
LDABFD71	fix	LP	4144530.5	706711.9375
LDABFD72	fix	LP	4144566.25	706706.375
LDABFD73	fix	LP	4144517.25	706746.25
LDABFD74	fix	LP	4144509	706681.375
LDABFD81	fix	VP	4144546	706911.8125
LDABFD82	fix	VP	4144582.5	706903.5
LDABFD83	fix	VP	4144537.25	706947.6875
LDABFD84	fix	VP	4144524.25	706886.3125
LDABFD92	fix	LP	4144596.75	707123.5625
LDABFD93	fix	LP	4144550	707164.75
LDABFD94	fix	LP	4144537.75	707102